University of Sussex

Non-Markovian effects & decoherence processes in open quantum systems

Graeme Pleasance

Submitted for the degree of Doctor of Philosophy

University of Sussex

September 2017

Dedicated to my parents.

Declaration

I hereby declare that this thesis has not been and will not be submitted in whole or in part to another University for the award of any other degree.

A paper has been published based on the work of chapter 6:

- Graeme Pleasance and Barry M. Garraway, *Application of quantum Darwinism to a structured environment*, Phys. Rev. A **96**, 062105 (2017).

Signature:

Graeme Pleasance

UNIVERSITY OF SUSSEX

Graeme Pleasance, Doctor of Philosophy

Non-Markovian effects & decoherence processes in open quantum systems

Summary

This thesis investigates two thematic lines of research, both underpinned by non-Markovian system-reservoir interactions in quantum optics. The overarching focus is on modelling the open system dynamics in a non-perturbative fashion, broadly on—though not restricted to—instances when the environment is structured.

A theory is developed by means of enlarging the open system over environmental degrees of freedom to include memory effects in its dynamics. This is achieved using an established technique that involves mapping a bosonic environment onto a 1D chain of harmonic oscillators. Within this setting, we apply a Heisenberg equation-of-motion approach to derive an exact set coupled differential equations for the open system and a single auxiliary oscillator of the chain. The combined equations are shown to have their interpretation rooted in a quantum Markov stochastic process. Including the auxiliary chain oscillator as part of the original system then enables us to obtain an exact master equation for the enlarged system, avoiding any need for the Born-Markov approximations. Our method is valid for a dissipative two-state system, with cases of multiple excitations and added driving discussed.

Separately, we apply the framework of quantum Darwinism to an atom-cavity system, and, subsequently, to a more general multiple-environment model. In both cases, the time-dependent spread of correlations between the open system and fractions of the environment is analysed during the course of the decoherence process. The degree to which information is redundant across different fractions is checked to infer the emergence of classicality. In the second case, we go further and present a decomposition of information in terms of its quantum and classical correlations. A quantitative measure of redundancy is also studied with regard to its ability to witness non-Markovian behaviour.

Besides fundamental interest, our results have application to quantum information processing and quantum technologies, keeping in mind the potential beneficial use of non-Markovian effects in reservoir engineering.

Acknowledgements

First and foremost, I would like to thank my parents who have continually supported me throughout my studies, even in the smallest things. I cannot express my gratitude enough for helping me to establish my place in the world and to get to where I am today.

Prior to starting my doctoral studies, my hope was to simply fulfil a desire to learn. Barry Garraway—my supervisor—has given me his time, space and encouragement to develop a much greater and deeper understanding of theoretical physics during these last four years, as well giving me the initial opportunity to start this adventure. For this I offer you my sincere and humble thanks. Importantly, too, for providing useful comments on the thesis.

I have had the benefit of meeting many people along the way. I give much thanks to Pedro who has been a great friend during our time in Brighton—his stimulating discussions and unique perspective on life will be missed. I also thank him for offering support during the write up of the thesis, despite not having the opportunity to say so in person.

I would too like to remember Elisa who I spent a great deal of time with during the first few years of my studies. Your care and affection during that era has shaped many good memories and has made the doctoral experience all the more worthwhile.

Also to friends in and around the department—Ezra, Hiroki, Nick, and others, and to my office mates Kathryn and Germán—I would like to extend my gratitude towards for having made this part of my life most enjoyable, as well as helping me improve my own capability as a scientist. Additionally to the friends I have been lucky to know since starting my undergraduate degree at the University of Birmingham; though I don't express it enough, I've have shared many good times with you all. Hopefully our get-togethers will continue long into the future.

I would finally like to give special appreciation to Jeremy Maris who has helped

me greatly with the use of the University of Sussex HPC. Many of the numerical results presented here wouldn't have been possible without his aid.

Contents

List of Figures viii

I Preface 1

1 Introduction 2

II Background 7

2 Theory of open quantum systems 8

2.1 Preliminaries 8

2.1.1 Closed quantum systems 8

2.1.2 Composite Hilbert spaces 13

2.1.3 Open quantum systems 15

2.2 Microscopic derivation of the Lindblad master equation 17

2.2.1 Born-Markov approximations 18

2.2.2 Decomposition of the interaction Hamiltonian 19

2.2.3 Secular approximation 21

2.3 Quantum dynamical maps and dynamical semigroups 24

2.3.1 Time-local master equations 25

3 The Heisenberg formalism 28

3.1 Outline 29

3.1.1 Rotating frame 31

3.1.2 Quantum optical Hamiltonian 34

3.1.3 Spectral density and memory effects 35

3.2 Exact Heisenberg picture dynamics . . . 36
3.3 The weak-coupling limit . . . 39
3.3.1 The Born-Markov approximations . . . 39
3.3.2 Markovian master equation . . . 41
3.4 Summary . . . 48

III Non-Markovian quantum dynamics of structured environments 49

4 Non-Markovian decay into a one-dimensional chain 50
4.1 Chain transformation . . . 51
4.1.1 Properties of orthogonal polynomials . . . 55
4.1.2 System-environment representation . . . 56
4.2 Spontaneous emission from a two-level system . . . 58
4.2.1 Damped Jaynes-Cummings model . . . 60
4.2.2 Parameters of the Hamiltonian . . . 62
4.2.3 Derivation of the dynamical equations for the atom and principal mode . . . 64
4.2.4 Noise term properties and interpretation . . . 69
4.3 The master equation . . . 76
4.3.1 Decay of a single excitation . . . 82
4.3.2 Decay of multiple excitations . . . 85
4.3.3 A driven two-level system . . . 87
4.4 Summary & discussion . . . 90

IV Quantum Darwinism 95

5 Emergence of classicality in a damped atom-cavity system 96
5.1 A basic example of quantum Darwinism . . . 97
5.1.1 Decoherence and pointer states . . . 98
5.1.2 Quantum Darwinism . . . 103
5.2 Dynamical model . . . 105
5.2.1 Solutions to the model . . . 105

5.2.2 Calculation of the quantum mutual information 109
5.3 Application of the quantum Darwinism framework 110
5.4 Total information and partial information plots 111
5.4.1 Dynamics of the total information 111
5.4.2 Partial information plots 113
5.5 Local information 117
5.6 Summary & discussion 122

6 A further application of quantum Darwinism to a structured environment 125
6.1 Dynamical model 127
6.1.1 Solutions to the model 128
6.1.2 Atom-pseudomode dynamics 131
6.2 Partial information plots 136
6.2.1 Case (i): atom and sub-environments 136
6.2.2 Case (ii): atom and pseudomodes 140
6.2.3 Accessible information and quantum discord 143
6.3 Maximisation of classical correlations 148
6.4 Non-Markovianity 150
6.4.1 Nondivisible maps 150
6.4.2 Redundancy 152
6.5 Summary and discussion 154

V Conclusions 157

7 Summary and outlook 158

Bibliography 163

A Notes on the Monte Carlo simulation 175

B Laplace transform solution of the state coefficients 182

C Accessible information and quantum discord 185

List of Figures

2.1 Time reversal in a closed quantum system 10

4.1 One-dimensional chain representation of the environment 57
4.2 Integration contours 61
4.3 The frequency kernels of a typical structured environment compared against the Markovian limit 73
4.4 Embedding of a single bosonic mode into a two-level system 79
4.5 Recurrence coefficients α_n and β_n vs. site index n 91

5.1 Observer monitoring a fragment of the environment 103
5.2 Modulus square of the atomic Green's function, $|G(t)|^2$ 107
5.3 Quantum mutual information for strong and weak system-environment coupling 112
5.4 Partial information plots in the weak coupling limit, $\Gamma = 10\Omega_0$ 115
5.5 Partial information plots in the strong coupling limit, $\Gamma = 0.1\Omega_0$ . . . 116
5.6 Partial information plots in the strong (moderate) coupling limit, $\Gamma = \Omega_0$ 117
5.7 Local information and excitation spectrum of the reservoir in the strong and weak coupling limits 120
5.8 Local information in the strong (moderate) coupling limit 122

6.1 Equivalent representations of the many-environment model 128
6.2 Excited population of the two-level atom and pseudomodes 132
6.3 Case (i): Partial information plot of the atom and sub-environments for strong (moderate) and weak system-environment coupling 136

6.4 Analytical estimates of the partial information plots compared against numerical results . . . 138
6.5 Case (ii): Partial information plots of the atom and pseudomodes for strong (moderate) and weak system-environment coupling, and for a large and small separation of decay timescales . . . 139
6.6 Purity of the atom-pseudomode density operator $\rho_{SP}(t)$ . . . 141
6.7 Case (i): Average of the classical and quantum correlations between the atom and fractions of sub-environments, compared with the partial information, in the strong and weak coupling limit . . . 145
6.8 Case (ii): Accessible information and quantum discord of the atom and pseudomodes in the strong and weak coupling limit . . . 146
6.9 Case (ii): Average of the classical and quantum correlations between the atom and fractions of pseudomodes, compared with the partial information, in the strong and weak coupling limit . . . 147
6.10 Case (ii): Accessible information and quantum discord of the full pseudomode environment with varying separation of timescales . . . 149
6.11 Redundancy $R_\delta = 1/f_\delta$ of information shared between the system and fractions of its environment . . . 153

Part I

Preface

Chapter 1

Introduction

Almost all quantum mechanical systems observed in the laboratory have been found to experience noise effects as a result of fluctuations in their local environment [1–6]. On one hand, this is unavoidable due to the fact that a system is never truly isolated from its surroundings. Indeed, for any microscopic system governed by the rules of either quantum or classical physics, the presence of noise is to be expected in a situation where fluctuations are freely left to influence the system's dynamics. What distinguishes a quantum system from a classical one—given the system is isolated from the environment—is that its statistics is formulated in terms of a state vector whose interpretation is based on the principle of superposition: inherently, the system can occupy one or many states with a certain (quantum) probability. According to the Schrödinger equation, the system exhibits a coherent dynamics in the sense that its superpositions are maintained over time. However, in an open and uncontrolled setting, quantum states are fragile, and environmental fluctuations tend to limit the coherent evolution to occur over a short timescale. Loss of such superpositions—known as decoherence—leads to an observable change from quantum to classical-like behaviour [7–11].

While most realisations of quantum systems have to be engineered to some degree (e.g. an atom in an optical cavity), there has been ongoing interest in implementing experiments where external fluctuations can be more reasonably controlled from the system being open by design—i.e. reservoir engineering [12, 13], rather than being an unintended consequence of random noise. Mitigating effects of dissipation and decoherence in this way, which are recognised as being detrimental to quantum

information processing [14, 15], is often necessary for quantum computation [16]. Therefore, understanding the types of decay processes that result from a quantum system coupling to its environment is critical to the development workable quantum technological devices.

One core part of this thesis is devoted to developing a novel framework that allows for the treatment of non-Markovian effects in open quantum optical systems [17]. The standard theoretical description of an open quantum system typically assumes that the reservoir is memoryless so that certain approximations can be made to its dynamics. Within a master equation approach, memory effects can be neglected by way of the Born-Markov approximations, which, provided the system-reservoir coupling is sufficiently weak, ensure that the final master equation describes a quantum Markov process whose generator is of a special Lindblad form[1] [18, 19]. Although their use tends to create an idealised picture of the actual dynamics, in many cases they serve as an excellent and valuable approximation since the resulting description is often much less challenging to deal with, and too they contextually provide a framework that is consistent with macroscopic (classical) thermodynamic laws. The subject of chapter 2 of the thesis is primarily devoted to the derivation of such a master equation. In the counter sense to this approach, the difficulty in modelling non-Markovian systems using a microscopic master equation arises due to non-trivial memory effects rendering the description based on the Born-Markov criteria obsolete. This happens in situations where, for example, the system-reservoir coupling is strong. Developing non-perturbative techniques to treat the dynamics of open systems is not only appealing out of theoretical curiosity, but also has a plethora of application to many relevant scenarios, such as the implementation of quantum heat engines [20, 21], understanding of energy excitation transfer in quantum biological systems [22], and photosynthetic complexes [23]; all where memory effects can play a significant role in the description. As well, it is thought non-Markovianity can be exploited as a resource in quantum information processing [24–26]—mainly to combat the exponential decay of coherences arising from occurrences of (Markovian) spontaneous emission into the environment.

[1]For conciseness, on some occasions we shall abbreviate the "Gorini-Kossakowski-Sudarshan-Lindblad form" to simply "Lindblad form".

Despite recent progress [27, 28], no general framework under which a non-Markovian system can be treated currently exists. An important class of methods used to extend the validity of certain master equations beyond the Born-Markov result are embedding methods, which we make the main focus our discussion. Broadly speaking, a non-Markovian system may be enlarged to a Markovian one by incorporating a number of auxiliary harmonic oscillator modes into its dynamics. This generally accounts for the non-Lindblad type evolution at the level of the original open system. Such approaches come under various guises—notable examples include the fictitious mode technique of Imamoglu [29, 30], the reaction-coordinate mapping [31–33], and a related effective mode representation, based on iteratively enlarging the open system over a set of collective degrees of freedom in the reservoir [34–36]. Embedding methods are appealing in their own right as generally the master equation of the enlarged system retains useful properties of its weak coupling counterpart. Indeed, since the ensuing equation is usually of Lindblad form, the master equation permits an unravelling of the combined dynamics of the original system and auxiliary degrees of freedom into pure quantum state trajectories [37]. Importantly, this avoids confronting issues surrounding the measurement-scheme interpretation of quantum trajectories for non-Markovian systems [38–40].

In the present work, we consider the specific techniques related to the pseudomode method [41, 42]. This method relies on making a connection between the shape of the reservoir spectral density (i.e. its frequency dependence), and the response the open system has by coupling to a number of damped pseudomodes to facilitate the derivation of exact non-perturbative master equation. The aim here is to extend the pseudomode treatment to a wider range of cases, for the reason that the approach offers a mathematically simple and intuitive account of how memory effects emerge in the open system dynamics. Indeed, it is precisely the link the pseudomodes have to the spectral density which gives better physical insight into the problem compared to other approaches used in the same structured reservoir setting, such as the resolvent operator method [17, 43]. In principle, the theory outlined in Ref. [41] can be extended to include cases of multiple excitation by applying a separate Fano diagonalisation procedure in which the open system is shown to couple to an analogous set of quasimodes [44–46]. However, because the original

pseudomode method employs an approach based on expanding the state vector of the total system in the one excitation sector, attempting to derive the theory for two, three e.t.c, excitations presents intractable difficulties. Its application is hence only straightforwardly demonstrated for the example of a singly excited two-level atom coupling to a structured reservoir. In our work, we generalise the pseudomode problem *per se* using a Heisenberg equation-of-motion approach to enable a description of multiple photon processes. By this, we expand the quantum Langevin equation of the system [2] over an auxiliary mode of the reservoir to find a closed Markovian dynamics for the enlarged system. In chapter 4 we develop the theoretical formalism that deals with the construction of the master equation starting in the Heisenberg picture. Initially, to gain a conceptual understanding for such techniques, we examine the weak coupling (Markov) limit of the dynamics for a bosonic system in chapter 3.

Working within the model of a two-level atom coupling to a large bosonic reservoir, in the second part of the thesis we focus on studying information flows between the atom and separate parts of the reservoir. This is done by quantitively analysing system-environment correlations produced during decoherence under the framework of quantum Darwinism [7, 47–56]. Based on the pioneering work of Zurek and collaborators, quantum Darwinism is concerned with using the idea of information redundancy to address the quantum-to-classical transition and in parallel the issue of a preferred basis in quantum theory: that is, to explain how objective behaviour in a quantum setting is feasible when states of parts of the environment correlate with the most "classical states" of an open system in a specific way. In this regard, classical behaviour is thought to emerge over time when many of the same copies of information about the classical states of the system are spread into many small parts of its environment, and so appear objective to an external observer (in other words, correlations between different parts are redundant [57]). Tracking the emergence of redundant information at the level of both system and environment has been shown to have importance in understanding how an open system can come to appear objective in prototypical models of decoherence, and even for generic models beyond the usual system-environment partitioning [58]. Recent studies have also sparked interest in applications beyond standard Markovian regimes [59, 60]. Here, it has

been found that memory effects tend to work against the spreading of redundant information, and thus prevent features of quantum Darwinism from emerging.

In chapter 5 we apply the quantum Darwinism framework to as of yet unexplored regime—that is, we study the aforementioned atom plus reservoir model, specifically framed in the setting of an atom coupled to a lossy cavity field (i.e. the damped Jaynes-Cummings model [1]). It turns out that redundant information proliferation occurs but only under the condition that the coupling strength of the atom to the reservoir is not too strong. Equivalently, non-Markovian effects prevent correlations between the atom and different collections of modes, on average, being uniformly spread across the reservoir. In chapter 6, we more or less generalise the contribution made from the previous chapter by considering a multiple-environment version of the model. Again we find similar redundancy features when the coupling is sufficiently weak. However, our most important result is that, by partitioning the correlations into their quantum and classical components, the classical part of the information is discovered to be non-redundant—despite prevalent redundancy of total information. Furthermore, in light of the pre-established connection between poor information redundancy and presence of non-Markovianity in the dynamics, we introduce a quantitative measure of redundancy and investigate its ability to act as a witness to non-Markovian behaviour.

Overall, the original contributions of this thesis make up two different but broadly related bodies of work, tied together by the theory of non-Markovian dynamics in quantum optics. Basic fundamentals in the theory of open quantum systems are presented in chapters 2-3. The first original part of the thesis, provided by chapter 4, deals with the derivation of a set of equations which allow the original non-Markovian dynamics of the system to be incorporated into a larger Markovian one by way of the pseudomode technique. The second part considers a more applied approach, motivated by gaining a deeper understanding of decoherence and the quantum-to-classical transition by using the tools of quantum Darwinism. This forms the body of work presented in chapters 5-6[2]. Finally, appendices A, B, C are provided at the end of the thesis.

[2]See the paper submitted for publication at the beginning of the thesis.

Part II

Background

Chapter 2

Theory of open quantum systems

This chapter introduces background material and is intended to serve as a foundation for much of the thesis. The analysis encountered here mostly relies on the treatment of open quantum systems given in the textbook of Breuer and Petruccione [1], with particular attention paid to the Markovian dynamics of open quantum systems. Bear in mind that this work is not meant to provide be complete review of the field—or to contain original content—but will selectively include material that will aid with conceptual understanding throughout. This goes for both chapters 2 and 3.

Section 2.1 gives a general overview of quantum theory applied to both closed and open physical systems, with attention paid closely to pure and mixed quantum states, measurement, and composite quantum systems. Section 2.2 presents a microscopic derivation of the Markovian quantum master equation, and, in section 2.3, culminates in a stricter formulation of Markovianity in terms of dynamical semigroups. This conveys a more general notion of dynamical maps in open quantum systems which we also discuss in relation to non-Markovian quantum processes.

2.1 Preliminaries

2.1.1 Closed quantum systems

Before we embark on formulating of the dynamics of open quantum systems, it is appropriate for us to present an overview of the standard theory of closed quantum systems. By this we consider time-dependent properties of states formed within a

Hilbert space $\mathcal{H}$, and as of yet introduce no partitioning of this space into subsystems (e.g. system and environment).

The time evolution of the state vector $|\psi(t)\rangle$ associated with the system is provided by the Schrödinger equation ($\hbar = 1$),

$$\frac{d}{dt}|\psi(t)\rangle = -iH(t)|\psi(t)\rangle\,. \tag{2.1}$$

Loosely, this describes how the probability densities of each of the basis states in $|\psi(t)\rangle$, which may be complex, evolve according to the Hamiltonian $H(t)$. Note the operator is assumed to have explicit time-dependence to include possible non-energy conserving effects in the dynamics, i.e. $\partial_t H(t) > 0$. The solution to (2.1) can be written as

$$|\psi(t)\rangle = U(t,t_0)|\psi(t_0)\rangle\,, \tag{2.2}$$

where $U(t,t_0)$ is a time evolution operator of the system. This maps the initial state $|\psi(t_0)\rangle$ at time t_0 onto the future state $|\psi(t)\rangle$ at $t > t_0$, and, since $U(t,t_0)$ is unitary, $U^\dagger(t,t_0) = U^{-1}(t,t_0)$, application of the operator conserves the inner product $\langle\psi(t)|\psi(t)\rangle = 1$. By inserting (2.2) into the Schrödinger equation, we find the time evolution operator satisfies the differential equation

$$\frac{d}{dt}U(t,t_0) = -iH(t)U(t,t_0), \tag{2.3}$$

which, from (2.2), is subject to the boundary condition

$$U(t_0,t_0) = 1 \quad \text{at} \quad t = t_0. \tag{2.4}$$

Equation (2.3) can be formally integrated to obtain the expression

$$U(t,t_0) = T_{\leftarrow}\exp\left[-i\int_{t_0}^{t} dt' H(t')\right], \tag{2.5}$$

with $T_{\leftarrow}$ the chronological time ordering operator that orders products of time-dependent operators so their time-arguments increase from right to left, as indicated by the direction of the arrow. If the time evolution governed by (2.2) occurs in an isolated setting, such that $\partial_t H(t) = 0$, the integral in (2.5) yields a simpler result:

$$U(t,t_0) = \exp\left[-iH(t-t_0)\right]. \tag{2.6}$$

Consequently, the time evolution of any closed quantum is reversible: that is, by evolving the state from $t_0 \to t$ and subsequently evolving it from $t \to t'$ via a

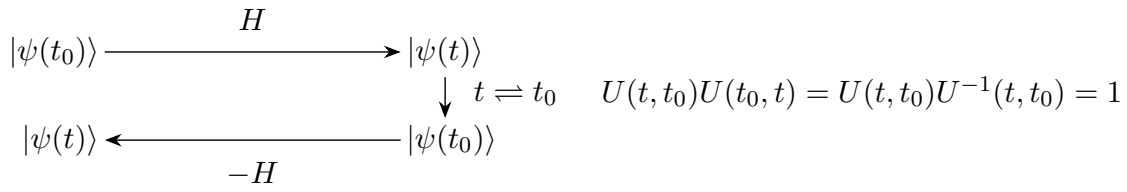

Figure 2.1: Pictorial representation of a time reversed quantum process. The evolution up to a time $t > t_0$ can be reversed by applying a unitary operator $U(t_0,t) = U^{-1}(t,t_0)$, the generator of which is given by $-H$.

different but equally timed process $U_r(t',t)$ with Hamiltonian H', we have

$$\begin{aligned} &|\psi(t_0)\rangle \longrightarrow |\psi(t)\rangle \\ &\longrightarrow |\psi(t')\rangle = U_r(t',t)\,|\psi(t)\rangle = |\psi(t_0)\rangle\,, \quad t \geq t_0. \end{aligned} \tag{2.7}$$

As (2.7) suggests, in order for the second time evolution to reverse the state back to $|\psi(t_0)\rangle$, the operator $U_r(t',t)$ must take the form $U_r(t',t) = U_r(t_0,t)$. Hence,

$$U_r(t_0,t) = U^{-1}(t,t_0) = \exp\left[-i(-H)(t-t_0)\right], \quad t \geq t_0, \tag{2.8}$$

such that (2.8) is associated with a real physical time evolution provided by the Hamiltonian $H' = -H$. This type of evolution is depicted schematically in Fig. 2.1. An important and contrasting feature of open quantum systems is that they are universally described by non-unitary processes. Indeed, while a time-dependent Hamiltonian $H(t)$ can account for external interactions, the system in question is still closed and has a unitary dynamics (i.e. the external system has no quantum dynamics of its own).

The above can be generalised to include states that cannot be represented by a single state vector. Usually this applies to cases when there is classical uncertainty in the preparation of $|\psi(t)\rangle$. To reflect such a case, a quantum state can instead be constructed out of many individual ensembles whose statistics are each described by a pure state $|\psi_j\rangle$. First we consider the most basic case where the states are time independent. According to classical probability theory, the statistics of the full ensemble can be realised by mixing together the given set of quantum states $\{|\psi_j\rangle\}$ weighted by the probabilities p_j:

$$\rho = \sum_j p_j\,|\psi_j\rangle\,\langle\psi_j| = \mathrm{E}\left[|\psi_j\rangle\,\langle\psi_j|\right], \tag{2.9}$$

where ρ is the *density matrix* or statistical operator, and $\mathrm{E}\left[\cdot\right]$ denotes the expectation value of some random variable r associated with the $j = j(r)$ index. Essentially, a mixed state forms part of the statistical mean that sums over each distinct subset of pure states. This is better illustrated by taking the average of an observable $R = \sum_j r(j) \left|r_j\right\rangle \left\langle r_j\right|$,

$$\langle R\rangle = \sum_j p_j \langle\psi_j|R|\psi_j\rangle = \sum_j p_j \langle\psi_j|r_j\rangle\langle r_j|R|\psi_j\rangle = \mathrm{tr}\left[R\,\rho\right], \tag{2.10}$$

where we have used the completeness relation $\sum_j \left|r_j\right\rangle \left\langle r_j\right| = 1$. As it should, Eq. (2.10) can be interpreted by the rules of classical (and quantum) probability. The trace of ρ taken using an arbitrary basis (the eigenbasis $\left|r_j\right\rangle$, for example) is thereby constrained to

$$\mathrm{tr}\left[\rho\right] = 1 \quad \text{from} \quad \sum_j p_j = 1, \tag{2.11}$$

along with hermiticity $\rho = \rho^\dagger$ and positivity $\rho > 0$. In a case where the states $\left|\psi_j\right\rangle$ gain time-dependence, clearly the density matrix ρ must coincide with that at the initial time $t = t_0$,

$$\rho(t_0) = \sum_j p_j \left|\psi_j(t_0)\right\rangle \left\langle\psi_j(t_0)\right|. \tag{2.12}$$

Using (2.2), it is straightforward to derive the form corresponding to the time evolved density matrix $\rho(t)$,

$$\rho(t) = \sum_j p_j U(t,t_0) \left|\psi_j(t_0)\right\rangle \left\langle\psi_j(t_0)\right| U^\dagger(t,t_0) = U(t,t_0)\rho(t_0)U^\dagger(t,t_0). \tag{2.13}$$

Taking its time-derivative and then applying (2.3) yields

$$\frac{d}{dt}\rho(t) = -i\left[H(t),\rho(t)\right], \tag{2.14}$$

The resulting dynamical equation is commonly known as the von Neumann or Liouville-von Neumann equation, which, in accordance with the classical Liouville equation can be written conveniently as

$$\frac{d}{dt}\rho(t) = \mathcal{L}(t)\rho(t), \tag{2.15}$$

where $\mathcal{L}(t)$ is the Liouvillian super-operator. Formally, a super-operator maps an operator onto another operator vector space, rather than a scalar. Equation (2.15) admits the general solution

$$\rho(t) = T_{\leftarrow}\exp\left[\int_{t_0}^{t} dt'\,\mathcal{L}(t')\right]\rho(t_0), \tag{2.16}$$

which again for a time independent process (2.6) reduces to $\rho(t) = \exp[\mathcal{L}t]\rho(t_0)$.

Note from here on it shall be assumed—without loss of generality—that $t_0 = 0$. In turn, $U(t, t_0)$ will have its notation replaced by $U(t)$.

Quantum measurements

While the time evolution of a closed system happens unitarily, to have a complete theory of quantum processes Eq. (2.1) has to be supplemented with a mathematical framework that describes instances when the system state is affected by measurement [14]. Under the collapse postulate, quantum measurements fundamentally account for a non-unitary type of process, since $\rho(t)$ is restricted to be observed in only one possible eigenstate of the measured observable.

Measurements themselves are described by a set of operators $\{M_m\}$, where the m index associates each operator (formed in $\mathcal{H}$) to a unique measurement outcome. For a pure state $|\psi\rangle$, a result m is recorded by an external observer with probability

$$p(m) = \langle\psi|M_m^\dagger M_m|\psi\rangle, \tag{2.17}$$

with the corresponding state after the measurement being given by

$$|\psi'_m\rangle = \frac{M_m\,|\psi\rangle}{\sqrt{\langle\psi|M_m^\dagger M_m|\psi\rangle}}. \tag{2.18}$$

The denominator is included to re-normalise $|\psi'\rangle$, so $\langle\psi'|\psi'\rangle = 1$. Note too that the operators satisfy the completeness relation

$$\begin{aligned} &\sum_m M_m^\dagger M_m = 1, \\ &\longrightarrow \sum_m \langle\psi|M_m^\dagger M_m|\psi\rangle = \sum_m p(m) = 1, \end{aligned} \tag{2.19}$$

as clearly probabilities must sum to unity. This can also be generalised to cases when measurements are performed on mixed states: again, the probability the result m is realised from the density matrix ρ is

$$p(m) = \mathrm{tr}\left[M_m^\dagger M_m \rho\right]. \tag{2.20}$$

Out of the full ensemble, if the initial state is $|\psi_j\rangle$, the corresponding state after measurement will be $|\psi_j^m\rangle = M_m\,|\psi_j\rangle\,/\sqrt{p(m|j)}$, having in the future sense been

obtained with a conditional probability $p(m|j) = \langle\psi_j|M_m^\dagger M_m|\psi_j\rangle$. Therefore, in summing all possible results arising from a measurement on (2.9) and using $p(j|m) = p(m|j)p_j/p(m)$ [61], the final density matrix reads

$$\rho_m = \sum_j p(j|m)\frac{M_m\left|\psi_j\right\rangle\left\langle\psi_j\right|M_m^\dagger}{p(m|j)} = \sum_j \frac{p_j M_m\left|\psi_j\right\rangle\left\langle\psi_j\right|M_m^\dagger}{\mathrm{tr}\left[M_m^\dagger M_m\rho\right]} = \frac{M_m\rho M_m^\dagger}{\mathrm{tr}\left[M_m^\dagger M_m\rho\right]}, \tag{2.21}$$

which leaves only the sub-ensemble ρ_m corresponding to a particular event m, out of that previously given by ρ.

Notice up to this point we have been describing selective measurements. These characterise situations when the post-measurement state is conditioned on an known outcome (i.e. the measurement record is "looked" at). For a non-selective measurement, the sub-ensembles of the density matrix are typically remixed according to the probabilities of each of their occurrence, where

$$\rho' = \sum_m p(m)\rho_m = \sum_m M_m\rho M_m^\dagger. \tag{2.22}$$

It is also worth emphasising that specific formulations of generalised measurement exist. Relevant examples include projective measurements and positive operator valued measures, which are encountered in chapter 6. These constitute a particular realisation of the current framework.

2.1.2 Composite Hilbert spaces

Here we briefly focus our attention on composite quantum systems. The idea that Hilbert space is an aggregate of its subsystems—or equally that it can partitioned into smaller constitute parts—is of special importance to the theory of open quantum systems, since the resulting formalism makes up a key part of the master equation derivation.

A core quantum postulate is that the Hilbert space of a composite quantum system is the tensor product space of the individual Hilbert spaces associated to its (distinguishable) subsystems. To illustrate this, let us specifically consider bipartite systems. If we have two quantum systems A and B with Hilbert spaces $\mathcal{H}_A$ and $\mathcal{H}_B$, using our previous notation, the composite state space is obtained through

$$\mathcal{H} \to \mathcal{H}_{AB} = \mathcal{H}_A \otimes \mathcal{H}_B. \tag{2.23}$$

With the fixed orthonormal bases $\{|\psi_j^A\rangle\}$ and $\{|\psi_j^B\rangle\}$ for $\mathcal{H}_A$ and $\mathcal{H}_B$, respectively, a given state in $\mathcal{H}$ may be expressed as

$$|\psi\rangle_{AB} = \sum_{i,j} c_{i,j} \, |\psi_i^A\rangle \otimes |\psi_j^B\rangle \,, \tag{2.24}$$

where $|\psi_i^A\rangle \otimes |\psi_j^B\rangle$ forms as basis for $\mathcal{H}_{AB}$, and $c_{i,j}$ are complex scalar coefficients. Introducing (2.24) naturally leads to the idea of entanglement in bipartite systems, since the above admits a general form which cannot factorised as $|\psi\rangle_A \otimes |\phi\rangle_B$. Moreover, if R_A is an operator acting in $\mathcal{H}_A$ and R_B an operator in $\mathcal{H}_B$, their tensor product is defined through the relation

$$(R_A \otimes R_B)(|\psi_i^A\rangle \otimes |\psi_j^B\rangle) = (R_A \, |\psi_i^A\rangle) \otimes (R_B \, |\psi_j^B\rangle), \tag{2.25}$$

which naturally extends to (2.24). In turn any operator R acting on $\mathcal{H}_{AB}$ can be written as a linear combination of operator products

$$R = \sum_k R_k^A \otimes R_k^B. \tag{2.26}$$

Because operators of $\mathcal{H}_A$ or $\mathcal{H}_B$ can be constructed unconditionally using the formula (2.26), observables of system A take a generic form $R_A \otimes 1_B$, while those of system B are represented by $1_A \otimes R_B$. Immediately we notice operators of different subsystems commute from the property (2.25).

Reduced density operator

Suppose, in a composite space, we only have direct access to the observables of one particular subsystem—say, system A. Under such circumstances, the expectation value of $R_A \otimes I_B$ can be correctly calculated using the reduced density operator ρ_A of the A subsystem: specifically,

$$\begin{aligned} \langle R_A \otimes 1_B \rangle &= \mathrm{tr} \left[R_A \otimes 1_B \, \rho_{AB} \right] \\ &= \mathrm{tr}_A \left[R_A \rho_A \right], \end{aligned} \tag{2.27}$$

with ρ_A defined through

$$\rho_A = \mathrm{tr}_B \, \rho_{AB}, \tag{2.28}$$

and where $\mathrm{tr}_{[.]}$ denotes the partial trace over the relevant subspace. The last line of (2.27) indicates that, by tracing out the marginal state ρ_B from ρ_{AB}, we recover a

density matrix entirely equivalent to the one in (2.9): or, in other words, ρ_A provides full knowledge of given subsystem when ignoring ρ_B. A proof of this is given in Ref. [4].

2.1.3 Open quantum systems

We now build on the concepts of section 2.1 to present a rigorous description of open quantum systems. In a quantum mechanical context, an open system S (called the "reduced system", or just "the system") is defined as a particular quantum system of interest which is assumed distinguishable from its surrounding environment E. The environment is assumed to contain a very large number of degrees of freedom compared to S, and, often since we have have limited knowledge of its microscopic properties, its influence on the system is modelled phenomenologically.

From their shared proximity the system and environment couple to each other, with their combined (closed) dynamics expressed in the von Neumann equation. However, from the intrinsic difficulty of tracking all components of E, one is not usually concerned about the impact the coupling has on the environment and so we look to ignore its state in (2.14). Not only is this practical, but in most cases a complete treatment of the full system-environment evolution is near impossible anyway due to complexity issues[1]: specifically, because each degree of freedom the system couples to generates its own equation of motion, if we were to solve (2.14) directly we foresee ourselves having the monumental task of solving a large (infinite) hierarchy of coupled differential equations. It is necessary then to restrict our interest only to the open system S.

To reflect us ignoring ρ_E, the time evolution of the open system is formulated in a reduced state space $\rho_S = \mathrm{tr}_E\, \rho$, where ρ is the density matrix of the closed $S + E$ system. Note the presence of noise in the open system dynamics introduces classical uncertainty and thus precludes a pure state description, i.e. (2.2). From (2.13) and (2.28), the time evolution of the reduced density matrix of the system is dictated via

$$\rho_S(t) = \mathrm{tr}_E \left[U(t)\rho(0)U^\dagger(t) \right]. \tag{2.29}$$

[1]While this is generally true, special cases exist where it is possible to have an analytical description of the full dynamics, as we shall see in chapters 5 and 6.

By taking partial trace of the von Neumann equation we also obtain

$$\frac{d}{dt}\rho_S(t) = -i\mathrm{tr}_E\left[H(t), \rho(t)\right]. \tag{2.30}$$

The idea is to use (2.29) to evaluate the observables of interest (2.27) pertaining to the reduced system. This is achieved through solving a closed form version of (2.30).

Interaction picture

Before we pursue a derivation of the Markovian density matrix equation for $\rho_S(t)$, at this point it is worthwhile introducing the transformation which maps states to the interaction picture. The transformation has immense practical use in the current open system setting while also being applicable to closed systems [62]. For this, we consider a generic Hamiltonian of the form $H = H_0 + \hat{H}_I(t)$, where it is assumed the eigenstates of H_0 are known, or equally, the free evolution is trivial in the absence of $\hat{H}_I(t)$. By defining $U_0(t) = \exp[-iH_0t]$, along with

$$U_I(t) = U_0^\dagger(t)U(t), \tag{2.31}$$

with $U(t)$ the familiar time evolution operator (2.6), it can be shown that the time-dependence gained in the density matrix (2.9)—through evolving a closed system—is split between operators and states according to

$$R_0(t) = U_0^\dagger(t)R(t)U_0(t) \quad \text{and} \quad \rho_I(t) = U_I^\dagger(t)\rho(0)U_I(t). \tag{2.32}$$

The density matrix $\rho_I(t)$ is referred to as the interaction picture density matrix. Note that its time evolution is only generated through H_I, and, since the expectation value (2.10) is unchanged by the mapping, Eq. (2.32) tends to provides an alternative—and usually simpler—framework to analyse. The time-derivative of (2.31) shows $U_I(t)$ to follow a differential equation similar to that in (2.3),

$$\frac{d}{dt}U_I(t) = -iH_I(t)U_I(t), \tag{2.33}$$

where we have adopted the following definition for the interaction Hamiltonian in the interaction picture:

$$H_I(t) = U_0^\dagger(t)\hat{H}_I(t)U_0(t). \tag{2.34}$$

Differentiating $\rho_I(t)$ in (2.32) then results in an interaction picture version of the von Neumann equation (2.14),

$$\frac{d}{dt}\rho_I(t) = -i\left[H_I(t), \rho_I(t)\right], \tag{2.35}$$

which shall be used as our starting point for the derivation of the Markovian master equation.

2.2 Microscopic derivation of the Lindblad master equation

Returning to the joint S+E system with Hilbert space $\mathcal{H} = \mathcal{H}_S \otimes \mathcal{H}_E$, from (2.26), we can expand the total Hamiltonian governing a generic time independent interaction as

$$H = H_S \otimes 1_E + 1_S \otimes H_E + H_I, \tag{2.36}$$

where H_S and H_E are the respective bare Hamiltonians of the open system and environment. The remaining term H_I is the interaction Hamiltonian, which induces the exchange of energy between the two subsystems. From now on we shall omit the identities 1_S and 1_E, e.g. in (2.36), since these have no effect beyond ensuring correct dimensionality.

Our aim is to use the density matrix $\rho_I(t)$ in (2.35) to find a closed dynamical equation for the open system. With this in mind, Eq. (2.35) is formally integrated to obtain

$$\rho_I(t) = \rho(0) - i\int_0^t dt' \left[H_I(t'), \rho_I(t')\right], \tag{2.37}$$

which is then inserted back into the von Neumann equation to yield an integro-differential equation for $\rho_I(t)$. This is our main quantity of interest. Considering that (2.37) describes the evolution of the closed $S + E$ system, we trace over the environment —as we did in (2.30)—to solely determine how $\rho_S(t)$ evolves in time. In doing so, we get

$$\frac{d}{dt}\rho_S(t) = -i\mathrm{tr}_E\left[H_I(t), \rho_I(0)\right] - \int_0^t dt' \,\mathrm{tr}_E\Big\{\left[H_I(t), \left[H_I(t'), \rho_I(t')\right]\right]\Big\}. \tag{2.38}$$

Here we drop the I-label on $\rho_I(t)$ and assume the derivation continues exclusively within the interaction picture.

2.2.1 Born-Markov approximations

At this point two key assumptions are made regarding (2.38):

(i) *Born approximation*: firstly, we assume that the total density matrix $\rho(t)$ of the closed system factorises as

$$\rho(t) \approx \rho_S(t) \otimes \rho_E, \tag{2.39}$$

at all times. Equation (2.38) then reduces to

$$\frac{d}{dt}\rho_S(t) = -i\mathrm{tr}_E\left[H_I(t), \rho(0)\right] - \int_0^t dt' \,\mathrm{tr}_E\Big\{\left[H_I(t), \left[H_I(t'), \rho_S(t') \otimes \rho_E\right]\right]\Big\}. \tag{2.40}$$

Note that (2.39) does not exclude the possibility of interaction between the two subsystems. More precisely, it assumes any correlations established between the open system and environment negligibly affect the time-dependent behaviour of the reduced system density matrix. This most likely reflects a situation where the environment is perturbed only slightly from its initial state by coupling to the system. Therefore, (2.39) ostensibly amounts to an assumption of weak system-environment coupling: that is, the "strength" of the Hamiltonian H_I has to be sufficiently weak for (2.40) to be valid in time-dependent perturbation theory.

(ii) *Markov approximation*: we now replace (2.40) with the following:

$$\frac{d}{dt}\rho_S(t) = -i\mathrm{tr}_E\left[H_I(t), \rho(0)\right] - \int_0^t dt' \,\mathrm{tr}_E\Big\{\left[H_I(t), \left[H_I(t'), \rho_S(t) \otimes \rho_E\right]\right]\Big\}. \tag{2.41}$$

where $\rho_S(t') \to \rho_S(t)$ in the integrand. Here we are prohibiting the evolution of $\rho_S(t)$ to depend only on its current state, rather than past states $\rho_S(t')$. This is justified provided that the reduced system evolves slowly over times during which the bath responds to the coupling. If we define τ_R as the relaxation time of the open system, and τ_B a typical variation time for the averaged terms inside the integral of (2.41), we are assuming

$$\tau_R \gg \tau_B, \tag{2.42}$$

For quantum optical systems—being our primary interest of the thesis—the timescales in question relate to the relevant frequency scales of the problem: for example, with a prototypical two-level system, the inverse of τ_R characterises its effective coupling strength to the bath, while the inverse of τ_B is provided by the optical transition frequency [63]. Given (2.42) holds, we can also push the upper limit of

integration to infinity since the integral terms evolving on the timescale τ_B will fall off quickly at long times. With a change of variable $t' \to t - t'$, Eq. (2.41) becomes

$$\frac{d}{dt}\rho_S(t) = -i\mathrm{tr}_E\left[H_I(t), \rho(0)\right] - \int_0^\infty dt'\, \mathrm{tr}_E\Big\{\left[H_I(t), \left[H_I(t-t'), \rho_S(t)\otimes\rho_E\right]\right]\Big\}. \tag{2.43}$$

When used together with (2.39), the picture we have under the Markov approximation is that the environment tends to relax quickly back to its original equilibrium state. This suggests the present bath dynamics cannot modify the future time evolution of the open system. With both approximations in place we then expect excitations to propagate away from the system (but not back), so as to induce wholly irreversible decay.

We finalise the previous steps by also assuming that

$$\mathrm{tr}_E\left[H_I(t), \rho(0)\right] = 0. \tag{2.44}$$

which is used to remove dependence of (2.43) on the initial conditions and thus guarantees a state independent master equation. It is emphasised (2.44) can always be fulfilled by appropriate renormalisation of the system Hamiltonian H_S (c.f. Ref. [64]). This leaves us to now systematically evaluate the correlation functions of

$$\frac{d}{dt}\rho_S(t) = -\int_0^\infty dt'\, \mathrm{tr}_E\Big\{\left[H_I(t), \left[H_I(t-t'), \rho_S(t)\otimes\rho_E\right]\right]\Big\}. \tag{2.45}$$

2.2.2 Decomposition of the interaction Hamiltonian

In what is to come, it will prove useful for us to write the interaction Hamiltonian H_I in terms of the eigenoperators of the open system Hamiltonian H_S, since, within the interaction picture, these will have simple exponential time-dependence in (2.43). The interaction Hamiltonian admits a general form

$$H_I = \sum_\alpha A_\alpha \otimes B_\alpha, \tag{2.46}$$

where A_α and B_α are operators of the system and environment, respectively. Note this form is non-unique and as such we additionally impose that $A_\alpha = A_\alpha^\dagger$ and $B_\alpha = B_\alpha^\dagger$. With ε denoting the eigenvalues of H_S, the decomposition we seek is obtained by projecting A_α onto the discrete eigenspace belonging to each ε:

$$A_\alpha(\omega) = \sum_{\varepsilon'-\varepsilon=\omega} |\varepsilon\rangle\langle\varepsilon| A_\alpha |\varepsilon'\rangle\langle\varepsilon'|, \tag{2.47}$$

where $|\varepsilon\rangle$ and $|\varepsilon'\rangle$ are the eigenstates of the same system Hamiltonian. The sum in this expression passes over all eigenvalues with a fixed difference given by ω. A desirable feature of (2.47) is that the operators satisfy

$$\begin{cases} \mathcal{L}_S A_\alpha(\omega) = i\left[H_S, A_\alpha(\omega)\right] = -i\omega A_\alpha(\omega), & (2.48) \\ \mathcal{L}_S A_\alpha^\dagger(\omega) = i\left[H_S, A_\alpha(\omega)\right] = i\omega A_\alpha^\dagger(\omega). & (2.49) \end{cases}$$

Notice $A_\alpha(\omega)$ is an eigenoperator of $\mathcal{L}_S = i[H_S, \cdot]$ with eigenvalue $-i\omega$, while $A_\alpha^\dagger(\omega)$ has eigenvalue $i\omega$ from the relation $A_\alpha(-\omega) = A_\alpha^\dagger(\omega)$. As we've predicted, mapping (2.47) to interaction picture shows

$$\begin{cases} e^{iH_S t} A_\alpha(\omega) e^{-iH_S t} = e^{-i\omega t} A_\alpha(\omega), & (2.50) \\ e^{iH_S t} A_\alpha^\dagger(\omega) e^{-iH_S t} = e^{i\omega t} A_\alpha^\dagger(\omega), & (2.51) \end{cases}$$

meaning that, together with the completeness relation $\sum_\omega A_\alpha(\omega) = A_\alpha$, the interaction Hamiltonian H_I (2.46) in the interaction picture [see (2.34)] can be written as

$$H_I(t) = \sum_{\alpha,\omega} e^{-i\omega t} A_\alpha(\omega) \otimes B_\alpha(t) = \sum_{\alpha,\omega} e^{i\omega t} A_\alpha^\dagger(\omega) \otimes B_\alpha^\dagger(t). \tag{2.52}$$

Here we have also defined the interaction picture operators of the environment,

$$B_\alpha(t) = e^{iH_E t} B_\alpha e^{-iH_E t}. \tag{2.53}$$

From our previous assumption (2.44), we find it necessary that

$$\langle B_\alpha(t) \rangle = \mathrm{tr}_E\left[B_\alpha(t)\rho_E\right] = 0, \tag{2.54}$$

which simply means the environment operators have to yield a zero expectation value.

By substituting (2.52) into the dynamical equation we had for the reduced density operator of the system (2.45), we obtain

$$\frac{d}{dt}\rho_S(t) = \sum_{\omega,\omega'} \sum_{\alpha,\alpha'} e^{i(\omega'-\omega)t} \Gamma_{\alpha,\alpha'}(\omega) \left[A_{\alpha'}(\omega)\rho_S(t) A_\alpha^\dagger(\omega') - A_\alpha^\dagger(\omega') A_{\alpha'}(\omega)\rho_S(t)\right] + \text{h.c.} \tag{2.55}$$

where

$$\Gamma_{\alpha,\alpha'}(\omega) = \int_0^\infty dt'\, e^{i\omega t'} \left\langle B_\alpha^\dagger(t) B_{\alpha'}(t-t') \right\rangle, \tag{2.56}$$

are the one sided Fourier transforms of the following reservoir correlation functions:

$$\left\langle B_\alpha^\dagger(t)B_{\alpha'}(t-t')\right\rangle = \mathrm{tr}_E\left[B_\alpha^\dagger(t)B_{\alpha'}(t-t')\rho_E\right]. \tag{2.57}$$

If we suppose the environment state ρ_E is stationary with respect to its own (self) Hamiltonian, i.e. $[H_E, \rho_E] = 0$, then using the cyclic property of the trace operation and (2.53) we can recast the above into a time homogenous form,

$$\begin{aligned}\mathrm{tr}_E\left[B_\alpha^\dagger(t)B_{\alpha'}(t-t')\rho_E\right] &= \mathrm{tr}_E\left[e^{iH_Et}B_\alpha^\dagger e^{-iH_Et}e^{iH_E(t-t')}B_\alpha e^{-iH_E(t-t')}\rho_E\right] \\ &= \mathrm{tr}_E\left[e^{iH_Et'}B_\alpha^\dagger e^{-iH_Et'}B_\alpha\rho_E\right] \\ &= \left\langle B_\alpha^\dagger(t')B_{\alpha'}(0)\right\rangle. \end{aligned} \tag{2.58}$$

Consequently, the function $\Gamma_{\alpha,\alpha'}(\omega)$ in (2.56) is time independent since the correlation functions only depend on the time difference between the operators $B_\alpha(t)$.

A precondition we originally attached to the use of the Markov approximation was that the terms in (2.55) do not "blow up" over a long time interval, partly to ensure the open system dynamics is irreversible and/or for any initial excitations to eventually decay from the system. In retrospect, extending the limit of integration to infinity is then justified if the characteristic time τ_B over which the correlation functions decay is fast compared to τ_R: or, equally, that there are no prolonged coherence effects within the bath. Supposing the environment comprises of a set of harmonic oscillators with a discrete frequency spectrum, it turns out correlation functions of the type (2.57) are quasi-periodic functions of t'—an artefact of the quantum recurrence theorem [65]. Therefore, the reservoir correlations functions generally inscribe coherent effects into the dynamics. To negate this, we require the spectrum to form a continuum of frequencies, which can be provided if the limit on the number of oscillators in the environment is taken to infinity. Under such circumstances we then have an infinitely long recurrence time so as to make the decay process irreversible. This case aside, if the environment is assumed to have infinitely many degrees of freedom, we shall refer to it as a *reservoir* for the remainder of the thesis.

2.2.3 Secular approximation

Currently we are in a position to make an additional step in the derivation of the Markovian master equation by way of the secular approximation. To proceed, let τ_S

denote a typical time scale by which the internal dynamics of the open system occurs. This timescale is typically quantified by $1/|\omega-\omega'|$ for $\omega \neq \omega'$, i.e. the reciprocal of the difference in the eigenoperator frequencies (2.48) and (2.49). Given the relaxation of the system happens much more slowly than its free time evolution set by H_S—that is, $\tau_S \ll \tau_R$—then the terms which stem from the $\omega \neq \omega'$ contributions to Eq. (2.55) oscillate rapidly and average to zero over times $t \approx \tau_R$. Ideally, removing these terms will incur no further changes to the dynamics of the open system. This leaves us with

$$\frac{d}{dt}\rho_S(t) = \sum_{\omega}\sum_{\alpha,\alpha'} \Gamma_{\alpha,\alpha'}(\omega)\left[A_{\alpha'}(\omega)\rho_S(t)A_{\alpha}^{\dagger}(\omega) - A_{\alpha}^{\dagger}(\omega)A_{\alpha'}(\omega)\rho_S(t)\right] + \text{h.c.} \tag{2.59}$$

For convenience, the Fourier transform of the reservoir correlation functions (2.56) can now be written into its real and imaginary parts:

$$\Gamma_{\alpha,\alpha'}(\omega) = \frac{1}{2}\gamma_{\alpha,\alpha'}(\omega) + iS_{\alpha,\alpha'}(\omega). \tag{2.60}$$

Standard matrix manipulation then reveals

$$S_{\alpha,\alpha'}(\omega) = \frac{1}{2i}\left[\Gamma_{\alpha,\alpha'}(\omega) - \Gamma_{\alpha',\alpha}^{*}(\omega)\right], \tag{2.61}$$

while

$$\gamma_{\alpha,\alpha'}(\omega) = \Gamma_{\alpha,\alpha'}(\omega) + \Gamma_{\alpha',\alpha}^{*}(\omega). \tag{2.62}$$

Notice the positioning of the indices α and α' in the above. The definitions of (2.61) and (2.62) suggest $S_{\alpha,\alpha'}(\omega)$ is hermitian and (2.62) is a positive matrix. We can then employ (2.58) to show that

$$\gamma_{\alpha,\alpha'}(\omega) = \int_{-\infty}^{\infty} dt'\, e^{i\omega t'}\left\langle B_{\alpha}^{\dagger}(t')B_{\alpha'}(0)\right\rangle, \tag{2.63}$$

and

$$S_{\alpha,\alpha'}(\omega) = \frac{1}{2i}\left[\int_{0}^{\infty} dt'\, e^{i\omega t'}\left\langle B_{\alpha}^{\dagger}(t')B_{\alpha'}(0)\right\rangle - \int_{0}^{\infty} dt'\, e^{-i\omega t'}\left\langle B_{\alpha}^{\dagger}(-t')B_{\alpha'}(0)\right\rangle\right], \tag{2.64}$$

where we've used

$$\begin{aligned}\Gamma_{\alpha',\alpha}^{*}(\omega) &= \int_{0}^{\infty} dt'\, e^{-i\omega t'}\left(\text{tr}_E\left[B_{\alpha'}^{\dagger}(t')B_{\alpha}(0)\right]\right)^{*} \\ &= \int_{0}^{\infty} dt'\, e^{-i\omega t'}\text{tr}_E\left[B_{\alpha}^{\dagger}(0)B_{\alpha'}(t')\right] \\ &= \int_{0}^{\infty} dt'\, e^{-i\omega t'}\left\langle B_{\alpha}^{\dagger}(-t')B_{\alpha'}(0)\right\rangle.\end{aligned} \tag{2.65}$$

Bear in mind that the last line uses (2.53) along with the cyclic property of the trace. Setting $t' \to -t'$ and switching the integration limits $(\infty, 0) \to (0, -\infty)$ also gets (2.63) from (2.62).

By substituting Eq. (2.60) into the current interaction picture master equation (2.59), we obtain the final result

$$\frac{d}{dt}\rho_S(t) = -i\left[H_{LS}, \rho_S(t)\right] + \sum_{\omega}\sum_{\alpha,\alpha'}\gamma_{\alpha,\alpha'}(\omega)\left[A_{\alpha'}(\omega)\rho_S(t)A_{\alpha}^{\dagger}(\omega) - \frac{1}{2}\left\{A_{\alpha}^{\dagger}(\omega)A_{\alpha'}(\omega), \rho_S(t)\right\}\right], \tag{2.66}$$

with $\{\cdot,\cdot\}$ indicating the anti-commutator, and H_{LS} defining the so-called Lamb shift Hamiltonian,

$$H_{LS} = \sum_{\omega}\sum_{\alpha,\alpha'} S_{\alpha,\alpha'}(\omega)A_{\alpha}^{\dagger}(\omega)A_{\alpha'}(\omega). \tag{2.67}$$

From (2.48) and (2.49), this term can quite easily been shown to commute with the unperturbed system Hamiltonian, $[H_S, H_{LS}] = 0$. The "Lamb shift" refers to the fact that H_{LS} acts to shift the energy levels of the system relative to those originally expressed in H_S as a direct result of the system-environment coupling.

In the interest of examining the Markovian properties (2.66), we note the above can be mapped back from the interaction picture: using (2.13), (2.31) and (2.32), while reintroducing the I-label to denote terms defined within the interaction picture, we have $\rho_S(t) = \exp[-iH_S t]\rho_S^I(t)\exp[iH_S t]$. Differentiating both sides of this gives

$$\frac{d}{dt}\rho_S(t) = -i\left[H_S, \rho_S(t)\right] + e^{-iH_S t}\left(\frac{d}{dt}\rho_S^I(t)\right)e^{iH_S t}. \tag{2.68}$$

As we shall see, the master equation pertaining to $\rho_S(t)$ can be identified with a particularly special *Lindblad form*. We now go on to sketch the formal mathematics underlying (2.66) which connects this form to that of a generic quantum Markov process.

2.3 Quantum dynamical maps and dynamical semigroups

Consider an initially uncorrelated product state $\rho(0) = \rho_S(0) \otimes \rho_E$ of the system and environment. After some time $t > 0$, the reduced density operator $\rho_S(t)$ from (2.29) reads

$$\rho_S(t) = \mathrm{tr}_E \left[U(t)(\rho_S(0) \otimes \rho_E)U^\dagger(t) \right]. \tag{2.69}$$

In general we can introduce a superoperator $\Phi(t,0)$ acting in the state space $S(\mathcal{H}_S)$ of the reduced system density matrices. Mathematically, it is defined as a linear map which maps $S(\mathcal{H}_S)$ to itself—that is,

$$\Phi(t,0) \; : \; S(\mathcal{H}_S) \longrightarrow S(\mathcal{H}_S). \tag{2.70}$$

If the state ρ_E of the environment remains fixed, then the transformation of $\rho_S(0)$ to $\rho_S(t)$ (2.69) can be characterised by the linear map $\Phi(t,0)$:

$$\rho_S(0) \mapsto \rho_S(t) = \Phi(t,0)\rho_S(0). \tag{2.71}$$

This is the quantum dynamical map evolving the open system state to a time t [66]. A requirement of (2.71) is that not only are the maps $\Phi(t,0)$ positive (i.e. they map positive operators to positive operators), but also completely positive [67]. Formally, a linear map (2.70) is completely positive if an only if it has a Kraus representation [68]: that is, for an operator A,

$$\Phi(t,0)A = \sum_j E_j(t) A \, E_j^\dagger(t), \tag{2.72}$$

where the dynamical map is trace preserving provided $\sum_j E_j^\dagger(t)E_j(t) = 1_S$. Note all physically valid processes must admit a representation provided by the above—see, for example, the operator-sum representation in Ref. [14]. According to (2.72), the form of $\Phi(t,0)$ also coincides with that of an operation describing a generalised quantum measurement (2.22). Intuitively this reflects a stochastic change in the operator $\rho_S(t)$ as it evolves through a noisy quantum channel.

An important and special example of a completely positive map is one fulfilling the semigroup property,

$$\Phi(t_1,0)\Phi(t_2,0) = \Phi(t_1+t_2,0), \quad \forall t_1, t_2 \geq 0. \tag{2.73}$$

The family of dynamical maps $\{\Phi(t,0)|t \geq 0\}$ describing the process in (2.71), together with the identity map $\Phi(0,0) = 1$, is referred to as a quantum dynamical semigroup [1]. Since under general mathematical conditions the semigroup can be written in an exponential form $\Phi(t,0) = \exp[\mathcal{L}t]$, having $\mathcal{L}$ as the infinitesimal generator of the semigroup, the quantum master equation associated with (2.73) is

$$\frac{d}{dt}\rho_S(t) = \mathcal{L}\rho_S(t), \tag{2.74}$$

which is identified as being intrinsically Markovian. Notice $\mathcal{L}$ is a super-operator and can be thought of as a generalisation of Liouvillian introduced in (2.15).

From the Gorini-Kossakowski-Sudarshan-Lindblad theorem [18, 19], it is well known that $\mathcal{L}$ is the generator of a semigroup of completely positive dynamical maps only if it admits the following generalised structure:

$$\mathcal{L}\rho_S(t) = -i\left[H_S, \rho_S(t)\right] + \sum_k \gamma_k \left[A_k \rho_S(t) A_k^\dagger - \frac{1}{2}\left\{A_k^\dagger A_k, \rho_S(t)\right\}\right]. \tag{2.75}$$

Master equations of this structure are said to be of *Lindblad form*. The Lindblad operators A_k represent the possible decay events governing the open system dynamics while γ_k are the associated decay rates. Notably, the master equation in (2.66) can be brought into the above form by diagonalising the matrices made from $\gamma_{\alpha,\alpha'}(\omega)$. As such the underlying dynamics of (2.66) is Markovian. We emphasise that it is precisely: (i) the assumption of weak coupling (2.39), and (ii) the removal of memory effects via the condition $\tau_R \gg \tau_B$ (2.42) which leads to an appropriate quantum mechanical description of a time-homogenous Markov process. Broadly speaking, the idea of (2.74) purporting to being Markovian is based on the (historical) assumption that the coefficients (2.75) are necessarily time independent to guarantee the absence of memory effects.

2.3.1 Time-local master equations

Of course, in situations where perturbation theory breaks down, e.g. when the coupling of the system to the environment is strong, we cannot expect the Lindblad equation (2.74) to give a reasonable description of the dynamics. In some cases, however, it possible to generalise (2.75) to

$$\frac{d}{dt}\rho_S(t) = \mathcal{K}(t)\rho_S(t), \tag{2.76}$$

with $\mathcal{K}(t)$ a time-dependent generator of the dynamics. Note this representation assumes the existence of the inverse map $\Phi^{-1}(t,0)$. Interestingly, there are known examples, such as the damped Jaynes-Cummings mode (see section 4.2.1), where the inverse of (2.70) cannot necessarily be obtained. Hall *et al.* have shown that any time-local master equation of the form (2.76) can expressed as [66, 69]

$$\begin{aligned}\mathcal{K}(t)\rho_S(t) =& -i\left[H_S(t),\rho_S(t)\right] \\ &+\sum_k \gamma_k(t)\left[A_k(t)\rho_S(t)A_k^\dagger(t)-\frac{1}{2}\left\{A_k^\dagger(t)A_k(t),\rho_S(t)\right\}\right].\end{aligned} \tag{2.77}$$

We notice this result naturally extends the previous Lindblad structure (2.75) to time-local generators, where the system Hamiltonian $H_S(t)$, decay operators $A_k(t)$, and each of the decay rates $\gamma_k(t)$, now have the possibility of being time-dependent. These "new" properties reflect on the inclusion of memory effects in the system dynamics, and thus on the potential of linear map—defined by

$$\Phi(t,0) = T_{\leftarrow}\exp\left[\int_0^t dt'\,\mathcal{K}(t')\right], \quad \forall t \geq 0, \tag{2.78}$$

to describe a non-Markovian process. However, it should be stated that the operator $\mathcal{K}(t)$ can be a generator of a Markovian dynamics if and only if it has the form (2.77) and $\gamma_j(t) \geq 0\,\forall j,t$ [70, 71]. We shall encounter a particular microscopic realisation of a time-local master equation during chapter 6.

Aside from the mathematical description given above, there exists other general means to study the dynamics of open quantum systems—a notable example being the Nakajima-Zwanzig projection operator technique [72, 73]. The importance of this technique stems from the fact that it provides an exact microscopic master equation for the reduced system density operator $\rho_S(t)$ of integro-differential form. Since this equation explicitly takes into account the influence of the past-time dynamics of the system on its current state, it is then suggested that the formulation of non-Markovian processes must rely on deriving a differential equation that is non-time local. However, contrary to this belief, there exists a way to specifically cast the exact master equation into the form (2.76), known as the time-convolutionless projection operator technique [74, 75].

While both approaches play a ubiquitous role in formulating a general theory of open quantum systems, our main line of investigation instead concerns embedding

methods, which tend to produce a master equation of Lindblad form as a result of redrawing the boundaries of the reduced system to include some "cut" of the environment. This system will be commonly referred to as the *enlarged system*. Despite the dynamics of the enlarged system always being Markovian, the dynamics of the original reduced system typically exhibits non-Lindbladian evolution as a result of its modification, and thus the form (2.75) is still appropriate.

Chapter 3

The Heisenberg formalism

It was shown in section 2.3 that the Gorini-Kossakowski-Sudarshan-Lindblad form (2.75) of the master equation necessitates a Markovian process. But to arrive at such an equation, some restrictive assumptions had to be imposed. The Born-Markov approximation, in particular, underpins much of the validity of the master equation by assuming weak system-environment coupling. To go beyond a Markovian description therefore requires us to depart from the methods of section 2.2.

To first motivate this, here we focus our attention on treating the theory of open quantum systems within the Heisenberg picture. We approach the problem by deriving the two key ingredients of the formalism: firstly, the so-called Heisenberg-Langevin equation, and secondly, the quantum Langevin equations. The Heisenberg-Langevin equation exists in parallel to the master equation in that it describes the same fundamental behaviours (e.g. dissipation, decoherence) but in terms of an observable $A(t)$ rather than the density matrix $\rho_S(t)$. The connection between the dynamics in the state and operator based pictures is rudimentary. By taking the time-derivative of the time-dependent form of (2.10), it is readily shown that

$$\frac{d}{dt}\langle A\rangle_t = \mathrm{tr}\left[\frac{d}{dt}A(t)\rho\right] = \mathrm{tr}_S\left[A\frac{d}{dt}\rho_S(t)\right]. \tag{3.1}$$

In the spirit of the pseudomode method [41], it will turn out to be advantageous to formulate the dynamics using the Heisenberg-Langevin equation, and then relate this to the Schrödinger picture using the above.

In the first part of the chapter we study the Heisenberg-Langevin equation under a generic Hamiltonian. We shall see a direct mapping via Eq. (3.1) is only possible if the time-derivative of $A(t)$ can be written solely in terms of a time-local set of

dynamical equations for the open system operators—namely, the quantum Langevin equations. Our intention is to demonstrate the feasibility of this approach to actually obtaining a valid master equation. The final parts of the chapter are then devoted to the derivation of the Markovian master equation as an initial proof of concept. The techniques developed here will eventually be put to original use during chapter 4, where applications to systems exhibiting strong coupling effects are considered.

The current chapter consists of three sections. The first section serves as an introduction to the generic model, which will later be tailored towards specific cases of interest. In section 3.1 we construct the exact Heisenberg-Langevin equations and quantum Langevin equations. In section 3.2 we focus on their application to the weak coupling limit, and subsequently provide a step-by-step derivation of the quantum optical master equation within the Heisenberg formalism. We summarise the chapter in section 3.4. It is pointed out that the techniques we employ in most parts are well known, and in particular are outlined in Refs. [2, 5, 76].

3.1 Outline

Since the Schrödinger and Heisenberg pictures are physically equivalent, the time evolution of any observable within the Heisenberg picture is generated through the global Hamiltonian of the open system, S, and the environment, E. As before, the Hamiltonian has the defining form

$$H = H_S + H_E + H_I, \tag{3.2}$$

It is usually considered that the system and environment are brought into contact at a time $t = 0$ when the Schrödinger and Heisenberg pictures coincide. To formally reflect this in Eq. (3.2), the interaction Hamiltonian can be amended to an explicitly time-dependent form $H_I(t) = \theta(t)H_I$, where the Heaviside distribution $\theta(t)$ is defined through

$$\theta(t) = \begin{cases} 1 & \text{if } t \geq 0 \\ 0 & \text{otherwise.} \end{cases} \tag{3.3}$$

This mathematically ensures that any interaction occurs over the time interval $[0, t]$. Although not explicitly written, the presence of $\theta(t)$ in the interaction H_I will be

implied based on the justification that the open system has been uncoupled from the environment since the distant past ($-\infty < t < 0$). On a similar level, we will assume initially uncorrelated subsystems in that the global state $\rho = \rho(0)$ is given by the direct product

$$\rho = \rho_S \otimes \rho_E, \tag{3.4}$$

which applies at all times the Heisenberg picture.

At this point we do not wish to specify the exact form of H_S. The environment, in the general case, is elected to comprise of a large collection of harmonic oscillators with frequencies ω_λ:

$$H_E = \sum_\lambda \omega_\lambda a_\lambda^\dagger a_\lambda. \tag{3.5}$$

The canonically conjugate operators a_λ and $a_\lambda^\dagger$ are the annihilation and creation operators of the λ mode of E, and satisfy the standard bosonic commutation relations

$$[a_\lambda, a_{\lambda'}^\dagger] = \delta_{\lambda,\lambda'}, \tag{3.6}$$

with $[a_\lambda, a_{\lambda'}] = 0$. On certain occasions we will endow the environment with an inner structure, such that H_E is made up from an ensemble of sub-environments with self energies H_{E_k}, where $k = 1, 2, \ldots \#E$ indicates each sub-environment E_k. In this case the Hamiltonian of the environment is written as

$$H_E = \sum_{k,\lambda} \omega_\lambda a_{k,\lambda}^\dagger a_{k,\lambda}, \tag{3.7}$$

where $H_E = \sum_k H_{E_k}$. Obviously, the above reduces to Eq. (3.5) for $k = 1$. The independency of the sub-environments ensures the bosonic operators $a_{k,\lambda}$ and $a_{k,\lambda}^\dagger$ still satisfy the canonical relations

$$[a_{k,\lambda}, a_{k,\lambda}^\dagger] = \delta_{k,k'}\delta_{\lambda,\lambda'}, \tag{3.8}$$

with all other commutators vanishing.

We are now in the position to write down the Hamiltonian of the system and environment including an explicit interaction. By combining equations (3.2) and (3.7), we have

$$H = H_S + \sum_{k,\lambda} \omega_\lambda a_{k,\lambda}^\dagger a_{k,\lambda} + \sum_{k,\lambda} \left(L + L^\dagger\right)\left(g_{k,\lambda}^* a_{k,\lambda} + g_{k,\lambda} a_{k,\lambda}^\dagger\right). \tag{3.9}$$

It is noted that the Hamiltonian coincides with generic one given by (2.46). The parameter $g_{k,\lambda} = |g_{k,\lambda}|e^{-i\varphi_{k,\lambda}}$ represents the coupling strength between the system and λ-mode of the k sub-environment, and, without loss of generality, are taken always to be real valued, i.e. $\varphi_{k,\lambda} = 0$. The interaction Hamiltonian is more conveniently expressed as

$$H_I = \sum_{k,\lambda} \left(L + L^\dagger\right) \left(B_k + B_k^\dagger\right), \tag{3.10}$$

with $B_k = \sum_\lambda g_{k,\lambda} a_{k,\lambda}$. In the following, the operators L and $L^\dagger$ are assumed to satisfy the eigenoperator relation

$$\begin{cases} [H_S, L] = -\varepsilon L, & (3.11) \\ [H_S, L^\dagger] = \varepsilon L^\dagger, & (3.12) \end{cases}$$

meaning that L lowers the energy of the open system by an amount $-\varepsilon$, while $L^\dagger$ raises the energy by an amount $+\varepsilon$. This is observed from the fact that H_S has the spectral decomposition

$$H_S = \sum_j \varepsilon_j \left|\varepsilon_j\right\rangle \left\langle\varepsilon_j\right|, \tag{3.13}$$

where $|\varepsilon_j\rangle$ are the energy eigenstates of the open system Hamiltonian. By virtue of the above eigenoperator relations, it is straightforward to check using (2.48) and (2.49) that $L\,|\varepsilon_j\rangle$ and $L^\dagger\,|\varepsilon_j\rangle$ are again eigenstates of H_S with the corresponding eigenvalues $\varepsilon_j - \varepsilon$ and $\varepsilon_j + \varepsilon$, respectively [1].

3.1.1 Rotating frame

Let us write the Hamiltonian (3.2) as

$$H = H_0 + H_I, \tag{3.14}$$

where clearly $H_0 = H_S + H_E$. Using the density matrix ρ of the entire system, the expectation value of an open system observable A can be manipulated as follows:

$$\begin{aligned} \langle A\rangle_t &= \mathrm{tr}\left[A\rho(t)\right] = \mathrm{tr}\left[A(t)\rho\right] \\ &= \mathrm{tr}\left[U_I^\dagger(t)\left(U_0^\dagger(t)\,A\,U_0(t)\right)U_I(t)\,\rho\right] \\ &= \mathrm{tr}\left[U_I^\dagger(t)A_0(t)U_I(t)\,\rho\right]. \end{aligned} \tag{3.15}$$

The first line of (3.15) simply expresses the physical equivalence of the Schrödinger and Heisenberg pictures. In the proceeding steps, we have made use of the unitary time-evolving operators $U_I(t)$ and $U_0(t) = \exp[-iH_0t]$ from Eq. (2.31), where

$$A_0(t) = U_0^\dagger(t)A(0)U_0(t), \tag{3.16}$$

and

$$A(t) = U^\dagger(t)A(0)U(t) = U_I^\dagger(t)\left[U_0^\dagger(t)A(0)U_0(t)\right]U_I(t). \tag{3.17}$$

In the interaction picture, $A_0(t)$ corresponds to a term whose time-dependence is gained from the transformation to a frame of reference rotating[1] with respect to the bare interaction, while the time evolution of ρ is generated via $\rho_I(t) = U_I(t)\rho(0)U_I^\dagger(t)$ from an initial state $\rho_I(0) = \rho(0)$—see (2.32). Using (3.17), the Heisenberg equation of motion $d_tA(t) = -i[A(t), H]$ can alternatively be written as

$$\frac{d}{dt}A(t) = -i[A(t), H_H(t)] + \frac{\partial A_{\circlearrowleft}(t)}{\partial t}, \tag{3.18}$$

where

$$\frac{\partial A_{\circlearrowleft}(t)}{\partial t} = U_I^\dagger(t)\frac{\partial A_0(t)}{\partial t}U_I(t). \tag{3.19}$$

In addition, we have defined the following quantity:

$$H_H(t) = U_I^\dagger(t)H_I(t)U_I(t), \tag{3.20}$$

with $H_I(t)$ taken from Eq. (2.34). The operator $H_H(t)$ is then the interaction Hamiltonian from (3.2) transformed to the Heisenberg picture. It is stressed that the rotating frame equation of motion is equivalent to the standard Heisenberg equation: all we have done is single out a term on the righthand side of Eq. (3.18) whose time-dependence has been provided by $U_0^\dagger(t)A(0)U_0(t)$. In turn, by making the identification

$$\frac{d}{dt}\hat{A}(t) = \frac{d}{dt}A(t) - \frac{\partial A_{\circlearrowleft}(t)}{\partial t}, \tag{3.21}$$

the Heisenberg equation is subsequently written in the compact form

$$\frac{d}{dt}\hat{A}(t) = -i\left[A(t), H_H(t)\right]. \tag{3.22}$$

[1]Eq. (3.16) is said to move the full system to a "rotating frame" in analogy to classical mechanics—a stationary position vector looks as though it is moving in a rotating reference frame.

Here, the dynamics of the observable is evaluated within a rotating frame picture, looking markedly similar to that of the standard interaction picture—that is, where the part (3.19) associated with the free evolution of the system is removed from the equation of motion. Note that, while Eq. (3.22) is not strictly of closed form, it will not be solved directly but used instead to obtain the associated master equation [c.f. (3.1)].

For an archetypal quantum optical system the timescale on which the open system freely evolves—typically characterised by the inverse of ε [see (3.11)]—is largely separated (in magnitude) from its relaxation time, such that $A_{\circlearrowleft}(t)$ oscillates quickly. In many cases it is beneficial to remove fast-evolving term to look at the slowly evolving contribution. Indeed, we will find that this has great utility in the derivation of the microscopic (Markovian) master equation, as was similarly done via the interaction picture transformation in section 2.1.3.

To transform a given operator O—either of the open system or environment—to the rotating frame picture, we expand Eq. (3.16) using the Baker-Hausdorff theorem [62]. This states that for non-commuting operators O and H_0, the following transformation property holds:

$$e^{iH_0t}Oe^{-iH_0t} = O + it\,[H_0, O] + \frac{(it)^2}{2!}\,[H_0, [H_0, O]] + \dots\,. \tag{3.23}$$

Armed with the commutation relations from equations (3.8) and (3.11)-(3.12), the Hamiltonian within the rotating frame (interaction) picture reads

$$H_I(t) = \sum_k \left(B_k^{(+)}(t)L + L^\dagger B_k^{(-)}(t) + L^\dagger B_k^{(+)\dagger}(t) + B_k^{(-)\dagger}(t)L \right), \tag{3.24}$$

where

$$B_k^{(-)}(t) = \sum_\lambda g_{k,\lambda} a_{k,\lambda} e^{-i(\omega_\lambda - \varepsilon)t}, \tag{3.25}$$

$$B_k^{(+)}(t) = \sum_\lambda g_{k,\lambda} a_{k,\lambda} e^{-i(\omega_\lambda + \varepsilon)t}, \tag{3.26}$$

have been defined from using that the operators of the open system transform to the new picture according to $e^{iH_St}Le^{-iH_St} = Le^{-i\varepsilon t}$ and $e^{iH_St}L^\dagger e^{-iH_St} = L^\dagger e^{i\varepsilon t}$. Notice that the time-dependence of the operators is explicit, in contrast to the Heisenberg picture evolution (3.22).

3.1.2 Quantum optical Hamiltonian

From now on we shall focus on the application of our methods to quantum optical systems. This allows to simplify the Hamiltonian (3.24) by use of the rotating wave approximation. For systems we are interested in, the counter-rotating terms oscillating at frequencies $\pm(\omega_\lambda + \varepsilon)$, such as $B_k^{(+)}(t)$, are assumed to evolve quickly in comparison to terms with exponents $\pm(\omega_\lambda - \varepsilon)$. Over any relevant timescale, e.g. a typical relaxation period of the system, the fast oscillating terms make a negligible contribution to the interaction, and therefore only the slowly evolving terms with exponents $\pm(\omega_\lambda - \varepsilon)$ are needed to be kept. In this ideal limit, the Hamiltonian reads

$$H_I(t) = \sum_k \left(L^\dagger B_k(t) + B_k^\dagger(t) L \right), \tag{3.27}$$

where $B_k^{(-)}(t)$ has been replaced by $B_k(t)$, and $B_k^{(+)}(t) \to 0$. Equation (3.27) now acts as the generator of the dynamics in (3.22). Accordingly, it will be used to compute the operator equations of motion during the next section.

Because we interested entirely in the open system dynamics, it is sufficient to rely on a course grained representation of the environment by which we smooth over microscopic detail to solely account for the collective influence of the modes. With a very large number of bosons, the mode spacing on the frequency line ω_λ should be very dense, meaning the that following replacement can be made:

$$\sum_\lambda \longrightarrow \int_0^\infty d\omega\, \rho_\omega, \tag{3.28}$$

where

$$\rho_\omega = \mathrm{tr}\left[\delta(\omega - H_E)\right] = \sum_\lambda \delta(\omega - \omega_\lambda), \tag{3.29}$$

is the density of states of the environment, i.e. $\rho_\omega d\omega_\lambda$ is defined to give the number of modes in the interval ω_λ to $\omega_\lambda + d\omega_\lambda$. The conversion in Eq. (3.28) amounts to replacing every individual oscillator of the environment, centred on the frequency ω_λ, by a continuous band of oscillators spread across a width $d\omega_\lambda$. An outcome of the rotating wave approximation is that it allows us to extend the lower limit of integration to $-\infty$,

$$\int_0^\infty d\omega \approx \int_{-\infty}^\infty d\omega. \tag{3.30}$$

Although this is really a tentative procedure, it is entirely reasonable because the counter-rotating terms, which we previously ignored, are highly non-resonant at negative frequencies. Thus the only significant contribution to the integral will be in the vicinity of $\omega \approx \varepsilon$ ($\varepsilon \gg 0$), meaning that no unphysical effects are added to the Hamiltonian by extending the frequency range to $(-\infty, \infty)$. The usefulness of (3.30) comes about in the weak coupling limit, where the open system dynamics can be show to follow that of a quantum Markov process [2].

While, on the face of it, the rotating wave approximation seems equivalent the secular approximation made in section 2.2.3, these are distinguished through the fact that each can lead to different forms of the master equation—see Ref. [3].

3.1.3 Spectral density and memory effects

By taking the continuum limit (3.28) together with rotating wave approximation (3.30), we are lead to define the memory kernel of the environment,

$$f(t-t') = \sum_{k,k'} \left[B_k(t), B_{k'}^\dagger(t') \right] = \int_{-\infty}^{\infty} d\omega J(\omega) e^{-i(\omega-\varepsilon)(t-t')}, \tag{3.31}$$

where we have also introduced the widely recognised *spectral density* function,

$$J(\omega) = \sum_{k,\lambda} (g_{k,\lambda})^2 \delta(\omega - \omega_\lambda). \tag{3.32}$$

Given that the spectral density fully characterises the statistical properties of the environment [77], the functional form of Eq. (3.32), to a large extent, influences the dynamics of the open system. In many physical examples of quantum optical systems, the spectral density is a slowly varying function in frequency. In these cases the frequency dependence of the parameters $g_k(\omega_\lambda)$ may be neglected if the function is reasonably flat over the bandwidth of the coupling. How are these properties reflected in the memory kernel? Since Eq. (3.31) is the Fourier transform of $J(\omega)$, its inverse width gives an estimate of the correlation time of the environment, i.e. the timescale by which the memory kernel decays. The original flatness of the spectral density then provides a time-domain function that is effectively delta correlated. This is an important feature seeing as the resulting open system dynamics is characteristic of white noise process, being inherently Markovian. Hence, we will tacitly assume a one-to-one correspondence between a "flat spectral density" and a

Markovian environment.

Conversely, there are instances when the system-environment coupling depends strongly on the frequency. The previous assumptions inevitably break down, and memory effects contained within the kernel become highly relevant over the timescale by which the open system evolves. Such behaviour is characteristic of a non-Markovian environment. Clearly, the boundary between Markovian and non-Markovian open quantum system dynamics can be gauged by the amount the spectral density depends on frequency. We will refer to an environment as being *structured* when the spectral density function does generally depend on frequency to a significant effect, in the opposite sense to a flat spectral density. Most of the thesis will focus on instances of non-Markovain behaviour arising from structured environments.

Note the concept of "non-Markovianity" here does not hinge on a strict definition, and is only used to refer examples where memory effects play a clear role in the dynamics of the open system, i.e. when the approximations used to derive the perturbative master equation are no longer valid. It is, however, worthwhile keeping in mind that mathematical definitions and quantifiers of non-Markovian processes do exist based on the notion divisibility of the dynamical map (2.78): see, for example Refs. [78–80].

3.2 Exact Heisenberg picture dynamics

In this section we review the quantum dynamics arising from the Hamiltonian (3.9). The most prevalent use of Heisenberg equations of motion as a way to treat Markovian dynamics is under the input-output formalism [2, 81], which for non-Markovian systems has been extended in Ref. [82]: other uses in this category include Refs. [83, 84].

We start by formulating the Heisenberg equation of motion for $\hat{A}(t)$ (3.22) using both open system and environment operators. This is is given by

$$\frac{d}{dt}\hat{A}(t) = -i\sum_k \left(\left[A(t), L^\dagger(t)\right] B_k(t) + B_k^\dagger(t) \left[A(t), L(t)\right] \right). \tag{3.33}$$

Note it is emphasised that

$$\begin{cases} L(t) = U_I^\dagger(t) L(0) U_I(t), \\ L^\dagger(t) = U_I^\dagger(t) L^\dagger(0) U_I(t), \end{cases} \tag{3.34}$$

while $A(t)$ adopts its previous definition from Eq. (3.17). Importantly, this convention for applying time-dependence to the operators A and L ($L^\dagger$) will be adopted for the current chapter and chapter 4. The operator $B_k(t)$ reads

$$B_k(t) = \sum_\lambda g_{k,\lambda} a_{k,\lambda}(t) e^{-i(\omega_\lambda - \varepsilon)t}, \tag{3.35}$$

where time-argument on the operator now denotes a Heisenberg picture evolution with respect to the transformation in Eq. (3.20). A closed form version of (3.33) is obtained by eliminating the dependence on the environment operators, whose equations of motion is given by

$$\frac{d}{dt} a_{k,\lambda}(t) = -i g_{k,\lambda} e^{i(\omega_\lambda - \varepsilon)t} L(t). \tag{3.36}$$

Formally integrating the above simply provides

$$a_{k,\lambda}(t) = a_{k,\lambda}(0) - i g_{k,\lambda} \int_0^t dt' e^{i(\omega_\lambda - \varepsilon)t'} L(t'), \tag{3.37}$$

where the result is now substituted into (3.35) to obtain the *Heisenberg-Langevin equation*,

$$\begin{aligned} \frac{d}{dt}\hat{A}(t) = \left[A(t), L^\dagger(t)\right] \left(\xi(t) - \int_0^t dt' f(t-t') L(t')\right) \\ + \left(\xi^\dagger(t) - \int_0^t dt' f^*(t-t') L^\dagger(t')\right) \left[L(t), A(t)\right], \end{aligned} \tag{3.38}$$

with $\xi(t)$ defined as

$$\xi(t) = -i \sum_{k,\lambda} g_{k,\lambda} a_{k,\lambda}(0) e^{-i(\omega_\lambda - \varepsilon)t}. \tag{3.39}$$

It can be seen that the original equation of motion for $A(t)$ now only depends the operators of the environment at the initial time $t = 0$. Additionally, the memory kernel appears in the form

$$f(t-t') = \sum_{k,\lambda} (g_{k,\lambda})^2 e^{-i(\omega_\lambda - \varepsilon)(t-t')}. \tag{3.40}$$

In Eq. (3.38), the integration over the past times makes it apparent that the memory kernel relates the current dynamics to the delayed back-action that the system

receives from coupling to the environment modes. This suggests an equation of integro-differential must be what describes a non-Markovian process. However, as discussed in section 2.3.1, in certain situations the master equation associated with (3.38) can be expressed in an approximate or even exact form which is local in time and captures the non-Markovian response of the system [85].

It is instructive to also derive an additional set of equations for the open system in terms of the operator $L(t)$. This is done by substituting A for each of these operators in Eq. (3.38): however, it is apt to have a consistent definition of the system operators in the rotating frame on both sides of the equation. For example, take $A = L$:

$$A(t) = U_I^\dagger(t)\left[U_0^\dagger(t)L(0)U_0(t)\right]U_I(t) = L(t)e^{-i\varepsilon t}, \quad A = L. \tag{3.41}$$

Assuming a rotating frame of reference, the lefthand side of the equation for $d_t A(t)$ can be computed using (3.21),

$$\begin{aligned}\frac{d}{dt}\hat{A}(t) &= \frac{d}{dt}\left(e^{-i\varepsilon t}L(t)\right) + i\varepsilon\, e^{-i\varepsilon t}L(t) \\ &= e^{-i\varepsilon t}\frac{d}{dt}L(t).\end{aligned} \tag{3.42}$$

Plugging this into Eq. (3.38) then yields the aforementioned *quantum Langevin equation* for $L(t)$:

$$\frac{d}{dt}L(t) = \left[L(t), L^\dagger(t)\right]B(t), \tag{3.43}$$

with $B(t)$ conveniently defined from

$$B(t) = \sum_k B_k(t) = \xi(t) - \int_0^t dt' f(t-t')L(t'). \tag{3.44}$$

The Heisenberg-Langevin equation can now be expressed as

$$\frac{d}{dt}\hat{A}(t) = \left[A(t), L^\dagger(t)\right]\left(\frac{d}{dt}L(t)\right) + \left(\frac{d}{dt}L^\dagger(t)\right)\left[L(t), A(t)\right], \tag{3.45}$$

where the dependence on the time convolved terms has been implicitly removed. By writing (3.33) solely in terms of the system operators and their time derivatives, it is clear that in order for the Heisenberg-Langevin equation to hold a time-local form, then so must the quantum Langevin equations.

So far, we have made no approximations in the derivation of the Heisenberg-Langevin equation and therefore it is exact, along with the dynamical equations for the coupling operators. We shall return to (3.43) and (3.45) during chapter 4 to formulate the non-Markovian dynamics of the relevant model.

3.3 The weak-coupling limit

The procedure detailed in Refs. [86, 87] makes use of the linear property of the Langevin equations to obtain their exact solutions, which are then used to rewrite the original differential equations for $L(t)$ [and $L^\dagger(t)$] in time-local form. The precise steps do not make explicit use of spectral density, and so the equations generally admit a kernel that can lead to non-Markovian behaviour. At the moment it is enough for us to resort to the Born-Markov approximations to evaluate the memory kernel explicitly, and as a result, place (3.43) in its destined form. We will go on to use the quantum Langevin equation to reproduce the Markovian master equation for an open bosonic system.

3.3.1 The Born-Markov approximations

Here, the spectral density function is taken to vary negligibly with respect to changes in frequency, and for all purposes is flat. The quantum Langevin equations can then be amended by use of the Markov approximation. Prior to this, we first make a change of variable to $\tau = t - t'$ in Eq. (3.44), such that

$$B(t) = \xi(t) - \int_0^t d\tau f(\tau) L(t-\tau). \tag{3.46}$$

The arguments of section 3.1.3 suggest the kernel is sharply peaked at the origin $\tau = 0$, but will eventually decline at a rate much faster than any timescale over which the system evolves. If γ sets the frequency scale at which the open system decays, i.e. in (2.66), then memory effects contained within $f(\tau)$ may be neglected under the assumption

$$\frac{1}{\varepsilon} \ll t \ll \frac{1}{\gamma}, \tag{3.47}$$

given this defines the weak coupling limit of the interaction. Equation (3.47) then provides the same level of approximation we previously encountered when assuming a large separation of timescales (2.42) in time-dependent perturbation theory. Again, the environment can be assumed to evolve negligibly from its initial state. Since the component freely evolving at the frequency ε has been extracted from the system operators, the term $L(t-\tau)$ evolves on a timescale characterised solely by $1/\gamma$. From Eq. (3.47), this occurs slowly with respect to changes in the memory kernel

(dictated by τ) and so the operator essentially remains static under the integral. We can then write [3],

$$\int_0^t d\tau f(\tau) L(t-\tau) \approx L(t) \int_0^t d\tau f(\tau). \tag{3.48}$$

From the reasoning outlined above, the righthand side of the equation will vary slowly with respect to changes in τ. The region of integration can then be safely extended by taking the limit $t \to \infty$, see Eq. (2.43). This leaves us to evaluate the integral over $\exp\left[\pm i(\omega-\varepsilon)\tau\right]$ as the dominant contribution towards the memory kernel. To do so, we make use of the formula

$$\lim_{t\to\infty} \frac{1}{\pi} \int_0^t d\tau\, e^{-i(\omega-\varepsilon)\tau} = \delta(\omega-\varepsilon) + \frac{i}{\pi} \text{P.V.} \frac{1}{\varepsilon-\omega}, \tag{3.49}$$

where P.V. indicates the principal value of a function $y(x)$ across an interval $-a \leq y(x) \leq a$, using the following definition ($|b| < |a|$) [4]:

$$\text{P.V.}\, y(x) = \lim_{\delta\to 0^+} \left[\int_{-a}^{b-\delta} dx' y(x') + \int_{b+\delta}^{a} dx' y(x') \right]. \tag{3.50}$$

Now, by substituting the above into Eq. (3.48) we can read off the real and imaginary parts of the memory kernel:

$$\text{Re}\left[f(t-t')\right] = \int_{-\infty}^{\infty} d\omega J(\omega) \cos[(\omega-\varepsilon)t] = \pi J(\varepsilon), \tag{3.51}$$

$$\text{Im}\left[f(t-t')\right] = \int_{-\infty}^{\infty} d\omega J(\omega) \sin[(\omega-\varepsilon)t] = \text{P.V.} \int_{-\infty}^{\infty} d\omega \frac{J(\omega)}{\varepsilon-\omega}. \tag{3.52}$$

Based on the frequency independence of the coupling constants $g_{k,\lambda}$, it is convenient for us to make the following replacement,

$$g_{k,\lambda} \longrightarrow g_{k,\varepsilon} = \sqrt{\frac{\gamma_k \Delta\omega_\varepsilon}{2\pi}}, \tag{3.53}$$

typically known under the first Markov approximation [2, 63]). This in turn provides

$$J(\varepsilon) = \sum_k \left(g_{k,\varepsilon}\right)^2 \rho_\varepsilon = \frac{\gamma}{2\pi}, \tag{3.54}$$

having identified the collective decay rate $\gamma = \sum_k \gamma_k$. Finally, inserting the real and imaginary components of $f(t-t')$ into Eq. (3.44), we find

$$B(t) = \xi(t) + \left(-i\Delta - \frac{\gamma}{2}\right) L(t), \tag{3.55}$$

where

$$\Delta = \text{P.V.} \int_{-\infty}^{\infty} d\omega \frac{J(\omega)}{\varepsilon - \omega}. \tag{3.56}$$

The quantum Langevin equation now becomes

$$\frac{d}{dt} L(t) = \left[L(t), L^{\dagger}(t)\right] \left\{ \left(-i\Delta - \frac{\gamma}{2} \right) L(t) + \xi(t) \right\}, \tag{3.57}$$

One notices that (3.57) is local in time, which indicates the system dynamics retains no memory of its previous state. This results from direct use of the weak coupling approximations.

The physical effect of each the terms in the curly brackets is briefly considered. Firstly, the term with an imaginary coefficient (3.52) indicates a renormalisation in the energy levels of the open system by an amount Δ. The Lamb shift generally only has quantitive importance to the dynamics and can in fact be removed altogether via an additional transformation into a new rotating frame. Secondly, the real term (3.51) accounts for losses via the damping effect of the environment. The full dissipative effect of the environment is connected to the individual rates

$$\gamma_k = 2\pi (g_{k,\varepsilon})^2 \rho_{\varepsilon}, \tag{3.58}$$

which are consistent with the emission rates obtained from applying Fermi's Golden rule. The last term $\xi(t)$, and its adjoint, act as a random noise that provide instantaneous "kicks" to the system during the course of its evolution.

3.3.2 Markovian master equation

Before substituting (3.57) into the Heisenberg-Langevin equation, we impose a bosonic relation on the open system,

$$[L, L^{\dagger}] = 1, \tag{3.59}$$

where the equal-time commutator is stationary, i.e. $[L(t), L^{\dagger}(t)] = 1$. It may appear that, by imposing Eq. (3.59), the Heisenberg-Langevin equation will have restricted use with (3.9). While this is certainly true, we will discover that the relation is a necessary condition to derive the quantum optical master equation and unfortunately constitutes a drawback of the current approach. From (3.57) and (3.38), we now

obtain

$$\frac{d}{dt}\hat{A}(t) = \left(-i\Delta - \frac{\gamma}{2}\right)\left[A(t), L^\dagger(t)\right] L(t) + \left(i\Delta - \frac{\gamma}{2}\right) L^\dagger(t)[L(t), A(t)] + \left[A(t), L^\dagger(t)\right]\xi(t) + \xi^\dagger(t)\left[L(t), A(t)\right]. \tag{3.60}$$

Expanding the commutators in the first line of Eq. (3.60) provides the alternative form

$$\frac{d}{dt}\hat{A}(t) = -i\Delta\left[A(t), L^\dagger(t)L(t)\right] + \gamma\left(L^\dagger(t)A(t)L(t) - \frac{1}{2}\left\{A(t), L^\dagger(t)L(t)\right\}\right) + \xi^\dagger(t)\left[L(t), A(t)\right] + \left[A(t), L^\dagger(t)\right]\xi(t), \tag{3.61}$$

where, by taking the expectation value of Eq. (3.61), it is finally left to consider

$$\frac{d}{dt}\langle\hat{A}\rangle_t = -i\Delta\Big\langle\left[A(t), L^\dagger(t)L(t)\right]\Big\rangle + \gamma\left(\left\langle L^\dagger(t)A(t)L(t)\right\rangle - \frac{1}{2}\Big\langle\left\{A(t), L^\dagger(t)L(t)\right\}\Big\rangle\right) + \Big\langle\xi^\dagger(t)\left[L(t), A(t)\right]\Big\rangle + \Big\langle\left[A(t), L^\dagger(t)\right]\xi(t)\Big\rangle. \tag{3.62}$$

Our task is to extract out moments from the last line of the equation in a way that is consistent with the Gorini-Kossakowski-Sudarshan-Lindblad theorem (2.75). Let us first inspect:

$$\begin{pmatrix}\Big\langle\xi^\dagger(t)\left[L(t), A(t)\right] \\ + \left[A(t), L^\dagger(t)\right]\xi(t)\Big\rangle\end{pmatrix} = \left\langle\xi^\dagger(t)L(t)A(t)\right\rangle + \left\langle A(t)L^\dagger(t)\xi(t)\right\rangle - \left\langle L^\dagger(t)A(t)\xi(t)\right\rangle - \left\langle\xi^\dagger(t)A(t)L(t)\right\rangle. \tag{3.63}$$

By writing the Hamiltonian as $H_I(t) \to gH_I(t)$ [1], the equation is read as a perturbative expansion in powers of the coupling constant g, given the strength of the system-environment coupling is assumed to be weak (i.e. the Born approximation). Equally, we can go on to consider the plausibility of de-correlating system and environment operators, so as to place (3.62) in a simpler form. In more precise terms, we examine under what conditions is it sufficient to write

$$\langle O_S^1(t)O_S^2(t)\ldots O_E^1(t)O_E^2(t)\ldots\rangle \approx \langle O_S^1(t)O_S^2(t)\ldots\rangle\langle O_E^1(t)O_E^2(t)\ldots\rangle, \tag{3.64}$$

for a collection of arbitrary system and environment operators. The above ignores modifications to the system dynamics that arise—let's say, on a characteristic timescale τ_B, when the system and environment are assumed to be in a correlated state.

Assuming this time is much smaller than any interval dt by which $A(t)$ appreciably changes, i.e. $A(t+dt) \approx A(t) + \frac{dA}{dt}dt$, the validity of (3.64) falls at the same level as the Born approximation. However, bear in mind this will only yield the correct dynamical result subject to taking the correct order of approximation [88].

Immediately factorising (3.63) provides first-order terms proportional to the average of the noise operator. In what follows the environment is assumed to be in thermal equilibrium with the system, such that ρ_E is given by

$$\rho_E = \frac{1}{Z_E}\exp\left[-\sum_{k,\lambda}\beta_k\left(\omega_\lambda - \mu_k\right)a^\dagger_{k,\lambda}a_{k,\lambda}\right], \tag{3.65}$$

with

$$Z_E = Z_{E_1}Z_{E_2}\ldots = \mathrm{tr}\left\{\prod_{k,\lambda}\exp\left[-\beta_k\left(\omega_\lambda - \mu_k\right)a^\dagger_{k,\lambda}a_{k,\lambda}\right]\right\} \tag{3.66}$$

the partition function of the grand canonical ensemble. The parameters $\beta_k = T_k^{-1}$ and μ_k are the inverse temperature (T_k) and chemical potential of the k sub-environment, respectively ($k_B = 1$). From the Gaussian property of ρ_E, we have

$$\langle\xi(t)\rangle_E = \mathrm{tr}\left[\xi(t)\rho_E\right] = 0, \tag{3.67}$$

meaning the first order contributions vanish for a thermal environment. This can be shown by taking the above trace using the Fock states of H_E. Notice as well that (3.67) can always be satisfied under the assumption $\mathrm{tr}_E\left[H_I(t), \rho(0)\right] = 0$ (2.44), and is subsequently vital to ensuring a master equation independent of the density matrix $\rho(0)$ [see Eq. (2.66)].

To continue to the next order of iteration, we return to the quantum Langevin equations and solve for $L(t)$ and its adjoint directly, which are then placed back into Eq. (3.63). We note that because the commutator of these operators is a scalar, the Langevin equation is guaranteed to be a first-order differential equation. The pertinence of this feature is that Eq. (3.57) admits the general solution

$$L(t) = G(t)L(0) + F(t), \quad \text{with} \quad G(0) = 1 \quad \text{and} \quad F(0) = 0. \tag{3.68}$$

If Eq. (3.59) does not hold, the equations will typically be non-linear in system operators and will thus be impossible to solve analytically. The precise form of $L(t)$ is found by differentiating the above and substituting the result into the quantum

Langevin equation:

$$\dot{G}(t)/G(t) = \left(i\Delta - \frac{\gamma}{2}\right), \qquad \dot{F}(t) = \left(i\Delta - \frac{\gamma}{2}\right) F(t) + \xi(t). \tag{3.69}$$

These are readily solved to give

$$L(t) = e^{i\Delta t - \gamma t/2} L(0) + (G * \xi)(t), \tag{3.70}$$

where the convolution $F(t) = (G * \xi)(t)$ is defined from

$$(G * \xi)(t) = \int_0^t dt' G(t-t')\xi(t') = \int_0^t dt' G(t')\xi(t-t'). \tag{3.71}$$

Since Eq. (3.70) is linear in the coupling strength, by substituting the solution to $L(t)$ into Eq. (3.63), we obtain

$$g \left\langle \xi^\dagger(t) L(t) A(t) \right\rangle = g\, e^{i\Delta t - \gamma t/2} \left\langle \xi^\dagger(t) L(0) A(t) \right\rangle + g^2 \left\langle \xi^\dagger(t) F(t) A(t) \right\rangle, \tag{3.72}$$

which is similarly performed with the other averages, e.g. $\left\langle A(t) L^\dagger(t) \xi(t) \right\rangle$. The first-order terms will vanish when factorising out either $\langle \xi(t) \rangle$ or $\langle \xi^\dagger(t) \rangle$, which suitably removes the influence of the noise operator at time t on the system operator at $t = 0$. Then, it is clear that we are only left to deal with second order contributions. Since the Markovian master equation in (2.66) is also evaluated to second order, it now makes sense at this stage to proceed with de-correlating each of the terms in (3.63).

It is implied through Eq. (3.1) that each $A(t)$ translates into a factor of $\rho_S(t)$ in the master equation. We foresee that the resulting master equation is therefore not of Lindblad form and so violates the positivity of the system density matrix. Indeed, making the decorrelation $\left\langle \xi^\dagger(t) F(t) A(t) \right\rangle \approx \left\langle \xi^\dagger(t) F(t) \right\rangle \langle A(t) \rangle$ leaves a factor of $\langle A(t) \rangle$, which includes none of the necessary coupling operators $L, L^\dagger$. To work around this issue we can attempt to rewrite Eq. (3.63) into a similar structure to the top line of (3.62). As an expedient method, the commutator $[L(t), L^\dagger(t)] = 1$ is inserted into each of the averages in a way that permits us to systematically factor out the environment operators from the righthand side of (3.72), and the like, to obtain the desired result. A working solution is found to yield the following:

$$\begin{aligned}
\begin{pmatrix} \left\langle \xi^\dagger(t) \left[L(t), A(t) \right] \right\rangle \\ + \left\langle \left[A(t), L^\dagger(t) \right] \xi(t) \right\rangle \end{pmatrix} &= g^2 C(t) \Big(\left\langle L^\dagger(t) A(t) L(t) \right\rangle + \left\langle L(t) A(t) L^\dagger(t) \right\rangle \Big) \\
&\quad - g^2 \left\langle \xi^\dagger F \right\rangle_t \Big(\left\langle A(t) L^\dagger(t) L(t) \right\rangle + \left\langle L(t) L^\dagger(t) A(t) \right\rangle \Big) \\
&\quad - g^2 \left\langle F^\dagger \xi \right\rangle_t \Big(\left\langle L^\dagger(t) L(t) A(t) \right\rangle + \left\langle A(t) L(t) L^\dagger(t) \right\rangle \Big) + O(g^3),
\end{aligned} \tag{3.73}$$

where the real quantity $C(t)$ is defined as

$$C(t) = \langle \xi^\dagger F \rangle_t + \langle F^\dagger \xi \rangle_t. \tag{3.74}$$

We now go about evaluating the moments using the Gibbs state (3.65). Firstly, by substituting $\xi(t)$ and $F(t)$ from (3.39) and (3.71) into the above, we obtain

$$\begin{aligned}\langle \xi^\dagger F \rangle_t = &\int_0^t dt'\, G(t-t') \\ &\times \sum_{k',k,\lambda',\lambda} g_{k',\lambda'} g_{k,\lambda} \langle a^\dagger_{k',\lambda'} a_{k,\lambda} \rangle^* \exp\left[i(\omega_\lambda - \varepsilon)t - i(\omega_{\lambda'} - \varepsilon)t' \right],\end{aligned} \tag{3.75}$$

and

$$\begin{aligned}\langle F^\dagger \xi \rangle_t = &\int_0^t dt' G^*(t-t') \\ &\times \sum_{k',k,\lambda',\lambda} g_{k',\lambda'} g_{k,\lambda} \langle a^\dagger_{k',\lambda'} a_{k,\lambda} \rangle \exp\left[-i(\omega_\lambda - \varepsilon)t + i(\omega_{\lambda'} - \varepsilon)t' \right],\end{aligned} \tag{3.76}$$

which is consistent with $\langle \xi^\dagger F \rangle_t = \langle F^\dagger \xi \rangle_t^*$ and $C(t) = 2\,\mathrm{Re}\left[\langle \xi^\dagger F \rangle_t \right]$. By using the identity

$$\langle a^\dagger_{k',\lambda'} a_{k,\lambda} \rangle = \delta_{k,k'} \delta_{\lambda,\lambda'} \bar{n}(\omega_\lambda), \tag{3.77}$$

Eqs. (3.76) and (3.75) can be expressed in terms of the *correlation function*:

$$\alpha_\beta(t-t') = \sum_{k,k'} \left\langle B^\dagger_k(t) B_{k'}(t') \right\rangle = \int_{-\infty}^{\infty} d\omega J(\omega) \bar{n}(\omega) e^{-i(\omega-\varepsilon)(t-t')}, \tag{3.78}$$

where again the quantity $\bar{n}(\omega)$ is the Bose-Einstein distribution of the environment. Since each of the sub-environments are held at the same (inverse) temperature β and chemical potential μ, then

$$\bar{n}(\omega) = \frac{1}{e^{\beta(\omega-\mu)} - 1}. \tag{3.79}$$

In turn the function $C(t)$ is given by

$$C(t) = \int_0^t dt' \left[G^*(t-t') \alpha_\beta(t-t') + \text{c.c} \right]. \tag{3.80}$$

It is tempting to re-use the argument of the last section which justified taking the limit $t \to \infty$. However, this would cancel the integral due to the presence of $G(t-t')$. To simplify Eq. (3.80) in line with the Born-Markov criteria we look at the correlation function instead. Again, because Eq. (3.79) varies slowly with respect to the oscillatory term, only its value at $\omega \approx \varepsilon$ is relevant as the integral

will average to zero quickly at any reasonable distance from this point. Thus the correlation function reduces to

$$\alpha_\beta(t-t') \approx \frac{\gamma\bar{n}_\varepsilon}{2\pi}\int_{-\infty}^{\infty} d\omega\, e^{-i(\omega-\varepsilon)(t-t')}, \tag{3.81}$$

where $\bar{n}_\varepsilon = (\exp[\beta(\varepsilon-\mu)]-1)^{-1}$. Now using the definition of the delta function

$$\delta(t-t') = \int_{-\infty}^{\infty}\frac{dx}{2\pi}\, e^{-ix(t-t')}, \tag{3.82}$$

and with a change of variable $x = \omega - \varepsilon$, Eq. (3.81) becomes

$$\alpha_\beta(t-t') = \gamma\bar{n}_\varepsilon\,\delta(t-t'), \tag{3.83}$$

which produces the delta correlated noise source characteristic of a Markovian environment [2]. In turn, $\langle\xi^\dagger F\rangle_t = \langle F^\dagger\xi\rangle_t = \gamma\bar{n}_\varepsilon/2$, where the factor of a half arises because the delta function is on the boundary of the integration region. The full second-order contributions to Eq. (3.62) are given by

$$\begin{aligned}\begin{pmatrix} \langle\xi^\dagger(t)\,[L(t),A(t)]\rangle \\ +\langle\big[A(t),L^\dagger(t)\big]\,\xi(t)\rangle \end{pmatrix} &= \gamma\bar{n}_\varepsilon\Big(\big\langle L^\dagger(t)A(t)L(t)\big\rangle + \big\langle L(t)A(t)L^\dagger(t)\big\rangle\Big) \\ -\frac{\gamma}{2}\bar{n}_\varepsilon\Big(\big\langle A(t)L^\dagger(t)L(t)\big\rangle &+ \big\langle L(t)L^\dagger(t)A(t)\big\rangle + \big\langle L^\dagger(t)L(t)A(t)\big\rangle + \big\langle A(t)L(t)L^\dagger(t)\big\rangle\Big).\end{aligned} \tag{3.84}$$

Putting all of this together provides

$$\begin{aligned}\frac{d}{dt}\langle\hat{A}\rangle_t = -i\Delta\Big\langle\,\big[A(t),L^\dagger(t)L(t)\big]\,\Big\rangle + \gamma(\bar{n}_\varepsilon+1)\left(\big\langle L^\dagger(t)A(t)L(t)\big\rangle - \frac{1}{2}\Big\langle\,\big\{A(t),L^\dagger(t)L(t)\big\}\,\Big\rangle\right) \\ + \gamma\bar{n}_\varepsilon\left(\big\langle L(t)A(t)L^\dagger(t)\big\rangle - \frac{1}{2}\Big\langle\,\big\{A(t),L(t)L^\dagger(t)\big\}\,\Big\rangle\right).\end{aligned} \tag{3.85}$$

The Heisenberg-Langevin equation has now been simplified to a time-local form, expressed only in terms of system operators. This fulfils the precondition attached to the use of Eq. (3.1), and therefore we may to transform Eq. (3.85) to the equivalent master equation.

First, we shift the time dependence from $A(t)$ onto the density matrix ρ_S, and use the cyclic property of the trace to move A so that it's positioned on the left most side of the trace. By then inserting the identity $U_0^\dagger U_0 = U_0 U_0^\dagger = 1$ between operators we obtain terms like $\mathrm{tr}_S[A\,L\rho_S(t)L^\dagger]$. Before we can consistently read of the master equation from Eq. (3.85), the same must also be done with the rotating

frame term (3.19) contained in $d_t\hat{A}(t)$. How this will modify the resulting master equation can be worked out by taking its expectation value:

$$\left\langle \frac{\partial A_{\circlearrowleft}}{\partial t} \right\rangle_t = \mathrm{tr}\left[U_I^\dagger(t)\frac{\partial A_0(t)}{\partial t}U_I(t)\rho\right] = \mathrm{tr}_S\left[\frac{\partial A_0(t)}{\partial t}\rho_S^I(t)\right]. \tag{3.86}$$

For a generic system operator $A_0(t) = e^{iH_St}Ae^{-iH_St}$, we find

$$\mathrm{tr}_S\left[\frac{\partial A_0(t)}{\partial t}\rho_S^I(t)\right] = -i\,\mathrm{tr}_S\big\{A\left[H_S,\rho_S(t)\right]\big\}, \tag{3.87}$$

which simply generates the fast unitary evolution associated with the system Hamiltonian H_S. Note that this term can easily be removed from the original von Neumann equation (2.30) via the transformation to the interaction picture (c.f. section 2.1.3). With this in mind, if we write each of the averages in Eq. (3.85) into the form $\langle A(t)(\dots)\rangle_t = \mathrm{tr}_S[A_0(t)(\dots)]$ and define $\rho_S^I(t) = U_0^\dagger(t)\rho_S(t)U_0(t)$ (2.32), such that

$$\begin{aligned}\frac{d}{dt}\langle A\rangle_t &= \frac{d}{dt}\mathrm{tr}_S\left[A_0(t)\rho_S^I(t)\right] \\ &= \mathrm{tr}_S\left[A_0(t)\frac{d}{dt}\rho_S^I(t)\right] - i\,\mathrm{tr}_S\big\{A\left[H_S,\rho_S(t)\right]\big\},\end{aligned} \tag{3.88}$$

then the last term in the above cancels with (3.87) in the Heisenberg-Langevin equation. Since the resulting equation is of closed form (achieved through inserting the identity where necessary), we can now read off the interaction picture master equation

$$\begin{aligned}\frac{d}{dt}\rho_S^I(t) = &-i\Delta\left[L^\dagger L,\rho_S^I(t)\right] + \gamma(\bar{n}_\varepsilon+1)\left(L\rho_S^I(t)L^\dagger - \frac{1}{2}\left\{L^\dagger L,\rho_S^I(t)\right\}\right) \\ &+ \gamma\bar{n}_\varepsilon\left(L^\dagger\rho_S^I(t)L - \frac{1}{2}\left\{LL^\dagger,\rho_S^I(t)\right\}\right).\end{aligned} \tag{3.89}$$

It is easy enough to derive the Schrödinger picture master equation by taking the time derivative of $\rho_S^I(t)$ [c.f. (2.68)]:

$$\frac{d}{dt}\rho_S^I(t) = i\left[H_S,\rho_S(t)\right] + U_0^\dagger(t)\left(\frac{d}{dt}\rho_S(t)\right)U_0(t). \tag{3.90}$$

Clearly, if we substitute this into (3.89) and rewrite the right side of the equation to only be in terms of the density operator $\rho_S(t)$ (again by inserting the identity), we finally retrieve the Schrödinger picture master equation

$$\begin{aligned}\frac{d}{dt}\rho_S(t) = &-i\Delta'\left[L^\dagger L,\rho_S(t)\right] + \gamma(\bar{n}_\varepsilon+1)\left(L\rho_S(t)L^\dagger - \frac{1}{2}\left\{L^\dagger L,\rho_S(t)\right\}\right) \\ &+ \gamma\bar{n}_\varepsilon\left(L^\dagger\rho_S(t)L - \frac{1}{2}\left\{LL^\dagger,\rho_S(t)\right\}\right),\end{aligned} \tag{3.91}$$

where

$$\Delta' = \varepsilon + \Delta. \tag{3.92}$$

Note the system Hamiltonian is diagonal in the operators L and $L^\dagger$, i.e. $H_S = \varepsilon L^\dagger L$, since L and $L^\dagger$ fulfil the eigenoperator relations (3.11) and (3.12). Our result is consistent with the Markovian master equation obtained for a single harmonic oscillator. We emphasise this as a direct consequence of the bosonic relation imposed in Eq. (3.59) and reflects a particular realisation of microscopic equation (2.66).

It's conclusive to say the method used to derive (3.85) has the potential to produce a valid phenomenological master equation, assuming a weak harmonic interaction H_I between the open system and the environment. We shall go on to examine how ideas of this chapter can be applied to more complicated examples which cannot be treated under the same perturbative assumptions.

3.4 Summary

In this chapter, we have worked through a derivation of the Heisenberg and quantum Langevin equations, starting with a generic form of the Hamiltonian in Eq. (3.9) for a quantum optical system in the non-Markovian regime. The utility of the Heisenberg-Langevin equation is that it acts as a gateway to an equivalent master equation description, as was established via the connection between the two pictures in Eq. (3.1). Importantly, it was found that the quantum Langevin equations must hold a time-local form, in any case, for a direct mapping to be possible.

In the forthcoming chapter we will consider specific examples of systems which generally exhibit non-Markovian behaviour. Since the Born-Markov approximations are no longer applicable, we shall rely of a class of methods that allows us include memory effects into the system dynamics by enlarging the open system of modes of the environment. The practicality of these methods lies in the fact the *enlarged* system is Markovian, and so techniques of this chapter can still be used to construct a master equation of Lindblad form, similar to (3.91), but valid in the case of strong system-environment interactions.

Part III

Non-Markovian quantum dynamics of structured environments

Chapter 4

Non-Markovian decay into a one-dimensional chain

As part of the last chapter we derived the exact quantum Langevin equations, which generally incorporate non-Markovian effects into the evolution of the open system operators. Beyond treating the dynamics under the Markov approximation the equations are mostly unwieldy to handle because of their time-convolved form. To circumvent this issue, in the current chapter we present a transformation that maps the original modes of the environment to a one-dimensional chain of harmonic oscillators with nearest neighbour interactions, following the techniques outlined in Refs. [89–92]. The motivation for using this transformation stems from the freedom it provides to partition the original environment into two parts: one part being given by an truncated chain—a small number of auxiliary modes—whose end interacts directly with the open system, and the other remaining part being a large Markovian bath.

The chain representation produces an intuitive physical picture where the coupling with the auxiliary modes introduces memory effects into the open system dynamics. This is important, as it suggests a natural compatibility with embedding methods. These methods involve systematically adding some auxiliary degrees of freedom into the system, i.e. the chain modes, as a way to make the enlarged system dynamics Markovian. Here, we shall focus on applying the techniques of the pseudomode method within the setting of the chain model. With the original method, the pseudomodes adopt the role of auxiliary variables based on the identification of an

auxiliary equation of motion, which can subsequently be used to derive a Markovian master equation for the enlarged system. In short, their conception is different to the (auxiliary) chain modes, in that they are connected directly to the poles of the spectral density when analytically continued to the complex plane. It is then of interest to see if such a "hybrid" method can be developed by combining the two paradigms.

Our overall aim is to exploit the chain representation, using the Heisenberg formalism, as a way to derive an auxiliary equation of motion—like that obtained using the pseudomode method—but with the advantage of being more general than the single excitation case of Ref. [41]. To achieve this, we formally expand the original set of dynamical equations of the open system to include those of an auxiliary set of harmonic oscillator(s) of the chain environment. We shall see that the auxiliary equation adopts the same role as quantum Langevin equation(s), and, as such, can be used with the Heisenberg-Langevin equation to derive an exact non-perturbative master equation for the enlarged system (the open system plus chain oscillators).

First, we introduce the details of the transformation and illustrate how it leads to a chain representation of the environment. This is, in part, to establish conventions with the reader. Next we formulate the Heisenberg and quantum Langevin equations for a two-level system, which are used to identify the auxiliary (pseudomode) equation. We go onto interpret our results within the framework of a bipartite system being damped by a homogenous tight-binding chain. This culminates in the derivation of the Markovian master equation for the enlarged system using the method set out in section 3.3.2. Finally, we discuss applications to systems of interest: specifically, the multiple excitation case and the driven qubit.

4.1 Chain transformation

We begin by considering a transformation to a new collective set of operators b_n ($b_n^\dagger$), defined in terms of the bosonic operators a_λ ($a_\lambda^\dagger$):

$$b_n = \sum_\lambda U_{\lambda,n} a_\lambda, \tag{4.1}$$

$$b_n^\dagger = \sum_\lambda U_{\lambda,n} a_\lambda^\dagger, \tag{4.2}$$

where $U_{\lambda,n}$ comprise the elements of some transformation matrix U. The above can be more conveniently written using the compact notation,

$$\vec{b} = U\vec{a} \tag{4.3}$$

$$(\vec{b})^* = U(\vec{a})^*, \tag{4.4}$$

where $\vec{a} = (a_0, a_1, \dots)^T$ and $\vec{b} = (b_0, b_1, \dots)^T$ are column vectors of the annihilation operators. These similarly define the vectors containing the creation operators $(\vec{a})^* = (a_0^\dagger, a_1^\dagger, \dots)^T$ and $(\vec{b})^* = (b_0^\dagger, b_1^\dagger, \dots)^T$.

To ensure the canonical bosonic commutation relation of Eq. (3.8) is preserved, the transformation matrix has to satisfy the dual orthogonality property

$$U^\dagger U = UU^\dagger = 1, \tag{4.5}$$

which, at this point, is the only constraint imposed upon (4.3). Here, we adopt the transformation initially proposed in Ref. [89], which parameterises the matrix elements $U_{\lambda,n}$ as follows:

$$U_{\lambda,n} = \delta_{\lambda,\lambda'} \frac{\tilde{g}_{\lambda'}\pi_n(k_{\lambda'})}{\rho_n} = \frac{\tilde{g}_\lambda \pi_n(k_\lambda)}{\rho_n}. \tag{4.6}$$

Here, $\pi_n(k_\lambda)$ are discrete *monic orthogonal polynomials* [93], $\tilde{g}_\lambda = \tilde{g}(k_\lambda)$ is a dimensionless coupling strength, and ρ_n a normalisation constant. Both $\pi_n(k_\lambda)$ and $\tilde{g}_\lambda$ are functions of a dimensionless variable $k_\lambda \in (-1, 1)$, which we will detail shortly. The polynomials hold the generic form

$$\pi_n(k_\lambda) = \sum_{m=0}^{n} c_m (k_\lambda)^m = (k_\lambda)^n + c_{n-1}(k_\lambda)^{n-1} + \dots \qquad n = 0, 1, 2 \dots, \tag{4.7}$$

where n indicates the order of the polynomial and $c_m \geq 0$ are real expansion coefficients. The fact that the coefficient of the leading order term is $c_n = 1$ defines the monic property of the polynomial, although this is a matter of choice and not of direct importance.

Since the transformation matrix has been fixed, it is instructive to first develop its use from the commutator $[b_n, b_{n'}^\dagger]$, where

$$\begin{aligned}\left[b_n, b_{n'}^\dagger\right] &= \sum_{\lambda,\lambda'} U_{\lambda,n} U_{\lambda',n'} \left[a_\lambda, a_{\lambda'}^\dagger\right] = \sum_\lambda U_{n,\lambda}^T U_{\lambda,n'} \\ &= \frac{1}{(\rho_n)^2} \sum_\lambda (\tilde{g}_\lambda)^2 \pi_n(k_\lambda)\pi_{n'}(k_\lambda).\end{aligned} \tag{4.8}$$

By construction, the bottom line of Eq. (4.8) assumes the orthogonality property:

$$\int_{-1}^{1} dk\, \widetilde{J}(k)\pi_n(k)\pi_{n'}(k) = (\rho_n)^2\delta_{n,n'}, \tag{4.9}$$

which subsequently yields the correct commutation relation $[b_n, b_{n'}^\dagger] = \delta_{n,n'}$. Note that we have provided the continuous polynomials $\pi_n(k)$ and spectral density

$$\widetilde{J}(k) = \sum_\lambda (\tilde{g}_\lambda)^2\delta(k - k_\lambda), \tag{4.10}$$

by taking the appropriate continuum limit [Eq. (3.28)]: we shall generally impose a continuum of modes as a way to remove finite size effects of the environment and introduce irreversible open syetem dynamics. In turn, the dual orthogonality property of the real matrix U is guaranteed through an equivalent formulation of (4.9) [93],

$$\sum_n \frac{1}{(\rho_n)^2}\pi_n(k_\lambda)\pi_n(k_{\lambda'}) = \frac{1}{(\tilde{g}_\lambda)^2}\delta_{\lambda,\lambda'}, \tag{4.11}$$

which we can then use to immediately define the inverse transformation,

$$\begin{aligned} a_\lambda &= \sum_n U_{\lambda,n} b_n, \\ a_\lambda^\dagger &= \sum_n U_{\lambda,n} b_n^\dagger, \end{aligned} \tag{4.12}$$

where $\vec{a} = U^T\vec{b}$ and $(\vec{a})^* = U^T(\vec{b})^*$. It is a straightforward procedure to show that $[a_\lambda, a_{\lambda'}^\dagger] = \delta_{\lambda,\lambda'}$ by making direct use of Eq. (4.11).

To now tie things together one has to specify the relation between the variable k_λ to the mode frequencies ω_λ, i.e. a one-to-one mapping $\omega_\lambda = \omega(k_\lambda)$, so that the transformation is consistent with the original Hamiltonian and spectral density. The Hamiltonian from Eq. (3.27)—in a non-rotating frame of reference—should hold the form [94]

$$H = H_S + \sum_\lambda \omega(k_\lambda)a^\dagger(k_\lambda)a(k_\lambda) + \sum_\lambda g(\omega(k_\lambda))\left(L^\dagger a(k_\lambda) + a^\dagger(k_\lambda)L\right), \tag{4.13}$$

where it is left to find explicit expressions for $\tilde{\omega}_\lambda = \tilde{\omega}(k_\lambda)$ (i.e. a scaled k_λ-space frequency) and $\tilde{g}_\lambda = \tilde{g}(k_\lambda)$. For simplicity, we set a linear relation $\tilde{\omega}_\lambda = k_\lambda = \omega_\lambda/\omega_c$, where ω_c is a maximum cut-off frequency that restricts the spectrum of the environment modes to the interval $(-\omega_c, \omega_c)$. Essentially, this follows by making the replacement

$$J(\omega) \longrightarrow J(\omega)\left[\theta(\omega - \omega_c) - \theta(\omega + \omega_c)\right], \tag{4.14}$$

where a finite support is necessary in most cases to guarantee convergence of the integral in Eq. (4.9). Notice we are also still assuming a symmetric range over negative frequencies through working in the quantum optical regime. We can figure out how the spectral density $\widetilde{J}(k)$ relates to the original function $J(\omega)$ by looking the definition in Eq. (3.32). Using the identity,

$$\delta(\omega - \omega_\lambda) = \frac{1}{\omega_c}\delta(k - k_\lambda), \tag{4.15}$$

the coupling parameters are

$$g(\omega(k_\lambda)) = \sqrt{\omega_c J(\omega(k_\lambda))dk}, \tag{4.16}$$

where dk is the spacing between individual modes on the k-axis. Here we have extracted the ω-dependence of the spectral density $J(\omega_\lambda) = (g_\lambda)^2\rho_\lambda$ onto the couplings—that is, basically, assuming a constant density of states. Since there are many possible factorisations of g_λ and ρ_λ which give the same spectral density, we have the freedom to adopt a convenient definition of g_λ (ρ_λ) to help in mapping the Hamiltonian in Eq. (4.13) to the original[1]. This freedom is also extended to how ω_λ is parameterised. Indeed, by choosing $\omega_\lambda = \omega_c k_\lambda$ and extracting the form of the spectral density onto $g(\omega(k_\lambda))$, we have shown via (4.15)-(4.16) that the mode structure of the environment is invariant under a uniform scaling of the frequencies;

$$\int d\omega \rho_\omega = \int dk \rho_k, \tag{4.17}$$

where the integral is taken over the same interval. To then re-produce a definition of $\tilde{g}(k_\lambda)$ that is consistent with (4.10), i.e. from $(\tilde{g}(k_\lambda))^2 = \widetilde{J}(k_\lambda)dk$, one chooses

$$J(\omega(k)) = \omega_c\, \widetilde{J}(k), \tag{4.18}$$

such that the coupling variables are related through $\tilde{g}(k_\lambda) = g(\omega(k_\lambda))/\omega_c$.

We now go on to detail some of the features of Eq. (4.6) that have later relevance in transforming the Hamiltonian (3.9) onto a chain structure.

[1]Formally, for an environment that is initially in Gaussian state, the dynamics of the open system is entirely encoded in spectral density [76]. Therefore changing the spectral parameters in a way that leaves $J(\omega)$ fixed does not alter the underlying physics of the problem.

4.1.1 Properties of orthogonal polynomials

A defining feature of the polynomials in Eq. (4.7) is that they satisfy a three-term recurrence property:

$$\pi_{n+1}(k) = (k - \alpha_n)\pi_n(k) - \beta_n \pi_{n-1}(k), \qquad n = 0, 1, 2, \dots , \tag{4.19}$$

with the universal boundary conditions $\pi_{-1}(k) = 0$ and $\pi_0(k) = 1$. We also introduce what are known as the recurrence coefficients of the polynomials,

$$\alpha_n = \frac{1}{(\rho_n)^2} \int_{-1}^{1} dk\, \widetilde{J}(k) k\, \pi_n(k)\pi_n(k), \qquad n = 0, 1, 2, \dots , \tag{4.20}$$

$$\beta_n = \frac{1}{(\rho_{n-1})^2} \int_{-1}^{1} dk\, \widetilde{J}(k) \pi_n(k)\pi_n(k), \qquad n = 1, 2, \dots , \tag{4.21}$$

with

$$\rho_n^2 = \int_{-1}^{1} dk\, \widetilde{J}(k)\pi_n(k)\pi_n(k). \tag{4.22}$$

The coefficients α_n and β_n are obtained in a similar recursive fashion to the polynomials $\pi_n(k)$, which are constructed via application of the Gram-Schmidt orthogonalisation procedure. Since $\pi_0(k)$ is defined arbitrarily in Eq. (4.19), we are able to freely choose the definition of β_0. It is typically convenient to employ

$$\beta_0 = \int_{-1}^{1} dk\, \widetilde{J}(k). \tag{4.23}$$

Moreover, the spectral density $\widetilde{J}(k)$ is said to belong to the Szegö class of measures if the following holds:

$$\int_{-1}^{1} dk \frac{\ln \widetilde{J}(k)}{\sqrt{1 - k^2}} > -\infty. \tag{4.24}$$

An important aspect of this class lies in the asymptotic properties of the recurrence coefficients. In the limit $n \to \infty$, the coefficients α_n and β_n converge to [93]

$$\lim_{n\to\infty} \alpha_n = 0, \qquad \lim_{n\to\infty} \beta_n = \frac{1}{4}. \tag{4.25}$$

While (4.24) will not be systematically checked against examples we go onto consider, the condition is known to be fulfilled for a wide range of spectral functions—in particular, those positive in the interval $k \in (-1, 1)$. This only places a mild constraint on the use of the mapping, and as such, $\widetilde{J}(k)$ is assumed to comply with (4.24) in the future case we consider.

4.1.2 System-environment representation

Here we recapitulate steps taken in Refs. [89, 92] to derive the new form of the Hamiltonian (4.13) in a representation provided by Eqs. (4.3), making use of the properties outlined in the last subsections. We start by applying the transformation (4.12) to the interaction term H_I:

$$\begin{aligned} H_I &= \sum_\lambda g_\lambda \left(L^\dagger a_\lambda + a_\lambda^\dagger L \right) \\ &= \sum_n \sum_\lambda \frac{g_\lambda \tilde{g}_\lambda}{\rho_n} \left(\pi_n(k_\lambda) L^\dagger b_n + \text{h.c.} \right) = \omega_c \sum_n \sum_\lambda \frac{(\tilde{g}_\lambda)^2}{\rho_n} \left(\pi_n(k_\lambda)\pi_0(k_\lambda) L^\dagger b_n + \text{h.c.} \right), \end{aligned} \tag{4.26}$$

where taking the continuum limit through $\sum_\lambda \to \int dk \rho_k$ gives

$$H_I = \omega_c \sum_n \frac{1}{\rho_n} \int_{-1}^{1} dk\, \widetilde{J}(k) \left(\pi_n(k)\pi_0(k) L^\dagger b_n + \text{h.c.} \right). \tag{4.27}$$

Employing the orthogonality criterion (i) then results in

$$H_I = \omega_c \sum_n \frac{(\rho_0)^2}{\rho_n} \delta_{0,n} \left(L^\dagger b_n + b_n^\dagger L \right) = \omega_c \rho_0 \left(L^\dagger b_0 + b_0^\dagger L \right). \tag{4.28}$$

Clearly from (4.23), $\rho_0 = \sqrt{\beta_0}$. For the bare Hamiltonian of the environment we apply a similar procedure:

$$\begin{aligned} H_E &= \sum_\lambda \omega_\lambda a_\lambda^\dagger a_\lambda \\ &= \omega_c \sum_\lambda \sum_{n,n'} k_\lambda U_{\lambda,n} U_{\lambda,n'} b_n^\dagger b_{n'} = \omega_c \sum_{n,n'} \frac{1}{\rho_n \rho_{n'}} \int_{-1}^{1} dk\, \widetilde{J}(k) k\, \pi_{n'}(k)\pi_n(k) b_n^\dagger b_{n'}, \end{aligned} \tag{4.29}$$

at which point we use the three-term recurrence relation (ii) to substitute in for $k\pi_n(k)$,

$$\begin{aligned} H_E &= \omega_c \sum_{n,n'} \frac{1}{\rho_n \rho_{n'}} \int_{-1}^{1} dk\, \widetilde{J}(k) \Big[\pi_{n+1}(k) + \alpha_n \pi_n(k) + \beta_n \pi_{n-1}(k) \Big] \pi_{n'}(k) b_n^\dagger b_{n'} \\ &= \omega_c \sum_{n,n'} \frac{1}{\rho_n \rho_{n'}} \int_{-1}^{1} dk\, \widetilde{J}(k) \Big[\pi_{n+1}(k)\pi_{n'}(k) + \alpha_n \pi_n(k)\pi_{n'}(k) + \beta_n \pi_{n-1}(k)\pi_{n'}(k) \Big] b_n^\dagger b_{n'}. \end{aligned} \tag{4.30}$$

Again, by orthogonality (4.9), the above reduces to the final form

$$H_E = \omega_c \sum_n \left(\sqrt{\beta_{n+1}} b_n^\dagger b_{n+1} + \alpha_n b_n^\dagger b_n + \sqrt{\beta_{n+1}} b_{n+1}^\dagger b_n \right), \tag{4.31}$$

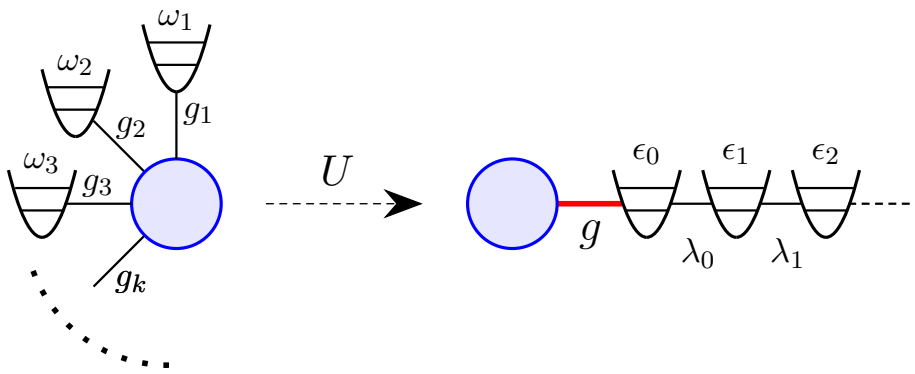

Figure 4.1: Schematic picture of the system-environment model before after applying the transformation U. (a) Shows a quantum system interacting with a bosonic environment with couplings g_λ and oscillator frequencies ω_λ. (b) Depicts an equivalent representation, where the quantum system couples to a 1D chain of oscillators with frequencies ϵ_n and inter-site couplings λ_n. The coupling to first mode is denoted g.

where we have used that $\sqrt{\beta_{n+1}} = \rho_{n+1}/\rho_n$ from Eq. (4.21). The labels in the last summation are also shifted by $n \to n+1$ as the first term in the sum is zero ($\pi_{-1}(k) = 0$). The global post-transform Hamiltonian then reads

$$H = H_S + g\left(L^\dagger b_0 + b_0^\dagger L\right) + \sum_n \left(\lambda_n b_n^\dagger b_{n+1} + \epsilon_n b_n^\dagger b_n + \lambda_n b_{n+1}^\dagger b_n\right), \tag{4.32}$$

where we have introduced the parameters

$$\epsilon_n = \omega_c \alpha_n, \qquad \lambda_n = \omega_c \sqrt{\beta_{n+1}}, \qquad n = 0, 1, 2, \ldots, \tag{4.33}$$

corresponding to the site energies and couplings between modes, respectively. Overall, based on the resulting structure of Eq. (4.32), we have shown the original bosonic environment (in a so-called "star" configuration) to be unitarily equivalent to that of a tight-binding model, i.e. a one-dimensional chain of oscillators with nearest neighbour interactions. Figure 4.1 displays the system-environment model before and after applying the transformation. Notice the system in unaffected by the mapping. In addition—and a feature we would like to emphasise—is that the coupling of the open system to the full environment of bosons has been incorporated into a collective interaction with just a *single* chain mode. The coupling strength of this interaction is

$$g = \omega_c \sqrt{\beta_0}. \tag{4.34}$$

We shall go on to show how such a mode plays an important role in dynamics, and for this reason will specially refer to it as the *principal mode* of the chain.

The main idea behind a similar class methods, which also involve mapping the environment to a linear one-dimensional chain, is to discretise the bath in such a way that appropriate numerical procedures can be used to solve for the dynamics of the full system [95]. The original mapping of a discretised bath onto a semi-infinite chain was first developed as part of the numerical renormalisation group (NRG) method by Wilson [96] to solve the quantum impurity (Kondo) problem, i.e. the coupling of a small system (magnetic impurity) to a continuous bath of fermions (bosons). Essentially the NRG method discretises the original spectral density of the model in such a way that the bath operators of the Hamiltonian can be transformed to form a new (discrete) set of modes in a 1D tight binding chain. Owing to the 1D structure of (4.32), Chin *et al* [89] have generalised this procedure (c.f. section 4.1) for the purpose simulating the exact dynamics of open systems using the t-DMRG (time-evolved density matrix renormalisation group) technique, having seen recent application to the spin-boson model [6, 77] within the context of photonic crystals [97] and pigment-protein complexes [90]. Instead, our treatment makes use of the Heisenberg formalism to investigate the dynamics arising out of this chain representation, in line with the techniques employed with the pseudomode method.

4.2 Spontaneous emission from a two-level system

Now that we have all technical requirements in place, we proceed by introducing some details of the model under study. The Hamiltonian of the full system is given by

$$H = \omega_0 \sigma_+ \sigma_- + \sum_\lambda \omega_\lambda a_\lambda^\dagger a_\lambda + \sum_\lambda g_\lambda \left(\sigma_+ a_\lambda + \text{h.c.} \right), \tag{4.35}$$

which describes the interaction between a two-level system, having ground and excited states denoted by $|g\rangle$ and $|e\rangle$, with a single bosonic environment. The system Hamiltonian is $H_S = \omega_0 \sigma_+ \sigma_-$, where the operators $\sigma_+ = \sigma_-^\dagger$ raise and lower the energy of the system by an amount ω_0. Mathematically, these operators are defined

as follows:

$$\sigma_- |e\rangle = |g\rangle\,, \quad \sigma_+ |g\rangle = |e\rangle \quad \text{and} \quad \sigma_-\sigma_+ |g\rangle = |g\rangle\,. \tag{4.36}$$

Notably, because the open system coupling operators in H_I satisfy the eigenoperator relations from (3.11) and (3.12), that is

$$[H_S, \sigma_-] = -\omega_0 \sigma_-, \tag{4.37}$$

$$[H_S, \sigma_+] = \omega_0 \sigma_+, \tag{4.38}$$

the Hamiltonian in Eq. (4.35) is valid within the rotating wave approximation, with non-energy conserving terms removed from the interaction.

To first derive the relevant dynamical equations in the Heisenberg picture, we map the Hamiltonian of the current model to the interaction picture using the bare Hamiltonian $H_0 = \omega_0 \sigma_+ \sigma_- + \sum_\lambda \omega_\lambda a_\lambda^\dagger a_\lambda$ [see Eq. (3.14)]. Doing so yields

$$H_I(t) = \sigma_+ B_1(t) + \text{h.c.}, \tag{4.39}$$

where the environment operator

$$B_1(t) = \sum_\lambda g_\lambda a_\lambda e^{-i(\omega_\lambda - \omega_0)t} \tag{4.40}$$

has the same definition as (3.25) but for a single environment. The Heisenberg-Langevin equation (3.38) in the rotating frame of reference is then

$$\begin{aligned} \frac{d}{dt}\hat{A}(t) = &- \int_0^t dt' \Big(f(t-t') \left[A(t), \sigma_+(t)\right] \sigma_-(t') + f^*(t-t') \sigma_+(t') \left[\sigma_-(t), A(t)\right] \Big) \\ &+ \left[A(t), \sigma_+(t)\right] \xi(t) + \xi^\dagger(t) \left[\sigma_-(t), A(t)\right], \end{aligned} \tag{4.41}$$

with

$$B_1(t) = i\xi(t). \tag{4.42}$$

To retrieve the quantum Langevin equation for $\sigma_-(t)$, let us recall the definitions of the Heisenberg picture operators $A(t)$, $\sigma_-(t)$ and $\sigma_+(t)$ from Eqs. (3.17) and (3.34). If, at $t = 0$, we set $A = \sigma_-$, then at a later time $t > 0$ the operators match as

$$A(t) = e^{-i\omega_0 t} \sigma_-(t), \quad A = \sigma_-. \tag{4.43}$$

From (3.42), the time-derivative of $A(t)$ within the rotating frame is

$$\frac{d}{dt}\hat{A}(t) = e^{-i\omega_0 t} \frac{d}{dt}\sigma_-(t), \tag{4.44}$$

and, since $H_I(t)$ has precisely the same form as Eq. (3.27), we can make direct use of (3.43) to obtain

$$\frac{d}{dt}\sigma_-(t) = -\sigma_z(t)\left\{\xi(t) - \int_0^t dt' f(t-t')\sigma_-(t')\right\}. \tag{4.45}$$

where we have also used the commutation relation $[\sigma_+, \sigma_-] = \sigma_z$ [5]. Note the above defines the equation of motion for its adjoint counterpart, $\sigma_+(t)$. Our next task is to evaluate the memory kernel

$$f(t-t') = \left[B_1(t), B_1^\dagger(t')\right] = \int_{-\infty}^{\infty} d\omega J(\omega) e^{-i(\omega-\omega_0)(t-t')}, \tag{4.46}$$

which will be left until an explicit form of the spectral density is adopted.

4.2.1 Damped Jaynes-Cummings model

From here on, we focus on a particular realisation of the Hamiltonian (4.35) to the damped Jaynes-Cummings model. Our specific choice model involves a two-level atom, which undergoes spontaneous emission induced by the quantised modes of an electromagnetic field, i.e. an environment of photons. The atom-field interaction stems from the coupling of the atomic electric dipole to the modes of an electromagnetic field, which here is taken under the dipole approximation. Incoherent losses from the atom occur as a result of uncontrolled fluctuations in the surrounding environment.

The spectral density typically associated with this model is phenomenologically characterised by a Lorentzian

$$J(\omega) = \frac{\Omega_0^2}{\pi}\frac{\Gamma/2}{(\omega_0 - \delta - \omega)^2 + (\Gamma/2)^2}, \tag{4.47}$$

where Γ defines the linewidth of the spectrum, δ is the detuning of the centre of the distribution from the atomic transition frequency, and Ω_0 is a measure of the total coupling strength of the atom-bath interaction. This is duly noted by applying the definition in Eq. (3.32),

$$\Omega_0^2 = \sum_\lambda (g_\lambda)^2. \tag{4.48}$$

In conjunction with the results obtained via the pseudomode method, when the environment is initially in the vacuum state the full system-environment dynamics are exactly solvable using Laplace transforms [88]. One of the reasons why the model

is of fundamental interest is that, for certain parameters of the spectral density, the solutions show distinct non-Markovian behaviour [1]. This is the regime we are intending to explore in the current chapter. At the moment, we shall impose no restrictions on the bath, apart from assuming it is initially in thermal equilibrium with the atom and at a finite temperature.

Considering we are working with a Lorentzian spectral density, the memory kernel (4.46) can be computed analytically by extending the domain integration to the complex ω-plane and employing Cauchy's residue theorem. Where the poles of Eq. (4.47) lie in the complex plane will determine the decay rate of the open system. The spectral density contains two simple poles in the upper and lower half planes, positioned at

$$z_{\pm} = \omega_0 - \delta \pm i\frac{\Gamma}{2}. \tag{4.49}$$

As $t \geq t'$, we are obliged to choose a semicircle contour in either the upper or lower half plane, depending on the sign of the exponent. For the memory kernel $f(t-t')$

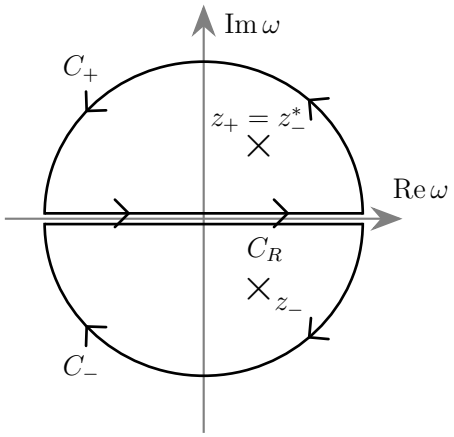

Figure 4.2: Contours used to evaluate the memory kernel function in equations (4.50) and (4.51). The ends points of C_R on the real line are taken to infinity, while Jordan's lemma ensures the integrals taken over the arcs $C_{\pm}$ vanish. Crosses show the locations of the poles.

appearing in Eq. (4.45), the full path of integration is given by a concatenation of the real line C_R and arc C_- joining the two ends at infinity—whereas, for $f^*(t-t')$ [i.e. in the conjugate equation $d_t\sigma_+(t)$], the integration contour is closed by a different arc C_+ to avoid divergence of the integral. Each of these two schemes are displayed

in Fig. 4.2. Since the exponential term is an entire function, it follows that

$$\begin{aligned} f(t-t') &= -2\pi i \,\mathrm{Res}\left[J(\omega), z_-\right] e^{-i(z_- - \omega_0)(t-t')}, \quad \omega \in \mathbb{C} \\ &= \theta(t-t')\Omega_0^2 \exp\left[\left(i\delta - \frac{\Gamma}{2}\right)(t-t')\right], \end{aligned} \tag{4.50}$$

and

$$\begin{aligned} f^*(t-t') &= 2\pi i \,\mathrm{Res}\left[J(\omega), z_+\right] e^{i(z_+ - \omega_0)(t-t')}, \quad \omega \in \mathbb{C} \\ &= \theta(t-t')\Omega_0^2 \exp\left[\left(-i\delta - \frac{\Gamma}{2}\right)(t-t')\right], \end{aligned} \tag{4.51}$$

where the Heaviside function $\theta(t)$ (3.3) is included to satisfy causality of the memory kernel. The quantum Langevin equation is then given by

$$\frac{d}{dt}\sigma_-(t) = -\sigma_z(t)\left\{\xi(t) - \Omega_0^2 \int_0^t dt' e^{(i\delta - \Gamma/2)(t-t')}\sigma_-(t')\right\}. \tag{4.52}$$

We shall use this equation at a later point to derive an exact set of dynamical equations for the open system plus environment in the chain configuration.

4.2.2 Parameters of the Hamiltonian

The purpose of introducing the chain transformation (section 4.1) has been to facilitate the derivation of an auxiliary equation which, along with the equation of motion for $\sigma_-(t)$ (4.52), fully describe the coupling of the atomic transition to a non-Markovian environment. Before we tackle this, we first compute the $n = 0$ recurrence coefficients of the Hamiltonian using the provided spectral density. The Hamiltonian in the new operator basis $\{b_n, b_n^\dagger\}_{n=0}^\infty$ reads

$$H = \omega_0 \sigma_+ \sigma_- + \Omega_0\left(\sigma_+ b_0 + b_0^\dagger \sigma_-\right) + \sum_n \left(\lambda_n b_{n+1}^\dagger b_n + \epsilon_n b_n^\dagger b_n + \mathrm{h.c.}\right), \tag{4.53}$$

where we have used that $g = \omega_c\sqrt{\beta_0} = \Omega_0$. This is easily seen from equations (4.23) and (4.48),

$$(g)^2 = \int_{-\omega_c}^{\omega_c} d\omega J(\omega) \approx \int_{-\infty}^{\infty} d\omega J(\omega) = \Omega_0^2. \tag{4.54}$$

The last line holds based on assuming the following relationship between parameters,

$$\omega_c \gg \omega_0 \gg \Gamma, \delta, \Omega_0. \tag{4.55}$$

Note that such a hierarchy implies the atomic transition frequency is well above zero, $\omega_0 \gg 0$, and again justifies the rotating wave approximation. It turns out

the integral can be made exact by altering the original transformation matrix (4.6) so that only terms for $n > 0$ have their support bounded by the Heaviside step functions in (4.14). We also find that the parameter ϵ_0 can be related to the spectral parameters of the model. This is checked from its definition (4.33),

$$\epsilon_0 = \omega_c \alpha_0 = \frac{1}{(\omega_c \rho_0)^2} \int_{-\omega_c}^{\omega_c} d\omega\, \omega J(\omega), \tag{4.56}$$

which, from (4.47), leads to the expression

$$\epsilon_0 = \omega_c \frac{1}{\pi} \int_{-1}^{1} dk \frac{k\,(\Gamma/2\omega_c)}{\left[(\omega_0 - \delta)/\omega_c - k\right]^2 + (\Gamma/2\omega_c)^2}, \tag{4.57}$$

where we have used $(\rho_0)^2 = \beta_0 = (\Omega_0/\omega_c)^2$ and $\pi_0(k) = 1$. Because the width Γ/ω_c will be very small for any reasonable selection of parameters, the above can be approximated by taking the "effective limit"

$$\epsilon_0 \approx \frac{\omega_c}{\pi} \lim_{\Gamma/\omega_c \to 0} \int_{-1}^{1} dk \frac{k\,(\Gamma/2\omega_c)}{\left[(\omega_0 - \delta)/\omega_c - k\right]^2 + (\Gamma/2\omega_c)^2}. \tag{4.58}$$

Now, since the Lorentzian is narrow compared to k, we can use the following definition of the delta function,

$$\lim_{\Gamma/\omega_c \to 0} \frac{1}{\pi} \left[\frac{(\Gamma/2\omega_c)}{k^2 + (\Gamma/2\omega_c)^2} \right] = \delta(k) \tag{4.59}$$

to obtain

$$\epsilon_0 \approx \omega_c \int_{-1}^{1} dk\, k\, \delta\left(k - \frac{(\omega_0 - \delta)}{\omega_c} \right) = \omega_0 - \delta. \tag{4.60}$$

The general argument to be made here is that the integrand falls off fast enough as $|k| \to \infty$, so as to be zero everywhere apart from at $k \approx (\omega_0 - \delta)/\omega_c$. Although (4.60) clearly results from an approximation, it should be attainable to arbitrary degree of accuracy seeing as ω_c can be taken to be as large as required—as long as all inner products (4.9) and moments, e.g. (4.20) and (4.21), converge.

The Hamiltonian of a Lorentzian environment coupled to a two-level system is then determined as

$$\begin{aligned} H = {} & \omega_0 \sigma_+ \sigma_- + (\omega_0 - \delta) b_0^\dagger b_0 + \Omega_0 \left(\sigma_+ b_0 + b_0^\dagger \sigma_- \right) \\ & + \lambda_1 \left(b_1^\dagger b_0 + \text{h.c.} \right) + \sum_{n>0} \left(\lambda_n b_{n+1}^\dagger b_n + \epsilon_n b_n^\dagger b_n + \text{h.c.} \right). \end{aligned} \tag{4.61}$$

For now, it will be convenient to partition (4.61) according to $H = \tilde{H}_S + \tilde{H}_I + H_R$, where

$$\begin{aligned}
\tilde{H}_S &= \omega_0 \sigma_+ \sigma_- + (\omega_0 - \delta) b_0^\dagger b_0, \\
\tilde{H}_I &= \Omega_0 \left(\sigma_+ b_0 + b_0^\dagger \sigma_- \right), \\
H_R &= \lambda_1 \left(b_1^\dagger b_0 + \text{h.c.} \right) + \sum_{n>0} \left(\lambda_n b_{n+1}^\dagger b_n + \epsilon_n b_n^\dagger b_n + \text{h.c.} \right).
\end{aligned} \tag{4.62}$$

Recurrence coefficients beyond $n = 0$ have to be computed numerically, though, as we will discover, this is not explicitly required for the application of our method.

4.2.3 Derivation of the dynamical equations for the atom and principal mode

To proceed, we go onto generate the Heisenberg equations of motion of the atom using the chain Hamiltonian (4.61). Bearing in mind that we're seeking a formulation of the dynamics consistent with (4.52), it is first necessary to transform Eq. (4.35) into a frame of reference which yields an equivalent dynamics for $\sigma_-(t)$ (σ_+). In the chain setting, our original choice of H_0 from $H = H_0 + H_I$, which included the bare energy terms of the atomic system plus environment of harmonic oscillators, is now defined as

$$H_0 = \omega_0 \sigma_+ \sigma_- + \sum_n \left(\lambda_n b_{n+1}^\dagger b_n + \epsilon_n b_n^\dagger b_n + \text{h.c.} \right). \tag{4.63}$$

For us it will actually be advantageous to adopt a different form, $H_0' = \tilde{H}_S + H_R$, using $\tilde{H}_S$ and H_R from (4.62):

$$H_0' = \omega_0 \sigma_+ \sigma_- + (\omega_0 - \delta) b_0^\dagger b_0 + \sum_{n>0} \left(\lambda_n b_{n+1}^\dagger b_n + \text{h.c.} \right). \tag{4.64}$$

This can be shown—when combined with the Heisenberg equation—to provide a dynamics equivalent to that of (4.52). We illustrate this by the following. Suppose we have the Heisenberg picture operator $\sigma_-(t)$—from (3.18), its equation of motion is given by

$$\begin{aligned}
\frac{d}{dt} \left(U_I^\dagger(t) U_0^\dagger(t) \sigma_- U_0(t) U_I(t) \right) = &- i \left[U_I^\dagger(t) U_0^\dagger(t) \sigma_- U_0(t) U_I(t), H_H(t) \right] \\
&+ U_I^\dagger(t) \frac{\partial}{\partial t} \left(U_0^\dagger(t) \sigma_- U_0(t) \right) U_I(t),
\end{aligned} \tag{4.65}$$

where

$$U_0(t) = e^{-iH_0 t} \quad \text{or} \quad U_0(t) = e^{-iH_0' t}. \tag{4.66}$$

Despite the lefthand side of (4.65) being fixed for any decomposition of H, each of the terms on the righthand side will be expected vary through the choice of either H_0 or H_0'. However, we notice $U_0^\dagger(t)\sigma_- U_0(t) = e^{-i\omega_0 t}\sigma_-$ for whatever choice is made. By writing the above in a way that is consistent with (3.22) and (4.44): that is, in a rotating frame where $-i\omega_0\sigma_-(t)$ is removed, we have

$$\frac{d}{dt}\sigma_-(t) = -i\left[\sigma_-(t), H_H(t)\right], \quad A(t) = e^{-i\omega_0 t}\sigma_-(t), \tag{4.67}$$

for both cases, thereby proving that the Heisenberg equation from (4.64) is equal to the quantum Langevin equation (4.45). This, as we shall see shortly, can be exploited to find our auxiliary equation.

We are now in a position to derive the Heisenberg equation of motion for $\sigma_-(t)$ by way of the chain Hamiltonian (4.53) and compare result to (4.52). Within the preferred frame of reference, rewriting (4.61) into the form of $H_H(t)$ and substituting this into (4.67) provides

$$\frac{d}{dt}\sigma_-(t) = i\Omega_0 e^{i\delta t}\sigma_z(t)b_0(t). \tag{4.68}$$

For the sake of completeness we can also derive the inversion rate of the atom,

$$\frac{d}{dt}\sigma_z(t) = i\,2\Omega_0\left(e^{-i\delta t}b_0^\dagger(t)\sigma_-(t) - \text{h.c.}\right). \tag{4.69}$$

Notice the definition of the time-evolved operator $b_0(t)$ ($b_0^\dagger(t)$) is consistent with (3.34) and carries no "hidden" time-dependence. By this we mean $U_0^\dagger(t)b_0U_0(t) = b_0e^{-i(\omega_0-\delta)t}$ clearly has an explicit and separable time-dependent factor, in turn helping to simplify the above. Unsurprisingly, this is what motivated original choice in defining the rotating frame using H_0'.

Now that we have two equivalent sets of differential equations for the open system operators, we can find an expression for $b_0(t)$ by equating (4.68) and (4.52),

$$b_0(t) = \frac{i}{\Omega_0}\xi(t)e^{-i\delta t} - i\Omega_0 e^{-\Gamma t/2}\int_0^t dt' e^{-(i\delta-\Gamma/2)t'}\sigma_-(t'). \tag{4.70}$$

Here, our attention is focussed on how the system dynamics can be represented via the use of such a solution. A representation we explored in the last chapter was

based on using the quantum Langevin equation(s) to obtain a master equation for the density matrix of the open system. Though a solution for $b_0(t)$ is at hand, we require its dynamical equation to be local in time if we are to pursue a master equation formulation of the dynamics. With this in mind, we take the time-derivative of $b_0(t)$,

$$\frac{d}{dt}b_0(t) = \frac{i}{\Omega_0}\frac{d}{dt}\left(\xi(t)e^{-i\delta t}\right) - i\Omega_0\frac{d}{dt}\left(e^{-\Gamma t/2}\int_0^t dt' e^{-(i\delta-\Gamma/2)t'}\sigma_-(t')\right), \tag{4.71}$$

where it is left to find a closed form expression of (4.71). To do this, we first inspect the noise operator $\xi(t)$. This was defined previously in chapter 3:

$$\xi(t) = -i\sum_\lambda g_\lambda a_\lambda e^{-i(\omega_\lambda-\omega_0)t}. \tag{4.72}$$

After applying the transformation (4.12) to the operators a_λ, the noise operator is given by

$$\xi(t) = -i\sum_n\sum_\lambda \frac{g_\lambda\tilde{g}_\lambda}{\rho_n}\pi_n(k_\lambda)b_n e^{-i(\omega_\lambda-\omega_0)t}, \tag{4.73}$$

which, in the continuum limit leads to

$$\xi(t) = -i\sum_n \frac{1}{\omega_c\rho_n}b_n\int_{-\omega_c}^{\omega_c} d\omega J(\omega)\pi_n(\omega/\omega_c)e^{-i(\omega-\omega_0)t}. \tag{4.74}$$

The above can be written in a more practical form by partitioning the sum into two parts:

$$\xi(t) = \xi_0(t) + \xi_c(t), \tag{4.75}$$

where we have defined

$$\xi_0(t) = -\frac{i}{\Omega_0}b_0\int_{-\omega_c}^{\omega_c} d\omega J(\omega)e^{-i(\omega-\omega_0)t}, \tag{4.76}$$

and

$$\xi_c(t) = -i\sum_n \frac{1}{\omega_c\rho_{n+1}}b_{n+1}\int_{-\omega_c}^{\omega_c} d\omega J(\omega)\pi_{n+1}(\omega/\omega_c)e^{-i(\omega-\omega_0)t}, \tag{4.77}$$

by making use of the identities $\pi_0(k) = 1$ and $\rho_0 = \Omega_0/\omega_c$. Note that the justification behind the cut-off frequency is made more concrete with (4.77): specifically, it is required to negate an otherwise infinitely rising noise spectrum contained in $\xi_c(t)$, which diverges as $\omega_c \to \infty$ [2].

Our task now is to place $\xi_0(t)$ and $\xi_c(t)$ into suitable forms. Remembering that ω_c can be taken to infinity for the $n = 0$ term in (4.74), we see (4.76) satisfies

$$\lim_{\omega_c\to\infty}\xi_0(t) = -i\frac{f(t)}{\Omega_0}b_0, \tag{4.78}$$

which can be evaluated in precisely the same way as Eq. (4.50)—that is, by analytic continuation of (4.47) to the complex plane and evaluating its poles using the residue theorem. In doing so, we find

$$\xi_0(t) = -\frac{2\pi}{\Omega_0}\text{Res}\left[J(\omega), z_-\right] e^{-i(z_- - \omega_0)t} b_0 = -i\theta(t)\Omega_0 \exp\left[\left(i\delta - \frac{\Gamma}{2}\right)t\right] b_0, \quad \omega \in \mathbb{C}. \tag{4.79}$$

The noise component $\xi_c(t)$ is a little trickier to manage seeing as it contains a product of the spectral density and orthogonal polynomials. It is appreciated that in order to produce a closed form expression for (4.71), $\xi_c(t)$ should be manipulated in such as way as to contain a real exponential term of the type in Eq. (4.79). Fortunately this can be achieved by use of the convolution theorem. By employing the previous definition of the convolution (3.71) from section 3.3.2, it is found—through its associative property—that

$$\xi_c(t) = -i\sum_{n=0}\frac{1}{\omega_c\rho_{n+1}} b_{n+1}\int_{-\infty}^{\infty} dt'\Bigg(\int_{-\infty}^{\infty} d\omega' J(\omega') e^{-i(\omega'-\omega_0)(t-t')} \times \frac{1}{2\pi}\int_{-\omega_c}^{\omega_c} d\omega\, \pi_{n+1}(\omega/\omega_c) e^{-i(\omega-\omega_0)t'}\Bigg), \tag{4.80}$$

where the Heaviside functions in (4.14) have been attached to the Fourier transform of the polynomials. Immediately we see the appearance of the memory kernel $f(t-t')$ whose explicit form is already known. We can then write

$$\xi_c(t) = -i\sum_{n=0}\frac{\Omega_0^2}{\omega_c\rho_{n+1}} b_{n+1}\int_0^t dt'\Bigg(e^{(i\delta-\Gamma/2)(t-t')} \times \frac{1}{2\pi}\int_{-\omega_c}^{\omega_c} d\omega\, \pi_{n+1}(\omega/\omega_c) e^{-i(\omega-\omega_0)t'}\Bigg). \tag{4.81}$$

Overall, we have the two noise contributions

$$\frac{i}{\Omega_0}\left(\xi_0(t)e^{-i\delta t}\right) = \theta(t) b_0 e^{-\Gamma t/2} \tag{4.82}$$

and

$$\frac{i}{\Omega_0}\left(\xi_c(t)e^{-i\delta t}\right) = \sum_{n>0}\frac{\Omega_0}{\omega_c\rho_n} b_n e^{-\Gamma t/2}\int_0^t dt'\Bigg(e^{-(i\delta-\Gamma/2)t'} \times \frac{1}{2\pi}\int_{-\omega_c}^{\omega_c} d\omega\, \pi_n(\omega/\omega_c) e^{-i(\omega-\omega_0)t'}\Bigg). \tag{4.83}$$

Plugging Eqs. (4.82)-(4.83) into (4.71) then determines our auxiliary equation of motion through the relation

$$\frac{i}{\Omega_0}\frac{d}{dt}\left(\xi(t)e^{-i\delta t}\right) = -\frac{\Gamma}{2}\left(\frac{i}{\Omega_0}\xi(t)e^{-i\delta t}\right) + \frac{\Omega_0}{2\pi}e^{-i\delta t}\sum_n \frac{1}{\omega_c\rho_{n+1}}b_{n+1}\int_{-\omega_c}^{\omega_c} d\omega\, \pi_{n+1}(\omega/\omega_c)e^{-i(\omega-\omega_0)t}. \tag{4.84}$$

Note that the evaluation of (4.70) proceeds in exactly the same way to obtain the adjoint equation for $b_0^\dagger(t)$.

Together with the atomic inversion rate (4.69), the dynamics of the system is completely described by the following coupled ordinary differential equations,

$$\begin{cases} \dfrac{d}{dt}\sigma_-(t) = i\Omega_0 e^{i\delta t}\sigma_z(t)b_0(t), & (4.85) \\ \dfrac{d}{dt}b_0(t) = -\dfrac{\Gamma}{2}b_0(t) - i\Omega_0 e^{-i\delta t}\sigma_-(t) - i\dfrac{\sqrt{\Gamma}}{2}b_{\rm in}(t), & (4.86) \end{cases}$$

where we have defined

$$b_{\rm in}(t) = i\frac{1}{2\pi}\sum_n \frac{2\Omega_0}{\omega_c\rho_{n+1}\sqrt{\Gamma}}b_{n+1}\int_{-\omega_c}^{\omega_c} d\omega\, \pi_{n+1}(\omega/\omega_c)e^{-i(\omega-\omega_0+\delta)t}. \tag{4.87}$$

The reason for including a factor of $2/\sqrt{\Gamma}$ in (4.87) will become clearer later. All in all, the equations of motion are exact and have been derived while making no particular assumptions on the properties of the chain [see Eq. (4.25)]. This has been made possible by exploiting analytical properties of the Lorentzian spectral density. In such a way, the dynamical equation for $b_0(t)$ has a direct one-to-one correspondence with the simple pole of (4.47). The fact there is a single lower-half plane pole in Eq. (4.47), combined with a single principal mode of the chain, has been crucial in being able to identify the expression in Eq. (4.70) leading to the auxiliary equation of motion.

As is already quite noticable, but worth emphasising, is that because Eq. (4.86) contains the effect of both damping and noise on the principal mode, it holds exactly the same form as the previously encountered quantum Langevin equations from section 3.3 (chapter 3), and indeed for Eq. (4.52) too. We can then attach similar physical meaning to each of the terms in (4.86).

For sake of clarity let us restate their interpretation. The first term describes

the effect of incoherent damping on the principal mode. The second accounts for a unitary time evolution—which, along with Eq. (4.85), is attributed to the direct coupling of the principal mode to the atomic transition. The last term on the righthand side, containing both real and imaginary components, can be interpreted as noise arising from random fluctuations along the part of the chain without the principal mode. This comes with the caveat of assuming initially factorising states of the system and bath, as we recall from Eq. (3.4). If this is the case then it seems reasonable to examine the statistics of the noise $b_{\text{in}}(t)$ as a way of characterising the properties of the chain environment; which, in turn, helps us to gain better insight into the system-environment dynamics contained in the equations of the atom (4.85) and principal mode (4.86).

4.2.4 Noise term properties and interpretation

Before we do this, it first proves instructive to formally establish idea of the operator $b_{\text{in}}(t)$ as a noise input to the dynamics. We look at the equal-time commutator of the conjugate pair of states $b_0(t)$ and $b_0^\dagger(t)$ using the solution in Eqs. (4.70):

$$\begin{aligned}\left[b_0(t), b_0^\dagger(t)\right] &= \frac{1}{\Omega_0^2}\left[\xi(t), \xi^\dagger(t)\right] \\ &\quad - \frac{1}{\Omega_0^2}\left\{\left[\xi(t), \int_0^t dt' f^*(t-t')\sigma_+(t')\right] - \left[\xi^\dagger(t), \int_0^t dt' f(t-t')\sigma_-(t')\right]\right\} \\ &\quad + \Omega_0^2 e^{-\Gamma t}\int_0^t dt' \int_0^t dt'' e^{-(\Gamma/2)(t'-t'')}\left[\sigma_+(t'), \sigma_-(t'')\right]. \end{aligned} \tag{4.88}$$

Since the time evolution of the operators is unitary, the above reduces to much simpler form

$$\left[b_0(t), b_0^\dagger(t)\right] = \frac{1}{\Omega_0^2}\left\{U^\dagger(t)\left[\xi(0), \xi^\dagger(0)\right]U(t)\right\}. \tag{4.89}$$

The relation

$$\left[\xi(t), \xi^\dagger(t')\right] = f(t-t') \tag{4.90}$$

can be substituted into (4.89) to show

$$\left[b_0(t), b_0^\dagger(t)\right] = \left[b_0, b_0^\dagger\right] = 1 \quad \text{from} \quad f(0) = \Omega_0^2, \tag{4.91}$$

as we would expect. By comparing the two equivalent expressions in (4.88) and (4.89), it is also revealed that

$$\left[b_0(t), b_0^\dagger(t)\right] = \frac{1}{\Omega_0^2}\left[\xi(t), \xi^\dagger(t)\right] = 1. \tag{4.92}$$

This indicates the bottom two lines of Eq. (4.88) make no contribution to the commutator [see Eq. (3.39)]. Therefore, the time-invariance of the canonical commutation relation is solely maintained by the noise operator $\xi(t)$. To gain a more precise understanding, we can convert (4.92) into a more suggestive form by writing $\xi(t) = \xi_0(t) + \xi_c(t)$ (4.75),

$$\frac{1}{\Omega_0^2}\left[\xi(t), \xi^\dagger(t)\right] = \frac{1}{\Omega_0^2}\left\{\left[\xi_0(t), \xi_0^\dagger(t)\right] + \left[\xi_c(t), \xi_c^\dagger(t)\right]\right\}, \tag{4.93}$$

where we have used that $[\xi_0(t), \xi_c^\dagger(t)] = [\xi_c(t), \xi_0^\dagger(t)] = 0$. From its definition in Eq. (4.76), it is easy to show the first term decays exponentially at a rate provided by Γ. As a result the equal-time commutator in Eq. (4.92) comprises the two following components,

$$\begin{cases} \left[\xi_0(t), \xi_0^\dagger(t)\right] = \Omega_0^2 e^{-\Gamma t}, & (4.94) \\ \left[\xi_c(t), \xi_c^\dagger(t)\right] = \Omega_0^2(1 - e^{-\Gamma t}). & (4.95) \end{cases}$$

Notice the commutator (4.95) is consistent with that obtained from (4.77) at $t = 0$ by the property

$$\xi_c(0) = -i\sum_n \frac{\omega_c}{\rho_{n+1}} b_{n+1}\left\{\int_{-\omega_c}^{\omega_c} dk\, \widetilde{J}(k)\pi_{n+1}(k)\pi_0(k)\right\} = 0. \tag{4.96}$$

Suppose we ignore $\xi_c(t)$ and have it set to zero. Without the presence of the second term, it is clear that (4.92) would only be satisfied at times which are short compared to the correlation time of the environment, i.e. $t \ll \tau_B$, where $\tau_B \sim 1/\Gamma$ [1]. Since the noise term $b_{\text{in}}(t)$ originates from the time-derivative of $\xi_c(t)$, as we recall from (4.84), the dynamical equations for the atom and principal mode are therefore unphysical for times $t > \tau_B$. It is this aspect which is used to justify its interpretation as a noise—in that it preserves the commutation relation (4.92).

Two-point commutator $[b_{\text{in}}(t), b_{\text{in}}^\dagger(t')]$

Now we move onto investigate at the statistical properties of Eq. (4.87). A possible way to understand the stochastic effects encoded in $b_{\text{in}}(t)$ is to compare its statistics to that of $\xi(t)$. Since our original motivation was to embed the non-Markovian dynamics of the atom into that of an enlarged Markovian system, it is of interest to see if the chain noise operator holds properties that would suggest it can be approximated as Markovian white noise (see section 3.1.3).

Because the environment containing the full λ-modes is assumed *not* to be memoryless, $\xi(t)$ typically displays signatures of non-Markovian behaviour. Indeed, given the spectral density is a Lorentzian, the memory kernel behaves much differently to what is expected in the Markovian case: that is, a locally peaked function around $t = t'$. Only in the flat Lorentzian limit $\Gamma \to \infty$ does Eq. (4.90) give delta correlated statistics, which in turn can be associated to a quantum Markov process (see section 3.1.3). We now check to see if these properties are carried over to the noise operator $b_{\rm in}(t)$.

To obtain an explicit expression for the two-point commutator of $b_{\rm in}(t)$, we start by writing Eq. (4.87) as

$$b_{\rm in}(t) = \sum_n v_{n+1}(t) b_{n+1}. \tag{4.97}$$

with

$$v_{n+1}(t) = i\frac{1}{2\pi}\sum_n \frac{2\Omega_0}{\omega_c \rho_{n+1}\sqrt{\Gamma}} \int_{-\omega_c}^{\omega_c} d\omega\, \pi_{n+1}(\omega/\omega_c) e^{-i(\omega-\omega_0+\delta)t} \tag{4.98}$$

The relevant non-zero commutator is given by

$$\left[b_{\rm in}(t), b_{\rm in}^\dagger(t')\right] = \sum_{(n,n')>0} v_n(t) v_{n'}^*(t') \left[b_n, b_{n'}^\dagger\right] = \sum_n v_{n+1}(t) v_{n+1}^*(t'), \tag{4.99}$$

which explicitly reads

$$\left[b_{\rm in}(t), b_{\rm in}^\dagger(t')\right] = \frac{4\Omega_0^2}{\Gamma\left(2\pi\omega_c\right)^2} \sum_n \int_{-\omega_c}^{\omega_c} d\omega \int_{-\omega_c}^{\omega_c} d\omega' \frac{\pi_{n+1}(\omega/\omega_c)\pi_{n+1}(\omega'/\omega_c)}{(\rho_{n+1})^2} \times e^{-i(\omega-\omega_0+\delta)t} e^{i(\omega'-\omega_0+\delta)t'}. \tag{4.100}$$

This can be put into a more intelligible form by defining the kernel $K(\omega, \omega')$,

$$K(\omega,\omega') = \sum_n \frac{\pi_{n+1}(\omega/\omega_c)\pi_{n+1}(\omega'/\omega_c)}{(\rho_{n+1})^2}, \tag{4.101}$$

where

$$\left[b_{\rm in}(t), b_{\rm in}^\dagger(t')\right] = \frac{4\Omega_0^2}{\Gamma\left(2\pi\omega_c\right)^2} \int_{-\omega_c}^{\omega_c} d\omega \int_{-\omega_c}^{\omega_c} d\omega' K(\omega,\omega') e^{-i(\omega-\omega_0+\delta)t} e^{i(\omega'-\omega_0+\delta)t'}. \tag{4.102}$$

Under the first Markov approximation the spectral density is replaced with $J(\omega) = \gamma_0/2\pi$ [see Eq. (3.54)], where $\gamma_0 = 4\Omega_0^2/\Gamma$ is the Markovian decay rate of the atom. Now, since the weight function $\widetilde{J}(k)$ is independent of frequency, the polynomials

$\pi_n(k)$ coincide exactly with the Legendre polynomials $P_n(k)$ [93]: these are defined with respect to the orthogonality relation

$$\int_{-1}^{1} dk\, P_n(k)P_{n'}(k) = (\rho_n)^2\delta_{n,n'}, \quad \text{where} \quad (\rho_n)^2 = \frac{2}{2n+1}. \tag{4.103}$$

In this particular case the kernel (4.101) $K(\omega,\omega') \to K_M(\omega,\omega')$ reads

$$K_M(\omega,\omega') = \frac{1}{2}\sum_n (2n+1)P_n(\omega'/\omega_c)P_n(\omega/\omega_c) - \frac{1}{2}. \tag{4.104}$$

having used $P_0(k) = 1$. We note the factor of $1/2$ on the righthand side of the above makes zero contribution to the double integral (4.101). This can be shown by evaluating the integral $\int_{-\omega_c}^{\omega_c} d\omega \exp[-i\omega t]$, which yields a factor of $\sim \sin(\omega_c t)/t$ for $\omega_c \gg \omega_0$. Since we are also assuming $t \gg 1/\omega_c$, the last term of (4.104) is zero for $t > 0$. Writing the above in the form

$$K_M(\omega,\omega') = \frac{1}{2}\sum_n (2n+1)P_n(\omega'/\omega_c)P_n(\omega/\omega_c), \tag{4.105}$$

then shows the kernel satisfies $K_M(\omega,\omega') \propto \delta(\omega-\omega')$ from the known identity [98]

$$\delta(k-k') = \frac{1}{2}\sum_n (2n+1)P_n(k')P_n(k). \tag{4.106}$$

Plugging (4.105) into (4.101) provides us with

$$\left[b_{\text{in}}(t), b_{\text{in}}^\dagger(t')\right] \sim \delta_c(t-t'), \tag{4.107}$$

where we have defined

$$\frac{1}{2\pi}\int_{-\omega_c}^{\omega_c} d\omega\, e^{-i(\omega-\omega_0+\delta)(t-t')} = \delta_c(t-t'). \tag{4.108}$$

This is a slowly varying function provided the timescales we are interested in fulfil $|t-t'| \gg 1/\omega_c$. Seeing as we are working in the regime set by Eq. (4.55), clearly, the inverse of the cut-off frequency defines fastest timescale of the problem, and so $\delta_c(t-t') \approx \delta(t-t')$. Taking the hard Markov limit $\Gamma \to \infty$ simply recovers the usual time-local features that we would envisage for a weakly perturbed atomic system.

We now examine the case of a more general Lorentzian coupling profile. Figure 4.3 shows the kernel $K(\omega,\omega')$ plotted as a function of ω (i.e. fixed ω') where it is taken up to the first N terms in its series. The plots have been obtained using a routine `stieltjes.m` from Ref. [99] which has been implemented with Mathworks

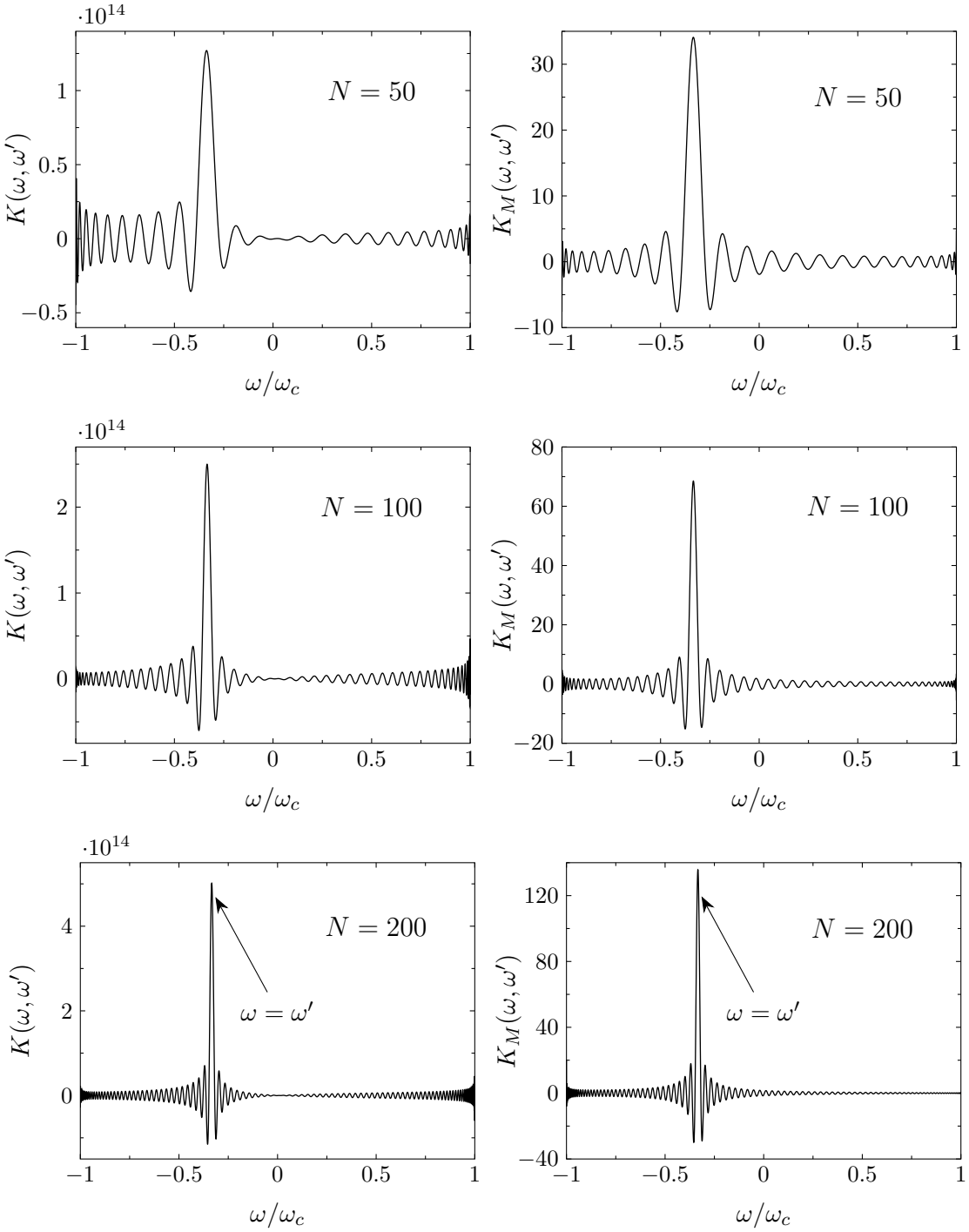

Figure 4.3: Frequency kernel (4.101) plotted as a function of ω for a varying number of terms N in its series, with $\omega' \approx -\omega_c/3$ and $\delta = 0$. The lefthand column (a,c,e) is shown for parameters $\Gamma = 0.1\Omega_0$, $\omega_0 = 10^{-2}\omega_c$, $\Omega_0 = 10^{-4}\omega_c$. The righthand column (b,d,e) shows the Markovian kernel $K_M(\omega, \omega')$ for comparison. Notice the different scaling between axes.

software, Matlab, for a fixed number of chain oscillators $n_c = 10^4$. For comparison, examples of the Markovian kernel $K_M(\omega, \omega')$ are displayed alongside those of

$K(\omega,\omega')$[2]. Let us first comment on the features of the Markovian kernel with reference to Eqs. (4.105) and (4.106). We immediately notice that the function is highly oscillatory, with a sharp peak centred on $\omega=\omega'$. It also has fringes which become more closely spaced together towards the edges of the plot. These features reinforce the idea that in limit $n_c, N\to\infty$, the kernel characterises a delta function, which, subsequently, leads to the two-point commutator in (4.107). Interestingly, for strong system-environment coupling, we a see striking qualitative resemblance between the kernel $K(\omega,\omega')$ and the Markovian one—the most important feature being a sharp localised peak at $\omega=\omega'$. We then expect (4.101) to converge to a delta function as $N\to\infty$. In fact, from Eq. (4.11), the continuum relation

$$\sum_n \frac{\pi_n(\omega/\omega_c)\pi_n(\omega'/\omega_c)}{(\rho_n)^2}=\frac{1}{\widetilde{J}(k)}\delta(k-k') \tag{4.109}$$

proves that the frequency kernel can be replaced by the following:

$$K(\omega,\omega')=\frac{1}{\omega_c^2}\sum_n \frac{\pi_{n+1}(\omega/\omega_c)\pi_{n+1}(\omega'/\omega_c)}{(\rho_{n+1})^2}\longrightarrow\frac{1}{J(\omega)}\delta(\omega-\omega'), \tag{4.110}$$

which indeed adopts the properties of a weighted delta function. Note the above is valid as the $n=0$ term in (4.109) makes no contribution under the integral. Therefore, without introducing any assumption on the commutator so far, the double integral in Eq. (4.102) reduces to

$$\left[b_{\rm in}(t),b_{\rm in}^\dagger(t')\right]=\frac{\gamma_0}{(2\pi)^2}\int_{-\omega_c}^{\omega_c}d\omega\frac{1}{J(\omega)}e^{-i(\omega-\omega_0+\delta)(t-t')}. \tag{4.111}$$

Here it is realised $b_{\rm in}(t)$ generally exhibits non-time local behaviour. In order to simplify the analysis, we look to impose a white noise approximation as a way to produce a time-local commutator. With a change of variable, (4.111) reads ($\omega_c\gg\omega_0$)

$$\left[b_{\rm in}(t),b_{\rm in}^\dagger(t')\right]\approx\frac{\gamma_0}{(2\pi)^2}\int_{-\omega_c}^{\omega_c}d\omega\frac{1}{J'(\omega)}e^{-i\omega(t-t')}, \tag{4.112}$$

where $J'(\omega)=J(\omega+\omega_0-\delta)$. For the timescales we are interested in [see (4.55)], if it's assumed the function $1/J'(\omega)$ is slowly-varying enough such that it can approximately be replaced by its value at $\omega\approx 0$ under the the integral ($J(0)=\gamma_0/2\pi$), then we in fact discover

$$\left[b_{\rm in}(t),b_{\rm in}^\dagger(t')\right]\approx\delta_c(t-t'),\qquad\forall t,t'\geq 0, \tag{4.113}$$

[2]From here on we assume $K(\omega,\omega')$ is amended to include the extra term $1/\rho_0^2$, which cancels in (4.102).

with $\delta_c(t-t')$ defined in Eq. (4.108). Notice the scaling adopted in (4.87) was made to ensure there are no extra factors in front of the delta function.

The above implies that it is adequate to approximate the two-point commutator as white noise in the current model. This is, of course, an idealisation of the actual effect the residual environment has on the principal mode of the the chain. However, the benefit of such a simplification—loss of exactness aside—is that it forms a dynamical picture which is much more intuitive and easier to understand than its alternative, as we shall go onto examine shortly. Indeed, in any case it is known that no noise is ever truly Markovian [100], but in many circumstances serves as a very good approximation. Note also that (4.111) is consistent with the result in the limit $\Gamma \to \infty$ (i.e. $J(\omega) = \gamma_0/2\pi$), where we expect $[b_{\rm in}(t), b_{\rm in}^\dagger(t')] = \delta_c(t-t')$.

Input-output representation

How do these results affect our current picture of the system-environment dynamics? Recall how $b_{\rm in}(t)$ encodes properties of the residual chain ($n > 0$). In view of the delta-commutator property (4.113), we can then deduce that the residual part of the chain has a Markovian dissipative effect on the dynamics. This would imply we can attach an input-output interpretation to the dynamical model, where $b_{\rm in}(t)$ acts in the same way as an "input field" in the Gardiner-Collet description of a conventional Markov stochastic process [2, 81]. To give weight to this idea, we replace $H_I(t)$ defined in (4.39) with the phenomenological (interaction picture) input-output Hamiltonian

$$H_{{\rm eff},I}(t) = \Omega_0 \left(e^{i\delta t}\sigma_+ b_0 + \text{h.c.}\right) + \sqrt{\Gamma}\left(b_{\rm in}^\dagger(t) b_0 + \text{h.c.}\right), \tag{4.114}$$

and attempt to show it can be used to reproduce Eqs. (4.85)-(4.86) using the Heisenberg equations. Because the atom only couples directly to the principal mode, it is easy verify that (4.85) results from placing the above into Eq. (4.67). The dynamical equations for the chain oscillators read

$$\frac{d}{dt}b_0(t) = -i\Omega_0 e^{-i\delta t}\sigma_-(t) - i\sqrt{\Gamma}b_{{\rm in},H}(t), \tag{4.115}$$

$$\frac{d}{dt}b_{n+1}(t) = -i\sqrt{\Gamma}v_{n+1}^*(t)b_0(t), \qquad n = 0, 1, \ldots, \tag{4.116}$$

where

$$b_{\text{in},H}(t) = \sum_n v_{n+1}(t) b_{n+1}(t). \tag{4.117}$$

By directly integrating (4.116) and substituting the result into (4.115), we obtain

$$\begin{aligned}\frac{d}{dt}b_0(t) = &-i\Omega_0 e^{-i\delta t}\sigma_-(t) - i\sqrt{\Gamma}b_{\text{in}}(t) \\ &- \Gamma\int_0^t dt' \sum_n v_{n+1}(t) v_{n+1}^*(t') b_0(t').\end{aligned} \tag{4.118}$$

Notice the last line contains the commutator (4.99). Applying the identities

$$\left[b_{\text{in}}(t), b_{\text{in}}^\dagger(t')\right] = \sum_n v_{n+1}(t) v_{n+1}^*(t') \approx \delta(t-t') \tag{4.119}$$

and

$$\Gamma\int_0^t dt' \delta(t-t') b_0(t') = \frac{\Gamma}{2} b_0(t) \tag{4.120}$$

thereby provides us with

$$\frac{d}{dt}b_0(t) = -\frac{\Gamma}{2}b_0(t) - i\Omega_0 e^{-i\delta t}\sigma_-(t) - i\sqrt{\Gamma}b_{\text{in}}(t). \tag{4.121}$$

Interestingly, the equation has the same form as (4.86) but with a different prefactor on the term $b_{\text{in}}(t)$. While this may be problematic, as part of the following section we shall prove—using the Heisenberg-Langevin equation—that in certain situations the phenomenological Hamiltonian (4.114) describing a quantum Markov stochastic dynamics is consistent with the dynamical equations (4.85)-(4.86) originating out of the chain Hamiltonian. Such consistency is important as it shows that the original setup, where the atom-reservoir interaction is characterised by a Lorentzian spectral density (4.47), is described equally in terms of an enlarged system in our chain model with Markovian damping. This is also reflected in the Lindbladian form of the master equation for the enlarged system, as we will now show.

4.3 The master equation

Since we have identified a time-local quantum Langevin equation, in this section we employ the techniques demonstrated in chapter 3 to derive the corresponding master equation. We reiterate that the main idea is to treat the dynamics of principal mode and the atom collectively in the Hilbert space of an enlarged system. In view

of (4.86), this system couples to a residual part of the environment through the principal mode, which acts to mediate the effect of dissipation on the atom.

To derive such a master equation, it is first acknowledged that the dynamical equations for $\sigma_-(t)$ and $b_0(t)$ should be consistent with the form of the Heisenberg-Langevin equation associated with the Hamiltonian (4.53). Let us recall parts of the formalism of section 3.2. Here, the operator equation of motion for L ($L^\dagger$), i.e the operator coupling the open system to the reservoir, is seen to determine the effect of dissipation and noise entering in from the term $B(t)$ [see Eq. (3.44)]. We then anticipate the same will be provided by the quantum Langevin equations for $b_0(t)$ and $b_0^\dagger(t)$. Obtaining the Heisenberg-Langevin equation will require treating the modes in the chain beyond $n = 0$ as an environment, acting on the enlarged system. This is necessary to ensure that the equation $d_t A(t)$ will result in a closed form expression with all environment (and noise) operators formally eliminated from the dynamics.

We notice this is made possible by virtue of the Szegö class property (4.25). Suppose we have an asymptotic region of the chain where the parameters ϵ_n and λ_n are independent of n. We can then show that the Hamiltonian of such a region can be expressed as a single quadratic term—like that in Eq. (3.5)—by a straightforward diagonalisation procedure. This is first illustrated by rewriting Eq. (4.53) into a more suitable form,

$$H = \omega_0 \sigma_+ \sigma_- + \Omega_0 \left(\sigma_+ b_0 + \text{h.c.}\right) + \sum_{n=0}^{m-1} \left(\lambda_n b_{n+1}^\dagger b_n + \epsilon_n b_n^\dagger b_n + \text{h.c.}\right) + \epsilon_m b_m^\dagger b_m + \sum_{n>m} \left(\lambda b_{n+1}^\dagger b_n + \epsilon b_n^\dagger b_n + \text{h.c.}\right). \tag{4.122}$$

The "flat" part of the chain, with Hamiltonian

$$H_R = \sum_{n>m} \left(\lambda b_{n+1}^\dagger b_n + \epsilon b_n^\dagger b_n + \text{h.c.}\right), \tag{4.123}$$

comprises a tridiagonal matrix, and is diagonalized by means of the following:

$$c_j = \sum_n V_{n,j} b_{n+m}, \tag{4.124}$$

$$c_j^\dagger = \sum_n V_{n,j} b_{n+m}^\dagger, \quad n, j = 1, 2, \dots, \tag{4.125}$$

with $H_R = V H_R V^T$ and $H_R = \text{diag}[\tilde{\omega}_1, \tilde{\omega}_2, \dots]$. The label m denotes the terminal mode of the chain, while the components of the matrix V are given in terms of a

Fourier sine transform on the n-modes,

$$V_{n,j} = \sqrt{\frac{2}{\pi}} \sin(nj), \qquad 0 \leq j \leq \pi. \tag{4.126}$$

The orthogonality property of the sine terms, which explicitly reads

$$\int_0^\pi dj \, \sin(nj) \sin(n'j) = \frac{\pi}{2} \delta_{n,n'}, \tag{4.127}$$

guarantees that the bosonic commutation relations of the principle mode are upheld. Furthermore, having the closure relation $\sum_{n=1}^{\infty} \sin(nj) \sin(nj') = \frac{\pi}{2} \delta_{j,j'}$ also provides

$$\left[c_j, c_{j'}^\dagger \right] = \delta_{j,j'}, \tag{4.128}$$

with all other commutators vanishing.

In order for the resulting Heisenberg-Langevin equation to match with the description provided by the quantum Langevin (4.86) it is necessary to assume $m = 0$, meaning the diagonalisation is taken over the full chain except for the principal mode. While the decomposition of the reservoir into a single damped oscillator and Markovian bath fits exactly with pseudomode description we duly recognise, however, there is no reason to make this choice without first checking for the convergence of the recurrence coefficients (4.33). In an effort to avoid having to rely on specific numerical traits of ϵ_n and λ_n to derive the master equation, currently we shall only pursue the fundamental case where a single harmonic oscillator is embedded into the open system, and as such take the residual chain (i.e. beyond $n = 0$) to be flat. The fact that the dynamics of the joint atom and principal mode conform to a quantum Markov process [cf. (4.114)] implies this is a reasonable approximation. We defer further discussion on this point to the final section of the chapter, section 4.4.

Single oscillator embedding: $m = 0$

In a setting where $m = 0$ the principal mode is locally coupled to a continuum of bosonic modes c_j ($c_j^\dagger$) which in turn interacts directly with the atom. This is clearly understood from the hierarchical structure of the Hamiltonian $H = H_S' + H_I' + H_R$, which has explicit components

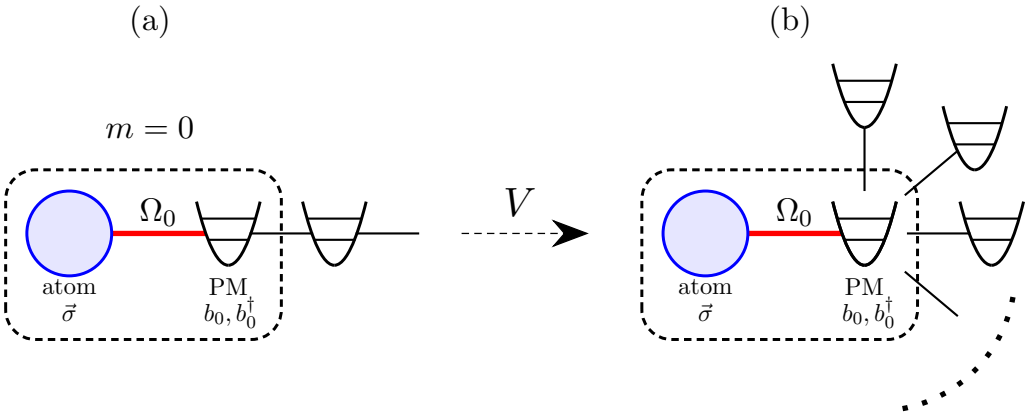

Figure 4.4: Schematic of the atom and environment. (a) Shows the full system representation prior to diagonalising (4.123) using V. Here, the principal mode (PM) is included into part of an enlarged system with the atom, assuming $m = 0$. (b) Depicts the enlarged system interacting locally with a continuum of normal modes.

$$\begin{cases} H'_S = \omega_0 \sigma_+ \sigma_- + (\omega_0 - \delta) b_0^\dagger b_0 + \Omega_0 \left(\sigma_+ b_0 + \text{h.c.}\right), \\ H'_I = \sum_j \kappa_j \left(b_0^\dagger c_j + \text{h.c.}\right), \\ H_R = \sum_j \tilde{\omega}_j c_j^\dagger c_j. \end{cases} \tag{4.129}$$

Figure 4.4 shows a schematic representation of the model. The normal mode frequencies $\tilde{\omega}_j$ and couplings κ_j of the reservoir R are defined as

$$\tilde{\omega}_j = -2\sqrt{\lambda}\cos(j), \tag{4.130}$$

$$\kappa_j = \sqrt{\frac{2\lambda}{\pi}}\sin(j), \tag{4.131}$$

where

$$\lambda = \omega_c \lim_{n\to\infty} \beta_n = \left(\frac{\omega_c}{2}\right)^2. \tag{4.132}$$

The reservoir has a plane wave excitation spectrum supported across $(-\omega_c, \omega_c)$ from the additional property $\lim_{n\to\infty} \epsilon_n = 0$. Note we have made the additional transformation $b_k \to (-1)^k b_k$ [92], so conveniently the lowest value of $j = j(\tilde{\omega})$ corresponds to ground state energy of the normal modes.

We can now apply the techniques of section 3.3.2 used in the derivation of the master equation (3.85), which here is to be performed in a rotating frame defined by the free Hamiltonian H'_0 (4.64). As was discussed at the beginning of the current section, this first requires us to obtain the Heisenberg-Langevin equation in the form

of (3.45). For brevity we will not work through the full steps of the derivation since the equation follows directly from the methods of the previous chapter. Instead, we just provide the result:

$$\frac{d}{dt}\hat{A}(t) = -i\left[A(t), H'_{S,H}(t)\right] + \left[A(t), b_0^\dagger(t)\right]\left(\frac{d}{dt}b_0(t) + i\Omega_0 e^{-i\delta t}\sigma_-(t)\right) + \left(\frac{d}{dt}b_0^\dagger(t) - i\Omega_0 e^{i\delta t}\sigma_+(t)\right)\left[b_0(t), A(t)\right], \tag{4.133}$$

This has been derived considering an observable of the enlarged system, i.e. $A(t) \to A_{SP}(t) \otimes 1_R$, and where $H'_S(t)$ is defined by

$$H'_{S,H}(t) = \Omega_0\left(e^{i\delta t}\sigma_+(t)b_0(t) + \text{h.c.}\right). \tag{4.134}$$

Notice the "H" label has been temporarily re-introduced to make clear that the time-dependence of $H'_{S,H}(t)$ originates from the (rotating frame) Heisenberg picture. Since (4.86) is time-local, it can be directly substituted into (4.133) along with its adjoint to provide us with

$$\begin{aligned}\frac{d}{dt}\hat{A}(t) = -i\left[A(t), H'_{S,H}(t)\right] &- \frac{\Gamma}{2}\left(\left[A(t), b_0^\dagger(t)\right]b_0(t) + b_0^\dagger(t)\left[b_0(t), A(t)\right]\right) \\ &+ \frac{\sqrt{\Gamma}}{2}\left(e^{-i\delta t}\left[A(t), b_0^\dagger(t)\right]b_{\text{in}}(t) + e^{i\delta t}b_{\text{in}}^\dagger(t)\left[b_0(t), A(t)\right]\right).\end{aligned} \tag{4.135}$$

Furthermore, taking the mean and expanding out of the commutators in the top line of (4.135) leads to

$$\begin{aligned}\frac{d}{dt}\langle\hat{A}\rangle_t = -i\left\langle\left[A(t), H'_{S,H}(t)\right]\right\rangle &- \frac{\Gamma}{2}\left(\left\langle A(t)b_0^\dagger(t)b_0(t)\right\rangle + \left\langle b_0^\dagger(t)b_0(t)A(t)\right\rangle - 2\left\langle b_0^\dagger(t)A(t)b_0(t)\right\rangle\right) \\ &+ \frac{\sqrt{\Gamma}}{2}\left(e^{-i\delta t}\left\langle\left[A(t), b_0^\dagger(t)\right]b_{\text{in}}(t)\right\rangle + e^{i\delta t}\left\langle b_{\text{in}}^\dagger(t)\left[b_0(t), A(t)\right]\right\rangle\right),\end{aligned} \tag{4.136}$$

where it is now left to evaluate the bottom row of (4.136).

Zero temperature environment

At this point we shall focus our attention on the zero temperature limit—that is, where the residual environment is initially in the vacuum state $|\{0\}\rangle_R = |0\rangle_R$. Because the reservoir is empty at $t = 0$ the average of $A(t)$ is taken with respect to

$\rho = \rho_{SP} \otimes (|0\rangle\langle 0|)_R$. The contribution from the last line of terms in Eq. (4.136) then vanishes since

$$b_{\rm in}(t)\,|0\rangle_R = 0 =_R \langle 0|\, b_{\rm in}^\dagger(t), \quad \text{from} \quad c_j\,|0\rangle_R = 0. \tag{4.137}$$

As a result, we obtain the equation

$$\begin{aligned}\frac{d}{dt}\langle \hat{A}\rangle_t = &-i\left\langle \left[A(t), H'_{S,H}(t)\right]\right\rangle \\ &-\frac{\Gamma}{2}\left(\left\langle A(t)b_0^\dagger(t)b_0(t)\right\rangle + \left\langle b_0^\dagger(t)b_0(t)A(t)\right\rangle - 2\left\langle b_0^\dagger(t)A(t)b_0(t)\right\rangle\right).\end{aligned} \tag{4.138}$$

We can readily identify the interaction picture master equation for our damped atom-oscillator system by following the same steps previously outlined in Eqs. (3.85)-(3.89). Through doing so, we get

$$\frac{d}{dt}\rho_{SP}(t) = \mathcal{L}_{SP}[\rho_{SP}(t)] = -i\left[H'_S(t), \rho_{SP}(t)\right] + \Gamma\,\mathcal{L}_{b_0}[\rho_{SP}(t)] \tag{4.139}$$

with

$$H'_S(t) = \Omega_0\left(e^{i\delta t}\sigma_+ b_0 + \text{h.c.}\right), \tag{4.140}$$

and

$$\mathcal{L}_{b_0}[\cdot] = b_0 \cdot b_0^\dagger - \frac{1}{2}\left\{b_0^\dagger b_0, \cdot\right\}. \tag{4.141}$$

Equation (4.139) is equivalent to the master equation obtained in Ref. [38] using the pseudomode method. Therefore, in the same way a Lorentzian spectral density associates with a single pseudomode, here the principal mode of the chain adopts the role of the pseudomode. In turn, the model can be directly mapped to the atom-cavity system, where the auxiliary mode is identified as the real leaky cavity mode with decay rate Γ.

Because the generator $\mathcal{L}_{SP}[\cdot]$ is of standard Liouvillian form the Lindblad theorem [cf. Eq. (2.75)] guarantees Eq. (4.139) to be Markovian. In view of this aspect, we notice the exact same averaged Heisenberg-Langevin equation (4.138) can be derived using the phenomenological Hamiltonian (4.114) and its associated quantum Langevin equation (4.121). Our current treatment is thus consistent with previous Markovian interpretation of the noise input $b_{\rm in}(t)$ for a vacuum reservoir. Note we can also use (4.124) to compute ensemble properties of the input noise. Starting with the correlation function

$$\left\langle b_{\rm in}(t)b_{\rm in}^\dagger(t')\right\rangle = \sum_{(n,n')>0} v_n(t)v_{n'}^*(t')\left\langle b_n b_{n'}^\dagger\right\rangle, \tag{4.142}$$

it can be shown that the bosonic expectation value $\langle b_n b_{n'}^\dagger \rangle$ satisfies

$$\left\langle b_n b_{n'}^\dagger \right\rangle = \sum_{j,j'} V_{n,j} V_{n',j} \left\langle c_j c_{j'}^\dagger \right\rangle = \delta_{n,n'}. \tag{4.143}$$

Hence, we have

$$\left\langle b_{\text{in}}(t) b_{\text{in}}^\dagger(t') \right\rangle = \sum_n v_{n+1}(t) v_{n'+1}^*(t') \approx \delta(t-t'), \tag{4.144}$$

with all other averages vanishing. Again, this demonstrates the applicability of Eqs. (4.85), (4.86) and (4.138) to collectively describing a Markovian stochastic process. The resulting dynamical picture we then have is straightforward to interpret: here, the atom-principal system experiences a bipartite Markovian dynamics from interacting with a residual (chain) reservoir. Non-Markovian effects in the atom are solely accounted for via its coupling to the auxiliary (prinicpal) mode.

4.3.1 Decay of a single excitation

To further illustrate the connection with the pseudomode method we consider a single initial excitation in the atom, with all other parts of the environment in vacuum. In such a case the dynamics can be formulated within the *single excitation manifold*, since the total excitation number $N = \sigma_+\sigma_- + b_0^\dagger b_0 + \sum_j c_j^\dagger c_j$ is a conserved quantity under the action of H: that is,

$$[H, N] = [H_S'(t) + H_I'(t), N] = 0, \tag{4.145}$$

with $H_I'(t)$ defined in the interaction picture with respect to H_0'.

Suppose now that the atom prepared in the state $|\psi\rangle_S = c_g |g\rangle + c_e(0) |e\rangle$. After a time t, the atom can at most randomly emit one photon into the reservoir through the principal mode, while its ground state—along with that of the environment—does not jointly evolve since $H|0\rangle = 0$. Here, $|0\rangle = |g\rangle \otimes |00\rangle$ indicates the ground state of the atom, principal mode and reservoir, respectively. The global solution can therefore be written as a pure state truncated in the one-excitation sector:

$$|\psi(t)\rangle = c_g |0\rangle + c_e(t)\sigma_+ |0\rangle + b(t) b_0^\dagger |0\rangle + \sum_j r_j(t) c_j^\dagger |0\rangle, \tag{4.146}$$

where the state coefficients satisfy

$$|c_g|^2 + |c_e(t)|^2 + |b(t)|^2 + \sum_j |r_j(t)|^2 = 1. \tag{4.147}$$

By sandwiching each of the terms in (4.85)-(4.86) between $\langle 0|$ and $|\psi(0)\rangle$, we can derive an equivalent set of equations describing the evolution of the coefficients (4.146) within the interaction picture. For example, with the relation

$$\langle 0|\, \sigma_-(t)\, |\psi(0)\rangle = \langle 0|\, \sigma_-\, |\psi(t)\rangle = c_e(t) \tag{4.148}$$

and similarly $\langle 0|\, b_0\, |\psi(t)\rangle = b(t)$, $\langle 0|\, \sigma_z(t)\, |0\rangle = -1$ and $\langle 0|\, c_j\, |\psi(0)\rangle = 0$, we obtain the following:

$$\frac{d}{dt}c_e(t) = -i\Omega_0 e^{i\delta t} b(t), \tag{4.149}$$

$$\frac{d}{dt}b(t) = -\frac{\Gamma}{2}b(t) - i\Omega_0 e^{-i\delta t} c_e(t). \tag{4.150}$$

For a Lorentzian spectral density (4.47) the exact same equations are generated by introducing an unnormalised state of the atom and principal mode,

$$|\widetilde{\psi}(t)\rangle = c_g\, |g,0\rangle + c_e(t)\sigma_+\, |g,0\rangle + b(t) b_0^\dagger\, |g,0\rangle\,, \tag{4.151}$$

where $|g,0\rangle$ explicitly denotes the ground state of the atom and principal mode (pseudomode). The state itself obeys the effective Schrödinger equation,

$$\frac{d}{dt}\, |\widetilde{\psi}(t)\rangle = -i\left(H'_S(t) - i\frac{\Gamma}{2} b_0^\dagger b_0\right) |\widetilde{\psi}(t)\rangle\,. \tag{4.152}$$

with effect of dissipation (and decoherence) accounted for through the non-hermitian Hamiltonian

$$H_{\text{eff}}(t) = H'_S(t) - i\frac{\Gamma}{2} b_0^\dagger b_0. \tag{4.153}$$

The physical interpretation attached to (4.152) is rooted in a stochastic description of the system dynamics. In this approach, the wavefunction $|\widetilde{\psi}(t)\rangle$ provides the evolution of the populations and coherences of the atom and cavity field under damping. This is noticed by initially writing master equation in form

$$\frac{d}{dt}\rho_{SP}(t) = -i\left[H_{\text{eff}}(t)\rho_{SP}(t) - \rho_{SP}(t) H_{\text{eff}}^\dagger(t)\right] + \Gamma\, b_0 \rho_{SP}(t) b_0^\dagger. \tag{4.154}$$

Now, by decomposing the density matrix into the mixture

$$\rho_{SP}(t) = \rho_{SP}^J(t) + \rho_{SP}^{NJ}(t), \tag{4.155}$$

we can associate the unconditioned dynamics of the atom and principal mode in Eq. (4.152) with the pure state $\rho_{SP}^{NJ}(t) = |\widetilde{\psi}(t)\rangle\langle\widetilde{\psi}(t)|$. Taking its time-derivative yields

$$\frac{d}{dt}\rho_{SP}^{NJ}(t) = -i\left[H_S'(t), \rho_{SP}^{NJ}(t)\right] - \frac{\Gamma}{2}\left\{b_0^\dagger b_0, \rho_{SP}^{NJ}(t)\right\}, \tag{4.156}$$

whose form agrees closely with the bracketed term on the righthand side of Eq. (4.154). We can then go onto derive an exact expression for the other term $\rho_{SP}^{J}(t)$ by considering the normalisation properties of $\rho_{SP}(t)$—that is, using the fact that the trace should fulfil $\mathrm{tr}\left[\rho_{SP}(t)\right] = 1$. Clearly this is made up from $\rho_{SP}^{J}(t)$, since

$$\mathrm{tr}\,\rho_{SP}^{NJ}(t) = \langle\widetilde{\psi}(t)|\widetilde{\psi}(t)\rangle \leq 1, \qquad t \geq 0. \tag{4.157}$$

Over a typical stochastic trajectory, the continuous dynamics of the atom and cavity mode will be interrupted by a jump process, which occurs at random time with given probability. Let us consider this in relation to $\rho_{SP}^{J}(t)$. Because the excitation is in the atom at $t = 0$, the additional term should account for the increase in the probability of the atom being left in the ground state after an emission of a photon. Equation (4.157) provides us with an expression for this probability, where $\mathrm{tr}\rho_{SP}^{J}(t) \equiv \Pi_g(t) = 1 - \langle\widetilde{\psi}(t)|\widetilde{\psi}(t)\rangle$. Taking the time-derivative of this yields

$$\frac{d}{dt}\Pi_g(t) = -\frac{d}{dt}\langle\widetilde{\psi}(t)|\widetilde{\psi}(t)\rangle = \Gamma|b(t)|^2. \tag{4.158}$$

We can interpret $d_t\Pi_g(t)$ as probability density of flux: in this sense, the probability $p(t)$ that the excitation decays between times t and $t + dt$ is given by

$$p(t) = \Gamma|b(t)|^2 dt. \tag{4.159}$$

Simply integrating Eq. (4.158) up to a time t then determines the probability of the atom and principal mode being in their ground state as function of time,

$$\Pi_g(t) = \Gamma\int_0^t dt'|b(t')|^2, \tag{4.160}$$

which is also understood as vacuum population of $S+P$. Note that, by construction, $|c_e(t)|^2 + |b(t)|^2 + \Pi_g(t) = 1$. The complete density matrix is therefore given as

$$\rho_{SP}(t) = \Pi_g(t)\,|g\rangle\langle g| \otimes (|0\rangle\langle 0|)_P + |\widetilde{\psi}(t)\rangle\langle\widetilde{\psi}(t)|_{SP}\,, \tag{4.161}$$

with it being straightforward to show that $\rho_{SP}(t)$ satisfies the master equation (4.139). To finalise our result in the single excitation limit, our solution in Eq.

(4.146) shows agreement with the stochastic approach. Indeed, by tracing out the environment state in the density matrix of the pure state (4.146) to obtain $\rho_{SP}(t) = \mathrm{tr}_R \left|\psi(t)\right\rangle \left\langle\psi(t)\right|$, we find

$$\rho_{SP}(t) = \sum_j |r_j(t)|^2 \left|g\right\rangle \left\langle g\right| \otimes \left(\left|0\right\rangle \left\langle 0\right|\right)_P + \left|\widetilde{\psi}(t)\right\rangle \left\langle\widetilde{\psi}(t)\right|_{SP}, \tag{4.162}$$

where we identify

$$\Pi_g(t) = \sum_{j,j'} \left\langle 0\right| c_j H_R c_{j'}^\dagger \left|0\right\rangle = \sum_j |r_j(t)|^2, \tag{4.163}$$

granted $c_j c_{j'}^\dagger \left|0\right\rangle_R = \delta_{j,j'} \left|0\right\rangle_R$. Equivalency of the populations $\Pi_g(t)$ and $\sum_j |r_j(t)|^2$ entirely makes sense from conservation of probability, seeing as the latter provides the vacuum population of the combined atom-pseudomode system. In light of the consistency between (4.146) and the mixed state solution (4.161) obtained via the pseudomode method, we proceed to now extend the formalism beyond the single excitation case.

4.3.2 Decay of multiple excitations

Because our treatment of the dynamics prior to arriving at the Heisenberg-Langevin equation (4.138) relies exclusively on Heisenberg picture operators, the only restrictive assumption we've made is to assume that the reservoir R is initialised in the vacuum state. Therefore, the master equation—which, interestingly, adopts the same form to usual single excitation pseudomode derivation—has been proven to be valid for any choice of state $\rho_{SP}(t)$ at $t = 0$. This allows us to go beyond usual applications of the method since we are not restricted to single excitation manifold. To this end, we can attempt to setup a generic solution to Eq. (4.139) by deriving a closed set of equations of motion for, e.g. $\langle\sigma_+\sigma_-\rangle_t$ and $\langle b_0^\dagger b_0\rangle_t$. As it happens these observables have an exact dynamics provided by the previous operator equations (4.85) and (4.86):

$$\frac{d}{dt}\langle\sigma_+\sigma_-\rangle_t = -2\Omega_0 \,\mathrm{Im}\left[e^{-i\delta t}\langle b_0^\dagger\sigma_-\rangle_t\right], \tag{4.164}$$

$$\frac{d}{dt}\langle b_0^\dagger b_0\rangle_t = -\Gamma\langle b_0^\dagger b_0\rangle_t + 2\Omega_0 \,\mathrm{Im}\left[e^{-i\delta t}\langle b_0^\dagger\sigma_-\rangle_t\right], \tag{4.165}$$

where we also have

$$\frac{d}{dt}\langle b_0^\dagger\sigma_-\rangle_t = -\frac{\Gamma}{2}\langle b_0^\dagger\sigma_-\rangle_t + i\Omega_0 e^{i\delta t}\left(\langle\sigma_+\sigma_-\rangle_t + \langle b_0^\dagger\sigma_z b_0\rangle_t\right). \tag{4.166}$$

Note it is sufficient to only assume the reservoir starts in the state $\rho_R = |0\rangle\langle 0|_R$ to obtain these expressions, so that any term containing $b_{\text{in}}(t)$ is zero. Other assumptions, e.g. the Born approximation, are unnecessary—as was implied during the derivation of the master equation (4.139).

The above equal-time differential equations make up part of a moment hierarchy [86, 101], which, in principle, can be used to compute any observable or state-based quantity of interest for the open system—with the disadvantage of not being practical to solve as generally the equations are not a closed set. While (4.164) and (4.165) are of closed form, Eq. (4.166) contains a surplus term depending on the inversion operator $\sigma_z(t)$ of the atom multiplying the creation/annihilation operators of the principal mode, adding a non-linear type effect on the dynamics. Such a term needs to be treated under approximation if the moment hierarchy is to be solvable analytically.

To explore this idea, it is worth examining the limit of weak excitation of the atom, that is $\langle\sigma_+\sigma_-\rangle_t \ll 1$. Under these circumstances we can make the replacement $\sigma_z(t) \to -1$ [87]. The plausibility of this approximation within the context of the moment hierarchy can be examined by looking back to the Heisenberg operator equations of the atom and principal mode, i.e. (4.85) and (4.86). Here, the equations are linear in the system operators and can be easily solved in the same way as the quantum Langevin equation (3.57) from section 3.3: in doing so, we also obtain solutions to (4.164)-(4.166). One finds that the observables of the atom-pseudomode system undergo damped Rabi oscillations. We notice this behaviour agrees with time evolution of the state coefficients when there is a single initial excitation in the system and for a Lorentzian spectral density. Indeed, by writing $\langle b_0^\dagger\sigma_z b_0\rangle_t = \langle b_0^\dagger b_0\sigma_z\rangle_t$, it follows that

$$\langle b_0^\dagger b_0\sigma_z\rangle_t = 2\langle b_0^\dagger b_0\sigma_+\sigma_-\rangle_t - \langle b_0^\dagger b_0\rangle_t. \tag{4.167}$$

Now taking the average with respect to the ket $|\psi(t)\rangle$ from Eq. (4.146), the term $\langle b_0^\dagger b_0\sigma_z\rangle_t$ reduces to

$$\langle b_0^\dagger b_0\sigma_z\rangle_t = -\langle b_0^\dagger b_0\rangle_t, \quad \text{for} \quad \langle N\rangle_t = 1. \tag{4.168}$$

The important point to realise is the dynamics remains exact even when $\sigma_z(t) \to -1$, so that, in this case, the moment equations (4.164)-(4.166) alone give a complete

description of the evolution of the system.

For multiple excitations, Eq. (4.168) can only be assumed to hold under approximation where $\sigma_z(t) \approx -1$. In an effort to avoid this we can take advantage of the fact that the total excitation number is conserved property of the Hamiltonian (4.35). With the number of initial excitations given by n, the commutator relation $[H, N] = 0$ (4.145) ensures n is a constant of motion and thus is fixed at all times. It is this feature which permits closure of the moment hierarchy with exact results. To illustrate this point, we revisit the above example where $n = 1$ to show how the equations can be numerically solved in the more general case where $1 < n < \infty$. As was shown, the moment hierarchy is restricted to a set of equations containing only first-order correlation functions of the atom and principal mode: here, it is simple to verify that next level terms—for example, $\langle b_0^\dagger b_0^\dagger b_0 b_0 \rangle_t$ or $\langle b_0^\dagger b_0 \sigma_+ \sigma_- \rangle_t$—vanish, whereas for $n = 2$ these terms will be non-zero. In the two-excitation case, by extrapolation, correlation functions beyond second order (e.g. $n = 3$) should make no contribution to the dynamics. It is then clear to see how these arguments extend to the general n-excitation case, which can be used to truncate the moment hierarchy to a finite set of equations.

For completeness, we compute the moment hierarchy to second order assuming a maximum of two excitations in the system,

$$\frac{d}{dt}\langle b_0^\dagger b_0 \sigma_+ \sigma_- \rangle_t = -\Gamma \langle b_0^\dagger b_0 \sigma_+ \sigma_- \rangle_t - \Omega_0 \mathrm{Im}\left[e^{-i\delta t} \langle \sigma_- b_0^\dagger b_0^\dagger b_0 \rangle_t \right], \tag{4.169}$$

$$\frac{d}{dt}\langle \sigma_- b_0^\dagger b_0^\dagger b_0 \rangle_t = -\Gamma \langle \sigma_- b_0^\dagger b_0^\dagger b_0 \rangle_t + i\Omega_0 e^{i\delta t} \left(\langle b_0^\dagger \sigma_z b_0 \rangle_t - \langle b_0^\dagger b_0^\dagger b_0 b_0 \rangle_t - \langle b_0^\dagger b_0 \rangle_t \right) \tag{4.170}$$

$$\frac{d}{dt}\langle b_0^\dagger b_0^\dagger b_0 b_0 \rangle_t = -2\Gamma \langle b_0^\dagger b_0^\dagger b_0 b_0 \rangle_t - \Gamma \langle b_0^\dagger b_0 \rangle_t + 4\Omega_0 \mathrm{Im}\left[e^{-i\delta t} \langle \sigma_- b_0^\dagger b_0^\dagger b_0 \rangle_t \right], \tag{4.171}$$

where each of the correlations functions are normal ordered. Higher order terms containing more than two consecutive factors of annihilation (lowering) operators, such as $\langle b_0^\dagger b_0^\dagger b_0 b_0 \sigma_+ \sigma_- \rangle_t$, are, of course, zero. The above equations, when used in conjunction with those in (4.164)-(4.166), in principal provide a complete solution to the problem.

4.3.3 A driven two-level system

The method we used to derive the master equation in Eq. (4.139) should also apply to the case when the atomic transition $|g\rangle \leftrightarrow |e\rangle$ is driven by an external field. Again,

in dealing with multiple excitations, this example is intractable to solve by simply expanding the state (4.146) in a truncated one-photon basis. A non-perturbative master equation for the enlarged system can be found as long as previous methods that went into proving (4.139) still apply.

To capture the effect of a monochromatic field driving the atom, the system Hamiltonian H_S from (4.35) is modified accordingly:

$$H_S(t) = \omega_0 \sigma_+ \sigma_- + \frac{\Omega_L}{2}\left(e^{-i\omega_L t}\sigma_+ + \text{h.c.}\right), \tag{4.172}$$

where Ω_L is the Rabi frequency of the field and ω_L its frequency. Note this form assumes the rotating wave approximation, which is valid in the case $|\omega_0 - \omega_L| \ll \omega_0$ of a nearly resonant driving field. The dynamics of the atom and principal mode are then formulated in a frame of reference moving with the driving field. In this way, we replace the open system term in H_0' (4.64) with $\omega_L \sigma_+ \sigma_-$. By following the exact procedure which lead to (4.68), we obtain

$$\frac{d}{dt}\sigma_-(t) = \sigma_z(t)\left\{i\Delta\sigma_-(t) + i\frac{\Omega_L}{2} + i\Omega_0 e^{i(\delta-\Delta)t}b_0(t)\right\}, \tag{4.173}$$

having defined $\Delta = \omega_0 - \omega_L$. We can also derive the quantum Langevin equation of the atom:

$$\frac{d}{dt}\sigma_-(t) = -\sigma_z(t)\left\{-i\Delta\sigma_-(t) - i\frac{\Omega_L}{2} + \xi(t) - \int_0^t dt' f(t-t')\sigma_-(t')\right\}, \tag{4.174}$$

where the memory kernel is replaced with

$$f(t-t') = \theta(t-t')\Omega_0^2 \exp\left[(-i\Delta + i\delta - \Gamma/2)(t-t')\right]. \tag{4.175}$$

Through equating (4.173) and (4.174), we retrieve almost the exact same solution for $b_0(t)$ given in Eq. (4.70):

$$b_0(t) = \frac{i}{\Omega_0}\xi(t)e^{-i(\delta-\Delta)t} - i\Omega_0 e^{-\Gamma t/2}\int_0^t dt' e^{-(-i\Delta + i\delta - \Gamma/2)t'}\sigma_-(t'). \tag{4.176}$$

It is quite straightforward to show the above leads to,

$$\frac{d}{dt}b_0(t) = -\frac{\Gamma}{2}b_0(t) - i\Omega_0 e^{-i(\delta-\Delta)t}\sigma_-(t) - i\frac{\sqrt{\Gamma}}{2}e^{-i\omega_L t}b_{\text{in}}(t), \tag{4.177}$$

while the noise term is given by

$$b_{\text{in}}(t) = i\frac{1}{2\pi}\sum_n \frac{2\Omega_0}{\omega_c \rho_{n+1}\sqrt{\Gamma}}b_{n+1}\int_{-\omega_c}^{\omega_c} d\omega\, \pi_{n+1}(\omega/\omega_c)e^{-i(\omega+\Delta-\delta)t}. \tag{4.178}$$

In this case, the quantum Langevin equation of the principal mode (4.177) has same form compared to when no driving field is present, i.e. by taking $\Delta \to 0$. Therefore, we can expect the method of substituting (4.174) and (4.177) into the Heisenberg-Langevin equation should follow in the same way as it did before, starting from Eq. (4.133). In fact, by applying this procedure, it can be shown that the exact master equation of the damped-driven qubit is given by

$$\frac{d}{dt}\rho_{SP}(t) = -i\left[H'_S(t), \rho_{SP}(t)\right] + \Gamma\mathcal{L}_{b_0}[\rho_{SP}(t)], \tag{4.179}$$

where

$$H'_S(t) = \Delta\sigma_+\sigma_- + \frac{\Omega_L}{2}\left(\sigma_+ + \sigma_-\right) + \Omega_0\left(e^{i(\delta-\Delta)t}\sigma_+ b_0 + \text{h.c.}\right). \tag{4.180}$$

The same master equation has been introduced by Whalen *et al.* [87] for the purpose of solving the dynamics of a driven qubit embedded in zero temperature bosonic environment [102]. In that paper, it appears no reference is given to the origin of the master equation—however, it possible to acquire their result by first modifying the Hamiltonian (4.35) in such a way as to separate the environment into a single damped oscillator and Markovian residual bath (see Fig. 4.4).

Though this is somewhat related to the transformation we initially used in section 4.1, our approach differs markedly in that it exploits the chain representation to derive all relevant dynamical equations with the Heisenberg picture—while they derive the master equation for the system and damped oscillator by way of the usual procedure [cf. section 2.2]. This follows the approach of Refs. [29, 30] and related methods [44]. Consequently, by arriving at the same exact result (4.179), our method is shown to be equally capable in describing the non-Markovian response of the qubit in the case of multi-photon excitation of the reservoir—both with driving and without. It is important to emphasise that the essence of our method comes from the pseudomode technique, which bases the formulation of the dynamics in terms of a set (operator) equations connected to the pole(s) of the spectral density, rather than by expanding the Liouville equation (2.38) for the enlarged system density matrix $\rho_{SP}(t)$ up to second order in the coupling strength of H'_I (4.129) and evaluating the result via the Born-Markov approximations.

4.4 Summary & discussion

In summary, we have provided an exact derivation of a master equation describing the non-Markovian damping of a two-level atom embedded in a environment (e.g. a quantum electromagnetic field) with a Lorentzian spectral density. Besides reproducing known results—specifically, in the instance where there is one excitation in the total system [1, 41], our method reveals a generalisation of the master equation (4.139) to cases involving multiple excitation of the reservoir. A prominent example we touched on being a driven-damped qubit system, having relevance in quantum information processing and applications of cavity QED.

We began the chapter by presenting a transformation that maps the original oscillator modes of the environment onto a one-dimensional chain. This new representation of the environment is generic, since the transformation itself leaves the open system unaffected and only requires knowledge of the form of the spectral density. As such, we have utilised this particular representation as a means to investigate the non-Markovian dynamics of a two-level atom interacting with a structured bosonic reservoir. By equating the Heisenberg (4.68) and quantum Langevin equations (4.52) of the atom, the original Heisenberg picture equations for the reduced system were expanded to include that of the principal mode, which together fully capture the system-environment dynamics in a non-perturbative fashion. The closure of the set dynamical equations for the atom plus oscillator system has been made possible on the basis that the spectral density only contains a single pole in the lower half complex plane.

We went on to derive an analytical expression for the two-point commutator of the noise operator $b_{\text{in}}(t)$ (with its adjoint), given in (4.102), and compare the generic result against the one obtained in the Markov limit. For a Lorentzian coupling profile, i.e when the system-environment coupling is typically strong, the noise input is seen to mimic the properties of a delta-correlated white noise—suggesting the model maps onto a Markovian stochastic process. Consequently, the combined dynamics of the atom and principal mode were shown to follow an interpretation along the same lines as the well known input-output formalism. Subsequent development of our framework then hinged on being able to partition the environment into a bipartite arrangement. This aspect was used to derive a time-local master equation for an em-

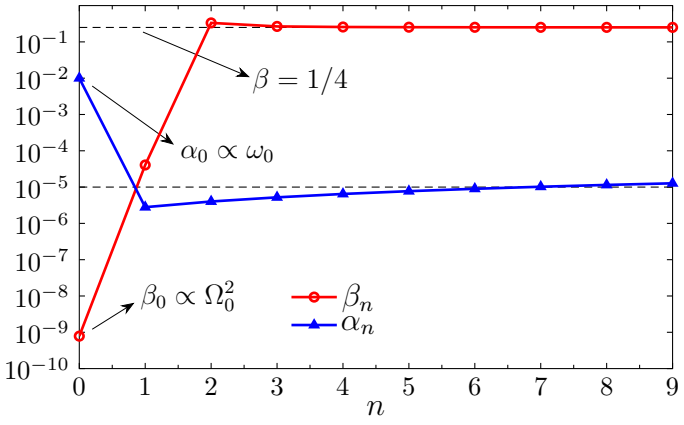

Figure 4.5: Recurrence coefficients shown according to the site index n of the chain oscillators, plotted for parameters $\omega_0 = 10^{-2}\omega_c$, $\Omega_0 = 10^{-4}\omega_c$, $\Gamma = 0.1\Omega_0$ ($\delta = 0$) pertaining to the spectral density (4.47). The coefficient β_n quickly converges to the asymptotic value $\lim_{n\to\infty}\beta_n = \beta = 1/4$ (4.25) around $n \approx 2$, while α_n approaches $\alpha \sim 10^{-5} \ll \omega_0/\omega_c$. The previously used stieltjes routine was implemented to obtain the coefficients via (4.20) and (4.21). Note small numerical discrepancies appear as artefact of the choice of routine (i.e. $\omega_c\sqrt{\beta_0} \lesssim \Omega_0$).

bedded system by way of the Heisenberg-Langevin and quantum Langevin equations (for the principal mode). The fact that the same master equation can equally be derived from the Hamiltonians (4.53), and (4.114), for a zero-temperature reservoir, demonstrates that the non-Markovian dynamics of the atom can be consistently mapped onto a bipartite Markovian dynamics.

Our method has appeal in keeping with the already established idea of Markovian embeddings from other works (cf. chapter 1). However, it is beneficial to the analysis to be somewhat critical with regards to the assumptions we've had to make. We take a brief opportunity to comment on these assumptions.

Firstly, let us address a point made in section 4.3 regarding flatness of the chain, where it was assumed the recurrence coefficients (4.20)-(4.21) were homogeneous beyond the principal mode, i.e $m = 0$. This case was originally implemented due to its inherent simplicity, while also providing a dynamical framework which appears to agree with the pseudomode method for a Lorentzian structured reservoir. The salient problem, however, is that such an assumption may idealise the true properties of the chain to a significant effect, and hence may compromise the validity of our

results. To highlight this, in Fig. 4.5 we plot numerical results obtained for the recurrence coefficients α_n and β_n across different n in the limit of strong system-environment coupling. We see β_n tends to come close to its asymptotic value (4.132) quickly, however, there is no immediate convergence past $n = 0$: indeed, we find a significant jump in value from $n = 2 \to n = 3$, with α_n having much less variation. This would imply having to embed two oscillators in the reduced system for the residual environment to fulfil its intended flatness. Furthermore, contrary to what one would expect, even when taking the Markov limit $\Gamma \to \infty$ the chain is found not to be perfectly flat. All in all, this could tend to suggest a lack of consistency between the assumptions we've made to derive (4.139) and properties of the chain coefficients. We make the case, however, that the numerics presented in Fig. 4.5 do not impact the validity of our method since the Lindblad form master equation (4.139) can be derived independently of the assumption $m = 0$. This is possible using the phenomenological Hamiltonian (4.114). Importantly, because $H_{\text{eff},I}(t)$ was introduced through the dynamical equation (4.86), which is in turn only connected to the pole contained with the complex spectral density (4.47), our statement is then justified on the basis that the properties of α_n and β_n are not invoked[3] prior to (4.129). While Eq. (4.139) should therefore be consistent with the representation where the chain is perfectly flat past $n = 0$, its validity is by no means restricted by such an assumption.

One might be tempted to suggest why the recurrence coefficients in Fig 4.5 do not appear to reflect the $m = 0$ result, i.e., a setting where a single auxiliary oscillator is damped by flat reservoir. My personal suspicion as to why the chain doesn't appear sufficiently flat around $n = 1$ is that it is a consequence of having to impose a finite cut-off frequency ω_c in the original chain transformation. We witness similar occasions where expected Markov features are not fully realised in the absence of $\omega_c \to \infty$. e.g. Eq. (4.108). In light of this, I believe the assumption of a perfect homogenous chain amounts to an idealisation of the true dynamics in the very same way as the white noise approximation. Hence, while not technically accounting for full effects, our model is assumed to replicate the exact dynamics of the atom to a

[3]Note the kernel (4.101) has implicit dependence on the recurrence coefficients: however, this was already shown to yield properties of a white noise process in (4.113).

high degree of accuracy. This is judged by the fact our results are consistent with pseudomode method.

Secondly an odd, if not problematic feature, is that the residual environment couples strongly to the principal mode due to $\omega_c/\Omega_0 \gg 1$. This has similarly been pointed out for the reaction coordinate mapping, which resembles the orthogonal polynomial chain mapping to a large extent. The issue here is that the implied assumption of there being only weak interactions between the enlarged system and residual environment are possibly unjustified within the chain representation: reviving the remark of Strasberg *et al.* [33],

> "It is not guaranteed that the resulting final SD (spectral density) is also weak in the sense that it is justified to consider only second order perturbation theory in the coupling to the residual baths [...] the resulting final SD in general depends on the shape of the initial SD and might be still large compared to parameters of the system."

One assurance to this concern is that Markov approximation is based on the flatness of the spectral density (see section 3.1.3). For an approximately homogenous chain, a microscopic theory can be used show the spectrum of the residual bath is given by a Wigner semicircle distribution [91], which, equivalently, is the spectral density of the Rubin model in an x-p coordinate representation [6, 103, 104]. For large ω_c the distribution provides a flat, memoryless bath, as necessary. Moreover, since we don't use second-order perturbation theory in our derivation, we avoid the need to assume the enlarged system and residual environment are weakly coupled.

Finally, let us reflect on a previously point made regarding already existing extensions of the standard pseudomode method, which have been demonstrated in Refs. [44–46]. Here, by use the Fano diagonalisation technique, an atom—or any open system for that matter—which couples to a structured bosonic reservoir is found to be equivalently described by its coupling to a set of damped quasimodes. In a way that is similar to what has been described in the current chapter (cf. section 4.3), the original environment is replaced by a bipartite structure comprising of an enlarged atom plus quasimode system, which in turn couples to a continuum of residual environment of harmonic oscillators. The interaction between the enlarged system and residual modes is treated assuming the relevant coupling constants α_j

are slowly varying functions in frequency across the range of interest, i.e. $\alpha_j \to \alpha$. Given this coupling is small, the resulting picture facilitates a standard derivation of a Born-Markov master equation for the enlarged system, where the time derivative of its density matrix is evaluated to second order in α. The important aspect is that the Lindblad form of the master equation in the extended Hilbert space of the atomic system is preserved. However, unlike the pseudomode method, since the transformation to the quasimode picture is based on rewriting the original Hamiltonian in terms an equivalent set of operators, the formalism incorporates the multiple excitation case into its approach. The quasimodes, in turn, are identified as pseudomodes through their connection to the poles of the spectral density—this is what justifies the extension of the pseudomode method to being able to treat the case of multi-photon processes.

A drawback of the quasimode method is that it forgoes the original simplicity of the pseudomode technique used to solve the single excitation case, and as a result can be complicated to apply practically in certain situations. Our treatment differs in that the master equation is explicitly derived from the Heisenberg operator equations within the chain setting. Under only weakly restrictive assumptions has this allowed us to extend the validity of the master equations to the case of multiple excitations in the atom and principal mode system. Comparatively, the benefit of our approach is that it's self-contained as well as being established within a more physically intuitive framework. The results of the current chapter may therefore offer a better foundation to work from for future applications. Indeed, since the master equation in Eq. (4.139) should be valid for any quantum optical system whose time evolution is mainly governed by $[H_S, x_j^{\pm}(t)] \approx \pm\omega_j x_j^{\pm}(t)$ [63], where $x_j^{\pm}$ are operators of the open system (e.g. $\sigma_j^{\pm} \to \sigma_{\pm}$ for a two-level system), then the methods of this chapter could be applied to model a variety of more complex non-Markovian systems, including the multi-level atom case described in Refs. [45, 46].

Part IV

Quantum Darwinism

Chapter 5

Emergence of classicality in a damped atom-cavity system

Quantum Darwinism seeks to provide an answer to the fundamental question of classicality in open quantum systems [47–52, 58, 105]. When a system interacts with its environment, superpositions of the reduced system tend to decay into mixtures of a certain stable macroscopic set of pure states, known as pointer states [106–108]. This description, referred to as decoherence [7, 9, 10], goes some way to explain the emergence of classical-like behaviour at the level of the reduced system. While decoherence can account for the removal of quantum interference phenomena, the description must be considered incomplete since it does not consider how the pointer states can be "found out" by an external observer, i.e. how information about these states becomes distributed into the environment. The relevant situation to understand is then one where many observers measure the environment, and in the process, gain certain information about the properties of the system through correlations shared with its measurement records. In the context of classicality, the state inferred by each observer should be unanimously agreed upon, and thus have objective properties [55, 109]. With this is mind, the basic question posed by quantum Darwinism—and the one we wish to address here—is the following: over the course of time, does the environment typically manage to acquire and maintain many of the same copies of information about the system's state as a result of the decoherence process?

The current chapter is devoted to investigating how such information is spread

within the environment of a paradigmatic model of quantum optics: specifically, the model of a two-level atom interacting a structured electromagnetic (bosonic) reservoir. The key idea is that of *redundancy* [7, 49–52]; or equally, how many copies of information regarding the atom are imprinted into the reservoir. In this way, the time-dependent nature of the correlations between the atom and different fractions of the reservoir is considered. These correlations are measured through the quantum mutual information [14, 110], which shall be our main point of focus in this chapter. An advantage of the model we shall go on to examine is that its dynamics is exactly solvable for a zero temperature reservoir [111], and as such, we can investigate full effects. While the atom-reservoir we consider is generic, we will envisage its particular application to a two-level atom coupled to a damped cavity field.

In the overall scheme of things, the ensuing work is intended to be studied as a toy model to recognise initial features of quantum Darwinism and develop a conceptual understanding of the problem. Later we shall propose a setup more relevant to actual experiments.

This chapter is organised as follows. In section 5.1 we provide an overview of the core aspects of decoherence theory and discuss their connection with the quantum Darwinism framework. Section 5.2 reintroduces the Jaynes-Cummings model for the single excitation case, where its solution is obtained and exploited to pursue an exact calculation of the quantum mutual information. Then, in section 5.4, we present numerical results for the partial information—the averaged amount of quantum information shared between the atom and parts of its environment—paying close attention to the formation of a "classical plateau" feature. Lastly, as a corollary to our main findings, in section 5.5 we study the properties of the local information in relation to the spontaneous emission spectra of the system.

5.1 A basic example of quantum Darwinism

We begin by illustrating the concepts of quantum Darwinism using a simple dynamical model, comprising a two-level system in contact with a number of identical quasi-spin systems. The current section closely follows the approach in Refs. [1, 48].

In the standard decoherence setting, it is necessary to presuppose that the system of interest—e.g. the two-level system—is initially uncorrelated and distinguishable from its environment, with the latter assumed to be macroscopic. While there is no *a priori* reason to believe such a partitioning agrees with any natural choice of system [112], we assume, at least in the setting where we intend to apply these concepts [cf. section 5.2.1], that no severe restrictions are placed on our work.

5.1.1 Decoherence and pointer states

Let us first consider the following initial state of the global system,

$$|\psi(0)\rangle_{SE} = (\alpha\,|0\rangle + \beta\,|1\rangle) \otimes |\phi_0(0)\rangle_E\,, \tag{5.1}$$

where the environment has a fixed inner structure $E = \otimes_{\lambda=1}^{\#E} E_\lambda$ made of mutually non-interacting sub-environments, E_k [51]. The environment is prepared in its ground state,

$$|\phi_0(0)\rangle = |\varepsilon_0^{(1)}, \varepsilon_0^{(2)}, \ldots, \varepsilon_0^{(\#E)}\rangle\,. \tag{5.2}$$

while the system starts in a superposition of $|0\rangle$ and $|1\rangle$ provided α and β satisfy $\alpha, \beta > 0$, with $|\alpha|^2 + |\beta|^2 = 1$. Here we study the time-dependence of the coherences and total correlations between the two subsystems. The interaction Hamiltonian H_I, from Eq. (2.46),

$$H_I = \sum_n S_n \otimes B_n = \sum_n |n\rangle\langle n| \otimes B_n, \qquad n = 0, 1, \tag{5.3}$$

is assumed to fulfil the property

$$[H_S, H_I] = 0 \quad \text{from} \quad \big[\,|n\rangle\langle n|\,, H_I\big] = 0. \tag{5.4}$$

Consequently, because $|\psi\rangle_S = \alpha\,|0\rangle + \beta\,|1\rangle$ is made from an arbitrary combination of the eigenstates of (5.3), its basis states are stationary in time. That's not to say $\rho_S(t)$ is time-independent: the open system is affected by dephasing, where randomisation of relative phases between the basis states tends to result in a loss of coherence. Because the system energy remains unchanged during this process, i.e. $d_t\,\langle H_S(t)\rangle = 0$, it suffices to ignore the contribution of H_S to the dynamics, meaning only the environment states evolve as $|\phi_n(0)\rangle \to |\phi_n(t)\rangle$. Thus the only timescales

of importance are those associated with the bath units. For a Hamiltonian given by $H = H_0 + H_I$ [cf. (3.14)], the propagator $U(t)$ within the interaction picture reads

$$U(t) = T_{\leftarrow}\exp\left[-i\int_0^t dt' \sum_n |n\rangle\langle n| \otimes B_n(t')\right], \tag{5.5}$$

where $B_n(t) = e^{iH_0 t} B_n e^{-iH_0 t}$, and $T_{\leftarrow}$ is the familiar time-ordering operator from (2.5). Note the propagator can also be expressed in terms of a Dyson series expansion [62]:

$$U(t) = 1 + \sum_{j=1}^{\infty}(-i)^j \int_0^t dt_n H_I(t_j) \int_0^{t_j} dt_{j-1} H_I(t_{j-1}) \ldots \int_0^{t_2} dt_1 H_I(t_1). \tag{5.6}$$

Under a unitary time evolution, $|\psi(t)\rangle_{SE} = U(t)\,|\psi(0)\rangle_{SE}$, the linearity of the Schrödinger equation, together with the commuting nature of the system and bath operators in Eq. (5.6), then ensures $|\psi(t)\rangle_{SE}$ has a unique form provided by

$$|\psi(t)\rangle_{SE} = \alpha\,|0\rangle\,|\phi_0(t)\rangle_E + \beta\,|1\rangle\,|\phi_1(t)\rangle_E\,, \tag{5.7}$$

where

$$|\phi_1(0)\rangle = |\varepsilon_1^{(1)}, \varepsilon_1^{(2)}, \ldots, \varepsilon_1^{(\#E)}\rangle\,, \tag{5.8}$$

and the time-evolved bath states are

$$|\phi_n(t)\rangle = T_{\leftarrow}\exp\left[-i\int_0^t dt' B_n(t')\right]|\phi_n(0)\rangle\,. \tag{5.9}$$

To inspect the density matrix of the open system, the environment degrees of freedom are traced out from the global state,

$$\begin{aligned}\rho_S(t) = \mathrm{tr}_E\big[(|\psi(t)\rangle\langle\psi(t)|)_{SE}\big] = |\alpha|^2\,|0\rangle\langle 0| + \alpha\beta^*\,|0\rangle\langle 1|\,\langle\phi_1(t)|\phi_0(t)\rangle \\ + |\beta|^2\,|1\rangle\langle 1| + \text{h.c.}\end{aligned} \tag{5.10}$$

Here we notice the time-dependence of the coherences in $\rho_S(t)$ (the off-diagonal terms) are determined by the overlap of the two environmental parts of the state [108], that is $\langle\phi_n(t)|\phi_{n'}(t)\rangle$, whereas populations contained in the diagonal elements remain static over time from $\langle\phi_n(t)|\phi_n(t)\rangle = 1$. Intuition would tell us to eventually expect

$$\langle\phi_n(t)|\phi_{n'}(t)\rangle \longrightarrow \delta_{n,n'} \tag{5.11}$$

on some timescale provided by microscopic details of the model, provided the thermodynamic limit $\#E \gg 1$ is fulfilled. This is certainly the case within a course-grained perspective, where the environment is assumed to contain a very large number of degrees of freedom.

Ultimately, the off-diagonal terms are found to decay either exponentially or with some exponential functional dependence, leading to a situation where the system density matrix approaches a completely diagonal representation as a result of the environment states (5.11) being mutually orthogonal. In the limit $t/\tau_D \to \infty$, with τ_D a typical decoherence time for the system, Eq. (5.10) has the following form:

$$\rho_S(\infty) = |\alpha|^2 \, |0\rangle \langle 0| + |\beta|^2 \, |1\rangle \langle 1| \, . \tag{5.12}$$

The interaction therefore singles out a preferred set of classical basis states—the pointer states—which are unique due to their stability with respect to coupling to the external reservoir. Since, in the asymptotic limit, $\rho_S(t)$ is given by an incoherent mixture of the eigenstates S_n (5.3) pertaining to the operator $O_S = \sum_{n,n'} \big(\langle n| \, O_S \, |n'\rangle \big) \, |n\rangle \langle n'|$, the density matrix of the reduced system mimics a classical ensemble. By this we mean interference terms are no longer present in the expectation value $\langle O_S \rangle_\infty = \mathrm{tr}_S \left[O_S \rho_S(\infty) \right]$, i.e.

$$\lim_{t\to\infty} \langle O_S \rangle_t = |\alpha|^2 \langle 0|O_S|0\rangle + |\beta|^2 \langle 1|O_S|1\rangle, \tag{5.13}$$

and thus the pointer observable behaves like a classical stochastic variable. Because (5.12) contains all accessible information about S and its probabilities, the lack of any coherent phase relation between states leads us to believe—under an ignorance (ensemble) interpretation[1]—that the system can be allocated to either one of the

[1] This regards the state as being in a *proper* mixture (i) rather than a *improper* mixture (ii) [10, 113]. The key difference between these two is stated as follows. A proper mixture, $\rho = \sum_n p_n \, |\psi_n\rangle \langle \psi_n|$, is constructed as an ensemble in the sense it has a given probability distribution $p_n = \mathrm{tr}\big[\, |\psi_n\rangle \langle \psi_n| \, \rho \big]$ of measuring the system in a preconceived state $|\psi_n\rangle$, if $\langle \psi_n | \psi_{n'} \rangle = \delta_{n,n'}$. Whereas, an improper mixture, like that found in Eq. (5.12), arises in a situation where the density matrix of a product space $H_1 \otimes H_2 \otimes \ldots$ is traced over to obtain the density operator of one of the subsystems. Hence an improper mixture is conceived from an understanding that the universe can be partitioned into fixed subsystems, such as system plus environment, with each having their own designated state, probabilities, and associated set of measurement outcomes; i.e. the same as (i). However, (i) and (ii) must be interpreted differently because (ii) cannot be assumed

pointers:

$$|\psi\rangle_S \longrightarrow |0\rangle\,, \quad \text{or}$$
$$|\psi\rangle_S \longrightarrow |1\rangle\,, \tag{5.14}$$

but clearly *not* both, in contrast to Eq. (5.1). After taking the trace, we find there is a reduction of the original superposition of system states to an apparent mixture of definite outcomes.

Nonetheless, while the original superposition $|\psi\rangle_S = \alpha\,|0\rangle + \beta\,|1\rangle$ becomes locally unobservable, it should be emphasised that coherences still exist in the global state vector $|\psi(t)\rangle_{SE}$. Again this is attributed to the linear nature of the Schrödinger equation. Yet, the steps leading to (5.12) end in a "different" evolution for the reduced system. As we've seen in (5.7), the first step involves the same linear (unitary) type of interaction, which brings the global state vector into a non-separable state $|\psi(t)\rangle_{SE} \neq |\psi\rangle_S \otimes |\psi(t)\rangle_E$. The "difference" then comes about from applying the nonlinear trace operation to get $\rho_S(t)$. However, because of the non-separability of the global state vector, the system $|\psi\rangle_S$ can neither be expressed as individual pure state or proper mixed state, and its properties (i.e. being in some fixed basis) are therefore ill-defined prior to measurement [9]. Since $|\alpha|^2$ and $|\beta|^2$ are interpreted as probabilities of actualising the system in either $|0\rangle$ or $|1\rangle$ after measurement, the trace must assume a collapse process occurs at some point in time for (5.12) to be understood as a true classical ensemble (cf. footnote 1). We generally regard the state to objectively exist when the environment modes are measured by a classical device, e.g. a photodetector.

Einselection and predictability

A defining feature of pointer states is that each can be perfectively distinguished under measurement, and as such they collectively form an independent set of measurement outcomes, $\langle n|n'\rangle = \delta_{n,n'}$, from the eigenstates of the system density matrix. This is an ensured consequence of environment-induced superselection [7, 108, 114] otherwise known as *einselection*, of the particular set of system states satisfying

to objectively exist under the standard orthodox interpretation if the reduced system is entangled with the bath—essentially, it's state is fundamentally indeterminate before measurement.

these properties. Any other state formed out of linear combination of $|n\rangle$ will undergo decoherence and the final density matrix cannot end up in a diagonal mixture of its original elements. Indeed, if we consider the example of a system prepared in an arbitrary pure state $|\psi\rangle_S^P$ with coefficients c_n, we notice the evolution

$$\rho_S(0) = \left(|\psi\rangle \langle\psi|_S \right)^P \xrightarrow{t} \sum_{n,n'} c_n^* c_{n'} |n\rangle \langle n'| \longrightarrow$$
$$\xrightarrow{t \gg \tau_D} \sum_n |c_n|^2 |n\rangle \langle n| = \rho_S(\infty), \tag{5.15}$$

is formally equivalently to S being acting upon by a non-selective measurement where a certain mixture of stable (pointer) states are picked from the full ensemble of possible results. The criteria used to identify the existence of these states in the final stage of (5.15) originates from the einselection identity:

$$\rho_S(\infty) = \sum_n S_n \rho_S(\infty) S_n, \tag{5.16}$$

where S_n, as we recall from (5.3), satisfies $S_n = S_n^\dagger$. We see in (5.16) that repeated measurement of the same observable (5.13) after einselection ($t \gg \tau_D$) always yields a complete record of the state $|\psi\rangle_S$ in one of its pointer outcomes—or, in opposite sense, the projection does not re-prepare the state in a new mixture of sub-ensembles comprising a different basis set. The density matrix $\rho_S(\infty)$ is therefore insensitive to (non-selective) measurements within the pointer state sector $\{S_n\}$ [114].

With regard to a classical description, the result in (5.16) is important as it naturally lends itself to the idea of predictability. By predictable, we mean the state $|\psi\rangle_S$ can be monitored continuously and that the observed result correlates exactly with what was previously found. Following (5.15), the irreversible nature of the system measurement going from $\rho_S(0) \to \rho_S(\infty)$ will grant unchanging and totally predictable outcomes: hence, to an external observer, it is as if S was originally classical. Decoherence then leads us to think of $\rho_S(\infty)$ as existing objectively, and whose state can be found through many independent observers without being perturbed.

Information flows

The einselection process is typically accompanied with a loss of (quantum) informa-

tion from the reduced system into its surroundings due to the off-diagonal terms of $\rho_S(t)$ decaying over time [7, 9]. Since information is in principle a conserved quantity, it seems pertinent to ask where or how this information is stored. As Zurek suggests [7, 47, 48], a natural extension to the decoherence program is to then include the whole environment—or fractions thereof—within the description rather than tracing out and excluding the role of the environment as we did previously in Eq. (5.10). This framework is summarised under a "environment as a witness" paradigm, depicted in Fig. 5.1. The key here is to know how decoherence spreads copies of information of the system's state to the observer during an evolution described by (5.7).

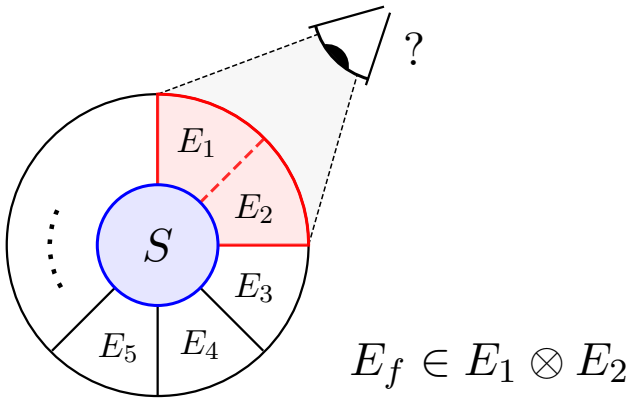

Figure 5.1: Diagrammatic representation of an observer monitoring a fragment E_f. The environment E is recognised to be made up of a fixed number of sub-environments. The question to be answered is: How much information does an observer gain about the system S from intercepting copies of its state in E?

5.1.2 Quantum Darwinism

Looking back at the example in Eq. (5.7), let us consider the effect decoherence has on shared correlations between the system and environment. Notably, pointer states preserve correlations with environment fragments as a result of the fixed structure of the global state $|\psi(t)\rangle_{SE} = \alpha\,|0\rangle\,|\varepsilon_0^{(1)}, \varepsilon_0^{(2)}, \ldots\rangle + \beta\,|1\rangle\,|\varepsilon_1^{(1)}, \varepsilon_1^{(2)}, \ldots\rangle$. These correlations hold certain information on the possible (pointer) states of the two-level system. The quantum mutual information (QMI) is the measure used to ascertain

what is known about the system by a fragment of the environment,

$$I(\rho_{SE_f}) = S(\rho_S) + S(\rho_{E_f}) - S(\rho_{SE_f}), \tag{5.17}$$

where E_f makes up a subdivision (in size) of E, see Fig. 5.1. The quantity $S(\cdot)$ is the von Neumann entropy, which, for an arbitrary density matrix ρ, is defined as [14, 110]

$$S(\rho) = -\mathrm{tr}[\rho \ln(\rho)] = -\sum_i \lambda_i \ln \lambda_i, \tag{5.18}$$

with λ_i its corresponding eigenvalues. Separately from the global state (5.7), lesser arrangements of composite system-fragment states ρ_{SE_f}—obtained by tracing out the remaining environment E/E_f—decohere over time, assuming E/E_f is of sufficient size to do so. If, in the limit $t/\tau_D \to \infty$, the overlap of the environment states satisfy $\langle \phi_n(t) | \phi_{n'}(t) \rangle_{E/E_f} \approx \delta_{n,n'}$, we end up with

$$\begin{aligned} \rho_{SE_f}(\infty) = \mathrm{tr}_{E/E_f}\left[(|\psi(t)\rangle \langle \psi(t)|)_{SE} \right] = |\alpha|^2 |0\rangle \langle 0| \otimes (|\phi_0(\infty)\rangle \langle \phi_0(\infty)|)_{E_f} \\ + |\beta|^2 |1\rangle \langle 1| \otimes (|\phi_1(\infty)\rangle \langle \phi_1(\infty)|)_{E_f}. \end{aligned} \tag{5.19}$$

Notice the original superposition of outcomes is reduced to a mixture containing the products of classical outcomes, e.g. $|0\rangle \otimes |\phi_1(\infty)\rangle_{E_f}$, similar to what we saw in (5.12). Substituting the above into Eq. (5.17) yields

$$I(\rho_{SE_f}) = S(\rho_S) \quad \text{from} \quad S(\rho_S) = S(\rho_{E_f}) = S(\rho_{SE_f}). \tag{5.20}$$

Therefore, the fragment retains a perfect record of the system pointer states. Because this condition is independent of the choice of E_f, many fragments contain copies of the same information on S. In the absence of entanglement this is restricted to the classical limit $I(\rho_{SE_f}) \leq \min\left[S(\rho_S), S(\rho_{E_f})\right]$, where $S(\rho_S) = -|\alpha|^2 \ln |\alpha|^2 - |\beta|^2 \ln |\beta|^2$ coincides with the classical Shannon entropy [14, 110]. While correlations form between the environment and other possible states of the system, it should be noted that only the pointer states have the ability proliferate classical information throughout the environment, which can reliably be accessed via measurement [50].

By token of (5.20), classical information is redundant since in principle an unconstrained number of observers can discover the state of the system through E_f. The redundancy of such information in itself—that is, roughly how many copies are imprinted across different fragments—can then be treated as a measure of classicality. Bear in mind, however, that here we've considered an illustrative example

only: in practice, copies will not store exactly this amount of information, which we waive, but $I(\rho_{SE_f}) = (1-\delta)S(\rho_S)$, with δ a small information deficit[2] ($\delta \ll 1$). This is now what we shall go on to test with our dynamical model by computing (5.17) for many choices of fragment state. Note that it is necessary by no means to have the condition (5.4) of an ideal measurement, and in the following, we also examine both effects of decoherence and dissipation on redundancy.

5.2 Dynamical model

As previously mentioned, the model system comprises a qubit interacting with a continuum of bosonic modes. Here we restrict our interest to the damped Jaynes-Cummings model: that is, a two-level atom coupled to a single-mode cavity, which in turns leaks into a vacuum reservoir. The reader is reminded this framework has already been outlined in section 4.2. Here, the coupling between atom and environment oscillators is characterised by a single Lorentzian spectral density. Throughout we will consider only resonant interactions, and so the distribution $J(\omega)$ is given by

$$J(\omega) = \frac{\Omega_0^2}{\pi} \frac{\Gamma/2}{(\omega-\omega_0)^2 + (\Gamma/2)^2}, \tag{5.21}$$

with the parameters being defined in the same way as they were in chapter 4. Note we also assume the environment to have an inner structure $E = \otimes_{\lambda=1}^{\#E} E_\lambda$ made up of sub-environments E_λ.

5.2.1 Solutions to the model

Consider the state vector in Eq. (4.146). In the current situation—when one excitation is present in the total system—a tractable way to study the dynamics is attainable by expanding state in the single excitation manifold, thanks to the property $[H, N] = [H_0 + H_I, N] = 0$ of the Hamiltonian (4.35). At $t = 0$, the initial state of the total system is

$$|\psi(0)\rangle = c_g |g, 0\rangle + c_e(0)\sigma_+ |g, 0\rangle , \tag{5.22}$$

[2]This is not to be mistaken for the detuning δ, which previously used the same symbol in chapter 4.

which after a time $t > 0$ evolves into

$$|\psi(t)\rangle = c_g |g,0\rangle + c_e(t)\sigma_+ |g,0\rangle + \sum_\lambda c_\lambda(t) a_\lambda^\dagger |g,0\rangle . \tag{5.23}$$

Recall that the annihilation and creation operators a_λ, $a_\lambda^\dagger$ fulfil $a_\lambda a_{\lambda'}^\dagger |0\rangle = \delta_{\lambda,\lambda'} |0\rangle$, while the atomic lowering and raising operators σ_- and σ_+ satisfy an algebra defined in Eq. (4.36). By substituting (5.23) into the Schrödinger equation $d_t |\psi(t)\rangle = -iH |\psi(t)\rangle$, within the interaction picture we obtain a set of coupled differential equations for the state coefficients $c_e(t)$ and $c_\lambda(t)$:

$$\frac{d}{dt} c_e(t) = -i \sum_\lambda g_\lambda \exp[-i(\omega_\lambda - \omega_0)t] c_\lambda(t), \tag{5.24}$$

$$\frac{d}{dt} c_\lambda(t) = -i g_\lambda \exp[i(\omega_\lambda - \omega_0)t] c_e(t). \tag{5.25}$$

Following the approach of Wigner-Weisskopf [115], we formally integrate (5.25) to get

$$c_\lambda(t) = -i g_\lambda \int_0^t dt' \exp[i(\omega_\lambda - \omega_0)t'] \, c_e(t'). \tag{5.26}$$

By then placing the result into (5.24) to arrive at an integro-differential equation

$$\frac{d}{dt} c_e(t) = -\int_0^t dt' f(t-t') c_e(t'), \tag{5.27}$$

with the memory kernel $f(t-t')$ given in (4.46). Since this equation is linear, its solution has the generic form $c_e(t) = G(t)c_e(0)$, with $G(t)$ the Green's function of the atom. Therefore, through taking the partial trace of $\rho(t) = |\psi(t)\rangle \langle\psi(t)|$ using the basis states $|0\rangle_E$ and $a_\lambda^\dagger |0\rangle_E$, the reduced density matrix of the atomic system can be written as [116]

$$\begin{aligned} \rho_S(t) = \mathrm{tr}_E\big[|\psi(t)\rangle \langle\psi(t)| \big] = \big(\rho_{gg} + (1 - |G(t)|^2)\rho_{ee}\big) |g\rangle \langle g| \\ + G^*(t)\rho_{ge} |g\rangle \langle e| + |G(t)|^2 \rho_{ee} |e\rangle \langle e| + \text{h.c.} \end{aligned} \tag{5.28}$$

The time evolution of population and coherences in (5.28) is then fixed according to the matrix elements

$$\begin{cases} \rho_{ee}(t) = |G(t)|^2 \rho_{ee} = |c_e(t)|^2, \\ \rho_{eg}(t) = G(t)\rho_{eg} = c_g^* c_e(t), \\ \rho_{ge}(t) = G^*(t)\rho_{ge} = c_e^*(t) c_g, \\ \rho_{gg}(t) = \big(\rho_{gg} + (1 - |G(t)|^2)\rho_{ee}\big) = 1 - |c_e(t)|^2, \end{cases} \tag{5.29}$$

with $\rho_{i,j} = \langle i| \rho_S |j\rangle$ $(i, j \in [g, e])$. It remains to determine $G(t)$ to have a full handle on the open system dynamics.

Because $\rho_S(t)$ only depends on couplings g_λ and parameters encoded in (5.21), the complete evolution of the system is solely determined by the form of the spectral density. For a Lorentzian, an analytical treatment of the full system-environment dynamics is possible by mapping $\rho_S(t)$ onto a enlarged system containing the original atom plus an extra pseudomode degree of freedom [41] (see section 4.3.1). As we know, the density matrix $\rho_{SP}(t)$ obeys the master equation (4.139),

$$\frac{d}{dt}\rho_{SP}(t) = -i\left[H'_S, \rho_{SP}(t)\right] + \frac{\Gamma}{2}\left(\left[a\rho_{SP}(t), a^\dagger\right] + \left[a, \rho_{SP}(t)a^\dagger\right]\right), \tag{5.30}$$

having

$$H'_S = \Omega_0\big(\sigma_+ a + \text{h.c.}\big), \tag{5.31}$$

and where the pseudomode adopts the role of the leaky cavity mode. Solving the

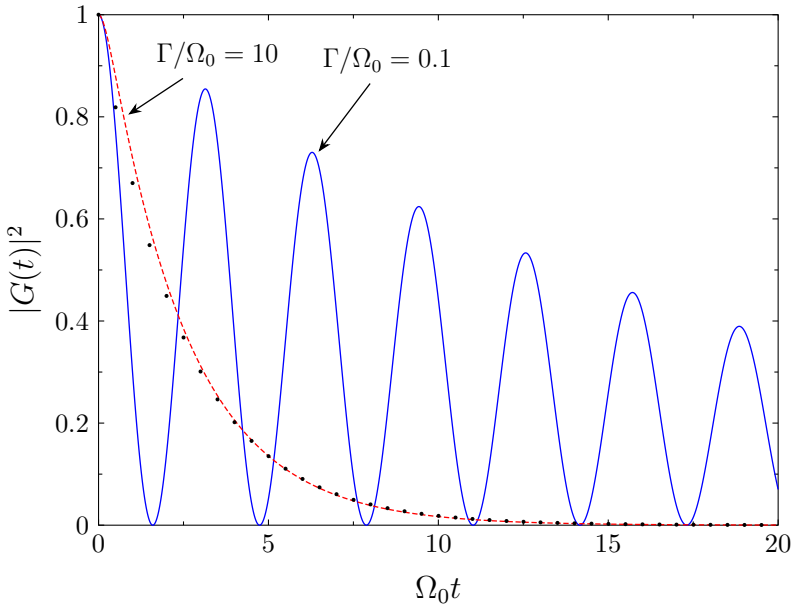

Figure 5.2: The function $|G(t)|^2$ [see Eq. (5.32)] plotted over time for $\Gamma = 0.1\Omega_0$ (blue solid curve) and $\Gamma = 10\Omega_0$ (red dotted curve). The solution obtained from the weak-coupling Markovian master equation is also shown (black points) for the latter choice of parameters.

master equation—either by numerically integrating or applying the Laplace transform method to the state coefficients in Eqs. (4.149)-(4.150)—and subsequently

tracing out the auxiliary variable from $\rho_{SP}(t)$ (4.161), then leads to an exact solution for the system density matrix, i.e. $\rho_S(t) = \mathrm{tr}[\rho_{SP}(t)]$. In doing so, we obtain the following expression for the Green's function:

$$G(t) = e^{-\Gamma t/4}\left[\cos\left(\frac{\Omega t}{2}\right) + \frac{\Gamma}{2\Omega}\sin\left(\frac{\Omega t}{2}\right)\right], \tag{5.32}$$

where

$$\Omega = \sqrt{4\Omega_0^2 - (\Gamma/2)^2}. \tag{5.33}$$

Figure 5.2 displays the behaviour of (5.32) for an initially excited atom, $c_e(0) = 1$. The atomic population shows qualitatively distinct behaviour depending on the values of the decay rate Γ and coupling strength Ω_0. The relaxation rate of the atom is provided by the Markovian decay rate $\gamma_0 = 4\Omega_0^2/\Gamma$. Within the strong coupling regime, $4\Omega_0 > \Gamma$, the population undergoes oscillatory dynamics and shows revivals at certain times. This is acknowledged to follow as a result of non-Markovian effects. By further increasing the coupling strength to $4\Omega_0 \gg \Gamma$, the atom dissipates more slowly and has more pronounced Rabi oscillations.

Alternatively, for weak coupling, $4\Omega_0 < \Gamma$, the population exponentially decreases in time. Likewise, it tends to approach its ground state faster than for strong system-environment coupling. However by taking the Markov limit $\Gamma \to \infty$: that is, when $4\Omega_0 \ll \Gamma$, the atom is perturbed weakly from its initial state and thus decays very slowly. In this instance, $|c_e(t)|^2$ conforms with the modified dynamics of the Lindblad master equation [1, 5], where

$$|G(t)|^2 \approx e^{-\gamma_0 t} \quad \text{for} \quad \frac{4\Omega_0}{\Gamma} \ll 1. \tag{5.34}$$

A complete solution to the problem is obtained by directly plugging $c_e(t)$ into Eq. (5.25) and integrating the result to obtain the reservoir coefficients $c_\lambda(t)$. The quantum mutual information can thus be calculated exactly from (5.17), allowing the time-dependent properties of the total system-fragment correlations to be studied fully within the scope of the current model. This we shall now go onto examine in detail.

5.2.2 Calculation of the quantum mutual information

The remaining states used to calculate (5.17), i.e. $\rho_{SE_f}(t)$ and $\rho_{E_f}(t)$, can straightforwardly be obtained by partitioning $|\psi(t)\rangle$ as follows:

$$|\psi(t)\rangle = c_g |g,0\rangle_{SE_f} |0\rangle_{E/E_f} + c_e(t) |e,0\rangle_{SF} |0\rangle_{E_f} + \sum_{\alpha,\lambda} c_{\mu_\alpha}(t) a^\dagger_{\mu_\alpha} |g,0\rangle_{SE_f} |0\rangle_{E_f} , \tag{5.35}$$

where as always the coefficients must satisfy

$$|c_g|^2 + |c_e(t)|^2 + \sum_\alpha \sum_\mu |c_{\mu_\alpha}(t)|^2 = 1. \tag{5.36}$$

Again [cf. (5.2) and (5.8)] the environment is formed out of a fixed composition of sub-environments $E = \sum_\alpha \otimes_{\mu_\alpha=1}^{\#E} E_{\mu_\alpha}$, each assigned to a mode labelled by μ. Though the index μ has a one-to-one association with each of the original λ-modes, its subscript α indicates the reservoir has been artificially partitioned into different Hilbert spaces. For a bipartite partition, we have $\alpha = \{1, 2\}$, and the operator $a^\dagger_{\mu_\alpha}$ (a_{μ_α}) belongs to the Hilbert space of the fragment or non-fragment depending on the assignment of α: for example, if $\alpha = 1$ is chosen to denote the state space of E/E_f, then $a_{\mu_1} a^\dagger_{\mu_1} |0\rangle_{E/E_f} = |0\rangle_{E/E_f}$. Importantly, the fragment E_f is independent of its complimentary part E/E_f, in the sense that

$$a_{\mu_\alpha} a^\dagger_{\mu'_{\alpha'}} |0\rangle = \delta_{\mu,\mu'}\delta_{\alpha,\alpha'}, \quad \text{and} \quad [a_{\mu_\alpha}, a^\dagger_{\mu'_{\alpha'}}] = \delta_{\mu,\mu'}\delta_{\alpha,\alpha'}. \tag{5.37}$$

To set notation we shall assign $\alpha = 1$ to E/E_f and $\alpha = 2$ to E_f. Hence, the fragment is arranged as $E_f = \otimes_{\mu=1}^{m} E_{\mu_2}$, where m indicates the number of quanta (modes) included within E_f. It should also be mentioned that different combinations of bath units (e.g. E_k, for $k = 1, 2 \ldots, \#E$) with fixed number $\#E$ will typically yield a different and unique choice of fragment, since each of the λ-modes have different frequencies and coupling strengths to the atom.

Using (5.35), we can now take the partial trace of $\rho(t) = |\psi(t)\rangle \langle\psi(t)|$ over the part of its Hilbert space containing either the complementary fragment E_{1-f} (i.e. not in E_f), or the complementary fragment plus the atom. That is we look to

compute

$$\begin{aligned}\rho_{SE_f}(t) &= \mathrm{tr}_{E/E_f}\left[\rho(t)\right] \\ &= \sum_{\mu} {}_{E/E_f}\langle 0|a_{\mu_1}\big(|\psi(t)\rangle\langle\psi(t)|\big)a^{\dagger}_{\mu_1}|0\rangle_{E/E_f} + {}_{E/E_f}\langle 0|\psi(t)\rangle\langle\psi(t)|0\rangle_{E/E_f},\end{aligned} \tag{5.38}$$

$$\rho_{E_f}(t) = \mathrm{tr}_S\left[\rho_{SE_f}(t)\right] = \langle g|\,\rho_{SE_f}(t)\,|g\rangle + \langle e|\,\rho_{SE_f}(t)\,|e\rangle\,, \tag{5.39}$$

which subsequently leads to

$$\rho_{E_f}(t) = \begin{pmatrix} 1-\sum_{\mu_2}|c_{\mu_2}(t)|^2 & c_g c^*_{1_{(2)}}(t) & c_g c^*_{2_{(2)}}(t) & \dots \\ c^*_g c_{1_{(2)}}(t) & |c_{1_{(2)}}(t)|^2 & c_{1_{(2)}}(t)c^*_{2_{(2)}}(t) & \dots \\ c^*_g c_{2_{(2)}}(t) & c_{2_{(2)}}(t)c^*_{1_{(2)}}(t) & |c_{2_{(2)}}(t)|^2 & \\ \vdots & \vdots & & \ddots \end{pmatrix}, \tag{5.40}$$

and

$$\rho_{SE_f}(t) = \left(\begin{array}{c|ccc|c} 1-|c_e(t)|^2-\sum_{\mu}|c_{\mu_2}(t)|^2 & \multicolumn{3}{c|}{\multirow{2}{*}{——}} & c_g c^*_{\{\mu_2\}}(t) & \multirow{2}{*}{——} & c_g c^*_e(t) & 0 \\ \multicolumn{1}{c|}{\vdots} & & & & & & & \\ \multicolumn{1}{c|}{c^*_g c_{\{\mu_2\}}(t)} & |c_{1_{(2)}}(t)|^2 & c_{1_{(2)}}(t)c^*_{2_{(2)}}(t) & \dots & c_{1_{(2)}}(t)c^*_e(t) & & & \\ \multicolumn{1}{c|}{\vdots} & c_{2_{(2)}}(t)c^*_{1_{(2)}}(t) & |c_{2_{(2)}}(t)|^2 & & \vdots & & & \vdots \\ \multicolumn{1}{c|}{c^*_g c_e(t)} & \vdots & & \ddots & & & & \\ \multicolumn{1}{c|}{} & c^*_{1_{(2)}}(t)c_e(t) & \dots & & |c_e(t)|^2 & & & \\ \hline 0 & & \dots & & & & & 0 \end{array}\right), \tag{5.41}$$

where the respective basis states, starting from the top left and moving to bottom right of (5.40) and (5.41), are

$$|0\rangle_{E_f}\,,\quad a^{\dagger}_{\{\mu_2\}}|0\rangle_{E_f} \tag{5.42}$$

$$|g,0\rangle_{SE_f}\,,\quad a^{\dagger}_{\{\mu_2\}}|g,0\rangle_{SE_f}\,,\quad |e,0\rangle_{SE_f}\quad a^{\dagger}_{\{\mu_2\}}|e,0\rangle_{SE_f}\,. \tag{5.43}$$

5.3 Application of the quantum Darwinism framework

As was touched upon in section 5.1, the successful emergence of quantum Darwinism is characterised by the presence of redundant classical information, needing the full

mutually induced decoherence of many different system-fragment combinations to emerge. Our objective is to use the QMI to gauge the extend to which correlations produced under the time evolution of (5.41) are shared universally between fragments: in other words, how many E_f communicate the same information about S. To this end, the size of a fragment is quantified by a fraction parameter f,

$$f = \frac{m}{\#E}, \qquad m = 1, 2, \dots, \#E, \tag{5.44}$$

where $0 \leq f \leq 1$ and $m = \dim E_f$. Notice that fractions are not just an aggregate of contiguous modes along the frequency line (i.e. $\lambda = 1, 2, \dots$): the modes are always assumed to be chosen at complete random.

The partial information [49, 52], denoted by $\langle I(f)\rangle$, is defined as the average of the QMI over random choices of fractions of size f. We are interested, of course, in identifying fragments which supply the classical information,

$$\langle I(f_\delta)\rangle = (1-\delta)S(\rho_S). \tag{5.45}$$

from which the redundancy measure R_δ is defined as [7, 50]

$$R_\delta = \frac{1}{f_\delta}. \tag{5.46}$$

Since the quantity f_δ indicates the threshold fragment size yielding $(1-\delta)S(\rho_S)$ information, (5.46) is the number of independent fragments that on average contain (5.45) information on the pointer states. Whilst, here, we shall not explicitly compute the redundancy R_δ, which we leave until chapter 6, it is straightforward to judge its time-dependent behaviour by observing how f_δ changes in the partial information plots.

5.4 Total information and partial information plots

5.4.1 Dynamics of the total information

First we study the dynamics of the QMI shared between the atom and full reservoir. Because the total state is initially pure, the joint entropy $S(\rho_{SE})$ vanishes due to the global entanglement of the atom and reservoir modes, so that the mutual information is given by [110]

$$I(\rho_{SE}) = 2\min\left[S(\rho_S), S(\rho_E)\right] = 2S(\rho_S). \tag{5.47}$$

If the two-level atom is prepared in the excited state then its entropy can be expressed analytically in terms of the binary entropy, $S(\rho_S) = h(|c_e(t)|^2)$, where

$$h(|c_e(t)|^2) = -|c_e(t)|^2 \ln |c_e(t)|^2 - (1 - |c_e(t)|^2) \ln (1 - |c_e(t)|^2), \quad \rho_S(0) = |e\rangle \langle e| . \tag{5.48}$$

Notice here that $|g\rangle$ and $|e\rangle$ adopt the role of pointer states, since with no initial coherences in the system, the density matrix $\rho_S(t)$ remains in a the diagonal form given by (5.12) at times $t > 0$.

In Fig. 5.3, we plot Eq. (5.48) against time and for different values of the coupling strength Ω_0. As one would expect, at short times, the atom quickly develops

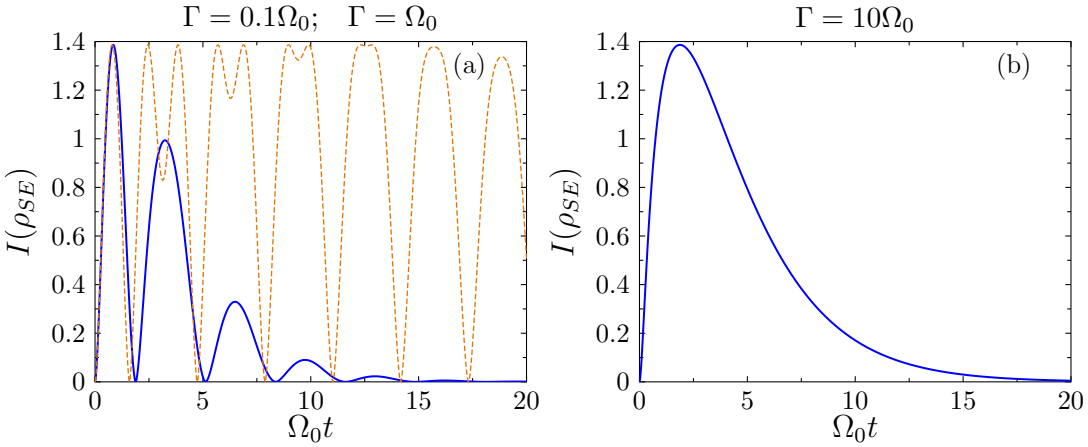

Figure 5.3: Quantum mutual information (5.47) as a function of time, plotted for various parameter values of Ω_0 and Γ. (a) QMI shown for strong (moderate) system-environment coupling, with $\Gamma = 0.1\Omega_0$ (orange dotted curve) and $\Gamma = \Omega_0$ (blue solid curve). (b) The weak coupling case where $\Gamma = 10\Omega_0$.

correlations with the reservoir, being accompanied with an increase in the marginal (atomic) entropy until $\rho_S(t)$ becomes maximally mixed. From this point onwards $S(\rho_S)$ tends to decrease as the atom relaxes to its ground state: whether the entropy also oscillates in time or not depends on the ratio of the parameters Ω_0/Γ (see Fig. 5.2). While it is tempting to think of the oscillations in the QMI has being a characteristic of memory effects, it is worth noting that sometimes total correlations increase as a result of the purity $p(t) = \mathrm{tr}[\rho_S^2(t)]$ decreasing in time, even when the coupling is weak. This can be shown by taking the time-derivative of (5.47):

$$\frac{d}{dt} I(\rho_{SE}) = -4 \left(\frac{d}{dt} |c_e(t)| \right) |c_e(t)| \ln \left(\frac{1 - |c_e(t)|^2}{|c_e(t)|^2} \right) . \tag{5.49}$$

With strong system-reservoir interactions there are clear time-dependent gains $d_t I(\rho_{SE}) > 0$ following times where $p(t)$ passes through a stationary point, i.e. when $d_t|G(t)| = 0$. Solving for $d_t I(\rho_{SE}) = 0$, the stationary points are noted to occur when $|c_e(t)| = \sqrt{1/2}$. Apart from this, other increases in the total QMI happen in parallel with $d_t|G(t)| > 0$. It is precisely these events which indicate re-correlation as a result of true non-Markovian effects in the open system dynamics [79, 80, 117] as we shall go on to discuss shortly with regard to the partial information.

Considering that the global system $S + E$ is bipartite, the entropy of entanglement $E(\rho_S) = -\mathrm{tr}_S[\rho_S \ln \rho_S]$ [14] exactly coincides with the von Neumann entropy $S(\rho_S)$ of the marginal system. The system-reservoir entanglement thus follows a similar pattern of behaviour as the excited state population of the atom, in the sense $E(\rho_S)$ has revivals starting at times

$$t_j = \frac{2}{\Omega}\left(\arctan\left(\frac{2\Omega}{\Gamma}\right) + j\pi\right), \qquad j = 1, 2, \ldots, \tag{5.50}$$

where the full state is momentarily separable (i.e. $G(t_j) = 0$)—as seen in Fig. 5.3. Intuitively, in the long time limit entanglement steadily dies off when the atomic population approaches zero.

5.4.2 Partial information plots

In order to examine the redundant recording of information in the environment, we employ a Monte Carlo procedure to randomly sample fractions f for every $m = 1, 2, \ldots \#E$. Further details on the Monte Carlo simulation are given in appendix A. The partial information is then computed by averaging over the ensemble of different $I(\rho_{SE_f})$. Numerical results are obtained for both strong and weak system-environment coupling for an initial density matrix $\rho(0) = |e\rangle\langle e| \otimes |0\rangle\langle 0|$.

Firstly, because the state in Eq. (5.23) remains pure throughout its time evolution, the partial information plots are antisymmetric about $f = 1/2$. This can be formally demonstrated by first partitioning $S+E$ into a bipartite Hilbert space containing a system-fragment arrangement SE_f and its complimentary fraction E_{1-f}. The Schmidt decomposition of $\rho_{SE}(t)$ reveals the entropies of the two constituent parts to fulfil $S(\rho_{SE_f}) = S(\rho_{E_{1-f}})$ and $S(\rho_{SE_{1-f}}) = S(\rho_{E_f})$. If we then use

$$I(\rho_{SE_f}) = S(\rho_S) - S(\rho_{SE_f}) + S(\rho_{SE_{1-f}}), \tag{5.51}$$

to sum the partial information of the two complementary fractions E_f and E_{1-f}, it turns out that [47, 49, 50]

$$2S(\rho_S) = I(\rho_{SE_{1-f}}) + I(\rho_{SE_f}), \tag{5.52}$$

which proves antisymmetry from the identity (5.47). Intuitively, as $f \to 1$, we obtain $I(\rho_{SE_{1-f}}) \to 0$ and so (5.52) recovers the full QMI of $S + E$.

Let us now focus on the case when the coupling between the atom and modes of the environment is weak; that is, for parameters $\Gamma = 10\Omega_0$. Figure 5.4 shows a complete time evolution of the partial information across many sizes of reservoir mode fractions. Initially after the system and reservoir are brought into contact, partial information grows rapidly as the interaction records information about the atom in the reservoir—coincidentally at the same rate at which the total information increases [cf. Fig. 5.3] . As decoherence sets in further the partial information increases more steeply to its maximum value around $f \approx 1$. From the antisymmetry property (5.52), the rise is matched by a gradually steeper gradient close to the origin. This in turn channels the middle region of the plot into a flat plateau shape, where its length indicates the availability of information $(1-\delta)S(\rho_S)$ from separate fractions of the environment. The level to which information is redundant is then qualitatively indicated by the length of this plateau. As the plateau grows in length and levels out over time, we eventually find that many fractions gain access to the same information about the two-level atom. In this way, redundancy clearly manifests since the difference between correlations in randomly selected fragments is only weakly dependent on f.

At short times, our numerical results show that for typical fragments of small or moderate size, the entropy $S(\rho_{E_f})$ is almost zero (less so in fragments centred close to the atomic frequency ω_0), whereas $S(\rho_S)$ and $S(\rho_{SE_f})$ are much larger and approximately equal as a consequence of fragile bipartite entanglement between the system-fragment and its complementary part: that is, tracing out E_{1-f} significantly diminishes correlations in the full system. If we also track the entropy of the same fragment towards the long time limit, we see $S(\rho_{E_f})$ tends to increase relative to $S(\rho_{SE_f})$ quickly from its initial value, but eventually equilibrates at

$$S(\rho_{E_f}) \simeq S(\rho_{SE_f}), \quad \text{for} \quad t \to \infty,\ f < 1, \tag{5.53}$$

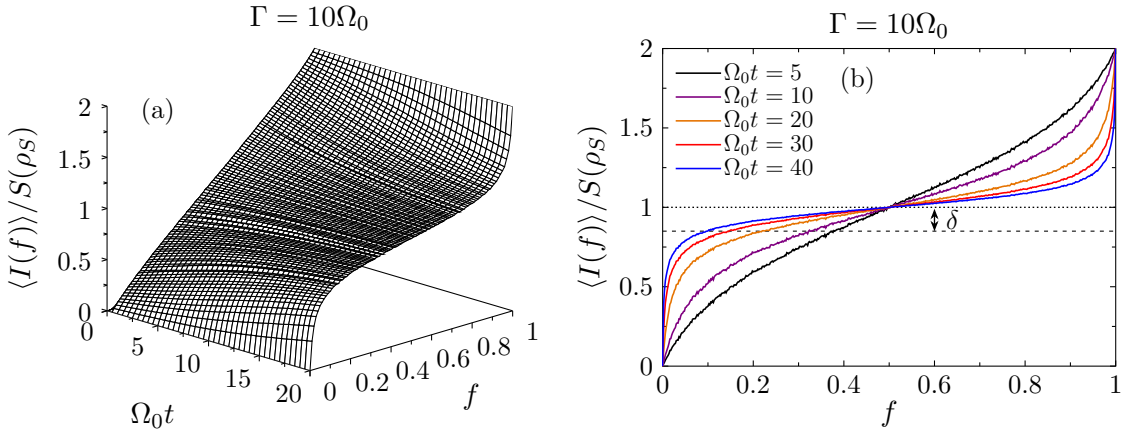

Figure 5.4: Partial information $\langle I(f)\rangle/S(\rho_S)$ shown for weak system-environment coupling, with $\Gamma = 10\Omega_0$. (a) The average of Eq. (5.17) taken from random fragments is plotted against time and fraction size f. (b) Representative snapshots of (a) for equal parameters. The intercept between the black dashed line (shown for $\delta = 0.15$) and each curve indicates the threshold fraction f_δ (5.45). Large redundancy, or small f_δ, reveals that spreading of correlations over time leads to the emergence of redundant information, indicated by the presence of the flat classical plateau.

once the fragment has recorded all possible information it can about the state of the atom. This type of evolution characterises successful quantum Darwinism, analogously fulfilling the redundancy condition in Eq. (5.19). Since this holds for most fractions, $I(\rho_{SE_f})$ declines to zero in line with the system entropy $S(\rho_S)$ [c.f. Fig. (5.3)]. Hence, while nearly all information on the atom is accessible from small fractions of E when $S(\rho_{E_f})$ grows to its maximum value, over time multipartite correlations also eventually decay as a result of the atom losing population. In the steady-state the system decouples from the environment—the global state converges to $\rho_{SE}(\infty) = |g\rangle\langle g| \otimes \rho_E(\infty)$, and, at this point, no information can be obtained from measurements on the environment.

In the case of strong system-environment coupling—shown in Fig. 5.5 for $\Gamma = 0.1\Omega_0$—rather than seeing a increasingly flat plateau form over time, we instead notice pronounced oscillations in the partial information. The process is clearly periodic: decay is followed partial recoherence of the state ρ_{SE_f}, which in turn is accompanied with a suppression in the plateau. While decoherence is not fully

reversible, the oscillations last over many relaxation periods and as a result the redundancy remains qualitatively small, see Fig. 5.5(b). This, of course, lies in direct contrast to the behaviour witnessed in the weak coupling limit.

Looking back at Fig. 5.2, we see that the time evolution of the partial information exactly matches the peaks and troughs in $|G(t)|^2$ at times (5.50). As we have noted from (5.49), at certain times revivals in the atomic population go hand in hand with recorrelation of the full state, which overall suggests memory effects impede the emergence of redundancy. Indeed, what we typically see for a fraction of a

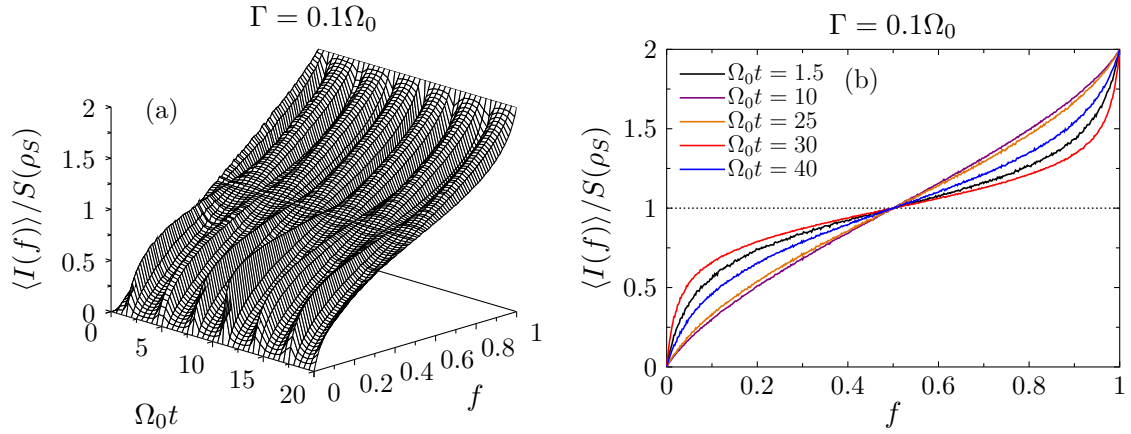

Figure 5.5: Partial information $\langle I(f)\rangle/S(\rho_S)$ shown for strong system-environment coupling. Details of the plots in (a) and (b) are provided in Fig. 5.4, except here with parameters $\Gamma = 0.1\Omega_0$. It can clearly be seen that a classical plateau does not form in the same way as in the Markovian case.

small (or moderate) size is that the entropy $S(\rho_{E_f})$ continuously oscillates in time. This is why the partial information develops "cusps" and does not exhibit a stable classical plateau. While such behaviour is prevalent in the early-time dynamics, it should be noted that a plateau does emerge for $\Omega_0 t \gg 1$ since the entropy converges to its fixed maximum value $S(\rho_{E_f})/S(\rho_{SE_f}) \simeq 1$ [c.f. Eq. (5.53)], at which point oscillations are no longer present (not shown). Though information redundancy can still be observed, clearly its rate of emergence is much slower than in the previously considered example.

To add to this, we also examine the intermediate regime in Fig. 5.6 for parameters $\Gamma = \Omega_0$. Again we find signatures of non-Markovianity in the partial information plots based on the oscillatory behaviour of the atomic population. However, at longer

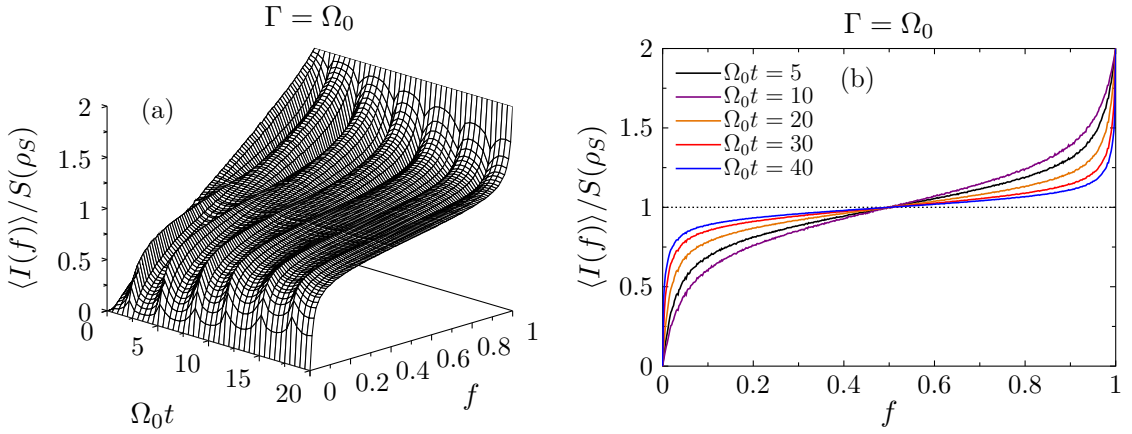

Figure 5.6: Partial information $\langle I(f)\rangle/S(\rho_S)$ shown for strong (moderate) system-environment coupling for parameters $\Gamma = \Omega_0$. Other details of the plots in (a) and (b) are given in Figs. 5.4 and 5.5. Notice oscillations occur in line with those in the atomic population, which tend to fade out at times when a classical plateau develops.

times we notice that a classical plateau very similar to the one in Fig. 5.4 develops. By considering this behaviour together with our last result (c.f. Fig. 5.5), we can see that memory effects tend to disrupt the emergence of redundancy—although, since revivals of the (average) system-environment correlations only affects the formation of the plateau at short times, the environment retains the capacity to record many local copies of the same information on the atom at long times even if the dynamics is strongly non-Markovian, i.e., $\Gamma \ll \Omega_0$.

5.5 Local information

While redundancy and entanglement emerge as a result of the global system-reservoir interaction, local correlations are also formed between the atom and small bands of oscillators. Our intention here is to then examine how information is dynamically distributed among individual modes, as opposed to that contained within larger fractions. The quantity of interest is

$$I(\rho_{SE_\lambda}) = S(\rho_S) + S(\rho_{E_\lambda}) - S(\rho_{SE_\lambda}), \tag{5.54}$$

which specifies the information shared about the atom with a bandwidth of modes spanning ω_λ and $\omega_\lambda + d\omega_\lambda$ about the atom: that is, a single sub-environment E_λ. In

the single excitation case this forms a measure of correlations for an effective two-qubit state, in the sense that one excitation at most can be in the atom or λ-mode of the reservoir.

To compute (5.54), we need to diagonalise each of the density matrices ρ_{E_λ} and ρ_{SE_λ}: with no initial coherences in S, it turns out that $\rho_{E_\lambda} = \mathrm{diag}\,(1-|c_\lambda(t)|^2, |c_\lambda(t)|^2)$. Diagonalising ρ_{SE_λ} yields its four eigenvalues λ_j $(j=1,2,3,4)$, which are given by

$$\lambda_1 = \lambda_3 = 0, \quad \text{and} \quad \lambda_4 = |c_e(t)|^2 + |c_\lambda(t)|^2, \quad \lambda_1 = 1-\lambda_4, \tag{5.55}$$

for each of the two qubits. The local QMI is thus

$$\begin{aligned} I(\rho_{SE_\lambda}) = h(|c_e(t)|^2) + \left(1-|c_\lambda(t)|^2\right)\ln\left(1-|c_\lambda(t)|^2\right) - |c_\lambda(t)|^2\ln|c_\lambda(t)|^2 - \left(|c_e(t)|^2\right. \\ \left. + |c_\lambda(t)|^2\right)\ln\left(|c_e(t)|^2+|c_\lambda(t)|^2\right) - \left(1-|c_\lambda(t)|^2-|c_e(t)|^2\right)\ln\left(1-|c_\lambda(t)|^2-|c_e(t)|^2\right). \end{aligned} \tag{5.56}$$

It proves useful at this point to introduce the following definition of the spontaneous emission spectrum [118, 119]:

$$S_a(\omega_\lambda, t) = \rho_\lambda \left\langle a_\lambda^\dagger a_\lambda \right\rangle_t, \tag{5.57}$$

remembering ρ_λ as the density of states from (3.29). This expresses the conditional probability of finding a photon of frequency ω_λ in the reservoir at a time t. For our initial pure state of $S+E$, the above reads

$$S_a(\omega_\lambda, t) = \rho_\lambda \left\langle \psi(t)\right| \left(1_S \otimes a_\lambda^\dagger a_\lambda\right) \left|\psi(t)\right\rangle = |c_\lambda(t)|^2 \rho_\lambda, \tag{5.58}$$

where $c_\lambda(t)$ are state coefficients of each of the reservoir modes in Eq. (5.23). Note the connection between the presence of local correlations and excitation of the reservoir modes. Thus, it is appreciated that the measure $I(\rho_{SE_\lambda})$ can be studied with regard to the time-dependent properties of the spectrum, as we will go onto establish shortly.

With this in mind, an important quantity to obtain is the steady state form of the emission spectrum, being calculated from $S_a(\omega_\lambda, \infty) = \lim_{t\to\infty} \rho_\lambda \left\langle a_\lambda^\dagger a_\lambda \right\rangle_t$. We discover that

$$S_a(\omega_\lambda, \infty) = \frac{16 J(\omega_\lambda)\left[(\delta_\lambda)^2 + (\Gamma/2)^2\right]}{\left|(2i\delta_\lambda - \Gamma/2)^2 + \Omega^2\right|^2} = \frac{8\Omega_0^2\Gamma}{\pi\left|(2i\delta_\lambda - \Gamma/2)^2 + \Omega^2\right|^2}, \tag{5.59}$$

with $\delta_\lambda = \omega_\lambda - \omega_0$. By substituting $|c_e(\infty)|^2 = 0$ into Eq. (5.56), the asymptotic value of $I(\rho_{SE_\lambda})$ is found to given by

$$I(\rho_{SE_\lambda}) = 0, \quad \text{for} \quad t \to \infty. \tag{5.60}$$

This is, of course, intuitive from the fact that the global state is separable at times $t \gg 1/\gamma_0$ when the atom has almost certainly emitted its photon into the reservoir. The final state of the bipartite system must then have the form

$$|\psi(\infty)\rangle = |g\rangle \otimes \sum_\lambda c_\lambda(\infty) a^\dagger(\omega_\lambda) |0\rangle . \tag{5.61}$$

It is noted the global entanglement (entropy) measure $E(\rho_S)$ (cf. section 5.4.1) also predicts the above, since $E(\rho_S) \to 0$ only occurs in the infinite time limit if $|\psi(\infty)\rangle = |g\rangle \otimes |\psi(\infty)\rangle_E$.

Based on having an analytic expression for the long-time reservoir population density (5.59) and the local information (5.56), it seems reasonable for us to now answer how correlations are distributed across the environment up until the point where the reservoir excitation probability $S_a(\omega_\lambda, t)$ approaches its stationary value (i.e. when $I(\rho_{SE_\lambda}) = 0$). In figures 5.7(a-b), the local information—plotted as a function of detuning from the atomic frequency ω_0—is shown alongside snapshots of itself in the long time limit, in addition to the excitation spectrum for $t \to \infty$. Notably, in Figs 5.7(c-d), there is an obvious resemblance between the atom-mode correlations and individual mode populations in both the strong and weak coupling regimes—more so with decreasing values of Γ. In view of this aspect, let us consider some particular features (5.54), starting with the case where the coupling Ω_0 is much larger than the linewidth; shown in Fig. 5.7(a).

Early exchange of population between the atom and reservoir results in time-dependent oscillations in $I(\rho_{SE_\lambda})$, as we could plausibly expect from the non-Markovian behaviour of $|G(t)|^2$ [cf. Fig. 5.2]. Furthermore, while at short times the atom-mode correlations are primarily spaced within a small band of modes centred on $\delta_\lambda \approx 0$, towards longer times these become increasingly concentrated in sidebands placed at $\omega_\pm - \omega_0$. This evolution in fact foreshadows the steady state behaviour of the population (5.59) shown by the inset in Fig. 5.7(c), which itself exhibits a doublet feature comprising of two sharp peaks separated by a distance $|\omega_\pm - \omega_\mp| = 2\Omega_0$. The effect we see in the local information is therefore a consequence of the vacuum

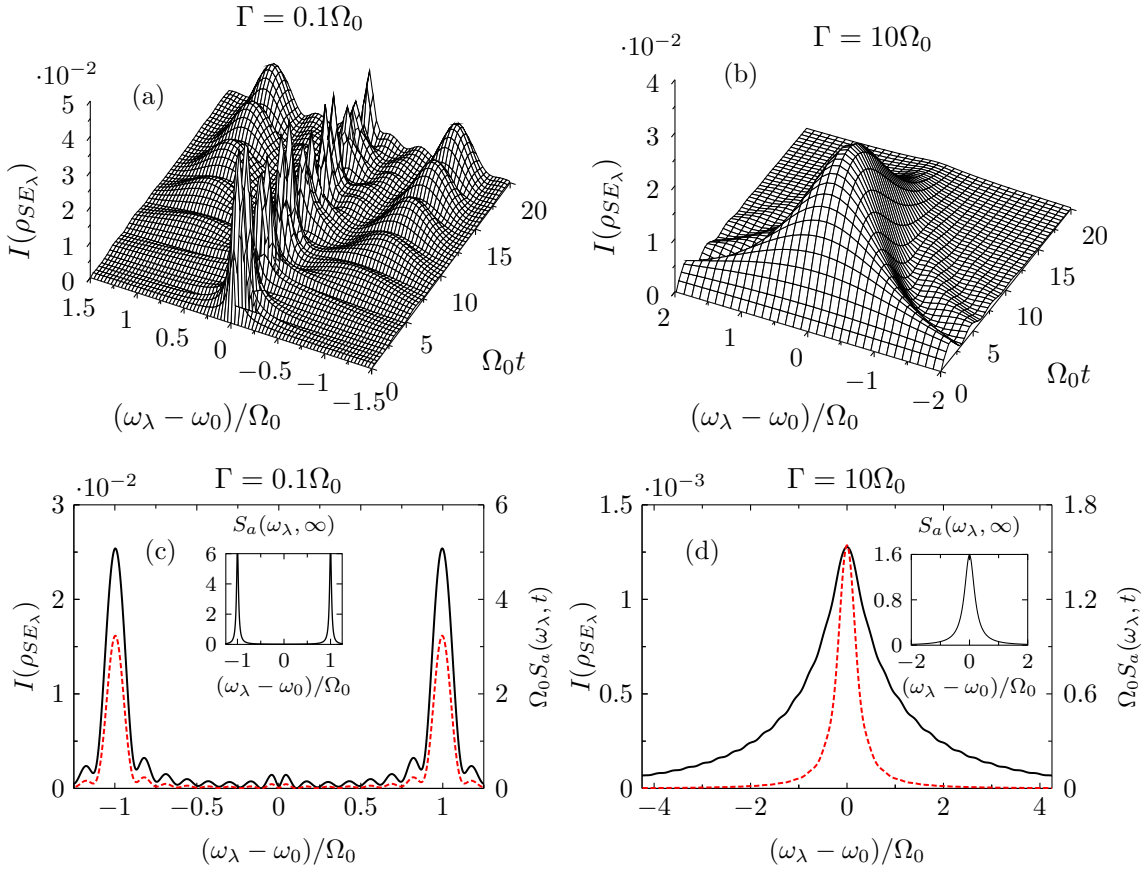

Figure 5.7: The local information $I(\rho_{SE_\lambda})$ plotted as a function of time, for parameters (a) $\Gamma = 0.1\Omega_0$ and (b) $\Gamma = 10\Omega_0$. The bottom row of plots compare (5.56) (black solid curve) against the excitation spectrum (5.58), shown at a times (c) $\Omega_0 t = 50$ and (d) $\Omega_0 t = 20$: respective parameters are the same as those in each of the above panels. Insets show the steady state spectra.

Rabi splitting [120].

On the other hand when the system-environment interactions are weak the spectrum shows no such response, see Fig. 5.7(b). Instead, at short times the atom-mode correlations spread across most of the reservoir due to non-resonant modes briefly participating in the dissipation process. At slightly longer times correlations are distributed over a Lorentzian-type shape with a width given by $\sim \gamma_0$, akin to what is observed in the Markov limit $\Gamma \to \infty$. Again we see that features of the spectrum $S_a(\omega_\lambda, t)$ are reflected in the local information during this point in the evolution. Further on, information decays significantly in line with the atomic

population—approaching zero as t increases further since no correlations can exist without excitation of the atom. Typically speaking, we also notice (5.56) decays more rapidly for weaker couplings relative to the case where $\Omega_0 \gg \Gamma$, which happens on time scale set by the rate of decay of the entropy $S(\rho_S)$.

Relation of local correlations to redundancy

On a final note, let us briefly return to the partial information plots of section 5.4.2 to consider how the local information relates to the growth of redundancy. In the weak coupling limit, if we inspect f_δ from the numerical data presented in Fig. 5.4, it is quite clearly found that redundancy proceeds on a timescale largely separated from that of decoherence τ_D, which sets the rate at which correlations between the atom and reservoir initially form (seen from the rate of increase of the partial information and total information $I(\rho_{SE})$ around $t \approx 0$). Looking at Fig. 5.7, it is interesting to note that the local information tends to fall off at these longer times when redundancy begins to emerge. Yet, for strong coupling in Fig. 5.5, local correlations persist well into this regime with there simultaneously being little redundancy. This indicates a possible connection between the successful storage of information at a local level (i.e. bands of oscillators), and suppression of redundant classical information on a larger "fraction scale".

To give more weight to this idea, in Fig. 5.8, we plot the local information within an intermediate coupling regime. Although peaks develop around the frequencies $\omega_\pm - \omega_0$ as they do in the strong coupling limit, the correlations decay much faster relative to the case $\Omega_0 \gg \Gamma$. As suggested, the correlations fall off on a timescale similar to one which equally sets the rate of decrease of f_δ (see Fig. 5.6). From this evidence we conjecture that local correlations in the reservoir are detrimental to the larger scale acquisition of information within fractions, that is, typically where $f \gg 1/\#E$. As we can imagine these two effects are not one and the same thing—redundancy stems from the information gained by a fraction of the reservoir as its modes decohere collectively along with the system (under the action of the remaining environment), while local information reflects on the information that is recorded by each individual oscillator [50].

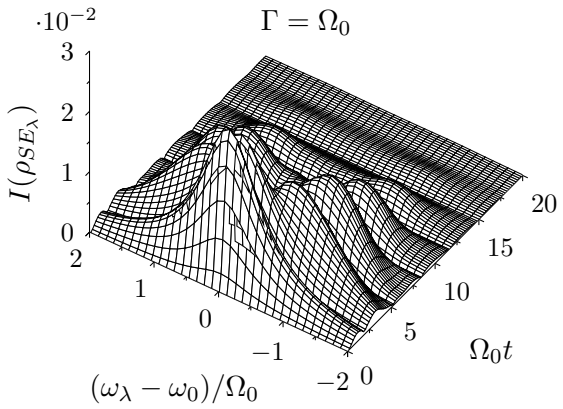

Figure 5.8: Local information (5.56) plotted as a function of time for parameters $\Gamma = \Omega_0$.

5.6 Summary & discussion

In this chapter we have studied emergent features of quantum Darwinism within the setting of a two-level atom coupled to a leaky cavity field. Our main line of inquiry has been to examine the underlying correlation structures of states associated jointly with the atom and different combinations of reservoir modes. To achieve this, we have computed the quantum mutual information (5.17) for such states, whose average across randomly chosen fractions of the environment provides an understanding on the information transfer happening as a result of decoherence. The QMI measure is practical and intuitive to interpret: if the partial information is found to be approximately independent of fraction size, then many fragments are known to gain access to the same information on the system pointer states. This is evidenced by the appearance of a flat plateau shape in the plots of $\langle I(f)\rangle$ at the classical boundary $f = f_\delta$ (5.45) (e.g. see Fig. 5.4), which is used to identify redundancy.

Since the solution to Eq. (5.23) is fully amendable for all possible coupling strengths—including the case when the environment is structured—we have also partly explored the effect non-Markovian behaviour has on the open system's ability to record classical copies of its own data in the environment. Indeed, our original motivation for applying the quantum Darwinism framework was that the model is

exactly solvable, and thus serves as an ideal testbed for future purposes.

Our goal was to numerically assess the partial information plots for various choices of spectral parameters Ω_0 and Γ. For weak system-environment coupling, not only was a classical plateau shown to form, but also that its length continuously increases over time, accompanied with a monotonic decrease in f_δ. Meanwhile, when the environment is structured, the long term storage of redundant information is strongly inhibited by the presence of memory effects. We recall that revivals in the atomic population lead to partial recorrelation of a typical system-fragment state, which subsequently contributes to the rollback of the decoherence process. Remarkably, in an intermediate regime $\Omega_0 \approx \Gamma$, despite memory effects still being influential to the dynamics, we have shown that significant redundancy does emerge at long times. Taking this into account, our preliminary conclusion is that quantum Darwinism (or redundancy) does emerge—taken with the caveat that for stronger couplings $\Omega_0 \gg \Gamma$, the non-Markovian response from the atom pushes back the formation of redundant information until very long times. In a regime where the atomic population oscillates in time, dissipation and decoherence can then be viewed as competing mechanisms with regard to the emergence of classicality: decoherence acts to proliferate copies of the system's state into the reservoir, while memory effects tend to disrupt this process until oscillations gradually fade out at longer times.

The last task was to study the information carrying capacity of individual reservoir modes as a means to acknowledge where information is locally recorded in the environment. This is quantified through the QMI shared between the atom and sub-environment of frequency ω_λ (5.54), which has been shown to follow a similar pattern of behaviour to the emission spectrum prior to the long time limit (see Fig. 5.7). For strong system-environment coupling, we established that local information develops Rabi sidebands symmetrically about the atomic frequency. Decreasing the coupling strength enough causes the doublet to be replaced by a Lorentzian profile with resonant modes containing most information. By comparing the different timescales on which local correlations disappear and $1/f_\delta$ increases, we also suggest a possible adverse influence local correlations have on the information capacity of "whole" fragments—those of moderate f-size that contain many modes and par-

ticipate in the decoherence process. This could be explored with greater detail in future work, and/or furthered to examine how multipartite correlations between mode fractions affect redundancy.

Finally, it should be emphasised that the general method of obtaining the partial information relies on sampling a bandwidth made up of a random selection of individual modes. This way of sampling, however, can be difficult to relate to how physical measurements could be made on the environment in the current model. To illustrate this point, consider a quantum Brownian particle oscillating under the dissipative action of a quantum field [1, 7, 52]. Usually in this setting excitations are scattered unpredictably from the particle into regions of the surrounding space: therefore, it seems reasonable that an observer could intercept information from a random bandwidth (in frequency space) when measuring a part of the particle's environment. Yet, for the atom-cavity model used in the chapter, it is not *a priori* obvious how to measure the environment in this way—indeed, measurements here are typically done in controlled manner over the full cavity bandwidth. The lack of a firm connection between our results and actual experiment is somewhat unsatisfactory for this reason. Part of our motivation for the next chapter is to then refine the current model to one that is grounded in a more realistic scheme.

Chapter 6

A further application of quantum Darwinism to a structured environment

At this point we have established the dynamical regimes for which quantum Darwinism emerges in the example of a dissipative two-level atom. In particular we found the transfer of redundant information into the environment to be most successful in the absence of memory effects. To build upon this foundation, we proceed down a similar path to one we previously explored, which involved us looking at how a system imprints copies of its own information into sub-environments. The exception here is that we promote the previous single bosonic reservoir to a multiple-environment model: more precisely, we deal with a setup where a two-level atom interacts with a large number of independent reservoirs of oscillators (see Fig. 6.1). As we shall see, since the spectral density of total environment may under certain conditions be expressed in terms of a single Lorentzian, like that in Eq. (5.21), the dynamical solution found in (5.32) for single reservoir coupling is also relevent to this case. The results we obtain here therefore encompass those of chapter 5, and, as such, stem from a generalisation of the previous model.

According to Ref. [41], each reservoir (sub-environment) may be replaced by a single pseudomode, meaning atom's dynamics is equally described by its coupling to many unconnected and damped oscillators. These are known to store information from which the atom can receive back at a later time [121]. In view of this, our

approach focuses on a partitioning of the environment into its memory part—the pseudomodes—and non-memory part, into which pseudomodes decay (see Fig. 4.4 for a single pseudomode illustration). We consider information storage in both of two separate cases: (i) in the full reservoirs, and (ii) in the memory part only. The main quantity of interest is still of course the QMI, provided as

$$I(\rho_{SX_f}) = S(\rho_S) + S(\rho_{X_f}) - S(\rho_{SX_f}). \tag{6.1}$$

However, we assign X_f (X) to fragments either made up of reservoirs E_f, or pseudomodes P_f, corresponding to cases (i) and (ii), respectively. By examining correlations selectively, our intent is to study where information is stored redundantly, and also how this process is affected by the mixing of the state $\rho_{SP_f} = \mathrm{tr}_{P/P_{1-f}}\rho_{SP}$ as it evolves under a noisy quantum channel in line with Refs. [53, 54]. We too establish how classical and quantum correlations are encoded between the system and environment fractions, the latter of which measured by the quantum discord [122, 123], to look more deeply at the degree to which *classical* information is redundant out of the total correlations.

Rather than keep a loose interpretation of memory effects, here we check the criteria that lead to poor Darwinism in chapter 5 with an actual witness of non-Markovianity [78–80]. This enables us to gain a consistent understanding on the role information back-flow from environment to the system [66, 124, 125] has on suppressing redundancy along with recorrelation effects. Additionally, it creates a formal link between the time-dependent behaviour of the partial information in the new and previous model to the non-Markovian dynamics of the atom.

First, we introduce the dynamical model in section 6.1 and proceed to obtain an exact solution for the state coefficients of the atom and pseudomode degrees of freedom. We identify a dynamical regime of interest where the atom shares significant correlations with the pseudomode part of the environment. Then, in sections 6.2, we study the partial information plots of cases (i) and (ii) and address the decomposition of the QMI (6.1) into its classical and quantum components. In section 6.3 we identify conditions which maximise classical atom-pseudomode correlations. Finally, we compute the redundancy from $R_\delta = 1/f_\delta$ (5.46) and relate its dynamical behaviour to that of the non-Markovian witness. A possible configuration the model applies to is a two-level atom coupled to a large cavity array, where each cavity field

leads into an external vacuum of modes.

6.1 Dynamical model

We start by considering a two-level atom (TLA) S interacting with an environment E of bosons. Our plan is to adopt the multiple-environment model from section 3.1: though for clarity we will briefly reiterate some ideas that were made in previous chapters, being relevant to the current model—see sections 4.3.1 and 5.2. Like before the environment is arranged as $E = \otimes_{k=1}^{\#E} E_k$ and is prepared in the vacuum state, where the index $k = 1, 2, \ldots, \#E$ labels individual fixed sub-environments E_k. An important difference here, however, is that the sub-environments now make up entire reservoirs, and *not* individual modes. In turn, each reservoir is comprised of harmonic oscillators with frequencies ω_λ. The Hamiltonian of the atom and environment are given by $H_S = \omega_0 \sigma_+ \sigma_-$ and $H_E = \sum_{k,\lambda} \omega_\lambda a^\dagger_{k,\lambda} a_{k,\lambda}$, respectively. Note too that variables between sub-environments commute as

$$[a_{k,\lambda}, a^\dagger_{k',\lambda'}] = \delta_{k,k'} \delta_{\lambda,\lambda'}, \tag{6.2}$$

which satisfy the familiar relation $a_{k,\lambda} a^\dagger_{k',\lambda'} |0\rangle = \delta_{k,k'} \delta_{\lambda,\lambda'} |0\rangle$. Within the rotating wave approximation and interaction picture, the total Hamiltonian reads

$$H_I(t) = \sum_k (\sigma_+ B_k(t) + \text{h.c.}), \tag{6.3}$$

where

$$B_k(t) = \sum_\lambda g_{k,\lambda} a_{k,\lambda} \exp[-i(\omega_\lambda - \omega_0)t], \tag{6.4}$$

and $g_{k,\lambda}$ is the coupling of the λ-mode in the k^{th} reservoir to the atom. In the following we consider spectral densities of the form

$$J(\omega) = \frac{\Omega_0^2}{2\pi} \sum_k \frac{w_k \, \Gamma}{(\xi_k - \omega)^2 + (\Gamma/2)^2}, \tag{6.5}$$

where Γ is the width and ξ_k the peak frequency of an individual Lorentzian, weighted by real positive constants w_k, satisfying $\sum_k w_k = 1$. For simplicity, we have imposed that each of the Lorentzian widths—associated with the coupling to each sub-environment—are the same.

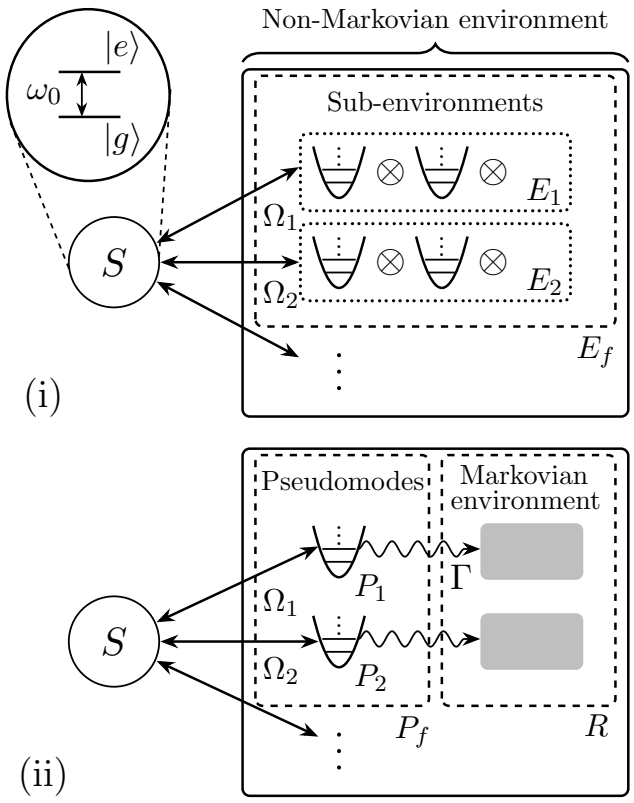

Figure 6.1: Schematic showing two dynamical representation of the model. (i) The qubit system S couples to many sub-environments $E_1, E_2, \ldots$ with strengths $\Omega_1, \Omega_2, \ldots$. (ii) An equivalent setup in terms of pseudomodes, labelled $P_1, P_2, \ldots$, which are each damped by independent Markovian reservoirs R at an equal rate Γ. The environment is sampled by constructing fragments out of the bare sub-environments E_f, or the pseudomodes, P_f, respectively.

6.1.1 Solutions to the model

Suppose the atom is initially prepared in the state $|\psi\rangle_S = c_g |g\rangle + c_e(0) |e\rangle$. As the number of excitations are conserved in this model [see Eq. (4.145)], the total state is restricted to the single excitation manifold, which at a time $t > 0$ admits the closed form

$$|\psi(t)\rangle = c_g |g, 0\rangle + c_e(t)\sigma_+ |g, 0\rangle + \sum_{k,\lambda} c_{k,\lambda}(t) a^\dagger_{k,\lambda} |g, 0\rangle . \tag{6.6}$$

The memory kernel is obtained by taking the continuum limit over all sub-environments as follows:

$$f(t - t') = \sum_{k,k'} \left[B_k(t), B^\dagger_{k'}(t') \right] = \int_{-\infty}^{\infty} d\omega J(\omega) e^{-i(\omega-\omega_0)(t-t')}. \tag{6.7}$$

By substituting (6.6) into the Schrödinger equation and eliminating the variables $c_{k,\lambda}(t)$, we get

$$\frac{d}{dt}c_e(t) = -\int_0^t dt' \sum_k \Omega_k^2 \exp[(-i(\xi_k - \omega_0) - \Gamma/2)(t-t')]c_e(t'), \tag{6.8}$$

where $\Omega_k = \sqrt{w_k}\Omega_0$ is defined as the coupling strength of the atom to the k^{th} reservoir. Because Eq. (6.5) is meromorphic and contains simple poles in the lower-half complex plane, we can then rewrite (6.8) into the following set of coupled differential equations:

$$\frac{d}{dt}c_e(t) = -i\sum_k \Omega_k e^{-i\Delta_k t} b_k(t), \tag{6.9}$$

$$\frac{d}{dt}b_k(t) = -\frac{\Gamma}{2}b_k(t) - i\Omega_k e^{i\Delta_k t}c_e(t), \tag{6.10}$$

having been defined in a new frame rotating frame with respect to the term $\sum_k \Delta_k a_k^\dagger a_k$ [see (3.16)], where $\Delta_k = \xi_k - \omega_0$. The coefficients

$$b_k(t) = -i\Omega_k e^{-\Gamma t/2}\int_0^t dt'\, e^{(i\Delta_k - \Gamma/2)t'}c_e(t') \tag{6.11}$$

are interpreted as those of pseudomodes. The dynamics of the combined atom-pseudomode degrees of freedom are formulated in terms of an exact Markovian master equation

$$\frac{d}{dt}\rho_{SP}(t) = -i[H_S'(t), \rho_{SP}(t)] + \Gamma\sum_k \mathcal{L}_{a_k}[\rho_{SP}(t)], \tag{6.12}$$

where a_k ($a_k^\dagger$) is the annihilation (creation) operator of the k-pseudomode, and

$$H_S'(t) = \sum_k \Omega_k \left(e^{-i\Delta_k t}\sigma_+ a_k + \text{h.c.}\right). \tag{6.13}$$

The master equation, as we would expect, has same structure as the one derived in Eq. (4.139) but this time with many possible independent decay channels. Therefore (6.12) has the solution

$$\rho_{SP}(t) = \Pi_g(t)\left|g\right\rangle\left\langle g\right| \otimes (\left|0\right\rangle\left\langle 0\right|)_P + \left|\widetilde{\psi}(t)\right\rangle\left\langle\widetilde{\psi}(t)\right|_{SP}, \tag{6.14}$$

with the unnormalised state vector $\left|\widetilde{\psi}(t)\right\rangle_{SP}$ provided by

$$\left|\widetilde{\psi}(t)\right\rangle_{SP} = c_g\left|g,0\right\rangle_P + c_e(t)\sigma_+\left|g,0\right\rangle_P + \sum_k b_k(t)a_k^\dagger\left|g,0\right\rangle_P. \tag{6.15}$$

In this context $|0\rangle_P$ denotes the pseudomode vacuum and $\Pi_g(t)$ its population,

$$\Pi_g(t) = \Gamma \int_0^t dt' \sum_k |b_k(t')|^2, \tag{6.16}$$

with the corresponding probability density of photon emission from the atom given by

$$\frac{d}{dt}\Pi_g(t) = \Gamma \sum_k |b_k(t)|^2. \tag{6.17}$$

Overall, the original environment is equally represented in terms of one with a bipartite inner structure, comprised of a set of uncoupled pseudomodes $P = \otimes_{k=1}^{\#E} P_k$ and Markovian reservoirs R. This picture is analogous to the structured atom-chain representation of the single environment model we saw in chapter 4. Indeed, the atom here interacts directly with the pseudomodes, which each in turn leak into R at a rate Γ (see Fig. 6.1).

Large environment limit $\#E \to \infty$

Since (6.9) and (6.10) are linear, exact solutions to the atom and pseudomode state coefficients in (6.15) may be found directly through numerical inversion of the equations. However, we consider the continuum limit of pseudomodes, and, more generally, of the sub-environments by taking $\#E \to \infty$. This allows analytical solutions to be obtained provided a suitable distribution for the weights $w_k = w(\xi_k)$ is assumed in the conversion

$$\sum_k \longrightarrow \int d\xi_k \rho_k, \tag{6.18}$$

done in a way analogous to (3.28), with ρ_k taken as the density of pseudomode states on the frequency line ξ_k. By replacing the weights in (6.5) with the quadrature $w_k = W(\xi_k)d\xi_k$, an equivalent form of the spectral density (6.5) is determined by the convolution $J(\omega) = (W * L)(\omega)$, where

$$(W * L)(\omega) = \int_{-\infty}^{\infty} d\xi\, W(\xi) L(\omega - \xi), \tag{6.19}$$

and $L(\omega) = \Gamma/[\omega^2 + (\Gamma/2)^2]$. Apart from the distribution $W(\xi)$ having to fulfil the normalisation condition,

$$\int_{-\infty}^{\infty} d\xi\, W(\xi) = 1, \tag{6.20}$$

its functional form is otherwise arbitrary. Based on the stipulation that (6.9) and (6.10) yield analytical solutions, a key result is that by choosing a single Lorentzian distribution,

$$W(\xi) = \frac{1}{\pi} \frac{\Gamma_W/2}{(\omega_0 - \Delta - \xi)^2 + (\Gamma_W/2)^2}, \tag{6.21}$$

with a width provided by Γ_W, Eq. (6.5) can be equivalently written as

$$J(\omega) = \frac{\Omega_0^2}{\pi} \frac{\Gamma_p/2}{(\omega_0 - \Delta - \omega)^2 + (\Gamma_p/2)^2}. \tag{6.22}$$

The parameter $\Gamma_p = \Gamma + \Gamma_W$ accounts for a broadening caused by the background pseudomode continuum. In addition, Δ is the detuning of the centre of this distribution from the atomic frequency: note this has a different symbol compared to what was used in chapter 4, in order to distinguish it from the information deficit δ.

Considering the formula (6.19) simply recovers a Lorentzian spectral density, the state coefficients in (6.6) and (6.15) have analytical solutions which are readily obtainable via the Laplace transform method. This aspect will conveniently be exploited to compute the QMI (6.1) exactly, in the same way as we did in section 5.2.2.

6.1.2 Atom-pseudomode dynamics

The master equation (6.12) provides fully amendable solutions for strong system-environment interactions, which are shown in Fig. 6.2 to illustrate their behaviour. We initially check the response of the atom by tracing out the pseudomodes from the density matrix $\rho_{SP}(t)$ (6.14). To construct a master equation for the atomic degrees of freedom, we note that $\rho_S(t)$ can be represented as a convex-linear combination

$$\rho_S(t) = (1-p)\,\mathrm{tr}_P\,|g,0\rangle\langle g,0|_P + p\,\mathrm{tr}_P\big[\Pi_g(t)\,|g,0\rangle\langle g,0|_P + |\widetilde{\psi}(t)\rangle\langle\widetilde{\psi}(t)|_{SP}\big], \tag{6.23}$$

where $0 \leq p \leq 1$ to ensure $\mathrm{tr}\,\rho_S(t) = 1$ for any initial pure or mixed state of the open system. By virtue of $a_k a_{k'}^\dagger\,|0\rangle = \delta_{k,k'}\,|0\rangle$, the trace in the above gives

$$\begin{aligned}\rho_S(t) = &\left\{(1-p) + p\left(|c_g|^2 + \Pi_g(t) + \sum_k |b_k(t)|^2\right)\right\}|g\rangle\langle g| + p|c_e(t)|^2\,|e\rangle\langle e| \\ &+ pc_g c_e^*(t)\,|g\rangle\langle e| + \mathrm{h.c.}\end{aligned} \tag{6.24}$$

Since the reduced system is spanned by two possible states, Eq. (6.24) also has the same form as the density matrix $\rho_S(t)$ in (5.28), similarly with $c_e(t) = G(t)c_e(0)$.

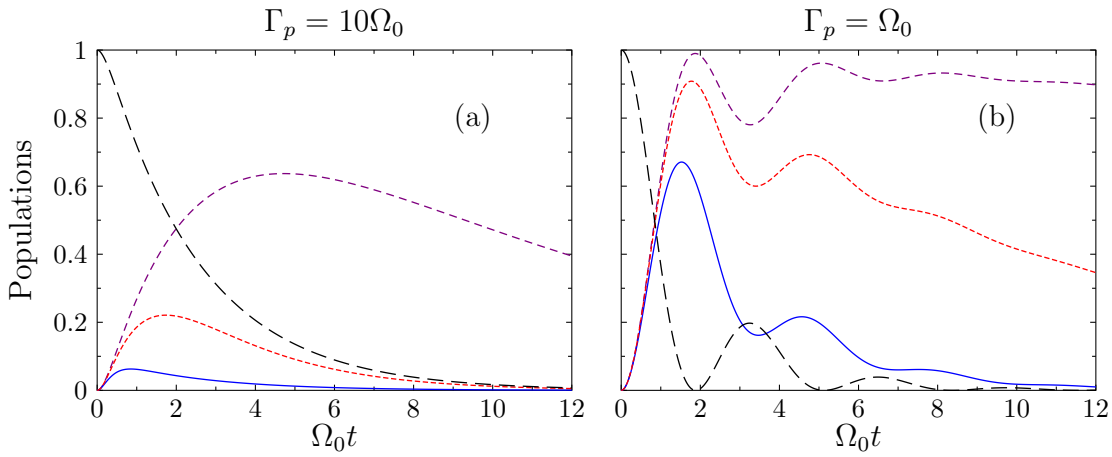

Figure 6.2: Time evolution of the populations $|c_e(t)|^2 = |G(t)|^2|c_e(0)|^2$ (black long-dashed) and $\sum_k |b_k(t)|^2$ for $c_e(0) = 1$. Parameters are $\Gamma = \{0.5, 0.1, 10^{-2}\}\Gamma_p$ (blue solid, red dotted, violet dashed lines) and $\Delta = 0$. (a) The weak coupling case $\Gamma_p = 10\Omega_0$. (b) The case of strong (moderate) system-environment coupling, $\Gamma_p = \Omega_0$.

From Ref. [111], it is known that the dynamics of this system is governed by the time-convolutionless master equation

$$\frac{d}{dt}\rho_S(t) = \Gamma(t)[\sigma_-\rho_S(t), \sigma_+] + \Gamma^*(t)[\sigma_-, \rho_S(t)\sigma_+], \tag{6.25}$$

where $\Gamma(t) = -d_t G(t)/G(t)$. By means of Laplace transforms, the exact solution to $G(t)$ taken from (5.27) and (6.7) is

$$G(t) = e^{(i\Delta/2 - \Gamma_p/4)t}\left[\cos\left(\frac{\Omega t}{2}\right) - \frac{(i\Delta - \Gamma_p/2)}{\Omega}\sin\left(\frac{\Omega t}{2}\right)\right], \tag{6.26}$$

with $\Omega = \sqrt{4\Omega_0^2 - (i\Delta - \Gamma_p/2)^2}$. Now, with the help of the Eq. (6.9), if we define the real coefficients

$$\gamma(t) = \Gamma(t) + \Gamma^*(t) = \sum_k 2\Omega_k \frac{\mathrm{Im}\left[e^{i\Delta_k t}c_e(t)b_k^*(t)\right]}{|c_e(t)|^2}, \tag{6.27}$$

$$s(t) = i\left[\Gamma^*(t) - \Gamma(t)\right] = \sum_k 2\Omega_k \frac{\mathrm{Re}\left[e^{i\Delta_k t}c_e(t)b_k^*(t)\right]}{|c_e(t)|^2}, \tag{6.28}$$

and subsequently use $\Gamma(t) = [\gamma(t) + is(t)]/2$ and $\Gamma^*(t) = [\gamma(t) - is(t)]/2$, the master equation for the two-level atom can be expressed in the canonical form [1, 69],

$$\frac{d}{dt}\rho_S(t) = -i\frac{s(t)}{2}[\sigma_+\sigma_-, \rho_S(t)] + \gamma(t)\mathcal{L}_{\sigma_-}[\rho_S(t)], \tag{6.29}$$

where $\gamma(t)$ is the decay rate and $s(t)$ the Lamb shift.

Importantly, the dynamics associated with (6.29) are known to be nondivisible and non-Markovian if $\gamma(t)$ takes negative values. It is instructive to consider this aspect with regard to the behaviour of (6.12). If we first differentiate $|c_e(t)|^2$ and apply (6.9) to the result, we obtain

$$\frac{d}{dt}|c_e(t)|^2 = i\sum_k \left(\Omega_k e^{i\Delta_k t} b_k^*(t) c_e(t) - \text{c.c.}\right), \tag{6.30}$$

which simply expresses the probability flux between the atom and pseudomodes. By then taking the time derivative of (6.24) and equating its ground state population with that from (6.29), i.e. the coefficient of $|g\rangle\langle g|$, we find, using Eqs. (6.30), (6.27) and (6.17), that the combined dynamics of the atom and pseudomodes is subject to the following relation:

$$\sum_k \left(\frac{\partial}{\partial t} + \Gamma\right)|b_k(t)|^2 = \gamma(t)|c_e(t)|^2. \tag{6.31}$$

The lefthand side of the above shows the rate of change the pseudomode population compensated against irreversible losses, occurring at a rate Γ. Notice the behaviour of $c_e(t)$ here follows exactly that of (5.32), except with a modified decay rate Γ_p. Given we want to compare $|c_e(t)|^2$ with the joint response of the pseudomode states using (6.31), we set $\Delta = 0$: this being the case we shall focus on from now on. In the strong coupling regime $4\Omega_0 > \Gamma_p$, the excited state population of the atom increases in time during intervals when $\gamma(t) < 0$, which, from (6.31), gives a simultaneous and equal decrease in the pseudomode population. Hence time-dependent revivals in the atomic population are exclusively linked to pseudomode depletion, neglecting the constant leakage of the pseudomode excitation to the external reservoirs. Also, with weak system-environment coupling, $4\Omega_0 < \Gamma_p$, the decay rate $\gamma(t)$ is positive at all times and the atom-pseudomode populations show no oscillations. Note too that when $\Gamma_p \to \infty$, we have $\gamma(t) \to \gamma_0$, where

$$\gamma_0 = 4\Omega_0^2/\Gamma_p. \tag{6.32}$$

Here the atom follows a time-independent Markov process. We therefore interpret the non-Markovian behaviour as being entirely causal to the back-flow of population and energy between the two. As discussed in Ref. [121], this indicates that the

pseudomode region P in Fig. 6.1 acts as a memory for the atom in the presence of strong interactions.

Separation of timescales

At this point it is worth further elaborating on the pseudomode population dynamics, which we examine via the density matrix $\rho_P(t) = \mathrm{tr}_S\, \rho_{SP}(t)$. Before we go into this, we first highlight the fact that the time evolution of $|G(t)|^2$ in (6.26) depends only on the memory kernel (6.7). In turn, this means the rate at which the atom decays is solely determined by the width Γ_p of the spectral density (6.22). One might intuitively expect something similar for the dynamics of the pseudomode coefficients $b_k(t)$. However, we actually discover two damping timescales that determine its evolution. Its solution, given by

$$\begin{aligned} b_k(t) = -\frac{4\Omega_k\, c_e(0)}{\left(i(2\Delta_k+\Delta)+\frac{\Gamma-\Gamma_W}{2}\right)^2+\Omega^2}\Bigg\{&\left(\Delta_k+\Delta+i\frac{\Gamma_W}{2}\right)e^{-\Gamma t/2} \\ &- e^{i\Delta_k t}e^{(i\Delta/2-\Gamma_p/4)t}\Bigg[\left(\Delta_k+\Delta+i\frac{\Gamma_W}{2}\right)\cos\left(\frac{\Omega t}{2}\right) \\ &- \left(\left(\frac{i\Delta-\Gamma_p/2}{\Omega}\right)\left(\Delta_k+\Delta/2-i\frac{\Gamma-\Gamma_W}{4}\right)+i\frac{\Omega}{2}\right)\sin\left(\frac{\Omega t}{2}\right)\Bigg]\Bigg\}, \end{aligned} \tag{6.33}$$

clearly separates into two parts, each with different and real exponential prefactors. This causes one part containing the sinusoidal terms to decay at a rate $\Gamma_p/4$, and the other static part to decay at a rate $\Gamma/2$. Because of "mixing" between terms in the population $\sum_k |b_k(t)|^2$, it is difficult to single out their individual effect in a typical time evolution, which generally shows complex behaviour. It becomes apparent, though, when we introduce a large separation of timescales through

$$\frac{1}{\Gamma_p} \ll t \ll \frac{1}{\Gamma}. \tag{6.34}$$

In Fig. 6.2, the effect of the fast and slow terms becomes increasingly noticeable towards the regime $\Gamma \ll \Gamma_p$. We see the fast terms decay quickly and predominantly influence the short time evolution, while the slow terms decline exponentially and thus survive into the long time limit.

In view of this, let us comment further on the dynamics in such a case where

Eq. (6.34) is valid. Within the strong coupling regime, there is a distinct cross-over owing to the fact that the fast oscillatory terms decay on the fixed timescale $t \sim O(1/\Gamma_p)$. The dynamics are then categorised into two phases. As we have seen, the short time evolution is characterised by memory effects where the qubit and pseudomode populations oscillate in time. When $t \gg 1/\Gamma_p$, the pseudomode population instead decays monotonically as ($c_e(0) = 1$)

$$\sum_k |b_k(t)|^2 \approx e^{-\Gamma t} \sum_k \frac{16\Omega_k^2 \left[\Delta_k^2 + (\Gamma_W/2)^2\right]}{\left|\left(2i\Delta_k + \frac{1}{2}(\Gamma - \Gamma_W)\right)^2 + \Omega^2\right|^2}. \tag{6.35}$$

At this point the atom has essentially relaxed and thus decoupled from the memory, i.e. $|G(\infty)|^2 \approx 0$. As a matter of interest, by evaluating the trace of $\rho_{SP}(t)$ over the system states we obtain

$$\rho_P(t) = \sum_{k,k'} b^*_{k'}(t) b_k(t)\, a_k^\dagger \left|0\right\rangle \left\langle 0\right|_P a_k + \Pi_g(t) \left|0\right\rangle \left\langle 0\right|_P, \qquad t \gg 1/\Gamma_p. \tag{6.36}$$

By then using (6.10) it is shown that $\rho_P(t)$ obeys the quantum master equation

$$\frac{d}{dt}\rho_P(t) = \Gamma \sum_k \mathcal{L}_{a_k}[\rho_P(t)], \qquad t \gg 1/\Gamma_p. \tag{6.37}$$

Similar phases also exist when the dynamics are Markovian given the solution (6.33) still comprises of fast and slow terms, where, at long times, the pseudomode population fulfils (6.35). Notice however that the cross-over isn't so distinct here since the fast terms do not decay on the same fixed timescale as before—with, of course, there being no oscillations. Nonetheless, there is still a transition to slow exponential decay close to when the atom has fully dissipated its energy.

When $t \ll 1/\Gamma$, Eq. (6.35) predicts that the pseudomodes tend to form a quasi-bound state at long times $\Omega_0 t \gg 1$ as a result of the cross-over, i.e. $\Gamma \ll \Gamma_p$. Although this occurs generally with respect to the coupling Ω_0, the excitation is most efficiently "trapped" by the pseudomodes in the strong coupling limit since increasing Γ_p (with the ratio Γ/Γ_p fixed) also increases the rate at which population leaks to the Markovian reservoir. Overall, we find the validity of Eq. (6.35) in describing the long time dynamics to only really be affected by the degree of separation between Γ and Γ_p. The trapping effect then appears to be a feature of the narrow-Lorentzian structure of $J(\omega)$. Indeed, taking the broad Lorentzian limit $\Gamma \approx \Gamma_p$ recovers the usual single pseudomode dynamics from Refs [41, 42], which

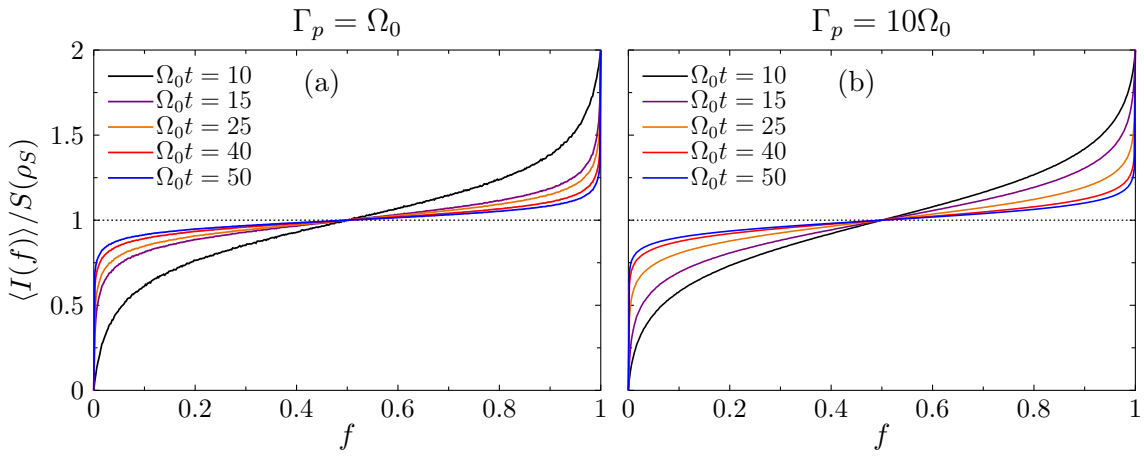

Figure 6.3: Partial information $\langle I(f)\rangle/S(\rho_S)$ shared between the atom and sub-environments ($X = E$), shown as a function of fraction size f at various times and for $\Delta = 0$, with parameters (a) $\Gamma_p = \Omega_0$ and (b) $\Gamma_p = 10\Omega_0$. The classical plateau appears for both the strong (moderate) and weak coupling—its length increases and becomes flatter as system-fragment states decohere over time.

does not display any of the trapping features seen here.

The presence of a large pseudomode population well into the long time limit suggests that a significant proportion of the total correlations of $S+E$ develop between the atom and memory region of the environment. Since we are working within the context of quantum Darwinism, it seems justified to ask if such correlations translate into redundant information. This is part of what we go onto consider in the following section.

6.2 Partial information plots

As we did in chapter 5, we again run a Monte Carlo simulation to compute the partial information $\langle I(f)\rangle$ by randomly sampling the QMI for different fraction sizes f. Numerical results are obtained assuming an initially excited atom. We now proceed by discussing each of the cases (i) and (ii) in turn.

6.2.1 Case (i): atom and sub-environments

Since the solution for the atomic state coefficient (6.26) is a generalised version of that given in (5.32)—likewise for the reservoir state coefficients (6.6) (see appendix

A), here we focus on dynamical regimes where redundancy is expected to emerge based on the results of section 5.4.2. Figure 6.3 shows the partial information plotted as a function of f for such cases. At short times, the atom's entropy $S(\rho_S)$ increases very quickly from zero in line with the entropy $S(\rho_{SE_f})$ of the atom plus an averagely chosen small (moderate) fraction of the environment. This effect—equivalent to what we saw in section 5.4.2—is based on the fast emergence of bipartite entanglement between the states of SE_f and E_{1-f}. As time progresses the entropy of the fragment E_f gradually increases relative to those of the other subsystems until it matches that of $S(\rho_{SE_f})$ at long times. Indeed, the total gain in $S(\rho_{E_f})$ over the course of the full time evolution measures the information fragments (on average) acquires about state of S. This steady increase in the system-fragment correlations is witnessed in the case of weak system-environment coupling, Fig. 6.3(a), which results in the substantial growth of a flat plateau shape in the partial information. Similar behaviour occurs for strong (moderate) coupling, the main difference being that there are times when f_δ (5.45) momentarily decreases due to oscillations of the plateau about $f = 1/2$. Overall, the dynamical features seen in the plots here are congruent with those in Figs. 5.4 and 5.6: the most important aspect being the emergence of redundancy at long times.

Before moving onto the next case we first examine a reduction of (6.1) to a much simpler analytical form, which we can use to check our numerical results. This is achieved by mapping the density matrix of a fragment state onto a single qubit [119]. Note the mapping is not specific to either case (i) or (ii), and, accordingly, we shall use it to approximate the QMI in both such cases. The ground state of the collective qubit is universally defined as $|\widetilde{0}\rangle_{X_f} = |\{0\}\rangle_{X_f}$, while here ($X_f = E_f$) the excited state is formed using

$$|\widetilde{1}\rangle_{E_f} = \frac{1}{\eta_{E_f}(t)} \sum_{k\in E_f,\lambda} c_{k,\lambda}(t)\,|1_{k,\lambda}\rangle\,, \tag{6.38}$$

where $k \in X_f$ denotes summation over objects in the fragment, and

$$\eta_{E_f}(t) = \sqrt{\sum_{k\in E_f,\lambda} |c_{k,\lambda}(t)|^2}. \tag{6.39}$$

By approximating

$$\eta^2_{E_f}(t) \approx f\eta^2_E(t) = f \sum_{k,\lambda} |c_{k,\lambda}(t)|^2\,, \tag{6.40}$$

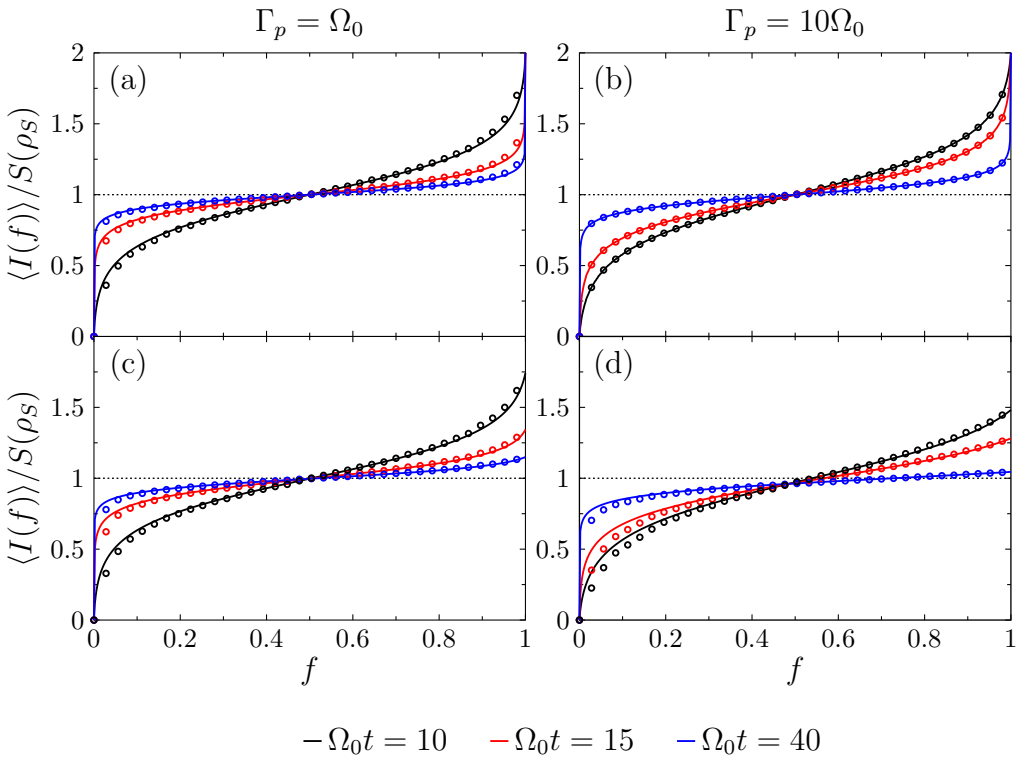

Figure 6.4: Analytical approximations of the partial information plotted at various times for $\Delta = 0$. In each panel, the coloured marks shows the corresponding numerical results. (a), (b) Average of $I(\rho_{SE_f})$ [Eq. (6.42)]. (c), (d) Average of $I(\rho_{SP_f})$ [Eq. (6.50)] for $\Gamma = 10^{-3}\Gamma_p$ ($X = P$). It can be seen that the approximate results fit the numerics accurately within the plateau region at longer times.

for all fraction sizes, the joint system-fragment state can be written as

$$\rho_{SE_f} = \begin{pmatrix} (1-f)\eta_E^2 & 0 & 0 & 0 \\ 0 & f\eta_E^2 & \sqrt{f}c_e^*\eta_E & 0 \\ 0 & \sqrt{f}c_e\eta_E & |c_e|^2 & 0 \\ 0 & 0 & 0 & 0 \end{pmatrix}, \tag{6.41}$$

being taken in the basis $\{|g,\widetilde{0}_{E_f}\rangle, |g,\widetilde{1}_{E_f}\rangle, |e,\widetilde{0}_{E_f}\rangle, |e,\widetilde{1}_{E_f}\rangle\}$. The eigenvalues of $\rho_{SE_f}(t)$ provide the following expression for the partial information of the "two-qubit" state,

$$I(\rho_{SE_f}) = h\left(|c_e(t)|^2\right) + h\big(\chi_E(f)\big) - h\big(\chi_E(1-f)\big), \tag{6.42}$$

where $h(x) = -x\ln x - (1-x)\ln(1-x)$ is taken from (5.48) and

$$\chi_E(f) = f\eta_E^2(t) \tag{6.43}$$

In Figs. 6.4(a-b) we see Eq. (6.42) reproduces the numerical results remarkably well, with only small discrepancies appearing at limiting values of the fraction size for $\Gamma_p = \Omega_0$, close to the boundaries of the plots at $f = 0$ and $f = 1$. Thus, our simple analytical model manages to predict the key features of the partial information plots to a good degree of accuracy.

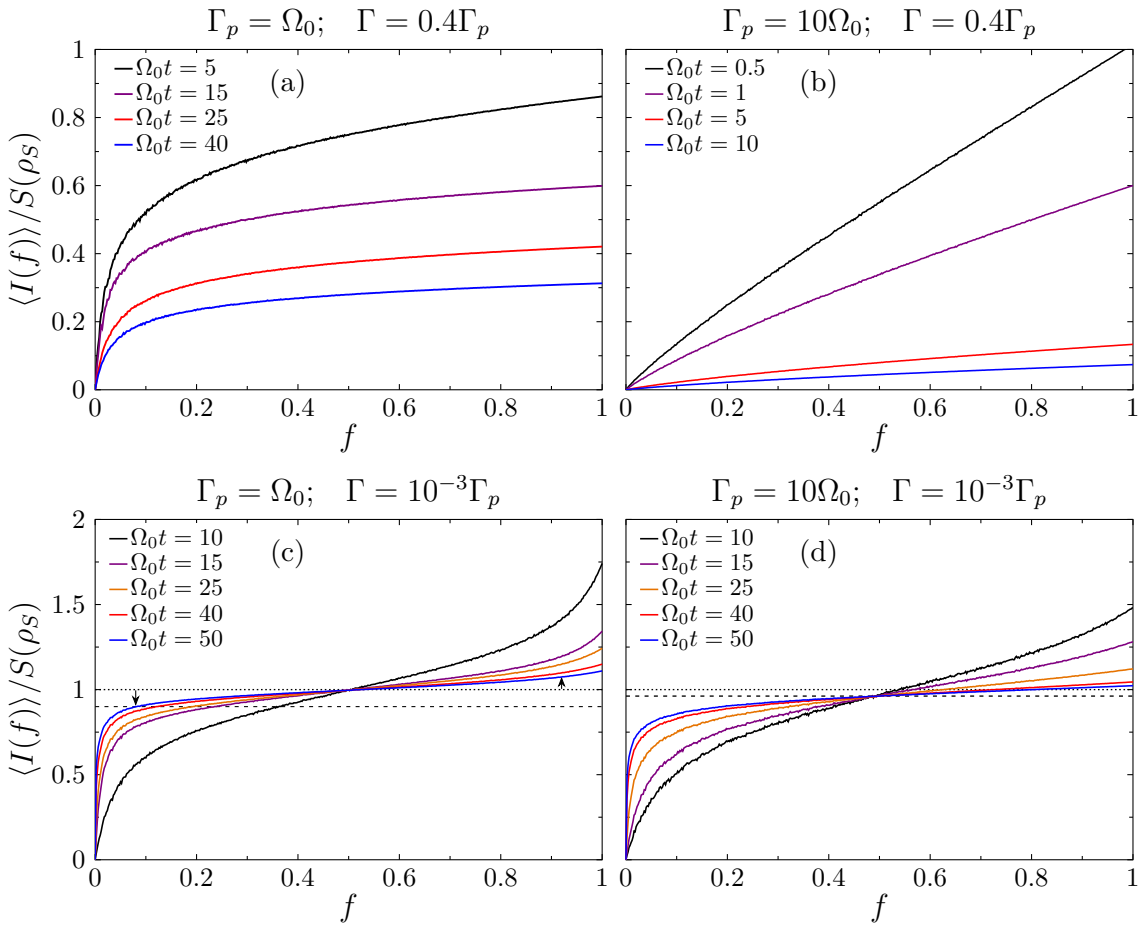

Figure 6.5: Partial information $\langle I(f)\rangle/S(\rho_S)$ of the atom and pseudomodes ($X = P$) shown at various times as a function of fraction size f. The lefthand column is for strong (moderate) coupling $\Gamma_p = \Omega_0$ while the righthand column is for weak coupling $\Gamma_p = 10\Omega_0$ (all $\Delta = 0$). Unlike case (i), correlations between the atom and pseudomodes are erased by evolving the state through noisy quantum channel, i.e. $I(\rho_{SP}) \leq 2S(\rho_S)$. (a), (b) $\Gamma = 0.4\Gamma_p$: The partial information dissipates quickly and no classical plateau forms, though for (a) qualitative information redundancy is noticeable. (c), (d) $\Gamma = 10^{-3}\Gamma_p$: A classical plateau is present within the long time limit. The arrows in figure (c) indicate that the partial information approximately retains its antisymmetry about $f = 1/2$, except at the boundary.

6.2.2 Case (ii): atom and pseudomodes

The global state becomes mixed beyond $t = 0$ and so the partial information plots do not acquire the same form. The QMI instead satisfies the inequality

$$I(\rho_{SP_f}) \leq I(\rho_{SE_f}), \qquad t \geq 0, \forall f, \tag{6.44}$$

where the upper bound is set by the strong sub-additivity of the von Neumann entropy [14]. As the equality only strictly holds at $t = 0$, Eq. (6.44) is understood from the idea that the state $\rho_{SP}(t)$ evolves under a noisy quantum channel where information irreversibly leaks out to the Markovian reservoir. The rate at which the vacuum state population increases signifies the noisiness of the channel. In view of this aspect, the top row of Fig. 6.5 shows the partial information plots of the qubit and pseudomodes within the lossy regime $\Gamma_p \approx \Gamma$, where the vacuum population $\Pi_g(t)$ increases significantly at short times. Here, correlations between the atom and pseudomodes typically decay quickly, though with strong system-environment interactions the QMI dissipates more slowly and redundant correlations have time to develop. In this instance we notice the appearance of a similar plateau feature from before.

Beyond simple inspection of the plots, however, it generally proves troublesome to compute values of f_δ using a fixed fraction size because of lack of antisymmetry in the partial information: that is, the plateau drops below the threshold $(1-\delta)S(\rho_S)$ for $\delta \ll 1$. This issue raises the question: are there circumstances where a quantitive analysis the redundancy using f_δ is possible? To answer this, we briefly look at how the time-dependent behaviour of the purity $p(t) = \mathrm{tr}\,\rho_{SP}^2(t)$ changes with respect to the parameters Γ, Γ_p and Ω_0. Figure 6.6 depicts this quantity for different values of the spectral widths and coupling strength. First, when $\Gamma \ll \Omega_0$, we notice the purity decays to it minimum value on the timescale $t \sim O(1/\Gamma)$ from the fact that the gradient of $p(t)$ is approximately ten times larger between $\Gamma_p = \Omega_0$ and $\Gamma_p = 10\Omega_0$ when $\Gamma = 10^{-3}\Gamma_p$. For $\Gamma \ll \Gamma_p$, we can then expect the information content of $\rho_{SP}(t)$ to stay closer to the equality of (6.44) than the examples seen in Figs. 6.5(a)-(b). This is because the purity declines more slowly when there is a large separation of timescales (assuming the same values of the coupling Ω_0 are used from before). As such, the partial information plots is expected to retain some of

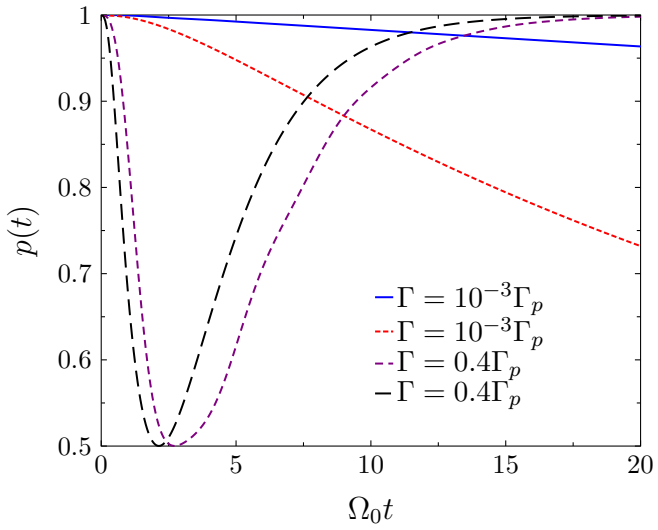

Figure 6.6: Time evolution of the purity $p(t) = \mathrm{tr}\,\rho_{SP}^2(t)$ for parameters $\Delta = 0$, $\Gamma_p = \Omega_0$ (blue solid, violet dashed curves) and $\Gamma_p = 10\Omega_0$ (red dotted, black long-dashed curves).

the antisymmetry features as those found previously in case (i).

Figures 6.5(c)-(d) show the development of a flat classical plateau over the time for parameters $\Gamma \ll \Gamma_p$. Small differences in the partial information plots are apparent between the strong and weak coupling limits as the rate at which purity decays slightly increases with higher values of Γ_p [see Fig. 6.6]. While Fig. 6.5(c) tends to deviate from a complete antisymmetric form at longer times, from the plot we see that, in relation to (5.52), the sum of the information for complimentary fragments satisfies

$$I(\rho_{SP_f}) + I(\rho_{SP_{1-f}}) \approx 2S(\rho_S), \quad \Gamma \ll \Gamma_p, \Omega_0, \tag{6.45}$$

provided $f < 1$. Crucially then, since the redundant information saturates to the limit $(1-\delta)S(\rho_S)$ ($\delta \ll 1$) once there is sufficient decoherence of fragment states, the measure R_δ can be used even without the atom-pseudomode state being pure. This is also clear from comparing these plots between the two cases (i) and (ii) at equal times, where both exhibit a fairly similar plateau.

We can map the state of a fragment P_f to that of a collective qubit, whose excited state is defined by

$$|\widetilde{1}\rangle_{P_f} = \frac{1}{\eta_{P_f}(t)} \sum_{k \in P_f} b_k(t)\,|1_k\rangle\,, \tag{6.46}$$

with normalization

$$\eta_{P_f}(t) = \sqrt{\sum_{k\in P_f} |b_k(t)|^2}. \tag{6.47}$$

Here, we look to follow a similar method that lead to a simple analytical expression for the partial information [see (6.40) and (6.41)], provided in (6.42), with the purpose of reproducing the results shown in Fig. 6.5. If we again assume on average that

$$\eta^2_{P_f}(t) \approx f\eta_P(t) = f\sum_k |b_k(t)|^2, \tag{6.48}$$

then the density matrix ρ_{SP_f} is given by

$$\rho_{SP_f} = \begin{pmatrix} \Pi_p + (1-f)\eta_P^2 & 0 & 0 & 0 \\ 0 & f\eta_P^2 & \sqrt{f}c_e^*\eta_P & 0 \\ 0 & \sqrt{f}c_e\eta_P & |c_e|^2 & 0 \\ 0 & 0 & 0 & 0 \end{pmatrix}, \tag{6.49}$$

using the basis states $\{|g,\widetilde{0}_{P_f}\rangle, |g,\widetilde{1}_{P_f}\rangle, |e,\widetilde{0}_{P_f}\rangle, |e,\widetilde{1}_{P_f}\rangle\}$. It turns out the partial information is given by

$$I(\rho_{SP_f}) = h\left(|c_e(t)|^2\right) + h\big(\chi_P^1(f)\big) - h\big(\chi_P^2(f)\big), \tag{6.50}$$

where the coefficients are

$$\begin{cases} \chi_P^1(f) = f\eta_P^2(t), \\ \chi_P^2(f) = (1-f)\eta_P^2(t) + \Pi_g(t). \end{cases} \tag{6.51}$$

In Figs. 6.4(c-d), results obtained from the approximate form of the partial information (6.50) are presented against the previously discussed numerical results at various times, with $\Gamma \ll \Gamma_p$ and $\Gamma_p = \Omega_0$. Our analytical formula shows remarkable agreement with the numerics, though small differences are noticeable: in particular, the partial information is slightly overestimated for small values of f. Regardless, the main features of these plots are captured, the most important being the increasing flattening of the plateau over time and subsequent emergence of redundant information.

Just as in case (i), a large redundancy here indicates widely accessible information on the system. However, because this information is located in the pseudomodes it reveals more about the interaction: specifically, that many classical records of

pointer states of the atom are held within the memory region of the environment. This differs with lossy interactions ($\Gamma \approx \Gamma_p$) where damping noise, reflected in behaviour of $\Pi_g(t)$, severely restricts the time window in which correlations can form before being decaying completely (see Fig. 6.5).

On the same point, it is noteworthy that the QMI of the full fraction of pseudo-modes decays on a much faster timescale than the redundant information (in the plateau region). For a small damping rate Γ, it is reasonable to question if this corresponds to a loss of quantum information from $S + P$, since the plateau sits approximately at the classical limit with most information lost from global correlations. Far from this case—particularly within the lossy regime—it is unclear if redundancy stems from the spreading of redundant classical copies of information into fragments, since the plateau falls well below this bound.

6.2.3 Accessible information and quantum discord

We shed light on the above discussion by considering the following definition of the QMI [122, 123]:

$$I(\rho_{SX_f}) = C(\rho_{SX_f}) + \bar{\delta}(\rho_{SX_f}), \tag{6.52}$$

where

$$C(\rho_{SX_f}) = \max_{\{M_j^{X_f}\}} \left[S(\rho_S) - S(\rho_S|\{M_j^{X_f}\}) \right], \tag{6.53}$$

$$\bar{\delta}(\rho_{SX_f}) = \min_{\{M_j^{X_f}\}} \left[S(\rho_{X_f}) - S(\rho_{SX_f}) + S(\rho_S|\{M_j^{X_f}\}) \right]. \tag{6.54}$$

The quantity $C(\rho_{SX_f})$ defines the upper limit of the Holevo bound [14, 126, 127]—the accessible information—which gives the maximum classical data provided by a quantum channel. Accordingly, the conditional entropy $S(\rho_S|\{M_j^{X_f}\})$ of the bipartite system is written as

$$S(\rho_S|\{M_j^{X_f}\}) = \sum_j p_j S\left(\rho_{S|M_j^{X_f}}\right), \tag{6.55}$$

which expresses the lack of knowledge in determining ρ_S when ρ_{X_f} is known. A measurement on the subsystem X_f is formulated in terms of the projectors $M_j^{X_f}$, where the post-measurement state of the qubit is

$$\rho_{S|M_j^{X_f}} = \frac{1}{p_j} \mathrm{tr}_{X_f} \left[M_j^{X_f} \rho_{SX_f} M_j^{X_f} \right], \tag{6.56}$$

with an outcome j obtained with probability

$$p_j = \mathrm{tr}_{S,X_f}\left[M_j^{X_f}\rho_{SX_f}\right]. \tag{6.57}$$

The second quantity $\bar{\delta}(\rho_{SX_f})$ defines a general measure of quantum correlations between the two subsystems, known as the quantum discord. Note the bar in (6.54) is used to distinguish the discord from the information deficit δ.

It is emphasised that the accessible information and discord are optimised through a choice of positive operator-valued measure (POVM) $\{M_j^{X_f}\}$. Our motivation for minimising the discord stems from wanting to examine the correlations least disturbed by measurement: that is, the correlations formed between fragments and the pointer states of the atom. Here, the measurement is formulated by mapping the relevant system-fragment to an effective two-qubit state, as was done with (6.38) and (6.47). The POVM $\{M_j^{X_f}\}$ $(j = 1, 2)$ then makes up a set of orthogonal projectors in the state space spanned by X_f—see details in appendix C.

Initially we compute (6.53) and (6.54) for the full system-environment ($f = 1$) of case (i) and find that the QMI is always shared equally between classical and quantum correlations when $I(\rho_{SE}) > 0$. This intuitively follows since the information encoded by classical data is limited to $S(\rho_S)$. The remaining information out of $S + E$ then has to make up the discord in equal amount assuming the state is pure, based on the global entanglement of the system and bath. Alternatively, for fractional states ($f < 1$) we find a more interesting, albeit complicated interplay between classical and quantum correlations. The quantities of interest here are the (averaged) partial accessible information $\langle C(\rho_{SX_f})\rangle$ and partial quantum discord $\langle\bar{\delta}(\rho_{SX_f})\rangle$, which from (6.52), fulfil the relation

$$\langle I(f)\rangle = \langle C(\rho_{SX_f})\rangle + \langle\bar{\delta}(\rho_{SX_f})\rangle. \tag{6.58}$$

In Fig. 6.7 we show plots of the average correlations for case (i). The most striking feature is the sharp rise in partial quantum discord around small fraction sizes. As quantum correlations generally decline in value for larger fractions, the accessible information grows linearly and as such is characteristic of non-redundant classical information—i.e. its partial information plot does not have to a flat plateau shape. Note also that the distribution of classical correlations between different arrangements of fragments is essentially static over time and independent of system-

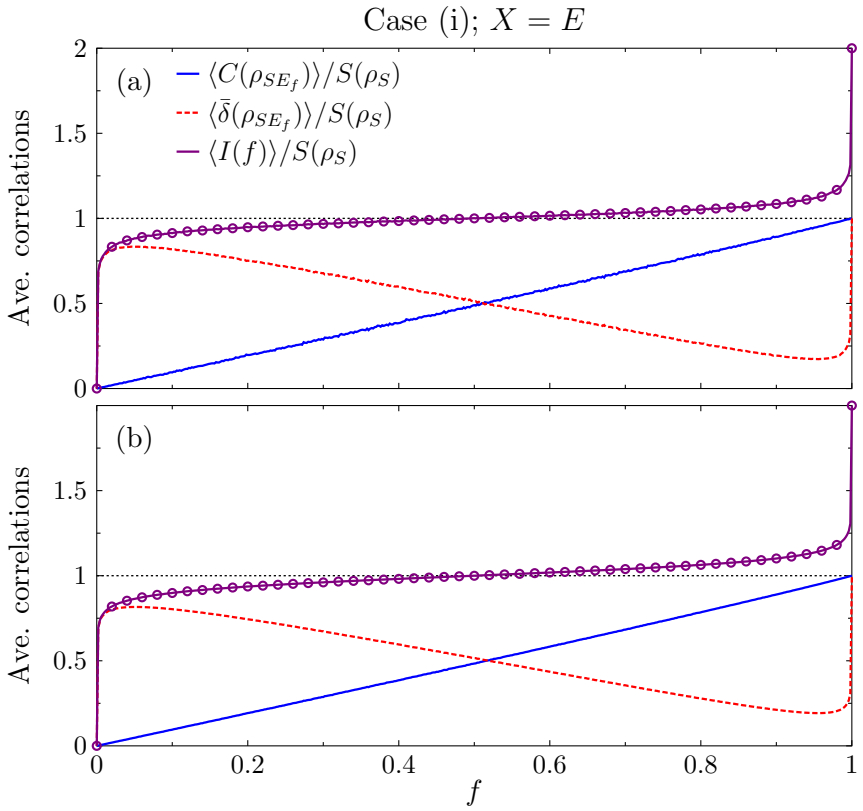

Figure 6.7: The partial accessible information (blue solid curve) and partial discord (red dotted curve) of the qubit and sub-environments, shown against the partial information (violet solid curve) with $\Delta = 0$. Snapshots of the average correlations at time $\Omega_0 t = 50$ for (a) $\Gamma_p = \Omega_0$ and (b) $\Gamma_p = 10\Omega_0$. The sum of the classical and quantum correlations (violet open points) are shown, too, indicating the validity of Eq. (6.58).

environment coupling strength. The discord, which takes large values in the majority of fractions, therefore indicates a clear disturbance to the overall state from performing local measurements on the pseudomode (memory) part of the environment. This behaviour reveals the evolution does *not* produce class of states exhibiting complete Darwinism.

Now turning our attention to case (ii), we address the dynamical behaviour of the correlations with respect to the full fraction of pseudomodes, displayed in Fig. 6.8. Let us start by considering the regime $\Gamma \ll \Gamma_p$. Remarkably, when the dynamics are non-Markovian, Eq. (6.53) stays close to its maximum value over the course of the interaction, and hence the classical correlations are robust to the noise influence of the Markovian environment. This is also true but to a lesser extent in

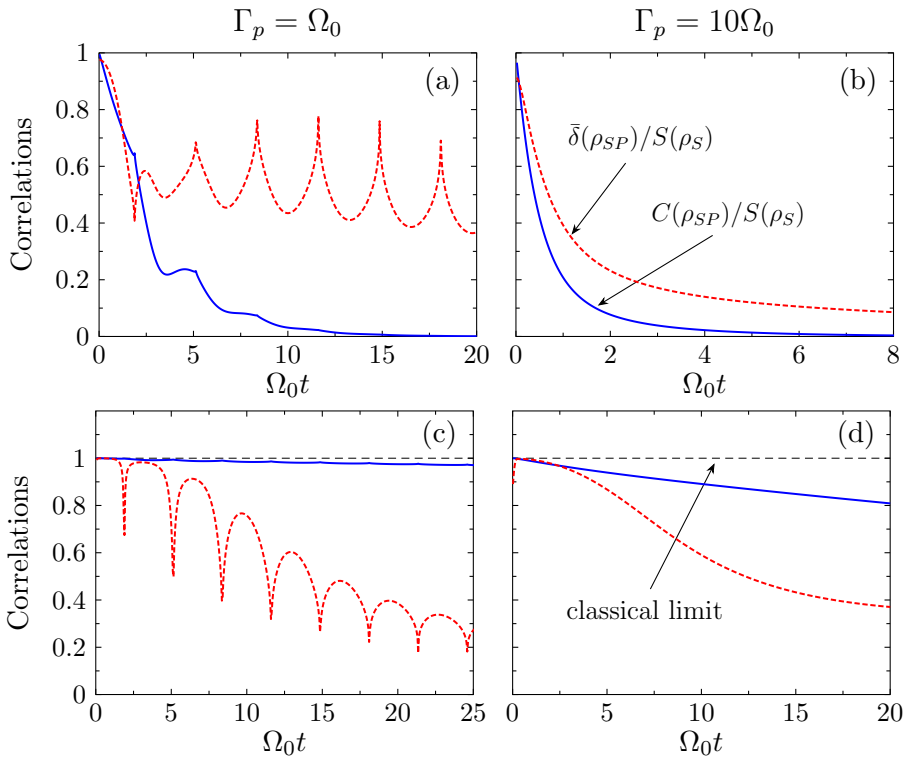

Figure 6.8: Accessible information (blue solid line) and quantum discord (red dotted line) between the atom and pseudomodes ($X = P$), taken from Eqs. (6.53) and (6.54), plotted as functions of time, with $\Delta = 0$. Panels in each column are shown for the same values of $\Gamma_p = \Omega_0$ (left) and $\Gamma_p = 10\Omega_0$ (right). (a), (b) $\Gamma = 0.4\Gamma_p$: classical correlations decay on a fast timescale and quickly approach zero. (c), (d) $\Gamma = 10^{-3}\Gamma_p$: quantum correlations mostly decay while remaining correlations stay close to the classical limit (indicated by the grey dashed line).

the case of Markovian dynamics—we recall that the effect of noise is more substantial with a higher rate of increase in vacuum population, which here increases the damping rate of the classical information by a factor proportional to Γ_p/Ω_0 (e.g. roughly ten times larger gradient between $\Gamma_p = \Omega_0$ and $\Gamma_p = 10\Omega_0$). In contrast, the quantum discord begins to decay at a faster rate. At longer times it can be seen that the quantum correlations become better protected against decoherence when the discord decreases more slowly. We examine the limiting case of this behaviour in section 6.3. Our current observation is that the dynamical behaviour of the classical correlations is qualitatively similar for both weak and strong (moderate) coupling.

In the regime $\Gamma \approx \Gamma_p$ [cf. Fig. 6.8(a)-(b)], a somewhat opposite effect occurs

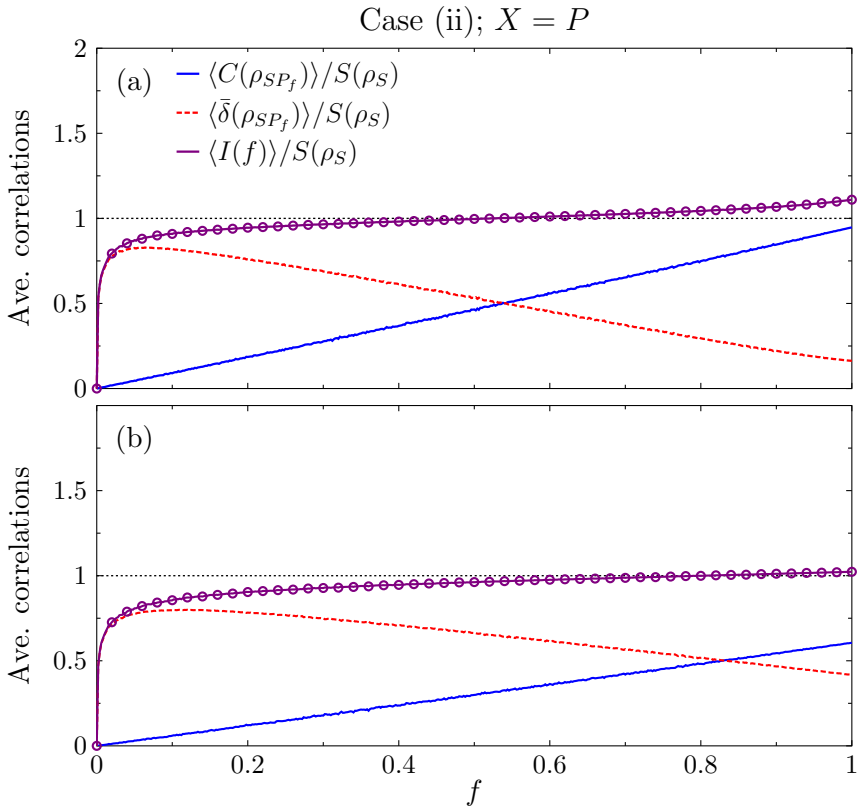

Figure 6.9: Partial information (violet solid curve), accessible information (blue solid curve) and quantum discord (red dotted curve) displayed at time $\Omega_0 t = 50$ for the atom and pseudomodes, where $\Gamma = 10^{-3}\Gamma_p$. Details of (a) and (b) are provided in Fig. 6.7. Open points show the sum of the averaged classical correlations and quantum discord, as in Eq. (6.58).

with respect to the full qubit-pseudomode information. In this instance, classical correlations disappear asymptotically in time so that eventually the quantum discord makes up all of the QMI. As almost no classical information is present even within the full memory region of the environment, from the partial information plot in Fig. 6.5 we find a case where quantum information is redundant since $\langle\bar{\delta}(\rho_{SP_f})\rangle \approx \langle I(f)\rangle$ and $\langle C(\rho_{SP_f})\rangle \approx 0$ must hold, regardless of fraction size. Moreover, Figs. 6.9(a)-(b) show these quantities plotted against f for a large separation of timescales $\Gamma \ll \Gamma_p$ in the strong and weak coupling limit, respectively. We see that the quantum and classical correlations mimic those in Fig. 6.7 for case (i), though clearly without a sudden increase in the discord at large f since the maximum available information is limited below $I(\rho_{SE})$ for a mixed state, even when a measurement of P is taken in the Schmidt basis of ρ_P.

Overall, we conclude that the emergence of a classical plateau—in the partial information plots of either case (i) or (ii)—does not guarantee that classical information is redundant. This reveals significant underlying differences between the partial information plots presented in Figs. 6.3 and 6.5 and those found in Refs. [57, 105]. For example, with an Ohmic environment interacting with a quantum Brownian oscillator, the quantum correlations (entanglement) are found to be suppressed for all but very large fraction sizes [57], meaning that the partial information plots alone reveal the presence of redundant classical correlations in the system. Here, we find that the same is not a sufficient condition for the redundancy of classical information, against what we originally interpreted as "successful" Darwinism in sections 5.4.2, 6.2.1 and 6.2.2. A similar point regarding the non-unique association of the classical plateau to purely classically correlated states has been made in Ref. [109].

6.3 Maximisation of classical correlations

So far, in studying case (ii) we have found that for a Lorentzian (6.22) with a highly peaked internal structure, $\Gamma \ll \Gamma_p$, the accessible information is non-redundant and significantly delocalized across the environment. As a corollary to the results of section 6.2, we examine the condtions under which the classical correlations are maximised against the quantum discord for the total state $\rho_{SP}(t)$.

Whether classical or quantum correlations are predominant has been shown not depend on the presence of memory effects in the dynamics. This suggests it depends only on the degree of separation of the timescales. In fact, numerical evidence shown in Fig. 6.10 reveals that decreasing the ratio Γ/Γ_p further slows down the decay of classical correlations compared to the plots shown in the bottom row of Fig. 6.8. If we observe the behaviour $C(\rho_{SP})$ at a fixed time, we see it grows larger by decreasing the value of Γ. This behaviour lies in contrast to the quantum correlations which tend to fall off more quickly, but can still make up a larger proportion of the total correlations given the QMI also dissipates more slowly. We postulate that in the idealised limit of Eq. (6.34), i.e. with a large separation of timescales:

$$\Gamma t \longrightarrow 0, \qquad \Gamma_p t \gg 1, \qquad \Omega_0/\Gamma_p = \text{fixed}, \tag{6.59}$$

the accessible information converges towards its maximum, thereby revealing that the full memory region of the environment acquires (almost all) classical data on the qubit state. Notice the limit $\Gamma_p t \to \infty$ (6.32) is avoided, as here the atom would approach the ground state with zero entropy, resulting in all correlations being lost. Let us now assume Eq. (6.59) holds. As t increases further, what we expect is for the discord to make up an increasingly smaller proportion of the QMI. Once we have $C(\rho_{SP}) \gg \bar{\delta}(\rho_{SP})$ in the very long time limit $\Gamma_p t \gg 1$, the state $\rho_{SP}(t)$ then shows robustness under non-selective measurements $\{M_j^P\}$ on the marginal subsystem P ($f = 1$). Writing this in terms of a local operation on P, $(\Lambda_P \otimes 1_S)\rho_{SP}(t)$, we should have

$$(\Lambda_P \otimes 1_S)\,\rho_{SP}(t) = \sum_j \left(1_S \otimes M_j^{P_f}\right) \rho_{SP}(t) \left(M_j^{P_f} \otimes 1_S\right) \approx \rho_{SP}(t). \tag{6.60}$$

Of course, the finite nature of the quantum correlations means our results do not provide an example of complete einselection [123], yet it can be appreciated that the state attains its most classical-like form when the dynamics fulfil (6.59). It is

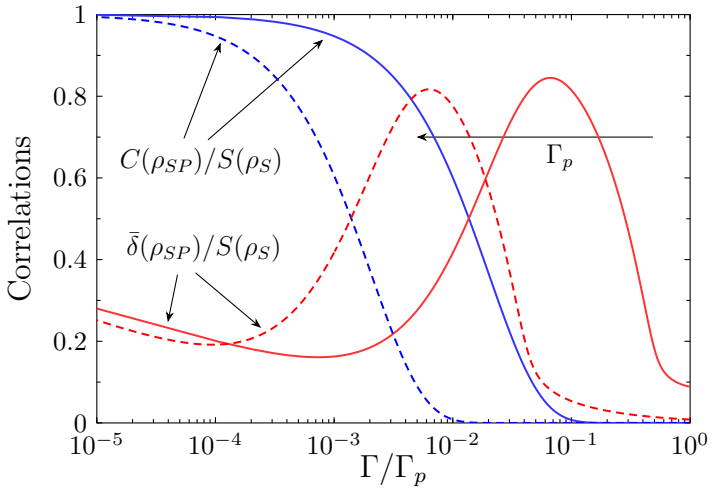

Figure 6.10: The accessible information (6.53) and quantum discord (6.54) for case (ii), plotted as a function of the decay rate Γ at time $\Omega_0 t = 50$ for $\Delta = 0$. Solid curves are obtained for $\Gamma_p = \Omega_0$ and dashed curves for $\Gamma_p = 10\Omega_0$.

also interesting to note how the slow loss of classical correlations occurs in line with the slow decay in the pseudomode population, which as we recall from section 6.1.2, occurs past the cross-over in dynamics at times $t \sim O(1/\Gamma_p)$.

6.4 Non-Markovianity

Here, we consider the relation between the non-Markovianity of the atomic dynamics and the redundancy. By this we formally expand on the findings of chapter 5 where memory effects were revealed to inhibit the emergence of a plateau in the partial information plots. Our current model provides a good foundation to investigate this connection as there is clear delineation of memory effects in terms of information back-flow to the open system, which, by construction, relates precisely to the two-level dynamics we studied in section 5.2.1. Note that this section draws heavily on concepts outlined in chapter 2—in particular, from section 2.3.

6.4.1 Nondivisible maps

We first illustrate the concepts surrounding non-Markovianity in this model by starting with the following definition. Let us state that if a dynamical map $\Phi(t,0)$ governing the point-to-point evolution

$$\rho_S(t_1) \longrightarrow \rho_S(t_2) = \Phi(t_2,t_1)\rho_S(t_1), \qquad t_2 \geq t_1 \geq 0, \tag{6.61}$$

is divisible into two completely positive and trace preserving maps (CPTP),

$$\Phi(t_3,t_1) = \Phi(t_3,t_2)\Phi(t_2,t_1), \qquad t_3 \geq t_2 \geq t_1, \tag{6.62}$$

then $\rho_S(t)$ undergoes a Markovian process. Here the notion of divisibility is enough to distinguish between what is considered Markovian and non-Markovian behaviour. However, it should be stressed that a CPTP map associated with a time-dependent Markov process, as in (6.62), is categorically different from that which forms a dynamical semigroup [1]—note the definition of the semigroup property from Eq. (2.73). Equation (6.29) adopts the time-local form,

$$\frac{d}{dt}\rho_S(t) = \left(\frac{d}{dt}\Phi(t,0)\right)\Phi^{-1}(t,0)\rho_S(t) = \mathcal{K}(t)\rho_S(t), \tag{6.63}$$

where time-dependent generator $\mathcal{K}(t)$ (2.76) of the relevant dynamical map is given by

$$\mathcal{K}(t)\rho_S(t) = -i\frac{s(t)}{2}\left[\sigma_+\sigma_-,\rho_S(t)\right] + \gamma(t)\left[\sigma_-\rho_S(t)\sigma_+ - \frac{1}{2}\left\{\sigma_+\sigma_-,\rho_S(t)\right\}\right]. \tag{6.64}$$

The time-local property of (6.64) is important as it allows one to categorise a quantum process in terms of the direction of information flow over the course of an evolution described by $\Phi(t,0)$. Indeed, the situation where a given amount of information leaks back to the open system has been shown to be intimately related to the non-Markovian properties of the quantum channel. The Breuer, Laine, Piilo (BLP) measure of non-Markovianity [79], as an example, is rooted in the particular interpretation of shared information as the distinguishability of a pair of input states $\{\rho_S^1, \rho_S^2\}$ to the channel. Their distinguishability is characterised by the trace distance $D(\rho_S^1, \rho_S^2)$, defined as

$$D(\rho_S^1, \rho_S^2) = \frac{1}{2}\mathrm{tr}\left|\rho_S^1(t) - \rho_S^2(t)\right|, \tag{6.65}$$

where $|A| = \sqrt{A^\dagger A}$. If the pair evolve under a divisible CPTP map, the rate of change in the trace distance over any given time interval is negative. One can then show that the distinguishability of the pair of states is a monotonically decreasing function in time—overall, corresponding to a continual loss of information from S to E [67]. Variation from this behaviour indicates that the process in nondivisible through reverse flow of information back to the open system. In terms of

$$\sigma(\rho_S^{1,2}(0), t) = \frac{d}{dt}D(\rho_S^1, \rho_S^2), \tag{6.66}$$

the quantum process is non-Markovian if and only if $\sigma(t) > 0$ at some point during the time evolution of the states $\rho_S^{1,2}(t)$.

Concerning our model, the trace distance between any two states $\rho_S^1(t)$ and $\rho_S^2(t)$ whose general form pertain to (5.29) can be expressed analytically as

$$D(\rho_S^1, \rho_S^2) = |G(t)|\sqrt{|G(t)|^2 a^2 + |b|^2}, \tag{6.67}$$

where $a = \langle e|\,\rho_S^1(0)\,|e\rangle - \langle e|\,\rho_S^2(0)\,|e\rangle = \rho_{ee}^1 - \rho_{ee}^2$ and $b = \langle e|\,\rho_S^1(0)\,|g\rangle - \langle e|\,\rho_S^2(0)\,|g\rangle = \rho_{eg}^1 - \rho_{eg}^2$. By then taking the time-derivative of (6.67) [128], we obtain

$$\sigma(t, \rho_S^{1,2}(0)) = \frac{2|G(t)|^2 a^2 + |b|^2}{\sqrt{|G(t)|^2 a^2 + |b|^2}}\frac{d}{dt}|G(t)|, \tag{6.68}$$

from which we see $\sigma(t)$ is only positive if $d_t|G(t)| > 0$ at any time t. This sets the condition for nondivisibility and thus non-Markovianity from the BLP measure [66]. Likewise, the equivalency

$$\sigma(t, \rho_S^{1,2}(0)) > 0 \longleftrightarrow \gamma(t) < 0, \tag{6.69}$$

means that information flows back to the system at times when there are revivals in the population. From this point of view, it is reasonable to suspect that memory effects will show up in the partial information plots at such times when the dynamics are non-Markovian. How the redundancy measure—defined in (5.46)—behaves with respect to changes in (6.67) is precisely the connection we aim to make with our results.

6.4.2 Redundancy

In Fig. 6.11, we show various values of the redundancy computed in both the strong and weak coupling limits. For $\Gamma_p = \Omega_0$, the detuning is taken to be non-zero for the practical reason that the map $\Phi(t,0)$ is noninvertible when $\Delta = 0$, and so no strict definition of divisibility exists in this case [67]. Though the timescale by which redundancy increases is largely separate from that which sets the decoherence rate of system-fragment states—in line with what was suggested in section —here we are not necessarily interested by the exact numerical value $R_\delta(t)$. Rather, we are concerned with its dynamical behaviour with respect to the time-dependent decay rate. Since the population dynamics of the pseudomodes is also influenced by the decay rate $\gamma(t)$ [cf. (6.31)], it is plausible to think that memory effects will also influence correlations between S and P. Therefore we have additionally computed the redundancy from the partial information plots of (ii)—using a large separation of timescales—to compare with the those of case (i).

First, in the strong coupling regime; Fig. 6.11(a), the key indication from our results is that the redundancy peaks and troughs almost exactly in line with the decay rate. Let us first consider case (ii) at time intervals during which $\gamma(t) > 0$. Here, the redundancy is seen to increase up until the point at which the decay rate suddenly becomes negative. It is noticed the plateau grows in length as the open system monotonously loses information into the environment. Then, as $\gamma(t)$ begins to grow from negative values—that is, when information flows back to atom, the redundancy plateau is suppressed considerably before increasing again at times when the decay rate becomes positive. Memory effects can also be seen to manifest in the redundancy calculated for case (i) at the same times. To further illustrate the connection between $R_\delta(t)$ and the trace distance measure, in Fig. 6.11(b) we plot

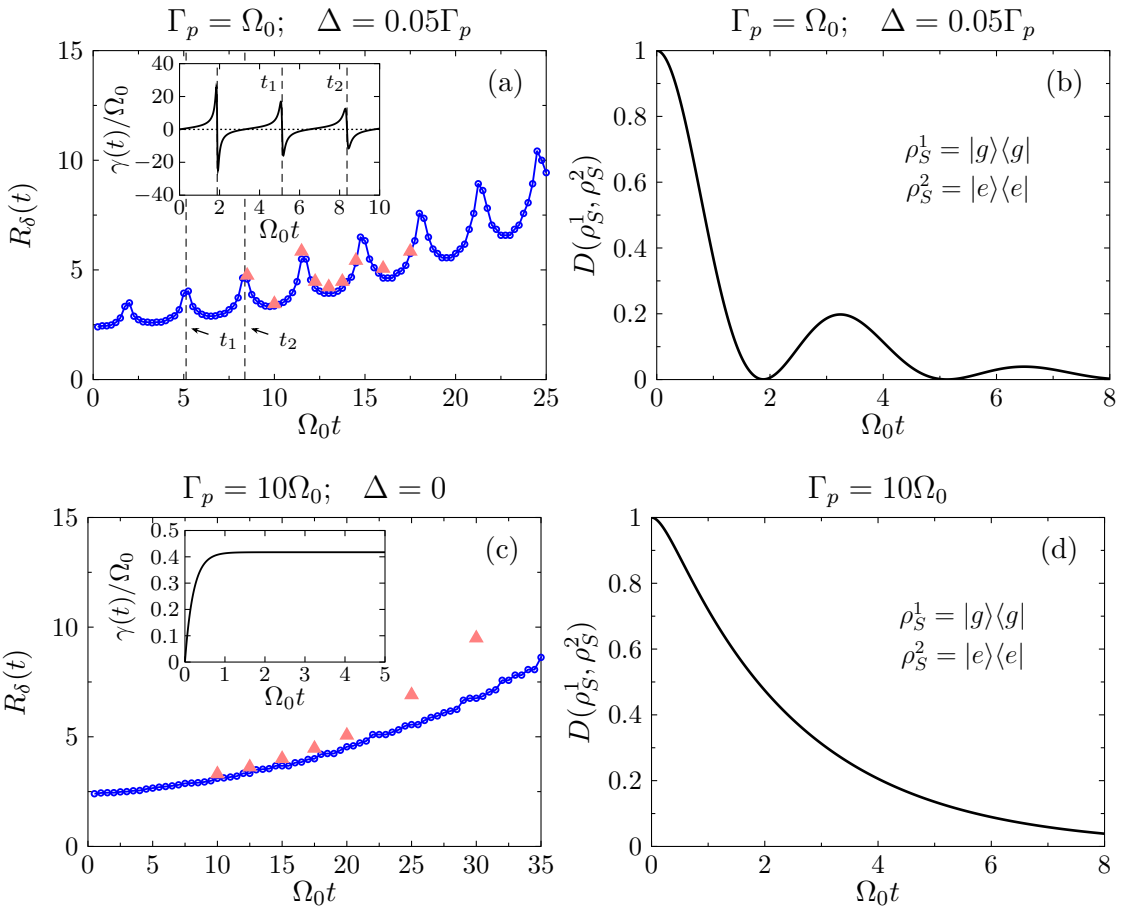

Figure 6.11: Redundancy (5.46) computed as a function of time for cases (i) (red triangles) and (ii) (blue marked line) with $\delta = 0.15$ (lefthand column), shown alongside the trace distance (righthand column). The insets display the decay rate $\gamma(t)$ from (6.27) for each set of parameters. (a), (b) $\Gamma_p = \Omega_0$ and $\Delta = 0.05\Gamma_p$: the dashed lines in (a) indicate times at which the redundancy peaks. (c), (d) $\Gamma_p = 10\Omega_0$ and $\Delta = 0$: in the weak coupling limit the redundancy (trace distance) monotonically increases (decreases) in time. Initial conditions used to compute Eq. (6.65) are shown.

(6.67) against time for the same set of parameters used in Fig. 6.11(a). If we take the input pair of states to be $\rho_S^1 = |e\rangle\langle e|$ and $\rho_S^2 = |g\rangle\langle g|$ for the simple reason that the trace distance is $D(\rho_S^1, \rho_S^2) = |c_e(t)|^2$, then oscillations in $D(\rho_S^1, \rho_S^2)$ evidently follow those in the redundancy and $\gamma(t)$, as we would justifiably expect.

Alternatively, in the weak coupling regime the plateau only continuously grows in length while the system undergoes a Markovian evolution [in both cases (i) and (ii)]. This firmly suggests the non-monotonicity of the redundancy captures the

non-Markovian dynamics of the atom—which, in this context, is clearly based on the same effective behaviour in the trace distance (6.67). We again point out the connection between quantum Darwinism and non-Markovianity has also been studied recently in Refs. [59, 60]. The authors find a similar effect, where information back-flow to the open system translates into poor Darwinism, i.e. a worsening of the plateau at these times. Equally, the trace distance shown in Fig. 6.11(d), which is plotted for the same reference pair of states from before, only decays exponentially over time.

Furthermore, the fact that the redundancy of cases (i) and (ii) shows similar dynamical behaviour suggests that the rollback of the plateau occurs specifically because of information back-flow from the pseudomodes (memory) to the atom. Indeed, consider the example of an initially excited atom for the same parameter as Fig. 6.11(a). What we find is that at times when $|G(t)|^2$ starts to increase, there is an accompanied increase in QMI of the atom and environment from its minimum zero value. This suggests correlations previously removed by dissipation redevelop because of information flow back at times when the redundancy decreases (cf. discussion in 5.4.2). Now, in the regime $\Gamma \ll \Gamma_p$, we notice the dynamics of total QMI between the atom and memory $I(\rho_{SP})$ faithfully coincides with that of $I(\rho_{SE})$. Thus we can associate the same recorrelation effect with revivals in the atomic population, which, from (6.31), occurs simultaneously with loss of population from the pseudomodes. Indeed, we find that the compensated rate of change of the pseudomode population (6.31) is negative during times when the trace distance is increasing. In this sense the energy/information received back by the atom from the pseudomodes can provide the physical mechanism for the drop in the classical plateau.

6.5 Summary and discussion

In this chapter, we have provided a detailed investigation into emergent features of quantum Darwinism by applying the framework to a two-level atom interacting with many sub-environments of bosons. The basis of our work derives from the idea that the original environment maps to a bipartite structure containing a memory and non-memory part. From this we have examined how information is encoded into

fractions of the environment in two separate cases: one where we constructed random fragments out of sub-environments [case (i)], and the other out of independent parts of the full memory [case (ii)]. Our main effort has been to recognise whether the emergence of redundant information occurs, and, if so, where into the environment such information is proliferated. By considering different dynamical regimes we identify instances in cases (i) and (ii) where redundant information forms close to the classical bound, implying "successful" Darwinism from the spreading of classical copies of information into the environment. This directly follows from the work of chapter 5 where we also saw the partial information develop (in certain regimes) an increasingly flat plateau over time.

Despite these signatures, which are usually is considered as a hallmark of successful quantum Darwinism, our results demonstrate a scenario where classical information (6.53) is precisely non-redundant. Consequently, we found the quantum discord (6.54) —taken from the partial information—to obtain relatively large values in small fractions of pseudomodes and/or sub-environments, realising the highly non-classical nature of a typical system-fragment state based on the fact it is disturbed significantly under local (projective) measurements.

In parallel we have analysed the dynamics of the classical and quantum correlations between the atom and memory region. In both cases—either when considering the partial correlations from fractions of the environment or full collection of pseudomodes—we have found qualitatively similar behaviour in the results across both the strong and weak coupling regimes. Substantial differences are only introduced through relatively varying the decay rates of the pseudomode population. For example, in the lossy regime; that is, where correlations and population are significantly damped in time, the QMI of the atom-pseudomode system shows asymptotically decaying classical correlations with prevalent discord. A regime where the pseudomodes maximise their classical correlations over the course of the dynamics has also been identified.

Finally, we have sought to cement the connection between the emergence of redundancy in the quantum Darwinism framework and non-Markovianity. Memory effects are characterised by the back-flow of information (and population) from the system to the environment, which in turn reflects the nondivisibility of the dynamical

map. We have shown that the redundancy plateau in the partial information plots, where it can be computed, is suppressed at times when information flows from the pseudomodes to the atom (see Fig. 6.11). Remarkably, the redundancy acts as a witness to non-Markovian behaviour in directly the same way as the trace distance does in the BLP measure.

Since the redundancy measure (5.46) is borne from the idea of information flowing out from the system to the environment, it seems intuitive to think that its ability to detect quantum memory effects should coincide with other information based witnesses to non-Markovianity [80, 117]. Looking ahead, this property could be possibly exploited to develop a novel quantifier of non-Markovianity based on information redundancy. Indeed this has been partly explored in Ref. [60] within the setting of a quantum Brownian motion model. Here they define the measure

$$\mathcal{N}_{f_\delta} = \int_{d_t f_\delta(t)>0} \frac{d}{dt} f_\delta(t) dt. \tag{6.70}$$

As we known from Fig. 6.11, the redundancy $R_\delta(t)$ temporally decreases when the threshold fraction f_δ increases at equal times. Evidence in the current setting suggests (6.70) only increases from a non-zero value for a non-divisible process. To further test the above as universal quantifier of non-Markovianity, it is then of interest to compare N_{f_δ} against the BLP measure for the dissipative two-level system. This is defined from trace distance quantity in (6.68):

$$\mathcal{N}(\Phi) = \max_{\rho_{1,2}(0)} \int_{\sigma(t)<0} dt\, \sigma(t, \rho_S^{1,2}(0)). \tag{6.71}$$

The measures in Eqs. (6.71) and (6.70) could too be analysed jointly for cases beyond our considered model.

Part V

Conclusions

Chapter 7

Summary and outlook

In this thesis we have studied several examples of non-Markovian behaviour in open quantum systems, with particular attention paid to the paradigmatic model of a two level-atom interacting with a zero-temperature bosonic reservoir. Firstly, we set out to investigate fundamental descriptions for the non-Markovian decay of the atom, and secondly, we sought to quantitatively measure how correlations are formed—in a multipartite sense—between the atom and reservoir. In each setting, memory effects are introduced into the open system dynamics by modifying the structure of the environment's spectral density so that it is non-flat for frequency scales of interest. When the spectral density is highly structured is this way, standard weak-coupling assumptions breakdown, and parts of the approach reviewed in chapters 2 and 3 are no longer applicable. As a result, our work has primarily been enabled by the use of non-perturbative pseudomode technique.

We began chapter 4 by addressing the application of the chain transformation [89–92] to the model in question. The reason for employing the transformation is because it naturally singles out an auxiliary part of the reservoir—the principal oscillator—which is responsible for an indirectly couples the atom to a residual continuum of modes. Choosing a Lorentzian spectral density, we exploited the chain representation to extend the original quantum Langevin equation of the atom (4.52) over that of the principal mode, resulting in a closed set of equations of motions for an enlarged system. The principal mode quantum Langevin equation (4.86) was identified through evaluating the residue of the single pole contained in the spectral density when extended to the complex frequency plane. Since this equation was

found to be reminiscent of the type used in the standard Markovian input-output formalism [2, 81], where $b_{\text{in}}(t)$ (4.87) adopts the role of an input field, we checked the two-point commutator of $b_{\text{in}}(t)$ (and its adjoint) against the result obtained in the flat spectrum limit: that is, in a regime where it was proven to represent a stochastic white noise. Under very reasonable assumptions, its statistics were found to replicate the usual properties of a Markovian noise even when the dynamics at the level of the reduced system (atom) was non-Markovian. Interestingly, the enlarged atom plus principal mode system can then be thought of as being acted upon by a noise which correlates with the dynamics on an infinitesimally short timescale.

To further understand this feature we proceeded to derive the master equation corresponding to the bipartite system. From truncating the chain at the first mode, we arrived at an equation of standard Lindblad form—exactly the result obtained by way of the pseudomode methods. In this regard, our main conclusion is that the non-Markovian process may be successfully mapped onto a bipartite Markovian dynamics when embedded into a one-dimensional bosonic chain. Our approach offers an immediate advantage over the pseudomode method since the derivation requires no initial assumptions on the combined state of the enlarged system. Importantly, the use of the Heisenberg formalism has shown the dynamics can—in principle—be solved for any number of initial excitations in the enlarged system (see section 4.3). Though it should be stated that the method is limited in practice due to Eqs. (4.169)-(4.171) becoming intractable to solve for a sufficiently large number of initial photon excitations in the system.

Next we analysed total correlations—as measured through the quantum mutual information—between the atom and different random fractions of its environment under the framework of quantum Darwinism, see chapter 5. This was considered in the setting of a two-level atom coupled to a single leaky cavity mode. Because the Jaynes-Cummings Hamiltonian (4.35) conserves excitation number, the first step—of course—for there only being a single total excitation, was to expand the full system-reservoir state in the one-excitation basis. The solutions we obtained were exploited to yield an exact calculation of the partial information. For weak and moderate system-reservoir coupling, it was noticed, in terms of the appearance of a classical plateau, that information becomes redundant on a timescale separate

from that at which initial correlations form between the system and reservoir. On the other hand, for strong interactions, temporal instances of recorrelation between the atom and the full reservoir was found to cause the plateau to oscillate well into the long time limit $\gamma_0 t \gg 1$. In the same dynamical regime, local correlations were seen to mostly be created in sidebands positioned around the atomic transition frequency. Since these correlations mimic the properties of the reservoir emission spectrum it then follows that the local information shows strong time-dependent oscillations. As with the QMI, this indicates the presence of recorrelation in the system, which as we found with the partial information, leads to poor redundancy. For weaker coupling, the local information grows initially but then tends to decay monotonically across all reservoir modes in line with the behaviour of the atomic population. Because the atom forms a non-Markovian system in the strong coupling limit, we concluded that the classical plateau (in the partial information plots) is negatively impacted by the presence of memory effects in the dynamics. This agrees with the analysis Refs. [59, 60] found for other models of dissipation.

We used chapter 6 to develop our model further for the purpose of investigating quantum Darwinism in a setting where a full part of the system (i.e. atom and pseudomodes) evolves under a noisy quantum channel. Here, the original environment was amended to comprise of many independent reservoir sub-environments. Because the Lorentzian form of the spectral density was shown to be maintained under certain conditions, the atomic dynamics is simply a generalisation of that from the previous case (i.e. section 5.2). Thus, we proceeded to compute the partial information exactly like before taking a singly-excited system, given the total Hamiltonian continues to conserve excitation number. The same classical features of redundancy emerge in the weak and strong-moderate coupling regimes. Yet, using definitions of accessible information (6.53) and quantum discord (6.54), total correlations were also partitioned into their respective classical and quantum counterparts. We subsequently exposed classical correlations to be non-redundant, regardless of the chosen coupling strength. This result has strong implications for future studies of quantum Darwinism and opens up broader questions into the relation between redundant information and multipartite quantum correlations [57], as well as the physical mechanisms that trigger their emergence. The same findings also support

the concern of Horodecki *et. al.* [109], which states that the criteria leading to (5.20) should be fundamentally checked at the level of states, rather than inferring the objective properties of the system using only the partial information and associated measures.

Furthermore, we have highlighted that instances of poor Darwinism tend to coincide with information back-flow from the open system to the environment. From this connection we found the redundancy measure R_δ to act as a witness to non-Markovian processes in the same way as the trace distance (6.65) does for nondivisible dynamical maps. Our future hope is that the results presented here, along with those of Refs. [59, 60], can be used to develop a novel quantifier of non-Markovianity.

Finally I conclude by considering some points that potentially merit further investigation. An immediate and natural extension to the work presented in chapter 4 is to apply our method to a case which involves multiple excitation of the reservoir. Although the formalism is generic, it could be relevant to describing, for example, the dynamics of a combined two-level atom and damped cavity field initialised in an entangled Bell-like state. Another possible direction is to apply the method to reservoirs whose spectral density is elected to take on a more complicated structure. Following Ref. [29] one could try modelling such a spectral density using a linear combination of Lorentzian functions. On the face of it, this type of approach looks to fit comfortably with our framework since the chain embedding can be straightforwardly extended to handle many Lorentzians: this would involve having to add extra modes of the chain (i.e. beyond $m = 0$) to the reduced system until the chain parameters converge. However, because identifying the quantum Langevin equation relies on the spectral density containing a single pole per principal mode, we anticipate having to first map the environment onto many independent sub-environments before applying our method. This would require *a priori* knowledge of what "structure" the environment needs in order for us to obtain the correct definition of $b_0(t)$ in (4.70), so as to produce to (4.86). Embedding certain problems can also quickly become impractical when having to incorporate a large number of oscillators into the system.

In summary, though the work of chapter 4 is far from being all encompassing, it still marks a significant step towards the development of a framework that, while

being based on the same intuitive principles of the pseudomode method, can too deal with processes involving multiphoton excitation of the reservoir (e.g. a dressed atomic system) by way of a Markovian master equation for the enlarged system. On top of this the results of chapter 5 and 6 offer new perspectives on quantum Darwinism within the scope of a singly excited atom emitting into a structured reservoir. This may perhaps drive a greater want of understanding on how quantum correlations between a system and parts of its environment evolve over the course of decoherence, which, as we can predict, will only build in relevance as we move closer towards the large scale fabrication of quantum technological devices.

Bibliography

[1] H. P. Breuer and F. Petruccione, *The theory of open quantum systems*. New York: Oxford University Press, 2002.

[2] C. W. Gardiner and P. Zoller, *Quantum Noise*. Berlin: Springer, 2005.

[3] H. J. Carmichael, *An Open Systems Approach to Quantum Optics*. Berlin: Springer-Verlag, 1993.

[4] Á. Rivas and S. F. Huelga, *Open Quantum Systems: An Introduction*. Berlin: Springer, 2012.

[5] W. H. Louisell, *Quantum Statistical Properties of Radiation*. New York: Wiley, 1973.

[6] U. Weiss, *Quantum Dissipative Systems*. Singapore: World Scientific, 2001.

[7] W. H. Zurek, "Decoherence, einselection, and the quantum origins of the classical," *Rev. Mod. Phys.*, vol. 75, no. 3, pp. 715–775, 2003.

[8] W. H. Zurek, "Decoherence and the transition from quantum to classical," *Physics Today*, vol. 44, no. 10, pp. 36–44, 1991.

[9] M. Schlosshauer, "Decoherence, the measurement problem, and interpretations of quantum mechanics," *Rev. Mod. Phys.*, vol. 76, no. 4, pp. 1267–1305, 2004.

[10] E. Joos, H. D. Zeh, C. Kiefer, D. Giulini, J. Kupsch, and I.-O. Stamatescu, *Decoherence and the appearance of a classical world in quantum theory*. New York: Springer, 2013.

[11] S. Haroche and J. M. Raimond, *Exploring the Quantum: Atoms, Cavities, and Photons*. Oxford: OUP, 2006.

[12] F. Verstraete, M. M. Wolf, and J. Ignacio Cirac, "Quantum computation and quantum-state engineering driven by dissipation," *Nat. Phys.*, vol. 5, no. 9, pp. 633–636, 2009.

[13] C. J. Myatt, B. E. King, Q. A. Turchette, C. A. Sackett, D. Kielpinskl, W. M. Itano, C. Monroe, and D. J. Wineland, "Decoherence of quantum superpositions through coupling to engineered reservoirs," *Nature (London)*, vol. 403, no. 6767, pp. 269–273, 2000.

[14] M. A. Nielson and I. L. Chuang, *Quantum Computation and Quantum Information*. Cambridge, England: Cambridge University Press, 2010.

[15] "Quantum coherence," *Nature (London)*, vol. 453, no. 1003-1049, 2008.

[16] G. M. Palma, K.-A. A. Suominen, and A. K. Ekert, "Quantum computers and dissipation," *Proc. Roy. Soc. Lond. A*, vol. 452, no. 1946, pp. 567–584, 1996.

[17] P. Lambropoulos, G. M. Nikolopoulos, T. R. Nielsen, and S. Bay, "Fundamental quantum optics in structured reservoirs," *Rep. Prog. Phys.*, vol. 63, no. 4, p. 455, 2000.

[18] G. Lindblad, "On the generators of quantum dynamical semigroups," *Comm. Math. Phys.*, vol. 48, no. 2, pp. 199–130, 1976.

[19] V. G., A. Kossakowski, and E. C. G. Sudarshan, "Completely positive dynamical semigroups of N-level systems," *Journal of Mathematical Physics*, vol. 17, no. 5, pp. 821–825, 1976.

[20] M. Esposito, M. A. Ochoa, M. A., and M. Galperin, "Quantum thermodynamics: a nonequilibrium Green's function approach," *Phys. Rev. Lett.*, vol. 114, p. 080602, 2015.

[21] D. Newman, F. Mintert, and A. Nazir, "Performance of a quantum heat engine at strong reservoir coupling," *Phys. Rev. E*, vol. 95, p. 032139, 2017.

[22] A. W. Chin, J. Prior, R. Rosenbach, F. Caycedo-Soler, S. F. Huelga, and M. B. Plenio, "The role of non-equilibrium vibrational structures in electronic coherence and recoherence in pigment-protein complexes," *Nat. Phys.*, vol. 9, no. 2, pp. 113–118, 2013.

[23] H. B. Chen, N. Lambert, Y. C. Cheng, Y. N. Chen, and F. Nori, "Using non-Markovian measures to evaluate quantum master equations for photosynthesis," *Sci. Rep.*, vol. 5, p. 12753, 2015.

[24] A. W. Chin, S. F. Huelga, and M. B. Plenio, "Quantum metrology in Non-Markovian environments," *Phys. Rev. Lett.*, vol. 109, p. 233601, 2012.

[25] B. Bellomo, R. Lo Franco, and G. Compagno, "Non-Markovian effects on the dynamics of entanglement," *Phys. Rev. Lett.*, vol. 99, p. 160502, 2007.

[26] B. Bylicka, D. Chruściński, and S. Maniscalco, "Non-Markovianity and reservoir memory of quantum channels: a quantum information theory perspective," *Sci. Rep.*, vol. 4, p. 5720, 2014.

[27] W.-M. Zhang, P.-Y. Lo, H.-N. Xiong, M. W.-Y. Tu, and F. Nori, "General non-Markovian dynamics of open quantum systems," *Phys. Rev. Lett.*, vol. 109, p. 170402, 2012.

[28] D. Tamascelli, A. Smirne, S. Huelga, and M. B. Plenio arXiv:1709.03509.

[29] A. Imamoglu, "Stochastic wave-function approach to non-Markovian systems," *Phys. Rev. A*, vol. 50, pp. 3650–3653, 1994.

[30] P. Stenius and A. Imamoglu, "Stochastic wavefunction methods beyond the Born-Markov and rotating-wave approximations," *Quantum and Semiclassical Optics: Journal of the European Optical Society Part B*, vol. 8, no. 1, p. 283, 1996.

[31] J. Iles-Smith, N. Lambert, and A. Nazir, "Environmental dynamics, correlations, and the emergence of noncanonical equilibrium states in open quantum systems," *Phys. Rev. A*, vol. 90, p. 032114, 2014.

[32] J. Iles-Smith, A. G. Dijkstra, N. Lambert, and A. Nazir, "Energy transfer in structured and unstructured environments: master equations beyond the Born-Markov approximations," *J. Chem. Phys.*, vol. 144, no. 4, p. 044110, 2016.

[33] P. Strasberg, G. Schaller, N. Lambert, and T. Brandes, "Nonequilibrium thermodynamics in the strong coupling and non-Markovian regime based on a reaction coordinate mapping," *New J. Phys.*, vol. 18, no. 7, p. 073007, 2016.

[34] K. H. Hughes, C. D. Christ, and I. Burghardt, "Effective-mode representation of non-Markovian dynamics: a hierarchical approximation of the spectral density. I. Application to single surface dynamics," *J. Chem. Phys.*, vol. 131, no. 2, p. 024109, 2009.

[35] K. H. Hughes, C. D. Christ, and I. Burghardt, "Effective-mode representation of non-Markovian dynamics: a hierarchical approximation of the spectral density. II. Application to environment-induced nonadiabatic dynamics," *J. Chem. Phys.*, vol. 131, no. 12, p. 124108, 2009.

[36] R. Martinazzo, B. Vacchini, K. H. Hughes, and I. Burghardt, "Communication: universal Markovian reduction of Brownian particle dynamics," *J. Chem. Phys.*, vol. 134, no. 1, p. 011101, 2011.

[37] A. A. Budini, "Non-Markovian quantum jumps from measurements in bipartite Markovian dynamics," *Phys. Rev. A*, vol. 88, p. 012124, 2013.

[38] K. Luoma, P. Haikka, and J. Piilo, "Detecting non-Markovianity from continuous monitoring," *Phys. Rev. A*, vol. 90, p. 054101, 2014.

[39] J. Piilo, S. Maniscalco, K. Härkönen, and K.-A. Suominen, "Non-Markovian quantum jumps," *Phys. Rev. Lett.*, vol. 100, p. 180402, 2008.

[40] J. Piilo, K. Härkönen, S. Maniscalco, and K.-A. Suominen, "Open system dynamics with non-Markovian quantum jumps," *Phys. Rev. A*, vol. 79, p. 062112, 2009.

[41] B. M. Garraway, "Nonperturbative decay of an atomic system in a cavity," *Phys. Rev. A.*, vol. 55, no. 3, pp. 2290–2303, 1997.

[42] B. M. Garraway, "Decay of an atom coupled strongly to a reservoir," *Phys. Rev. A.*, vol. 55, no. 6, pp. 4636–4639, 1997.

[43] S. Bay, P. Lambropoulos, and K. Mølmer, "Fluorescence into flat and structured radiation continua: an atomic density matrix without a master equation," *Phys. Rev. Lett.*, vol. 79, pp. 2654–2657, 1997.

[44] B. J. Dalton, S. M. Barnett, and B. M. Garraway, "Theory of pseudomodes in quantum optical processes," *Phys. Rev. A*, vol. 64, p. 053813, 2001.

[45] B. J. Dalton and B. M. Garraway, "Non-Markovian decay of a three-level cascade atom in a structured reservoir," *Phys. Rev. A*, vol. 68, p. 033809, 2003.

[46] B. M. Garraway and B. J. Dalton, "Theory of non-Markovian decay of a cascade atom in high-Q cavities and photonic band gap materials," *J. Phys. B: At. Mol. Opt. Phys.*, vol. 39, no. 15, p. S767, 2006.

[47] W. H. Zurek, "Quantum Darwinism," *Nat. Phys.*, vol. 5, no. 3, pp. 181–188, 2009.

[48] W. H. Zurek, "Quantum Darwinism, classical reality, and the randomness of quantum jumps," *Physics Today*, vol. 67, no. 10, pp. 44–50, 2014.

[49] R. Blume-Kohout and W. Zurek, "A simple example of "quantum Darwinism": redundant information storage in many-spin environments," *Found. Phys.*, vol. 35, no. 11, pp. 1857–1876, 2005.

[50] R. Blume-Kohout, *Decoherence and Beyond*. PhD thesis, University of California, Berkeley, 2005.

[51] R. Blume-Kohout and W. H. Zurek, "Quantum Darwinism: entanglement, branches, and the emergent classicality of redundantly stored quantum information," *Phys. Rev. A*, vol. 73, p. 062310, 2006.

[52] R. Blume-Kohout and W. H. Zurek, "Quantum Darwinism in quantum Brownian motion," *Phys. Rev. Lett.*, vol. 101, no. 24, 2008.

[53] M. Zwolak, H. T. Quan, and W. H. Zurek, "Quantum Darwinism in a mixed environment," *Phys. Rev. Lett.*, vol. 103, no. 11, 2009.

[54] M. Zwolak, H. T. Quan, and W. H. Zurek, "Redundant imprinting of information in nonideal environments: objective reality via a noisy channel," *Phys. Rev. A.*, vol. 81, no. 6, 2010.

[55] H. Ollivier, D. Poulin, and W. H. Zurek, "Objective properties from subjective quantum states: environment as a witness," *Phys. Rev. Lett.*, vol. 93, p. 220401, 2004.

[56] R. Brunner, R. Akis, D. K. Ferry, F. Kuchar, and R. Meisels, "Coupling-induced bipartite pointer states in arrays of electron billiards: quantum Darwinism in action?," *Phys. Rev. Lett.*, vol. 101, p. 024102, 2008.

[57] J. P. Paz and A. J. Roncaglia, "Redundancy of classical and quantum correlations during decoherence," *Phys. Rev. A*, vol. 80, no. 4, 2009.

[58] F. G. S. L. Brandão, M. Piani, and P. Horodecki, "Generic emergence of classical features in quantum Darwinism," *Nat. Comm.*, vol. 6, no. 7908, 2015.

[59] G. L. Giorgi, F. Galve, and R. Zambrini, "Quantum Darwinism and non-Markovian dissipative dynamics from quantum phases of the spin-1/2 XX model," *Phys. Rev. A.*, vol. 92, no. 2, 2015.

[60] F. Galve, R. Zambrini, and S. Maniscalco, "Non-Markovianity hinders quantum Darwinism," *Sci. Rep.*, vol. 6, no. 19607, 2016.

[61] G. Grimmett and D. Stirzaker, *Probability and Random Processes*. Oxford New York: Oxford University Press, second edition ed., 1992.

[62] J. J. Sakurai and J. Napolitano, *Modern Quantum Mechanics*. Pearson Education International, 2nd edition ed., 2011.

[63] A. J. Daley, "Quantum trajectories and open many-body quantum systems," *Adv. Phys.*, vol. 63, no. 2, pp. 77–149, 2014.

[64] J. Jeske, *Spatially Correlated Decoherence: Understanding and Exploiting Spatial Noise Correlations in Quantum Systems*. PhD thesis, School of Applied Science, RMIT University, 2014.

[65] P. Bocchieri and A. Loinger, "Quantum recurrence theorem," *Phys. Rev.*, vol. 107, pp. 337–338, 1957.

[66] H. P. Breuer, "Foundations and measures of quantum non-Markovianity," *J. Phys. B: At. Mol. Opt. Phys.*, vol. 45, no. 15, 2012.

[67] H. P. Breuer, E. M. Laine, J. Piilo, and B. Vacchini, "Colloquium: non-Markovian dynamics in open quantum systems," *Rev. Mod. Phys.*, vol. 88, no. 2, 2016.

[68] K. Kraus, *States, Effects, and Operations*, vol. 190. Berlin: Springer-Verlag, 1983.

[69] M. J. W. Hall, J. D. Cresser, L. Li, and E. Andersson, "Canonical form of master equations and characterization of non-Markovianity," *Phys. Rev. A*, vol. 89, p. 042120, 2014.

[70] Á. Rivas, S. F. Huelga, and M. B. Plenio, "Quantum non-Markovianity: characterization, quantification and detection," *Rep. Theor. Phys.*, vol. 77, no. 9, p. 094001, 2014.

[71] D. Chruściński and A. Kossakowski, "Markovianity criteria for quantum evolution," *J. Phys. B: At. Mol. Opt. Phys.*, vol. 45, no. 15, p. 154002, 2012.

[72] S. Nakajima, "On quantum theory of transport phenomena: steady diffusion," *Prog. Theor. Phys.*, vol. 20, no. 6, pp. 948–959, 1958.

[73] R. Zwanzig, "Ensemble method in the theory of irreversibility," *J. Chem. Phys.*, vol. 33, no. 5, pp. 1338–1341, 1960.

[74] S. Chaturvedi and F. Shibata, "Time-convolutionless projection operator formalism for elimination of fast variables. applications to Brownian motion," *Z. Phys. B*, vol. 35, no. 3, pp. 297–308, 1979.

[75] F. Shibata, Y. Takahashi, and N. Hashitsume, "A generalized stochastic Liouville equation. Non-Markovian versus memoryless master equations," *J. Stat. Phys.*, vol. 17, no. 4, pp. 171–187, 1977.

[76] I. de Vega and D. Alonso, "Dynamics of non-Markovian open quantum systems," *Rev. Mod. Phys.*, vol. 89, p. 015001, 2017.

[77] A. J. Leggett, S. Chakravarty, A. T. Dorsey, M. P. A. Fisher, A. Garg, and W. Zwerger, "Dynamics of the dissipative two-state system," *Rev. Mod. Phys.*, vol. 59, pp. 1–85, 1987.

[78] M. M. Wolf, J. Eisert, T. S. Cubitt, and J. I. Cirac, "Assessing non-Markovian quantum dynamics," *Phys. Rev. Lett.*, vol. 101, p. 150402, 2008.

[79] H. P. Breuer, E. M. Laine, and J. Piilo, "Measure for the degree of non-Markovian behavior of quantum processes in open systems," *Phys. Rev. Lett.*, vol. 103, no. 21, 2009.

[80] Á. Rivas, S. F. Huelga, and M. B. Plenio, "Entanglement and Non-Markovianity of quantum evolutions," *Phys. Rev. Lett.*, vol. 105, p. 050403, 2010.

[81] C. W. Gardiner and M. J. Collett, "Input and output in damped quantum systems: quantum stochastic differential equations and the master equation," *Phys. Rev. A*, vol. 31, pp. 3761–3774, 1985.

[82] J. Zhang, Y.-x. Liu, R.-B. Wu, K. Jacobs, and F. Nori, "Non-Markovian quantum input-output networks," *Phys. Rev. A*, vol. 87, p. 032117, 2013.

[83] J. D. Cresser, "A Heisenberg equation-of-motion derivation of stochastic Schrödinger equations for non-Markovian open systems," *Laser Phys.*, vol. 10, no. 1, pp. 337–347, 2000.

[84] L. Diósi, "Non-Markovian open quantum systems: input-output fields, memory, and monitoring," *Phys. Rev. A*, vol. 85, p. 034101, 2012.

[85] L. Mazzola, E. M. Laine, H. P. Breuer, S. Maniscalco, and J. Piilo, "Phenomenological memory-kernel master equations and time-dependent Markovian processes," *Phys. Rev. A*, vol. 81, p. 062120, 2010.

[86] S. J. Whalen, *Open quantum systems with time-delayed interactions*. PhD thesis, The University of Auckland, 2015.

[87] S. J. Whalen and H. J. Carmichael, "Time-local Heisenberg-Langevin equations and the driven qubit," *Phys. Rev. A*, vol. 93, p. 063820, 2016.

[88] S. M. Barnett and P. M. Radmore, *Methods in Theoretical Quantum Optics*. New York: Oxford University Press, 1997.

[89] A. W. Chin, Á. Rivas, S. F. Huelga, and M. B. Plenio, "Exact mapping between system-reservoir quantum models and semi-infinite discrete chains using orthogonal polynomials," *J. Math. Phys.*, vol. 51, no. 9, p. 092109, 2010.

[90] J. Prior, A. W. Chin, S. F. Huelga, and M. B. Plenio, "Efficient simulation of strong system-environment interactions," *Phys. Rev. Lett.*, vol. 105, p. 050404, 2010.

[91] A. W. Chin, S. F. Huelga, and M. B. Plenio arXiv:1112.6280.

[92] M. P. Woods, R. Groux, A. W. Chin, S. F. Huelga, and M. B. Plenio, "Mappings of open quantum systems onto chain representations and Markovian embeddings," *J. Math. Phys.*, vol. 55, no. 3, p. 032101, 2014.

[93] W. Gautschi, *Orthogonal Polynomials*. New York: Oxford University Press, 2004.

[94] I. de Vega and M.-C. Bañuls, "Thermofield-based chain-mapping approach for open quantum systems," *Phys. Rev. A*, vol. 92, p. 052116, 2015.

[95] R. Bulla, H.-J. Lee, N.-H. Tong, and M. Vojta, "Numerical renormalization group for quantum impurities in a bosonic bath," *Phys. Rev. B*, vol. 71, p. 045122, 2005.

[96] K. G. Wilson, "The renormalization group: Critical phenomena and the Kondo problem," *Rev. Mod. Phys.*, vol. 47, no. 3, pp. 773–840, 1975.

[97] J. Prior, I. de Vega, A. W. Chin, S. F. Huelga, and M. B. Plenio, "Quantum dynamics in photonic crystals," *Phys. Rev. A*, vol. 87, p. 013428, 2013.

[98] A. Peres, *Quantum Theory: Concepts and Methods*. Berlin: Springer, 1995.

[99] W. Gautschi, "A MATLAB suite of programs for generating orthogonal polynomials and related quadrature rules.".

[100] G. W. Ford, J. T. Lewis, and R. F. O'Connell, "Quantum Langevin equation," *Phys. Rev. A*, vol. 37, pp. 4419–4428, 1988.

[101] H. J. Carmichael, *Statistical Methods in Quantum Optics 1: Master Equations and Fokker-Planck Equations*. Physics and Astronomy Online Library Springer, 1999.

[102] H. Z. Shen, M. Qin, X.-M. Xiu, and X. X. Yi, "Exact non-Markovian master equation for a driven damped two-level system," *Phys. Rev. A*, vol. 89, p. 062113, 2014.

[103] E. Fick and G. Sauermann, *The quantum statistics of dynamic processes*. Berlin: Springer-Verlag, 1990.

[104] R. J. Rubin, "Momentum autocorrelation functions and energy transport in harmonic crystals containing isotopic defects," *Phys. Rev.*, vol. 131, pp. 964–989, 1963.

[105] M. Zwolak and W. H. Zurek, "Complementarity of quantum discord and classically accessible information," *Sci. Rep.*, vol. 3, 2013.

[106] W. H. Zurek, S. Habib, and J. P. Paz, "Coherent states via decoherence," *Phys. Rev. Lett.*, vol. 70, no. 9, pp. 1187–1190, 1993.

[107] W. H. Zurek, "Pointer basis of quantum apparatus: into what mixture does the wave packet collapse?," *Phys. Rev. D*, vol. 24, no. 6, pp. 1516–1525, 1981.

[108] W. H. Zurek, "Environment-induced superselection rules," *Physical Review D*, vol. 26, no. 8, pp. 1862–1880, 1982.

[109] R. Horodecki, J. Korbicz, and P. Horodecki, "Quantum origins of objectivity," *Phys. Rev. A.*, vol. 91, no. 3, 2015.

[110] S. M. Barnett, *Quantum Information*. Oxford New York: Oxford University Press, 2009.

[111] C. Anastopoulos and B. Hu, "Two-level atom-field interaction: exact master equations for non-Markovian dynamics, decoherence, and relaxation," *Phys. Rev. A.*, vol. 62, no. 3, pp. 033821–033821, 2000.

[112] R. E. Kastner, "Classical selection and quantum Darwinism," *Physics Today*, vol. 68, no. 5, pp. 8–9, 2015.

[113] P. B. P. J. Lahti and P. Mittelstaedt, *The Quantum Theory of Measurement*. Berlin: Springer, 1991.

[114] W. H. Zurek, "Preferred states, predictability, classicality and the environment-induced decoherence," *Prog. Theor. Phys.*, vol. 89, no. 2, pp. 281–312, 1993.

[115] V. Weisskopf and E. Wigner, "Berechnung der natürlichen linienbreite auf grund der diracschen lichttheorie," *E. Z. Physik*, vol. 63, no. 1, pp. 54–73, 1930.

[116] B. Vacchini and H. P. Breuer, "Exact master equations for the non-Markovian decay of a qubit," *Phys. Rev. A*, vol. 81, p. 042103, 2010.

[117] S. Luo, S. Fu, and H. Song, "Quantifying non-Markovianity via correlations," *Phys. Rev. A*, vol. 86, p. 044101, 2012.

[118] I. E. Linington and B. M. Garraway, "Control of atomic decay rates via manipulation of reservoir mode frequencies," *J. Phys. B: At. Mol. Opt. Phys.*, vol. 39, no. 16, p. 3383, 2006.

[119] C. Lazarou, K. Luoma, S. Maniscalco, J. Piilo, and B. Garraway, "Entanglement trapping in a nonstationary structured reservoir," *Phys. Rev. A.*, vol. 86, no. 1, 2012.

[120] S. M. Dutra, *Cavity Quantum Electrodynamics: The Strange Theory of Light in a Box*. Hoboken, New Jersey: John Wiley and Sons, Inc., 2005.

[121] L. Mazzola, S. Maniscalco, J. Piilo, K.-A. Suominen, and B. Garraway, "Pseudomodes as an effective description of memory: non-Markovian dynamics of two-state systems in structured reservoirs," *Phys. Rev. A.*, vol. 80, no. 1, 2009.

[122] L. Henderson and V. Vedral, "Classical, quantum and total correlations," *J. Phys. A: Math. Gen.*, vol. 34, no. 35, pp. 6899–6905, 2001.

[123] H. Ollivier and W. Zurek, "Quantum discord: a measure of the quantumness of correlations," *Phys. Rev. Lett.*, vol. 88, no. 1, pp. 179011–179014, 2002.

[124] F. F. Fanchini, G. Karpat, B. Çakmak, L. K. Castelano, G. H. Aguilar, O. J. Farías, S. P. Walborn, P. H. S. Ribeiro, and M. C. de Oliveira, "Non-Markovianity through accessible information," *Phys. Rev. Lett.*, vol. 112, p. 210402, 2014.

[125] S. Haseli, G. Karpat, S. Salimi, A. S. Khorashad, F. F. Fanchini, B. Çakmak, G. H. Aguilar, S. P. Walborn, and P. H. S. Ribeiro, "Non-Markovianity through flow of information between a system and an environment," *Phys. Rev. A*, vol. 90, p. 052118, 2014.

[126] A. S. Holevo, "Bounds for the quantity of information transmitted by a quantum communication channel," *Probl. Peredachi Inf.*, vol. 9, pp. 3–11, 1973.

[127] V. Vedral, "The role of relative entropy in quantum information theory," *Rev. Mod. Phys.*, vol. 74, pp. 197–234, 2002.

[128] E. M. Laine, J. Piilo, and H. P. Breuer, "Measure for the non-Markovianity of quantum processes," *Phys. Rev. A*, vol. 81, p. 062115, 2010.

[129] E. C. Anderson, "Monte Carlo methods and importance sampling." Unpublished lecture notes, 1999.

[130] A. Datta. arXiv:0807.4490.

Appendix A

Notes on the Monte Carlo simulation

Here we detail the procedure used to find a Monte Carlo estimate of the averaged quantum mutual information $\langle I(f)\rangle$ in sections 5.4 and 6.2. The content of this appendix is outlined as follows: First, the method used to sample fragments is proposed. I later explore the problems faced with this method for $\#E \gg 1$ and briefly discuss the use of sampling from a test distribution rather than the true underlying distribution of fragment combinations to remedy this. I find good results are obtained by giving importance to sub-environments located towards the edges of the distribution.

The environment E[1] has a fixed inner structure $E = \otimes_{k=1}^{\#E} E_k$, where each sub-environment E_k is uniquely identified by the label $k = 1, 2, \ldots, \#E$. A fragment is constructed out of an aggregate of m sub-environments, whose size f—defined in (5.44)—depends only on the number of sub-environments included within the fragment. We calculate the partial information by first generating a random number of sub-environments m, and averaging the QMI (5.17) or (6.1) over the total number of samples taken for each particular fraction size. This is then carried out for every possible f value to fully construct $\langle I(f)\rangle$.

To illustrate how the procedure works, suppose we have random variable X that

[1]Note the methods of this appendix generally apply within the multiple-environment setting—that is, the partial information is sampled from the pseudomodes P in the same way as it is done for E.

generates the number of sub-environments m in a sample fragment by way of a given probability distribution. For a random sample of length n, we take our samples from a sequence of i.i.d. random variables $\{X_1, X_2, \ldots, X_{n_s}\}$ $(j = 1, 2, \ldots n_s)$, which are used to compute expectation value of X:

$$\langle X \rangle = \frac{1}{n_s} \sum_{j=1}^{n_s} X_j. \tag{A.1}$$

Ideally, the average number of samples obtained for each m should be distributed according to the number of ways m sub-environments can be combined to produce a fragment of size f_m. It is then necessary for us to choose a probability distribution that generates an appropriate "spread" of X across the sample space. For current purposes we adopt the the binomial distribution $p_X(m)$, where

$$p_X(m) = \frac{\#E!}{m!(\#E - m)!} p^m (1-p)^{\#E-m}, \tag{A.2}$$

and p is probability of "success" of a Bernoulli trial—in analogy, a sample X is drawn by the tossing a fair coin sequentially for $m = 1, 2, \ldots, \#E$, with the number of successes (e.g. heads) generating the number of sub-environments. Since the number of possibilities for arranging m within a fixed total number $\#E$ goes as the coefficient $\binom{\#E}{m}$, we symmetrise the distribution by setting $p = 1/2$ in the above, yielding

$$p_X(m) = \frac{\#E!}{m!(\#E - m)!} \left(\frac{1}{2}\right)^{\#E}, \quad p = \frac{1}{2}. \tag{A.3}$$

We can make the connection between the expected number of drawn samples for each m and the probability distribution (A.2) using the (weak) law of large numbers [61]. This states that, in the limit $n_s \to \infty$, the sample average (A.1) converges to the average of the binomial distribution μ:

$$\mu = \lim_{n_s \to \infty} \langle X \rangle = \sum_m p_X(X = m) m. \tag{A.4}$$

Therefore, the expected number of samples for each m, given by E[no. m] $= n_s p_X(m)$, converges proportionally to the binomial coefficient (A.3) as we intended.

For a large total number of sub-environments $\#E \gg 1$, the binomial distribution (A.2) tends to a Gaussian $N(\mu, \sigma^2)$ with mean $\mu = \#E/2$ and variance $\sigma^2 = \#E/4$ [61]. In our case this is very well satisfied since the total number of sub-environments

taken is approximately of the order $\#E \sim 100$. Equation (A.3) may then be written as

$$p_X(m) \approx N(\mu, \sigma^2) = \frac{1}{\sigma\sqrt{2\pi}} \exp\left[-\frac{(m-\mu)^2}{2\sigma^2}\right], \quad m = 1, 2, \ldots \#E. \tag{A.5}$$

Once a sample number of sub-environments is generated, we must subsequently generate a specific combination out of $X = m$ indicated by $\{m\} = \{k_1, k_2, \ldots, k_m\}$. The value of the k-index refers to the ordering of sub-environments on the frequency line, i.e. $E_k \to E(\omega_k)$, where $\omega_k = \omega_0 - \Delta + x_k$, and

$$\begin{aligned} x_k &= -\Lambda + (k-1)\Delta x, \\ \Delta x &= \frac{2\Lambda}{\#E - 1}, \qquad k = 1, 2, \ldots, \#E. \end{aligned} \tag{A.6}$$

Note $x_k = [-\Lambda, \ldots, \Lambda]$ are frequencies renormalised to be centred on zero, with Λ an arbitrary cut-off frequency (other parameters are defined in the main text). Another random variable Y is then used to successively draw m samples of $k_1, k_2, \ldots$ of frequency x_k from the uniform distribution

$$U_Y(k) = \begin{cases} 1/\#E & \text{if} \quad 1 \leq k \leq \#E \\ 0 & \text{otherwise,} \end{cases} \tag{A.7}$$

where each are generated with equal probability $\Pr(Y = k) = 1/\#E$. This is done on the grounds that no particular arrangement of sub-environments should be biased for. In addition, when a sub-environment Y is taken, it is eliminated from the set such that no sub-environment can be picked more than once. Therefore, the probability of picking a combination $\{m\}$ is

$$\Pr(\{m\}) = \frac{m!(\#E - m)!}{\#E!}. \tag{A.8}$$

Partial information estimate

Repeatedly taking samples of X to (1): choose m, and Y to (2): choose a combination of sub-environments $\{m\}$, eventually allows us to compute an estimate for the partial information. This is found using

$$\langle \widetilde{I}(f_m) \rangle = \frac{1}{n(m)} \sum_{k=1}^{n(m)} I_k(f_m), \tag{A.9}$$

where $I_k(f_m)$ is the quantum mutual information of an arrangement $\{m\}$ and $\langle\widetilde{I}(f_m)\rangle$ the Monte Carlo estimate of the partial information. From (A.5), the expected number of samples generated for each m is

$$n(m) \approx \mathrm{E}[\text{no. } m] = n_s p_X(m), \quad n_s \gg 1. \tag{A.10}$$

The actual partial information $\langle I(f_m)\rangle$ is defined as the average of $I(f_m)$ across every possible combination of sub-environments $\{m\}$, that is

$$\langle I(f_m)\rangle = \sum_{\{m\}} \Pr(\{m\}) I(f_m). \tag{A.11}$$

In the same way as Eq. (A.4), the estimate of the partial information $\langle\widetilde{I}(f_m)\rangle$ converges to $\langle I(f_m)\rangle$ probability wise through the weak law of large numbers (PandRP): (plot histogram to show)

$$\lim_{n_s\to\infty} \Pr(|\langle I(f_m)\rangle - \langle\tilde{I}(f_m)\rangle| \geq \varepsilon) = 0, \tag{A.12}$$

where ε arbitrarily small. While the above determines how the mean of the sample estimate converges in the limit $n_s \to \infty$—i.e, that (A.9) coincides with the expectation value $\langle I(f_m)\rangle$ in (A.11)—what it does not describe is the behaviour of the fluctuations in $\langle\tilde{I}(f_m)\rangle$ or the rate at which convergence occurs. Since sampling a large part of the sample space is necessary for (A.12) to even approximately hold, knowing how the estimate behaves with respect to the sample size n_s is important as it affects the accuracy of the Monte Carlo simulation. The central limit theorem describes such a phenomena—formally, it states that, for a sequence of i.i.d. variables $\{I_1(f_m), I_2(f_m), \dots\}$ with mean $\langle I(f_m)\rangle$ and variance $\sigma_{I,m}$, the distribution associated to the variable $\sqrt{n(m)}(\langle\tilde{I}(f_m)\rangle - \langle I(f_m)\rangle)/\sigma_{I,m}$ converges to [61]

$$\lim_{n\to\infty} \frac{(\langle\tilde{I}(f_m)\rangle - \langle I(f_m)\rangle)}{\sigma_{I,m}/\sqrt{n(m)}} = \lim_{n\to\infty} Z_n \to N(0,1), \tag{A.13}$$

that is, a standard normal (Gaussian) distribution $N(0,1)$. What the central limit theorem reveals is that fluctuations (reflected in the variance) of the random variable Z_n remain constant as $n(m)$ grows in size. However, as Z_n is scaled by a factor $\sqrt{n(m)}$, the fluctuations in $\langle\tilde{I}(f_m)\rangle$ must scale by an equal inverse factor to keep the spread in Z_n constant. This scaling can in turn be used to characterise how the

variance of the Monte Carlo estimate $\langle\widetilde{I}(f_m)\rangle$ changes with $n(m)$:

$$\begin{aligned}\mathrm{var}(\langle\widetilde{I}(f_m)\rangle) &= \mathrm{var}\left(\frac{1}{n(m)}\sum_{k=1}^{n(m)} I_k(f_m)\right), \\ &= \frac{1}{n(m)}\mathrm{var}(I(f_m)), \\ &= \frac{\sigma_m^2}{n(m)}, \end{aligned} \tag{A.14}$$

where again the variables $I_k(f_m)$ are assumed independent. Note the final line expresses the fact that the variance in the Monte Carlo estimate decreases proportionally with $n(m)$. Therefore, increasing the sample number shrinks the error incurred in the estimate $\langle\tilde{I}(f_m)\rangle$ by a factor of $1/\sqrt{n(m)}$, which, according to (A.13), is distributed as a Gaussian for $n(m) \gg 1$.

A summary of the complete sampling procedure is then stated as follows:

1. Use the test distribution in Eq. (A.5) to generate a sample of X. The value of $X = m$ is realised with probability $\Pr(X = m) = p_X(m)\Delta m$.

2. Generate a combination of sub-environments $\{m\}$ using the random variable Y, where m samples are drawn from the uniform distribution (A.7).

3. Compute $I_k(f_m)$ and store its value. Repeat from the first step, such that 1.—3. are performed n_s times.

4. When all samples of X are taken, find the partial information using Eq. (A.9). Use the results to construct $\langle I(f)\rangle$.

Importance sampling

Unfortunately, a critical issue with Eq. (A.3) being a very good fit to a Gaussian is that the tails of the distribution (A.5) are sampled with incredibly small probability, even for a very large n_s. Not only then is $n(m)$ much smaller than the number of fragment combinations for each m in the marginals of the Gaussian, so the error in (A.14) is large, but in a typical simulation these regions are found to not be sampled at all. This is problematic as we need to draw a sufficient number of m values (i.e. $n(m) \gg 1$) from all parts of this distribution to accurately construct the partial information, while too having to keep n_s small enough as to

prevent severe computational inefficiency. With the current procedure this seems difficult to achieve. To tackle this problem we instead make use of a method akin to importance sampling [129]. Here, the random variable X used to draw a random number of sub-environments in a fragment is chosen to be picked from a different "test" distribution rather than the Gaussian. The idea is that this new distribution reduces the error in $\langle \widetilde{I}(f_m) \rangle$ enough to give reasonable results but is also efficient from a Monte Carlo standpoint.

If we denote the test distribution $h_X(m)$, a new Monte Carlo estimate for the partial information [i.e. (A.9)] is provided by

$$\langle I_h(f_m) \rangle = \frac{1}{n_h(m)} \sum_{k=1}^{n_h(m)} I_k(f_m), \tag{A.15}$$

with $n_h(m) = n_s h_X(m)$ giving the expected number of samples for $X = m$. The error in the estimate of the partial information associated with this distribution is thus proportional to $1/\sqrt{h(m)}$. We can gauge the relative error in the test distribution in comparison to the previous Gaussian—or target—distribution via

$$\frac{\tilde{\sigma}_{h,m}}{\tilde{\sigma}_{P,m}} = \sqrt{\frac{p_X(m)}{h_X(m)}}, \tag{A.16}$$

where $\tilde{\sigma}_{p,m} = \sigma_m/\sqrt{n(m)}$ and $\tilde{\sigma}_{h,m} = \sigma_m/\sqrt{n_h(m)}$ are the standard deviations of the sample estimate. The value of the ratio (A.16) clearly depends on our choice for the test distribution. It turns out the error can be minimised across all m if we take [129]

$$|h_X(m)| \sim \alpha\, p_X(m), \tag{A.17}$$

where $\alpha \gg 1$, so that Eq. (A.16) goes like $1/\sqrt{\alpha}$. Of course, if this holds for all m then the test distribution will have to be arbitrarily close to the the target (Gaussian) distribution, and we revert back to the same problem.

For simplicity, let us take $h_X(m)$ to be the uniform distribution. In the marginal regions of the binomial distribution, our choice of distribution in (A.17) turns out to be advantageous to sample from since we are "over-sampling" relative to the target distribution $p_X(m)$ due to $\alpha \gg 1$. Consequently the error on the Monte Carlo estimate tends to be very small. Nonetheless, as we approach values closer to the centre of the distribution, $p_X(m)$ will quickly rise above $h_X(m)$ and we will have the opposite effect from $\alpha \ll 1$. Within this region we will thus be "under-sampling"

against the target distribution—the ratio in (A.16) will be very large, and sampling from the test distribution is disadvantageous compared to (A.5).

Despite this apparent drawback, what the above doesn't consider is intrinsic uncertainty in the partial information $\langle I(f_m)\rangle$: that is, the magnitude of the standard deviation $\sigma_{I,m}$ defined in (A.14). If this value is sufficiently small in regions where the error is predicted to be large then it is still possible to get good numerical results for $\langle \tilde{I}(f_m)\rangle$ despite the aforementioned under sampling. This informs us that lots of samples in this region are "irrelevant" to computing the partial information, and thus we can afford to massively under sample from the target distribution and still get a reasonably accurate estimate of the partial information. In Fig. 6.4 we compare our Monte Carlo results against analytical approximations of $\langle I(f)\rangle$ [cf. (6.42)-(6.50)], and generally find a high level of agreement between the two.

In light of the above, our Monte Carlo procedure is amended to sample fragments by first drawing a value for m from the uniform distribution $h_X(m)$. Note however, that for ease of implementation the results presented in chapters 5 and 6 are actually realised by first taking $\tilde{n}_s$ predetermined samples $\#E$ times for each $m = 1, 2, \ldots \#E$. A sub-environment combination is then drawn randomly for each realisation of $X = m$ using (A.7). Within the limit $\tilde{n}_s \gg 1$, this coincides with the previously considered method of randomly generating the number of sub-environments in a fragment, since from $\tilde{n}_s = n_s h_X(m)$, where $h_X(m) = 1/\#E$, the eventual bin count (E(no. m)) between the two methods is the same.

Appendix B

Laplace transform solution of the state coefficients

For the multiple-environment model considered in section 6.1, if we impose the limit $\#E \to \infty$ we can then replace the spectral density (6.5) in such a way as to produce the following integro-differential equation:

$$\frac{d}{dt}c_e(t) = -\Omega_0^2 \int_0^t dt' \exp\left[(i\Delta - (\Gamma + \Gamma_W)/2)(t-t')\right] c_e(t'), \tag{B.1}$$

where

$$f(t-t') = \Omega_0^2 \exp\left[i\Delta(t-t') - \left(\frac{\Gamma + \Gamma_W}{2}\right)(t-t')\right], \tag{B.2}$$

is obtained from (6.7) and (6.22), with the above parameters defined in section 6.1.1. One way of solving (B.1) is by means of the Laplace transform method. We define the Laplace transform a time domain function $y(t)$ as follows:

$$\tilde{y}(s) = \mathcal{L}[y](s) = \int_0^\infty dt\, e^{-st} y(t), \quad s \in \mathbb{C}, \tag{B.3}$$

where the tilde hat is used to indicate the function is defined in Laplace space. By now applying the above to both sides of (B.1) and making use of the convolution property $\mathcal{L}[x * y](s) = \tilde{x}(s)\tilde{y}(s)$, we find

$$s\tilde{c}_e(s) - c_e(0) = -\tilde{f}(s)c_e(s), \tag{B.4}$$

which can subsequently be re-arranged into the form

$$\tilde{c}_e(s) = \frac{c_e(0)}{s + \tilde{f}(s)}. \tag{B.5}$$

Having

$$\tilde{f}(s) = \mathcal{L}[f](s) = \frac{\Omega_0^2}{s - \left(i\Delta - \frac{\Gamma+\Gamma_W}{2}\right)} \quad \text{for} \quad \text{Re}(s) > 0, \tag{B.6}$$

the Laplace coefficient in Eq. (B.5) can be inverted to to obtain $c_e(t) = \mathcal{L}^{-1}[\tilde{c}_e(s)](t)$, where

$$\begin{aligned} c_e(t) &= G(t)c_e(0), \\ &= c_e(0)e^{(i\Delta/2-\Gamma_p/4)t}\left[\cos\left(\frac{\Omega t}{2}\right) - \frac{(i\Delta - \Gamma_p/2)}{\Omega}\sin\left(\frac{\Omega t}{2}\right)\right]. \end{aligned} \tag{B.7}$$

Here, $G(t)$ is the same atomic Green's function we defined in (6.26), while $\Gamma_p = \Gamma + \Gamma_W$ is an additive decay rate. This result can be used in conjunction with (6.11) to determine an analytical expression for the pseudomode coefficients $b_k(t)$. Employing the integration formulae

$$\begin{cases} \displaystyle\int dt\, e^{\alpha t}\cos\beta t = \frac{e^{\alpha t}}{\alpha^2+\beta^2}\left(\alpha\cos\beta t + \beta\sin\beta t\right), & \text{(B.8)} \\ \displaystyle\int dt\, e^{\alpha t}\sin\beta t = \frac{e^{\alpha t}}{\alpha^2+\beta^2}\left(\alpha\sin\beta t - \beta\cos\beta t\right), & \text{(B.9)} \end{cases}$$

one can then show we arrive at the analytical result quoted in Eq. (6.33).

Something I would also like to emphasise is that the state coefficients of the multiple-environment model (B.7) are considered a generalisation of those associated to the state vector (5.23) in the original single-environment (damped Jaynes-Cummings) model. Evidently, if we take the limit $\Gamma_W \to 0$ and solve for $c_e(t)$ in the above using the same Laplace transform method, we recover the Green's function solution (5.32) found in the case of a single Lorentzian reservoir. This follows from the fact that the spectral densities of the multiple-environment model and the damped Jaynes-Cummings model in this limit are both given by

$$J(\omega_\lambda) = \frac{1}{2\pi}\frac{\Omega_0^2\Gamma}{(\omega_0 - \Delta - \omega_\lambda)^2 + (\Gamma/2)^2}. \tag{B.10}$$

For the sake of completeness, we can further demonstrate correspondence between the two models by finding the state coefficients of the reservoir modes $c_{k,\lambda}(t)$ appearing in (6.6). Integrating its equation of motion and applying the above formulae

yields

$$c_{k,\lambda}(t) = -\frac{4g_{k,\lambda}c_e(0)}{(i(2\delta_\lambda+\Delta)-\Gamma_p/2)^2+\Omega^2}\Bigg\{\left(\delta_\lambda+\Delta+i\frac{\Gamma_p}{2}\right) - e^{i\delta_\lambda t}e^{(i\Delta/2-\Gamma_p/4)t}\Bigg[\left(\delta_\lambda+\Delta+i\frac{\Gamma_p}{2}\right)\cos\left(\frac{\Omega t}{2}\right) - \left(\left(\frac{i\Delta-\Gamma_p/2}{\Omega}\right)(\delta_\lambda+\Delta/2+i\Gamma_p/4)+i\frac{\Omega}{2}\right)\sin\left(\frac{\Omega t}{2}\right)\Bigg]\Bigg\}, \tag{B.11}$$

where $\delta_\lambda = \omega_\lambda - \omega_0$ and $\Omega = \sqrt{4\Omega_0^2-(i\Delta-\Gamma_p/2)^2}$. We notice the timescale associated with the decay the coefficient $c_{k,\lambda}(t)$ depends exclusively on the width of the Lorentzian spectral density in Eq. (6.22) in the same way as $c_e(t)$. Taking $\Gamma_W \to 0$ and restricting the description to a single environment ($k = 1$) then provides the exact reservoir state coefficients $c_{\lambda,1}(t) = c_\lambda(t)$ for the atom-cavity model in section 5.2, again as a result of the equivalence between the two spectral densities.

Appendix C

Accessible information and quantum discord

To gain a clear understanding on the distinction between classical and quantum information, we use the Holevo quantity (6.53) introduced in 6.2.3 to gauge the information accessible via measurements on X_f. This information is limited by the type of measurement used. Because the QMI is invariant to how $C(\rho_{SX_f})$ and $\bar{\delta}(\rho_{SX_f})$ are assigned, the quantum discord, in turn, is required to be minimised over all measurement bases $\{M_j^X\}$ to avoid erroneous results. The POVM that fulfils this condition has been shown by Datta to be formulated using rank one projectors [130].

In order to realise the measurement in terms such projectors, we make use of the fact that both the sub-environments and pseudomodes—or fractions thereof—can collectively be mapped to a single qubit. As stated in the main text, the ground state of the qubit is defined from the vacuum of X_f: $|\widetilde{0}\rangle_{X_f} = |\{0\}\rangle_{X_f}$, while the excited state $|\widetilde{1}\rangle_{X_f}$ is formed through (6.38) and (6.47). Let us write the complete set of local orthogonal projectors in terms of the qubit states,

$$M_1^{X_f} = \frac{1}{2}\left(1_{X_f} + \vec{r}\cdot\vec{\sigma}\right), \tag{C.1}$$

$$M_2^{X_f} = \frac{1}{2}\left(1_{X_f} - \vec{r}\cdot\vec{\sigma}\right), \tag{C.2}$$

where $\vec{r} = (\sin\theta\cos\phi, \sin\theta\sin\phi, \cos\theta)^T$ is the Bloch vector, and $\vec{\sigma} = (\sigma_x, \sigma_y, \sigma_z)^T$ contains the Pauli operators constructed from the basis $\{|\widetilde{0}\rangle_{X_f}, |\widetilde{1}\rangle_{X_f}\}$, along with the identity 1_{X_f}. The accessible information and discord are then extremized with

respect to the free choice of angles $\theta \in [0, \pi)$ and $\phi \in [0, 2\pi)$.

Remembering from (6.56) that the conditional state is

$$\rho_{S|M_j^{X_f}} = \frac{1}{p_j} \mathrm{tr}_{X_f} \left[(1_S \otimes M_j^{X_f}) \rho_{SX_f} (M_j^{X_f} \otimes 1_S) \right], \qquad j = 1, 2, \tag{C.3}$$

for each measurement one obtains

$$\rho_{S|M_j^{X_f}} = \frac{1}{p_j} \Big(A_j(\theta) \left|g\right\rangle \left\langle g\right| + C_j(\theta) \left|e\right\rangle \left\langle e\right| + B_j(\theta, \phi) \left|e\right\rangle \left\langle g\right| + \text{h.c.} \Big). \tag{C.4}$$

After much algebra it is possible to show that

$$\begin{cases} A_j(\theta) = \dfrac{1}{2} \left\{ \Pi_f(t) + \eta_f^2(t) + (-1)^{j-1} \cos\theta \left[\eta_f^2(t) - \Pi_f(t) \right] \right\}, \\ B_j(\theta, \phi) = \dfrac{1}{2} (-1)^{j-1} \sin\theta \, e^{-i\phi} \eta_f(t) c_e(t), \\ C_j(\theta) = \dfrac{1}{2} |c_e(t)|^2 \Big(1 + (-1)^j \cos\theta \Big), \end{cases} \tag{C.5}$$

where, for $\sigma_z^S = \left|e\right\rangle \left\langle e\right| - \left|g\right\rangle \left\langle g\right|$, the probabilities of each outcome are

$$p_j = \frac{1}{2} \left\{ 1 + (-1)^j \cos\theta \left[\langle \sigma_z^S \rangle + 2\Pi_f(t) \right] \right\}. \tag{C.6}$$

The coefficients $\eta_f(t)$ and $\Pi_f(t)$ are also given by

$$\eta_f(t) = \begin{cases} \sum_{k \in E_f, \lambda} |c_{k,\lambda}(t)|^2, & \text{if } X = E, \\ \sum_{k \ni P_f} |b_k(t)|^2, & \text{if } X = P, \end{cases} \tag{C.7}$$

and

$$\Pi_f(t) = \begin{cases} |c_g|^2 + \sum_{k \ni E_f, \lambda} |c_{k,\lambda}(t)|^2, & \text{if } X = E, \\ |c_g|^2 + \sum_{k \ni P_f} |b_k(t)|^2 + \Pi_g(t), & \text{if } X = P, \end{cases} \tag{C.8}$$

where $k \ni X_f$ denotes summation over objects *not* in the fragment.

Finally, by diagonalizing (C.4) its eigenvalues are obtained and substituted into (6.55) to evaluate the conditional entropy. We get

$$S(\rho_{S|\{M_j^{X_f}\}}) = -\sum_{i,j=1,2} p_j \lambda_{i,j} \ln \lambda_{i,j}, \tag{C.9}$$

where

$$\lambda_{i,j} = \frac{A_j(\theta) + C_j(\theta) + (-1)^i \sqrt{\left[A_j(\theta) - C_j(\theta)\right]^2 + 4|B_j(\theta,\phi)|^2}}{2p_j}. \tag{C.10}$$

From this expression it is easy to see that the conditional entropy is invariant with respect to ϕ.